Reinforcement learning-based thermal comfort control for vehicle cabins

Hintea, Diana

Award date:
2015

Awarding institution:
Coventry University

Reinforcement Learning-based Thermal Comfort Control for Vehicle Cabins

Diana Cristina Hintea

A thesis submitted in partial fulfilment
of the University's requirements for the Degree of
Doctor of Philosophy

September 2014

Coventry University
Faculty of Engineering and Computing

Abstract

Vehicle Heating, Ventilation and Air Conditioning (HVAC) systems aim to ensure that passengers are thermally comfortable. However, thermal comfort is influenced by a large number of environmental variables and, furthermore, thermal preferences can vary greatly between individuals due to physiological, behavioural and cultural factors. This means that, generally, occupants need to adjust the nominally "comfortable" HVAC settings in order to achieve and maintain thermal comfort. This thesis established that, in order to develop efficient HVAC control algorithms, there is a need to i) sense a range of variables beyond air temperature, and ii) adopt learning-based techniques to take into account user preferences.

This thesis proposes a novel reinforcement learning-based HVAC controller combined with virtual sensing to enable energy-efficient, comfort-oriented, high-level HVAC control.

Towards this goal, the thesis first explores which of the thermal comfort models presented in the literature is the most suitable for real-time use in an HVAC system. The evaluation is based on data gathered from experimental trials with human subjects conducted over a wide range of conditions. Nilsson's equivalent temperature-based model is shown to provide the highest correlation scores with the subjective occupant comfort data. Furthermore, Nilsson's model has the advantage of estimating local (not only overall) thermal sensation and requiring only two input parameters—the clothing index and equivalent temperature.

Although equivalent temperature is shown to be necessary for estimating thermal comfort, it cannot feasibly be measured in real-time in a manufactured vehicle . Therefore, this thesis introduces a novel concept, called Virtual Thermal Comfort Sensing (VTCS), a method that estimates occupant body part equivalent temperatures from a minimalistic set of inexpensive cabin environmental sensors. Implementing VTCS within a vehicle cabin consists of two stages. First, using a mutual information-based approach, the set of cabin environmental sensors that correlate well with the body part equivalent temperatures is selected. Second, Multiple Linear Regression (MLR) is applied to infer the occupant body part equivalent temperatures from the selected cabin environmental sensors. MLR was selected as the most suitable learning method out of seven different approaches, based on the estimation accuracy provided and the processing time required for the estimation. The VTCS approach was evaluated using empirical data and provided an average Root Mean Square Error (RMSE) of 1.41 ℃ across environmental conditions characterised by cabin interior temperature rates of change of up to 6 ℃ per minute, ambient temperature differences up to 6 ℃ per experimental trial, varying ambient wind, solar load and precipitation.

Finally, this thesis proposes an innovative reinforcement learning-based controller that phrases the control specification in terms of an overall objective function based on the thermal comfort of the passengers and the energy consumption. The performance metric used in evaluating the controller was the *reward*—a measure quantifying how thermally comfortable the occupant is and the amount of energy consumed. The proposed controller was evaluated through simulation within both single-zone and multi-zone scenarios and it exceeded the performance of a basic controller and a fuzzy logic-based controller by a factor of 2.15 and 1.7, respectively. These results translate into an average of 29.05% energy saving over 200 testing scenarios when compared to the fuzzy logic-based controller, while thermal comfort was achieved and maintained successfully.

The combination of the VTCS and the reinforcement learning-based controller sets the benchmark for future HVAC systems aimed at delivering true occupant comfort. Furthermore, the techniques described in this thesis can be transferred to a wide variety of applications such as skin temperature-driven control or HVAC control in buildings.

Acknowledgements

Pursuing a PhD degree was one of my dreams in life and a dream does not come true without hard work, dedication and most importantly, the support of many people.

Firstly, I would like to thank my Director of Studies, Dr. James Brusey. I am deeply indebted to him for the fundamental role he played in my doctoral work. James provided me the guidance, assistance and expertise that I needed. Also, he offered me valuable feedback, advice and encouragement at all times. I quite simply cannot imagine a better adviser.

Further, I would like to thank my second supervisor, Prof. Elena Gaura. She provided me with fantastic research opportunities within the past years. Through her drive and determination, I always found myself highly motivated to work harder towards answering the research questions and to see the bigger picture. Elena's support and constructive criticism have helped me immensely.

I would also like to thank my colleagues from Cogent Computing research centre for delivering wonderful projects together and for proof-reading my thesis in the last stages.

Special thanks go to my friends (they know who they are) for their constant support. Cracking a few jokes amongst friends can be magic sometimes and takes the pressure away.

I heartily thank my mom and dad. My love for them is without limits and I would not have made it this far without them. My parents have always provided unconditional love and care, making continuous sacrifices in order for me to achieve my dreams. Moreover, my dad has been my model since I was a little girl and he has always inspired my love for academia and research. There's no better way to say thank you than through a PhD thesis!

Lastly, I want to thank Reda, my other half. There are no words to convey how much I appreciate what he has done for me. He continuously instilled confidence in me, had faith in me and my intellect at all times and provided boundless love. I'm looking forward to travelling the world together!

Contents

List of Figures

List of Tables

List of Algorithms

Acronyms

AC	Air Conditioning
ASHRAE	American Society of Heating, Refrigerating and Air-Conditioning Engineers
ANN	Artificial Neural Network
ATC	Automatic Temperature Control
AWM	Advantage West Midlands
AET	Average Equivalent Temperature
CO_2	Carbon Dioxide
CO	Carbon Oxide
CCARC	Cogent Computing Applied Research Center
CFD	Computational Fluid Dynamics
CMAC	Cerebellar Model Articulation Controller
CV	Cross-Validation
ERDF	European Regional Development Fund
HVAC	Heating, Ventilation and Air Conditioning
KNN	K-Nearest Neighbour
LCVTP	Low Carbon Vehicle Technology Project
LS-SVM	Least Squares Support Vector Machine
LOSOCV	Leave-One-Subject-Out-Cross-Validation
LOTOCV	Leave-One-Trial-Out-Cross-Validation
IR	Infrared
ISO	International Organization for Standardization
JLR	Jaguar Land Rover
MDP	Markov Decision Process
MTV	Mean Thermal Vote
MEMS	Micro-Electro-Mechanical Systems
MIRA	Motor Industry Research Association
MLP	Multilayer Perceptron
MLR	Multiple Linear Regression
MARS	Multivariate Adaptive Regression Splines
NREL	National Renewable Energy Laboratory

PMV	Predicted Mean Vote
PPD	Predicted Percent Dissatisfied
PCA	Principal Component Analysis
RAM	Random Access Memory
RBF	Radial Basis Function Network
RF	Random Forest
REPTree	Reduced Error Pruning Tree
RST	Resultant Surface Temperature
RFID	Radio-Frequency IDentification
RMSE	Root Mean Square Error
TD	Temporal Difference
VTCS	Virtual Thermal Comfort Sensing
WEKA	Waikato Environment for Knowledge Analysis

Nomenclature

T_o	outside temperature (K)
T_H	head equivalent temperature (K)
T_F	foot equivalent temperature (K)
T_b	block temperature (K)
$T_b^{'}$	updated block temperature (K)
T_a	cabin air temperature (K)
$T_a^{'}$	updated cabin air temperature (K)
T_i	vent air temperature (K)
T_x	cabin temperature considering recirculation (K)
T_e	occupant overall equivalent temperature (K)
V_h	head vent air flow (ls^{-1})
V_f	foot vent air flow (ls^{-1})
T_h	head vent air temperature (K)
T_f	foot vent air temperature (K)
C_a	specific heat capacity of air ($Jkg^{-1}K^{-1}$)
C_s	specific heat capacity of steel ($Jkg^{-1}K^{-1}$)
m_i	mass of air at input (kg)
m_a	mass of air (kg)
v_i	volume of air at input (L)
A_r	air recirculation amount
R_h	radiant heat (W)
S_l	solar load (W)
Q_a	cabin heat energy sum (J)
Q_b	block heat energy sum (J)
$Q_{conv_{1\rightarrow 2}}$	heat energy transferred via convection from body 1 to body 2 (J)
$Q_{cond_{1\rightarrow 2}}$	heat energy transferred via conduction from body 1 to body 2 (J)
$Q_{r_{1\rightarrow 2}}$	heat energy transferred via radiation from body 1 to body 2 (J)
Q_R	heat energy radiated by the road (J)
Q_S	heat energy absorbed from the sun (J)
Q_O	heat energy given off by occupant (J)
Q_{lg}	ambient loss / gain load (J)
Q_i	energy input for heating (J)
Q_c	energy input for cooling (J)
h_c	heat transfer coefficient
ε_g	emissivity of glass
σ	Stefan-Boltzmann constant
A	area of the material (m^2)
l	coefficient of thermal transfer loss (WK^{-2})
ρ_s	density of steel (kgm^{-3})
ρ_a	density of air (kgm^{-3})
v_s	volume of the block structure (m^3)
a	subscript denoting cabin air
b	subscript denoting block
o	subscript denoting outside air
E_c	heat exchange by evaporation on the skin
C_r	heat exchange by convection in breathing
E_r	evaporative heat exchange in breathing

H	sensitive heat losses
I_{cl}	insulating clothing value (clo, 1 clo= 0.155 $\mathrm{Km^2W^{-1}}$)
t_a	air temperature (℃)
t_{cl}	clothing surface temperature (℃)
t_r	mean radiant temperature (℃)
v_a	relative air velocity ($\mathrm{ms^{-1}}$)
M	metabolic rate (met, 1 met = 58.2 $\mathrm{Wm^{-2}}$)
h_c	convection heat transfer coefficient ($\mathrm{Wm^{-2}K^{-1}}$)
h_r	radiation heat transfer coefficient ($\mathrm{Wm^{-2}K^{-1}}$)
W	external work ($\mathrm{W\times m^{-2}}$)
p_a	partial water vapour pressure (Pa, 1 Pa=$\mathrm{Nm^{-2}}$)
f_{cl}	clothing surface area factor
R	radiation heat exchange ($\mathrm{Wm^{-2}}$)
C	convective heat exchange ($\mathrm{Wm^{-2}}$)
t_{eq}	equivalent temperature (℃)
t_s	local surface temperature (℃)
F_{cl}	reduction factor for sensible heat exchange (ND)
hcal	heat transfer coefficient
RST	resultant surface temperature (℃)
Q	body heat gain or loss ($\mathrm{Wm^{-2}}$)
ε_s	sensor emissivity (ND)
ε_a	emissivity of ambient air (ND)
σ	Stefan-Boltzmann constant ($\mathrm{Wm^{-2}K^{-4}}$)
S_{ov}	overall thermal sensation
$S_{i,\mathrm{local}}$	local thermal sensation for segment i
$S_{i,\mathrm{static}}$	static thermal sensation for segment i
$S_{i,\mathrm{dynamic}}$	dynamic thermal sensation for segment i
T_{core}	core temperature
T_i	skin temperature at segment i
$T_{i,\mathrm{set}}$	set-point skin temperature for segment i
$T_{v,\mathrm{set}}$	overall set-point skin temperature
$T_{i,\mathrm{offset}}$	offseted skin temperature for segment i
$T_{v,\mathrm{offset}}$	offseted overall skin temperature
T_v	overall skin temperature
C	thermal comfort coefficients
w_i	weights for the different body parts
$C_{i,\mathrm{local}}$	local thermal comfort for segment i
t	discrete time step
T	final time step of an episode
s_t	state at t
a_t	action at t
r_t	reward at t
R_t	return (cumulative discounted reward) following t
$R_t^{(n)}$	n-step return
R_t^{λ}	λ-return
Π	policy
$\Pi(s)$	action taken in state s under deterministic policy Π
$\Pi(s,a)$	probability of taking action a in state s under stochastic policy Π
S	set of all non-terminal states
S^+	set of all states, including the terminal state
$A(s)$	set of actions possible in state s
$P^a_{ss'}$	probability of transition from state s to state $s^{'}$ under action a

$R^a_{ss'}$	expected immediate reward on transition from s to s' under action a
$V^\Pi(s)$	value of state s under policy Π
$V^\star(s)$	value of state s under the optimal policy
V, V_t	estimates of V^Π or $V^\star$
$Q^\Pi(s,a)$	value of taking action a in state s under policy Π
$Q^\star(s,a)$	value of taking action a in state s under the optimal policy
Q, Q_t	estimates of Q^Π or $Q^\star$
$e_t(s)$	eligibility trace for state s at t
$e_t(s,a)$	eligibility trace for a state-action pair
γ	discount-rate parameter
ε	probability of random action in ε-greedy policy
α, β	step-size parameters
λ	decay-rate parameter for eligibility traces

Chapter 1

Introduction

Vehicle Heating, Ventilation and Air Conditioning (HVAC) systems have long held an elusive promise of ensuring that passengers are thermally comfortable. However, despite substantial effort into improving such systems, by individually controlling multiple zones within the cabin for example, they are still acknowledged to provide inadequate comfort in some situations.

Firstly, current HVAC approaches are focused on set-point control of cabin environmental parameters, such as air temperature. However, in many circumstances, occupants need to further adjust this set-point in order to make themselves comfortable. This is expected, as human thermal comfort depends on other factors in addition to current air temperature, such as heat radiated from the instrument panel, contact heat from the seat or steering wheel, air flow circulating within the cabin and solar radiation [46, 59]. Moreover, thermal preferences can vary greatly between individuals due to physiological factors as well as behavioural and cultural preferences [27].

Secondly, set-point based HVAC approaches consume considerable energy [109, 110]. Mola [108], for example, argued that, in order to develop an efficient controller, one needs to estimate occupant thermal comfort as accurately as possible in order to determine exactly the amount of power that must be used. With the introduction of hybrid and electric vehicles, more energy efficient approaches to HVAC control are called for, potentially based on more targeted conditioning of occupied cabin areas and driven by an estimate of the occupants' thermal comfort perceptions of the environment rather than set-point temperatures [96, 108]. Therefore, HVAC systems need to control occupant thermal comfort, not just air temperature or a combination of air temperature and humidity. Improving the internal efficiency of the HVAC system itself is another solution, however this is not part of the aim of this work.

Two factors have inspired the work in this thesis. The first is the lack of empirical work in the area of thermal comfort in vehicles, a gap that must be filled in order for the state-of-the-art to progress, as indicated by Hoof [152]. Existing thermal comfort models provide a method for estimating occupant thermal comfort. However, a key difficulty with these models is that they may not produce accurate comfort estimates for the car cabin environment [152]. If a comfort testing methodology is to be considered

authoritative, the thermal comfort model used must be validated to ensure that it agrees with passenger opinion. However, to the author's knowledge, there is no empirical evaluation of these models in real-world car cabin conditions.

The second factor is the desire to improve the way HVAC systems are designed. The author proposes, therefore, an innovative approach based on virtual sensing that will greatly simplify the HVAC control specification by phrasing it in terms of an overall objective function based on the thermal comfort of the passengers. This approach constitutes an objective measure that can be used to compare controllers with each other and should be particularly useful for control engineers when testing improvements to the system. The virtual sensing and objective function approaches are built upon to produce an innovative solution for thermal comfort control in vehicle cabins: a reinforcement learning-based heating and cooling controller is proposed and evaluated, focusing on optimising occupant thermal comfort and energy consumption. This type of control aims to set the benchmark for future HVAC systems.

The rest of this chapter is organised as follows. The motivation for the work is presented in Section 1.1. The research methodology is discussed next in Section 1.2, followed by the research questions addressed by this thesis in Section 1.3. The contributions to knowledge are then presented in Section 1.4, together with the list of publications that have resulted from the work in this thesis in Section 1.6. Finally, Section 1.5 presents the thesis structure, while the contributed work is acknowledged in Section 1.7.

1.1 Motivation

Electric and hybrid vehicles are a rapidly growing area of development, driven by concerns regarding the environment and the depletion of fossil fuels. However, their range and performance are severely impacted by the energy consumption of traditional HVAC systems. Thus, they require that the comfort control is energy efficient. Moreover, ensuring thermal comfort is an important occupant safety factor, impacting, for example, on the driver's attentiveness to traffic [23, 29, 33]. Significant effort has, therefore, been focused on researching and developing methods for intelligently controlling the HVAC unit [5, 89, 108]. However, ensuring efficient vehicular HVAC control is a challenging task, due to the following cabin and occupant related factors:

1. Cabin

   (a) The car cabin is a transient environment [29]. Average cabin air temperature rates of change of up to 9 ℃ per minute have been experienced in realistic conditions in trials performed by the author (as presented in Chapter 3).

(b) The outside environment affects the cabin in a non-uniform way [91].

(c) The car cabin is a non-uniform thermal environment. Large differences in temperature between adjacent locations within the cabin (up to 7 ℃ between the chest and foot zones) have been experienced in the experimental trials conducted by the author.

(d) Radiant heat asymmetry occurs due to the close proximity of the cabin windows, dashboard and walls to the occupant [29].

(e) Modern vehicle cabins use heated or cooled surfaces, such as seats or steering wheels that further impact on the occupants' body part thermal comfort [51, 83, 119, 132].

2. Occupant

(a) Thermal preferences can vary greatly between individuals due to physiological, behavioural and cultural factors [27].

(b) Pre-conditioning occupants at a particular temperature before they get into the car affects their perception of thermal sensation and comfort (as shown in Chapter 3, hypothesis **H3.3**).

(c) Unlike in building environments, cabin occupants are fixed in position and, therefore, do not have the ability to make themselves more comfortable by moving to another location. This reduced control also affects the perception of thermal comfort.

The traditional approach used for conditioning vehicle cabins and buildings is via the use of HVAC systems with control based on set-point temperatures. This type of system takes as input a desired set-point temperature (for example 22 ℃) and the control system aims to maintain that temperature. This approach is not optimal, either with regards to ensuring occupant thermal comfort or in terms of energy efficiency [96].

The power consumption of the HVAC system can be reduced in a number of ways, such as by achieving more efficient high-level control or by improving the physical system itself. This work focuses on restating the task for the HVAC system as being one of maintaining *occupant thermal comfort*.

Occupant thermal comfort, however, is a difficult metric to estimate and control, even more so in car cabin environments due to the factors previously listed. It has long been established that thermal comfort is influenced by a variety of factors in addition to air temperature [46, 59]. Thermal comfort is generally affected by three types of parameters:

- Environmental parameters (such as air velocity, air temperature, relative humidity and mean radiant temperature).

- Physiological parameters (such as skin temperatures, core temperatures and metabolic rate).

- Other parameters such as clothing thermal resistance.

Furthermore, it has been shown that pre-conditioning, acclimatisation and personal preferences have a large impact on thermal comfort. Particularly, Fanger's results show that at least 5% of a population will be dissatisfied for any given conditions [47]. Experimental evidence presented in this thesis and also reflected in prior literature [6, 18, 21, 23, 60, 81] shows that:

1. Thermal neutrality defines the temperatures in an optimum state that guarantee overall occupant thermal comfort. For a given population, thermal neutrality does not occur at one particular air temperature value. The empirical results in this thesis show that, while a cabin average air temperature of 25 ℃ produces a neutral thermal sensation for drivers in some cases, influencing factors caused thermal neutrality to occur within a wider range (between 19 ℃ and 29 ℃).

2. In the case of extreme winter and summer conditions, both the occupant and the cabin are naturally pre-conditioned to a very low or high temperature. Perception of thermal comfort is influenced by these conditions and, therefore, thermal comfort is likely to be different at the same car cabin air temperature. Experimental results confirm that thermal neutrality occurs at different average cabin temperatures based on the pre-conditioning of the subject (for example, thermal neutrality is reached approximately 3 ℃ lower with cold pre-conditioning).

3. Solar loading is another factor that influences thermal comfort. Results in this thesis show that additional solar loading causes the thermal sensation for a given air temperature to be generally warmer. Also, in the case of asymmetry in the solar load, the side of the subject's body exposed to solar loading was often reported as being at a lower comfort level than the unexposed side.

The above indicates that, in order to develop efficient HVAC control algorithms, there is a need to 1) *sense more than just air temperature* and 2) *utilise thermal comfort estimates for cabin occupants in the control feedback loop.* However, no mathematical model is able to satisfy the thermal comfort preferences of all cabin occupants. Moreover, the relationship between thermal comfort and the environmental variables being measured is non-linear [37]. *Therefore, learning-based control is needed that fulfils the above capabilities.* The development of such a mechanism lies at the core of this thesis.

1.2 Methodology

This thesis draws from several collaborative projects between leading automotive companies (Jaguar Land Rover (JLR), Ricardo and Motor Industry Research Association (MIRA)) and research partners (Coventry University and Warwick University) aimed at introducing new, low carbon vehicle components and manufacturing techniques. The projects are: the Low Carbon Vehicle Technology Project (LCVTP), Automatic Temperature Control (ATC) and STRIVE (further detailed in Section 1.7). These collaborations highlight the practical nature of the work performed by the author and its potential impact on the automotive industry.

The work in this thesis followed two methodological strands. The first strand is experimental and is aimed at critically evaluating and selecting an optimal thermal comfort model from the literature, as well as developing a Virtual Thermal Comfort Sensing (VTCS) approach that estimates occupant body part equivalent temperature from minimalistic and inexpensive cabin environmental sensors. This work provides the foundation for comfort-based HVAC control.

A significant gap exists in the literature regarding research performed using car cabin experimental data. Many car cabin comfort evaluations are based on simulation models and are limited by the constraints introduced by the simulation packages and the models used. A strength of this work, therefore, comes from the fact that the thermal comfort related analysis conducted is based on gathered empirical data—both cabin environmental sensor data and subjective occupant reports. This data was used to determine which existing thermal comfort model best matches the thermal comfort level of car cabin occupants. As described in Chapter 4, the experimental data was gathered from a number of trials that include both steady-state conditions and conditions normally expected while driving and in which subjective comfort measures were sought from human participants.

Another use of the empirical data was to develop an in-depth understanding of the relationship between various cabin environmental sensors. Knowledge of these relationships was essential for the VTCS development. In order to develop the VTCS method, seven equivalent temperature estimation techniques were implemented and evaluated (see Chapter 5) based on the data collected.

The second methodological approach is simulation-based and was used in the development of a reinforcement learning-based heating and cooling controller that maximises occupant thermal comfort while minimising the energy consumption. The concept of reinforcement learning is described in detail in Section 2.6. Once the optimum policy is learnt through simulation, the policy can be transferred into the vehicle, where the controller can be fine-tuned for the real cabin and HVAC system, and additional learning of user preferences can occur. As a result, a better control policy can be achieved. The development

of a real-time system is, however, beyond the scope of this thesis.

The work in this thesis uses existing statistical and machine learning techniques in order to develop novel paradigms in the area of vehicular thermal comfort control. As shown in this thesis, the methods are generic and can be used within a number of other applications, such as HVAC systems for trains, planes or buildings. This section provided an overview of the methodology used to develop the work here. In summary, to develop and evaluate the methods presented in this thesis, the author has taken an approach of both empirical data-based evaluation and simulation-based evaluation.

1.3 Research questions

As previously described, this thesis focuses on 1) the evaluation of existing thermal comfort models on data gathered in a variety of environmental vehicle cabin conditions, 2) the development of VTCS that enables cabin occupant body part equivalent temperature to be estimated and 3) the development and evaluation of a reinforcement learning-based HVAC control algorithm aimed at maximising the thermal comfort of passengers while reducing the energy consumption. There are several research questions that this work aims to answer, as follows:

RQ1: Is there an existing thermal comfort model that is suitable for real-time use in an HVAC system and if so, which is it?

This question pertains to whether there is a thermal comfort model in the state-of-the-art that is suitable for vehicular control. The four models implemented and evaluated on gathered empirical data are: the Predicted Mean Vote (PMV), Zhang's model, Taniguchi's model and Nilsson's model. In order to decide the most suitable thermal comfort model, the correlation score with subjective occupant comfort data is taken into consideration, as well as characteristics of the model such as whether it can estimate local thermal comfort and the number of parameters it requires as input. This work is described in Section 4.3.

RQ2: Can an optimum set of cabin environmental sensors be defined for estimating occupant body part equivalent temperature, given realistic constraints?

The location and type of cabin environmental sensors that actuate the HVAC control are usually selected according to cost and aesthetics. These sensors, however, may not be suitable for effective HVAC control. A mutual information-based sensor selection technique combined with virtual sensing allows occupant body part equivalent temperature to be estimated and used as the basis

for more effective HVAC control. Therefore, the first step is to determine the feasibility of selective cabin sensor locations for this method and demonstrate what these locations might be. The method is provided in Section 5.1.

RQ3: Which is the most suitable machine learning technique for estimating occupant body part equivalent temperature from a set of cabin environmental sensors?

As stated in Section 2.3, it is not feasible to directly measure occupant body part equivalent temperature in vehicles. Therefore, machine learning approaches should be considered in order to estimate the occupant equivalent temperatures. Seven machine learning methods were implemented and evaluated. The criteria for selecting the best method were: i) the error between the values estimated and the values actually observed and ii) the processing time required for the estimation to be performed on an unseen data set. The latter is important to take into account given the real-time potential application of this methodology. This work is described in Section 5.2.

RQ4: Is it possible to represent the state of the cabin environment in such a way that it fulfils the Markov Decision Process (MDP) criteria?

This question asks whether the car cabin environment can be represented to fulfil the MDP criteria. In order for an environment to fulfil the MDP criteria, the representation of the state needs to be Markovian (that is, the state comprises all the necessary information and this information suffices in order to decide the next action). In general, the aim is to express the state in a compact way, so that the complexity of the problem is significantly reduced. Creating a compact Markovian state representation for this particular HVAC control algorithm is a problem discussed in Section 6.2.

RQ5: Can a reinforcement learning-based heating and cooling control policy provide performance beyond the current state-of-the-art?

This question asks whether an efficient reinforcement learning-based controller that maximises occupant thermal comfort while minimising the associated energy consumption can provide a better performance than state-of-the-art approaches. In order to compare the performance of various control algorithms, a performance metric has to be defined. The method of quantifying performance is an important design decision and for this application the basic metric of performance is the *reward*—a number quantifying the combination of how far the occupant equivalent temperature is from the comfortable range and how much energy is consumed. This is discussed in Chapter 6.

1.4 Contributions to knowledge

In answering the research questions listed in Section 1.3, the following contributions to knowledge were made:

1. The identification and evaluation (based on gathered empirical data) of the most suitable existing thermal comfort model to be used for vehicular heating and cooling control. This work is presented in Chapter 4.

2. A method for developing VTCS to actuate the heating and cooling control. The method consists of:

   (a) A method that selects the optimum set of cabin environmental sensors and their associated locations for estimating occupant body part equivalent temperature. This is reported in Chapter 5.

   (b) An equivalent temperature estimation machine learning-based method. The method was selected out of seven different methods based on accuracy and processing time. This is also reported in Chapter 5.

3. A reinforcement learning-based policy design for producing an energy efficient comfort-oriented heating and cooling controller, which outperforms current state-of-the-art methods. This work is presented in Chapter 6.

1.5 Thesis structure

This chapter has presented an introduction to this thesis, including the motivation for the work, the methodology adopted, the research questions and contributions to knowledge. The rest of this thesis is organised as follows:

Chapter 2 discusses relevant background literature to the topics introduced throughout this thesis. The chapter reviews thermal comfort in car cabins and existing thermal comfort models, introduces background on the equivalent temperature concept, reviews tools for measuring thermal comfort in car cabins, presents techniques for estimating and predicting cabin environmental parameters and reviews existing HVAC control systems. The chapter also presents background on reinforcement learning theory and related applications.

Chapter 3 offers an overview of the system developed within this thesis and discusses the real-time potential of this application.

Chapter 4 presents empirical work in the area of vehicular thermal comfort. The chapter describes the experimental data used for the analysis, both cabin environmental sensor data and subjective occupant reports, gathered from a number of trials that include both steady-state conditions and conditions normally expected while driving. This data was used to answer thermal comfort related research questions and to determine which existing thermal comfort model best matches the thermal comfort level of car cabin occupants.

Chapter 5 draws on experimental data to investigate methods of providing accurate thermal comfort estimates along with the use of virtual sensing in the car cabin. The chapter introduces a novel method, named VTCS, that estimates occupant body part equivalent temperatures from inexpensive cabin environmental sensors and evaluates the method on offline real-world data sets.

Chapter 6 proposes and evaluates a reinforcement learning-based HVAC control algorithm, an innovation in the area of vehicular thermal comfort-oriented control. The algorithm is evaluated through simulation within two different scenarios.

Chapter 7 concludes the work by presenting answers to research questions proposed in this chapter and future directions of the work.

This thesis has three distinct, but inter-related paths , namely occupant thermal comfort, thermal comfort estimation and heating and cooling control algorithms. The casual reader may be interested only in thermal comfort models, for example. In this case, the relevant parts that should be read are in Chapters 2 and 4, as they provide an overview of existing thermal comfort models (Chapter 2) and an evaluation of the existing thermal comfort models on empirical data (Chapter 4).

For readers more interested in estimating occupant thermal comfort, Chapters 2 and 5 provide a description of related works (Chapter 2) and a methodology for designing a VTCS approach that estimates occupant body part equivalent temperatures from cabin environmental sensors (Chapter 5).

For readers more interested in thermal comfort-based control algorithms, Chapter 2 provides an overview of related works. Chapter 2 also provides an overview of the reinforcement learning theory behind the work in this thesis. Chapter 6 presents the design, implementation and evaluation of the reinforcement learning-based controller.

1.6 Publications

The work described in this thesis has lead to the following publications:

Journal

- Diana Hintea, James Brusey, Elena Gaura: Reinforcement Learning-based Thermal Comfort Control for Vehicle Cabins. To be submitted toApplied Thermal Engineering.

Conference Proceedings

- Diana Hintea, John Kemp, James Brusey, Elena I. Gaura, Neil Beloe: Applicability of Thermal Comfort Models to Car Cabin Environments. Proceedings of the 11th International Conference on Informatics in Control, Automation and Robotics ICINCO (1) 2014: 769–776; Austria, Vienna, 1-3 September, 2014; ISBN: 978-989-758-039-0.
- Diana Hintea, James Brusey, Elena I. Gaura, John Kemp, Neil Beloe: Comfort in Cars - Estimating Equivalent Temperature for Comfort Driven Heating, Ventilation and Air Conditioning (HVAC) Control. Proceedings of the 10th International Conference on Informatics in Control, Automation and Robotics ICINCO (1) 2013: 507–513; Iceland, Reykjavik, 29-31 July, 2013; ISBN: 978-989-8565-70-9.
- Diana Hintea, James Brusey, Elena I. Gaura, Neil Beloe, David Bridge: Mutual Information-based Sensor Positioning for Car Cabin Comfort Control. Proceedings of the 15th International Conference on Knowledge-Based and Intelligent Information and Engineering Systems KES (3) 2011: 483–492; Germany, Kaiserslautern, 12-14 September, 2011; ISBN: 978-3-642-23853-6.

Patents and disclosures

- Diana Hintea, James Brusey, Neil Beloe: Reinforcement Learning-based HVAC Control - in draft.

Appendix B offers more information on the publications and technical reports.

1.7 Acknowledgement of contributed work

Little research is carried out in its entirety by an individual, particularly in the case of highly practical work such as the research presented in this thesis. This section details the contribution made by other researchers that have aided the work presented in this thesis.

Designing the occupant thermal comfort trials, detailed in Section 4.1, benefited from the expertise of Dr. Doug Thake within the Health and Life Sciences Faculty of Coventry University, Neil Beloe at JLR and Dr. David Bridge at MIRA Ltd. The data sets deriving from the trials and used to evaluate a series of thermal comfort models in Chapter 4 and the VTCS method in Chapter 5 were provided by Dr. John Kemp in the Cogent Computing Applied Research Center (CCARC).

The evaluation of the reinforcement learning-based heating and cooling controller, detailed in Chapter 6, was made possible using a cabin simulation provided by Neil Beloe at JLR. The simulation was provided in an Microsoft Excel spreadsheet and translated into Java by the author. The Java reinforcement learning software support libraries used in the development of the algorithm were created by Dr. James Brusey, the Director of CCARC.

This thesis draws from several collaborative projects between automotive companies and research partners with the goal of introducing innovative, low carbon vehicle components and manufacturing techniques. The projects are the LCVTP, ATC and STRIVE. The LCVTP was a collaborative research project between various research partners and automotive companies, revolutionising the way vehicles are powered and manufactured. The project partners included JLR, Ricardo, MIRA LTD., Tata Motors European Technical Centre, WMG, Zytek, and Coventry University. The LCVTP included 15 automotive technology development work-streams that delivered technological and socio-economic outputs benefiting the West Midlands Region. The £19 million project was funded by Advantage West Midlands (AWM) and the European Regional Development Fund (ERDF). ATC was a collaborative research project between CCARC and JLR aimed at developing a revised automatic temperature controller. STRIVE was a collaborative research project between CCARC and JLR looking into innovative approaches that improve the effectiveness and efficiency of heating and cooling systems in vehicles.

Chapter 2

Literature Review

The work reported in this thesis draws on domains such as thermal comfort models, tools for measuring thermal comfort in vehicles, machine learning techniques for estimating cabin environmental parameters, Heating, Ventilation and Air Conditioning (HVAC) control algorithms and reinforcement learning applications. This chapter therefore describes the state-of-the-art of these domains and its relationship to the work here.

Section 2.1 gives an overview of existing thermal comfort models. The most widely used tools to measure thermal comfort within vehicles are summarised in Section 2.2. The concept of equivalent temperature is introduced in Section 2.3, along with modalities of measurement and validation within transient and inhomogeneous environments. Section 2.4 describes machine learning-based methods that are applied to estimating cabin environmental parameters. An overview of HVAC control algorithms with applicability both in the buildings and vehicular domains is presented in Section 2.5. Section 2.6 presents reinforcement learning theoretical aspects and related applications. Finally, Section 2.7 summarises the chapter.

2.1 Thermal comfort models

Thermal comfort and thermal sensation are complex parameters, depending on variables such as local air flow temperature [121, 166], air velocity [68, 170, 171], relative humidity [1, 3], and solar load [40, 68]. Extensive research has gone into developing thermal comfort models that take as input measurable parameters such as air temperature, mean radiant temperature or skin temperature and output a thermal comfort or thermal sensation index. A thermal index is a single number that represents the degree of thermal comfort people are perceiving. Thermal comfort models are needed in order to estimate the occupant thermal comfort level without requiring subjective feedback, for automatic control loops and in situations where you cannot place a person into the desired location. Jones [82] states that all thermal models have several limitations, such as: i) the model must be precisely and unequivocally defined (code provided), ii) the use of the model must be carefully and precisely limited to the conditions for which it

Table 2.1: Existing thermal comfort models.

Author	Year	Local or overall	Environment type
Gagge et al. [59]	1967	Local	Steady-state
Fanger [46]	1970	Overall	Steady-state
Wyon et al. [164]	1985	Local	Steady-state
Taniguchi et al. [147]	1992	Overall	Non-uniform
Matsunaga et al. [103]	1993	Overall	Steady-state
Wang [165]	1994	Overall	Transient
De Dear [38]	1998	Overall	Steady-state
Nilsson [115]	2004	Local and overall	Steady-state and non-uniform
Arens et al. [7, 8]	2006	Local and overall	Transient: Uniform and non-uniform
Zhang [172]	2003	Local and overall	Transient: Uniform and non-uniform
Fiala et al. [52]	2010	Local and overall	Transient

is validated and iii) the model is no better than the inputs provided to it. Detailed reviews of thermal comfort models are given in [2, 26, 41, 42, 72, 122].

Table 2.1 presents the thermal comfort models in the state-of-the-art. Four models are implemented and evaluated in this thesis, namely Fanger's Predicted Mean Vote (PMV), Taniguchi's model, Zhang's model and Nilsson's model (see Section 2.1.1 to Section 2.1.4). With regard to other models, Matsunaga et al. [103] adopted, for example, the concept of Average Equivalent Temperature (AET) in order to compute the PMV sensation index. The AET is a surface area-weighted value for three body parts: the head with a weight of 0.1, the abdomen with a weight of 0.7 and the feet with a weight of 0.2. Because the end product is the PMV index, the thermal comfort model of Matsunaga et al. is not evaluated in this thesis.

The Berkeley advanced human thermal comfort model [7, 8] is used in multiple works [19, 57]. The Berkeley model uses 16 body segments (head, chest, back, pelvis, left and right lower arms, left and right upper arms, left and right hands, left and right lower legs, left and right thighs, and left and right feet) that correspond to the Berkeley thermal manikin. Each segment of the manikin integrates a clothing layer and four body layers (core, muscle, fat, and skin tissues). Taking into account various physiological mechanisms such as sweating, metabolic heat production and vasoconstruction, the model predicts human physiological responses to non-uniform and transient thermal environments. The advantages are that the model can predict more accurately the effects of thermally asymmetric environments and that the segmentation of the model corresponds to the UC Berkeley thermal manikin. The virtual manikin in the software model estimates occupant skin temperatures and Zhang's model is further applied to calculate thermal sensation and thermal comfort. As this thesis is concerned with empirical results rather than simulation-based results, only Zhang's model is evaluated. For the same reason, the thermal comfort

model developed by Fiala et al. [52] is not considered.

Gagge *et al.* [59] presented a thermal comfort model suitable for low and medium activity levels—the Pierce two-node model. The model is based on sweating and body heat generation and splits the human body in two thermal nodes: the skin and the core, each with corresponding heat balance equations. Within this model, the human body is divided into 16 segments. Gagge *et al.* introduced the concept of effective temperature, which is a combination of air temperature and relative humidity. The model was validated experimentally, with some parameters set to a constant value, such as the humidity or the clothing insulation. Furthermore, a thermal sensation index (TSENS) is formed as a linear regression from the standard environment temperature parameter and the water vapour pressure at this particular temperature.

The following subsections discuss the thermal comfort models evaluated in this thesis.

2.1.1 Predicted Mean Vote

Fanger [46, 47, 48] developed the PMV model in 1967 and to this date it is still the most widely used thermal comfort model. The main advantages of PMV are the standardisation of its implementation (in the International Organization for Standardization (ISO) and American Society of Heating, Refrigerating and Air-Conditioning Engineers (ASHRAE) standards) and that if some of the constituent parameters cannot be measured, they can be approximated without introducing a significant error in the resulting PMV index. However, PMV was never intended to be applied in transient, inhomogeneous conditions. Moreover, the state-of-the-art does not contain any validation of the model in various conditions within vehicular environments.

PMV was developed based on thermo-regulation and heat balance theories. These theories are based on human bodies employing physiological processes in order to maintain a balance between the heat produced by metabolism and the heat lost from the body. The PMV index is computed using the following formula:

$$\mathrm{PMV} = \left[0.303 \times e^{-0.036M} + 0.028\right] \times L \tag{2.1}$$

$$L = (M - W) - H - E_c - C_r - E_r \tag{2.2}$$

where L is the thermal load (that is, the difference between the internal heat production and the heat loss to the environment), M is the metabolic rate, W is the external work, H is the sensible heat loss, E_c is the heat exchange by evaporation on the skin, E_r is the evaporative heat exchange in breathing and C_r is the heat exchange by convection in breathing.

Table 2.2: PMV thermal sensation index.

-3	Cold
-2	Cool
-1	Slightly cool
0	Neutral
1	Slightly warm
2	Warm
3	Hot

The remaining variables in equation (2.2) can be calculated as:

$$H = 3.96 \times 10^{-8} \times f_{cl} \times \left[(t_{cl} + 273)^4 - (t_r + 273)^4\right] - f_{cl} \times h_c \times (t_{cl} - t_a) \tag{2.3}$$

$$E_c = 3.05 \times [5.73 - 0.007 \times (M - W) - p_a] - 0.42 \times [(M - W) - 58.15] \tag{2.4}$$

$$C_r = 0.0014 \times M \times (34 - t_a) \tag{2.5}$$

$$E_r = 0.0173 \times M \times (5.87 - p_a) \tag{2.6}$$

$$t_{cl} = 35.7 - 0.028 \times (M - W) - R_{cl} \times [(M - W) - E_c - C_r - E_r] \tag{2.7}$$

$$h_c = \begin{cases} 2.38 \times |t_{cl} - t_a|^{0.25}, & \text{for } 2.38 \times |t_{cl} - t_a|^{0.25} \geq 12.1 \times \sqrt{v_a} \\ 12.1 \times \sqrt{v_a}, & \text{for } 2.38 \times |t_{cl} - t_a|^{0.25} < 12.1 \times \sqrt{v_a} \end{cases} \tag{2.8}$$

$$f_{cl} = \begin{cases} 1 + 1.29 \times I_{cl}, & \text{for } I_{cl} \leq 0.078\,\mathrm{m}^2 \\ 1 + 0.645 \times I_{cl}, & \text{for } I_{cl} > 0.078\,\mathrm{m}^2 \end{cases} \tag{2.9}$$

$$R_{cl} = 0.155 \times I_{cl} \tag{2.10}$$

where t_{cl} is the average surface temperature of the clothed body (℃), f_{cl} is the clothing surface area factor, t_a is the air temperature (℃), h_c is the convection heat transfer coefficient ($\mathrm{Wm^{-2}K^{-1}}$), I_{cl} is the insulating clothing value (clo), R_{cl} is the clothing thermal insulation (clo), v_a is the air velocity ($\mathrm{ms^{-1}}$) and t_r is the mean radiant temperature (℃).

The model combines the effect of four physical variables (air velocity, mean radiant temperature, air temperature and relative humidity) and two personal variables (activity level and clothing insulation) and outputs an index that can be used to predict thermal comfort, presented in Table 2.2.

The index corresponds to the ASHRAE thermal sensation scale and it is defined as the average thermal sensation felt by a large group of people in a space. Fanger validated and refined the comfort equation

Table 2.3: Intervals of validity for the PMV input parameters according to the ISO 7730 standard.

Parameter	Interval
Air temperature	10–30 ℃
Mean radiant temperature	10–40 ℃
Air velocity	0–1 $\mathrm{m \times s^{-1}}$
Relative humidity	30–70%
Clothing insulation	0–2 clo (0–0.31 $\mathrm{K \times m^2 \times W^{-1}}$)
Activity level	0.8–4 met (46–232 $\mathrm{W \times m^{-2}}$)

with data from previous thermal comfort studies combined with his own, with the number of participants summing up to approximately 1400. Fanger stated that the PMV model should be used with care for indexes below -2 and above $+2$ and that significant errors can appear in hot environments. Also, Fanger provides validity intervals for the input parameters of the model (shown in Table 2.3).

Following from PMV, Fanger developed an additional index, called the Predicted Percent Dissatisfied (PPD). This index can be directly calculated from the PMV index and predicts the percentage of people who are likely to be dissatisfied with a given thermal environment. PPD is computed using:

$$\mathrm{PPD} = 100 - 95 \times e^{(-0.03353 \times \mathrm{PMV}^4 - 0.2179 \times \mathrm{PMV}^2)} \tag{2.11}$$

As stated by Charles [24], a large number of researchers made efforts to prove the validity of the PMV model. Humphreys *et al.* [77] show that the accuracy of the PMV model is higher when sedentary activities are conducted and light clothing is used, and is lower for heavier clothing and higher activity levels. Schiller [137] and Oseland [123] show that the PMV model over-predicted or under-predicted the neutral temperature within a 2–4 ℃ error margin, with other findings suggesting that subjects are more sensitive to changes in temperature than the PMV model would predict. Measurement errors (due to the difficulty of measuring these six parameters in field settings) and contextual assumptions (such as individual preferences [53, 76, 161], building differences [38, 153], outdoor climate and behavioural and psychological adaptation) are the main factors that can contribute to discrepancies between the thermal sensation of a subject and the calculated PMV index.

Van Hoof [152] conducted a study based on Fanger's thermal comfort model. While discussing PMV's applicability to transient conditions, Van Hoof highlighted that the model is only valid for stable conditions. Van Hoof concluded that there is a lack of PMV assessment in transient environments and that extensive research is still required. Also, body parts experience local discomfort and thermal sensation levels differ from each other and from the overall sensation [7, 8, 111]. Therefore, a big disadvantage of the PMV model is that it is unable to differentiate between thermal sensations at different body parts,

which would be very useful in the case of vehicular HVAC control systems.

Despite these disadvantages, PMV is evaluated in this thesis due to its popularity and the need, as pointed out in the literature, for empirical evaluation.

2.1.2 Taniguchi's model

Skin temperature is shown to be a good predictor of local and overall thermal sensation in the state-of-the-art [12, 15, 17, 25, 156, 168], especially in the case of extremities such as face and hands. Taniguchi [147] developed a Multiple Linear Regression (MLR)-based model that relates average facial skin temperature and its rate of change to occupant Overall Thermal Sensation (OTS) in a vehicle environment. The model was developed based on a series of human subject tests and is calculated as:

$$\text{OTS} = 0.81 \times (T_f - 33.9) + 39.1 \times \frac{dT_f}{dt} \tag{2.12}$$

where T_f is the face skin temperature and $\frac{dT_f}{dt}$ is the face skin temperature rate of change.

A significant disadvantage of this model is not taking into account that the thermal sensation of body segments other than the face also impacts the overall body thermal sensation. Moreover, the model does not allow the computation of local thermal sensation. However, it would be interesting to see the correlation between facial skin temperature and thermal comfort reports within a variety of trials and whether this model matches more accurately subjective thermal comfort than more complex skin temperature-based models, such as Zhang's.

2.1.3 Zhang's model

Zhang *et al.* [173, 174, 175] developed local and overall thermal sensation and comfort models targeted at transient, non-uniform conditions. The models are based on skin temperatures along with core temperature, if available. A nine-point analogue scale and a six-point analogue scale (as shown in Table 2.4) are used for expressing thermal sensation and thermal comfort, respectively.

Zhang *et al.* carried out experimental tests at UC Berkeley during January to mid August 2002, with subjects placed into chambers of uniform temperature and with heated or cooled air applied individually to 19 body areas. The tests were carried out in a climate-controlled wind tunnel, consisting of both cold and hot test cases and covering a temperature range of -23.3 ℃ to 43 ℃. Throughout these tests, subjects adjusted the HVAC settings to their preference. Skin temperature was measured at 19 locations using thermocouples, while core temperature was measured using an ingestible temperature device. Zhang *et*

Table 2.4: Zhang's thermal sensation and comfort scales.

-4	Very cold
-3	Cold
-2	Cool
-1	Slightly cool
0	Neutral
1	Slightly warm
2	Warm
3	Hot
4	Very hot

-3	Very uncomfortable
-2	Uncomfortable
-1	Just uncomfortable
1	Just comfortable
2	Comfortable
3	Very comfortable

al. stated that certain body parts, such as the back and chest, have a bigger impact on the overall thermal sensation, whereas others, such as hands and feet, have a smaller impact. Based on the experimentation, thermal sensation and comfort equations were developed using the measured skin temperature, mean skin temperature and core temperature, along with subjective reports. Local thermal sensation at segment i is calculated as:

$$T_{i,\text{offset}} \leftarrow T_i - T_{i,\text{set}} \tag{2.13}$$

$$T_{v,\text{offset}} \leftarrow T_v - T_{v,\text{set}} \tag{2.14}$$

$$m = [C_{1,i}] \times [T_{i,\text{offset}}] - K_{1,i} \times ([T_{i,\text{offset}}] - [T_{v,\text{offset}}]) \tag{2.15}$$

$$S_{i,\text{static}} = 4 \times \left(\frac{2}{1 + e^{-m}} - 1 \right) \tag{2.16}$$

$$S_{i,\text{dynamic}} = C_{2,i} \times \frac{dT_{\text{i}}}{dt} + C_{3,i} \times \frac{dT_{\text{core}}}{dt} \tag{2.17}$$

$$S_{i,\text{local}} = S_{i,\text{static}} + S_{i,\text{dynamic}} \tag{2.18}$$

where $T_{i,\text{offset}}$ is the offseted skin temperature for segment i, $T_{v,\text{offset}}$ is the offseted overall skin temperature, T_i is the skin temperature for segment i, T_v is the overall skin temperature, $T_{i,\text{set}}$ is the set-point skin temperature for segment i, $T_{v,\text{set}}$ is the overall set-point skin temperature, T_{core} is the core temperature, $S_{i,\text{local}}$ is the local thermal sensation for segment i, $S_{i,\text{static}}$ is the static thermal sensation for segment i, $S_{i,\text{dynamic}}$ is the dynamic thermal sensation for segment i and C and K are pre-established coefficients. The overall thermal sensation S_{ov} is calculated as the weighted average of the local sensation for each of the body segments:

$$S_{ov} = \frac{\sum_i^n w_i \times S_{i,\text{local}}}{\sum_i^n w_i} \tag{2.19}$$

where i is the index for the body part segment, n is the total number of body parts, $S_{i,\text{local}}$ is the local

thermal sensation for segment i and w_i is the weight of segment i.

Local thermal comfort at segment i is described by the following formula:

$$C_{i,\text{local}} = \left(\frac{C_1 + C_2 \times S_{ov}}{e^{5\times(S_i+[C_3]\times S_{ov})}+1} + C_4 + C_5 \times S_{ov}\right) \times (S_{i,\text{local}} + C_3 \times S_{ov}) + C_6 + C_7 \times S_{ov} \quad (2.20)$$

where $S_{i,\text{local}}$ is the local thermal sensation for segment i, S_{ov} is the overall thermal sensation and C are pre-established thermal comfort coefficients.

Zhang *et al.* validated the models against subjective reports. The coefficient of determination (R^2) for the overall thermal sensation model was 0.95 and the standard deviation of residuals was 0.54. On the other hand, for the overall thermal comfort model the coefficient of determination was 0.89 and the standard deviation of the residuals was 0.78.

Zhang's model was developed to accommodate non-uniform conditions, however, no validation of the model within daily driving scenarios or other typical conditions encountered in vehicular environments exists in the state-of-the-art. Zhang's model has been criticised for not including the main parameters contributing to thermal comfort (air velocity, air temperature and mean radiant temperature) [47, 81]. Luo *et al.* [95] also criticise the model, citing that "the mathematical model is not practicable as it is limited by having too many coefficients, and because of the experiment's limitation, the regression analysis result cannot be assured either". Furthermore, they criticise the body part set-point temperature approach of the model (Zhang *et al.* omit specifications related to the use of set-point temperatures). Cheng [26] points out that Zhang *et al.* focused more on cooling down body parts in warm environments than on warming up body parts in cool environments during the experiments. In addition, Zhang *et al.* did not vary the influence of local stimulation duration and intensity throughout their tests.

The main advantage of Zhang's model over PMV is its ability to determine local thermal sensation indexes. Even if the overall thermal sensation is neutral, some body parts can still experience discomfort, for example when the vent air flow is directed towards them. With the introduction of heated/cooled seats and steering wheels, the impact of individual body part sensation on overall thermal sensation is even higher due to the direct contact with these elements.

2.1.4 Nilsson's model

Nilsson [115] proposed clothing independent thermal comfort zones for 18 different body parts based on equivalent temperatures. Equivalent temperature, as further discussed in Section 2.3, is formally defined as the uniform temperature of an imaginary enclosure with air velocity equal to zero in which a person will

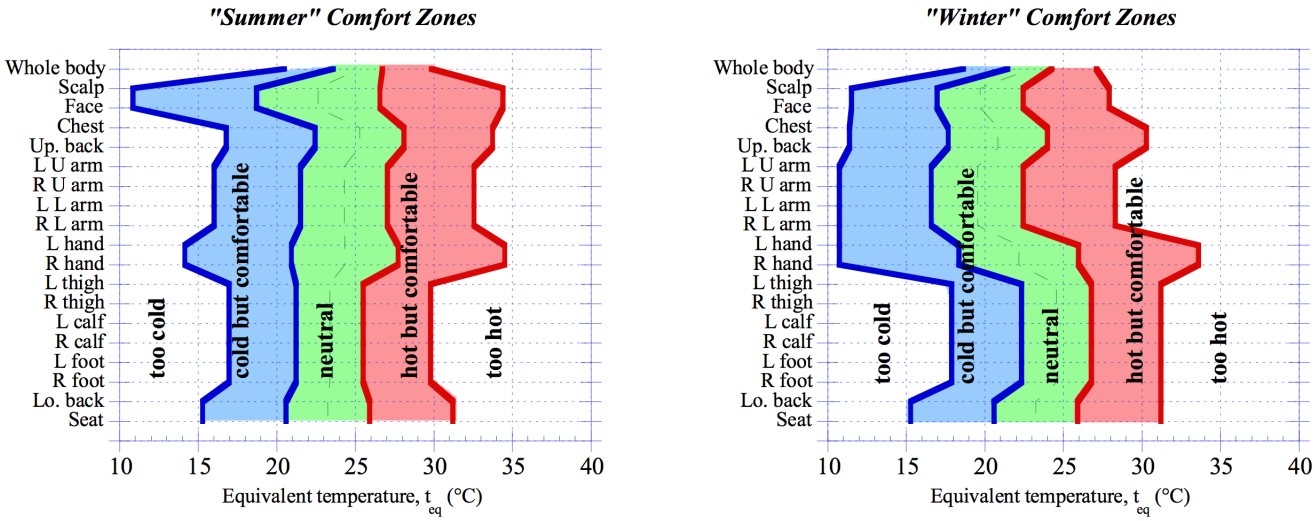

Figure 2.1: Nilsson's clothing-independent thermal sensation diagrams [115].

exchange the same dry heat by radiation and convection as in the actual non-uniform environment [113]. Equivalent temperature can be computed based on environmental parameters (air temperature, mean radiant temperature, air flow and clothing index) or it can be "more" directly measured with appropriate instruments [113]. Once equivalent temperature is calculated, the local and overall thermal sensation level can be estimated using the diagrams in Figure 2.1. Nilsson developed this model experimentally.

A gap in the literature that this thesis responds to is the lack of empirical evaluation of thermal comfort models within vehicular environments in order to establish whether any of them is suitable for comfort-oriented HVAC control. According to the author's knowledge, no empirical data-based evaluation of the four thermal comfort models discussed in this section exists in the state-of-the-art. These models are implemented and evaluated within various conditions in Chapter 3.

2.2 Tools for measuring car cabin thermal comfort

Various tools exist for measuring the basic climatic parameters (air temperature, mean radiant temperature and air flow), the equivalent temperature or the PMV index in vehicular environments. This section gives an overview of such tools and discusses their applications and limitations.

2.2.1 Sensors measuring individual variables

Silva [32] describes the sensors used for measuring the basic climatic parameters: air temperature, mean radiant temperature and air velocity. The most common choices of sensors are:

- Air temperature—measured with liquid-in-glass, pressure bulbs, bimetallic thermometers, thermocouples, thermistors or resistance temperature devices.
- Mean radiant temperature—measured with black globe thermometers or estimated from an equation consisting of surrounding surface temperatures and shape factors.
- Air velocity—measured using hot-wire anemometry or laser Doppler velocimeters.

Madsen [97] highlighted the problems associated with measuring the individual parameters and using them as input to a formula to calculate PMV. It would be much faster, simpler and more accurate to have an instrument that directly measures the effect of air temperature, mean radiant temperature and air velocity—a thermal comfort sensor.

2.2.2 Comfort sensors

Madsen and Olesen [97, 98, 120] presented the notion of a "comfort meter", together with its requirements in terms of size, shape, radiation properties, surface temperature and orientation. The aim of the device was to measure the dry heat emittance from a person to their surroundings. The instrument allowed setting the activity level, clothing index and the vapour pressure.

Kumar *et al.* [90] addressed the issue of thermal comfort real-time assessment in buildings by developing a PMV-based thermal comfort smart sensor. Four physical parameters (humidity, temperature, Carbon Dioxide (CO_2) and Carbon Oxide (CO)) were measured by the system and the sensors were selected based on several criteria (sensitivity, low cost, fast response time, high stability, low dependency on humidity, low power consumption, and compact size). The PMV index was computed in three different ways: taken from occupants' survey, using the ISO 7730 calculation procedure, and through the prototype monitoring system. Results showed that the PMV computed using ISO 7730 and the proposed monitoring system were within 0.5 error on the thermal comfort scale but deviated significantly to that of the survey. Kumar *et al.* explained the large deviation as being due to the adaptive nature of occupants, which is very difficult to define and derive mathematically. They recommended carrying out a large number of experiments and applying the data to train a neural network.

Lee [92] combined optical design, Micro-Electro-Mechanical Systems (MEMS) technology and wireless communication to build a sensor network that performs environmental thermal comfort calculation. Thirty eight subjects participated in experiments within a classroom, recording their thermal comfort index on the PMV scale. The thermal comfort index estimated by the designed system had a correlation of 0.95 with the subjective readings.

Figure 2.2: The Flatman support manikin, with the associated eight dry heat loss transducers and logger.

An example of a commercial comfort meter is the one developed by LumaSense Technologies[1]. The comfort sensors are placed on a support manikin called “Flatman”, used in the experimental trials performed in this thesis. Flatman holds up to eight INNOVA MM0057 dry heat loss transducers (shown in Figure 2.2) and outputs the PMV thermal comfort level as well as the equivalent temperature at eight locations.

Comfort sensors that can directly measure dry heat loss and calculate equivalent temperature are therefore available on the market, but they are large and the use of several (6–8) is required in order to accurately predict thermal comfort. On the other hand, developing a bespoke sensor system that measures four different parameters for computing the PMV index introduces a cost and measurement error associated with each instrument individually. The method in this thesis accurately estimates body part equivalent temperature using only two basic, inexpensive sensors.

2.2.3 Thermal manikins

Manikins are a widely used tool within the automotive field due to the following advantages:

1. They are suitable for investigations under harsh conditions that simulate extreme environments.

[1]LumaSense Technologies The INNOVA ”Flatman” Manikin: `http://www.lumasenseinc.com/EN/products/thermal-comfort/flatman/the-manikin-innova-flatman.html`

Table 2.5: Existing thermal manikins.

Author	Year	Number of sections
Wyon *et al.* [164]	1985	17
Madsen *et al.* [100]	1986	16
Tanabe *et al.* [146]	1994	20
Rugh *et al.* [130, 131]	2004	120
Nilsson *et al.* [116]	2007	18

2. They avoid biased subjective estimates of thermal comfort as reported by humans.

3. They rely on the physics and biophysics of heat exchange to evaluate human thermal comfort.

4. They can provide a reproducible, rapid and accurate simulation of the physical processes of heat loss to the environment.

5. The values obtained can serve directly as input for existing thermal comfort models.

Thermal manikins were first manufactured in the 1960's and have developed significantly since. Manikins use a heating system based on electrical resistances coiled around different sections, under their "skin" layer. The number of manikin sections varies, reaching up to 120 for the one described by Rugh *et al.*. The manikins relevant to the work here are listed in Table 2.5.

Wyon *et al.* [164] described a new method of measuring heat loss within car cabins via a full-size, clothed thermal manikin, Voltman. The manikin consists of 17 sections and it ensures even heat distribution and rapid response to environmental changes.

Madsen *et al.* [100] developed a thermal manikin at the Technical University of Denmark that measures clothing index values and also evaluates the indoor thermal climate. Fitted with pliable joints, the manikin consists of 16 sections with individual heating systems. The equivalent temperature of each section, together with the PMV index, can be computed based on the measured heat loss.

Tanabe *et al.* [146] described a method for measuring thermal comfort in non-uniform environments using a thermal manikin with controlled skin surface temperature. An equivalent temperature model was proposed and discussed, together with a method to calculate the PMV index. The manikin, seated at a desk in a larger workstation, was tested in an office with a floor-supply air distribution system. Cool air was delivered through a floor module, while heat sources were used to simulate typical office load distributions and densities. Equivalent temperature was shown to be a useful tool in detecting the effects of asymmetries in heat sources and airflow.

Rugh *et al.* [130, 131] presented the "ADAM" thermal manikin, developed by the National Renewable Energy Laboratory (NREL). A series of tools were developed: a thermal comfort manikin (consisting

of 120 separate controlled zones and capable of simulating human heating, sweating and breathing), a physiological model and a psychological model, together assessing thermal comfort in transient non-homogeneous environments. Skin temperatures were estimated within 1 ℃ Root Mean Square Error (RMSE), except the foot and hand, which reached errors up to 4 ℃. The predicted thermal sensation for most body parts matched the subjective data within 1 unit on the sensation scale (-4 to 4), reaching up to 3 units for hands and feet, while the overall sensation matched the subjective readings within 0.5 units RMSE.

Nilsson *et al.* [116] developed a virtual thermal manikin, MANIKIN3, for use in Computational Fluid Dynamics (CFD) simulations. In order to have a full understanding of thermal comfort estimation, they looked at human subjective reports such as PMV and PPD and at manikin measurements. A computer model was developed based on CFD with 18 zones, with the surface temperature regulated continuously through an iterative process. Results illustrated that the set of equations used in the simulations agreed with real life measurements in different environments. The use of input data from CFD calculations produced reasonable results, especially in relatively homogeneous climates, such as offices, but have to be further tuned in order to be reliable in environments such as car cabins.

Martinho *et al.* [102] evaluated equivalent temperature-based thermal comfort in a variety of conditions: different air inlet settings, different air velocities and temperatures and with or without a thermal manikin within the car cabin model. One goal was to compare the body part equivalent temperature measured by the thermal manikin with the body part equivalent temperature computed from measuring the basic climatic parameters (air temperature, mean radiant temperature and air velocity) using equation (2.24) on page 29. When the overall equivalent temperature measurements were compared, the difference was less than 1 ℃ on average. However, when the individual body part equivalent temperatures were compared, significant differences were found (higher than 2 ℃).

Many thermal manikins have been developed for research purposes, but there are also commercial thermal manikins available, such as the one developed by PT Teknik[2]. An optional feature of this manikin is the comfort meter which measures equivalent temperature, operative temperature and the PMV comfort level. Thermal manikins are the preferred tool for assessing thermal comfort in vehicular environments. However, although they are a good research tool, thermal manikins are not appropriate for production vehicles because of the large amount of power they require, their size and their positioning requirements. Therefore, suitable tools must be developed as an alternative and the work in this thesis fulfils this need.

[2]PT Teknik Comfort: `http://pt-teknik.dk/driver.html`

2.2.4 Infrared thermal imaging

For the purpose of temperature measurement, particularly in locations where sensors cannot easily be affixed, Infrared (IR) measurements are a common choice. Even though IR cameras are a promising tool for evaluating the conditions of transient environments such as car cabins, few research projects have made use of it.

Genno *et al.* [61] presented a method of measuring skin temperature using IR cameras. Their previous research suggested that facial skin temperature (for example, the cheeks, nose and ears) can be used to estimate human thermal sensation. The proposed method aimed to identify the desired body parts within the image using image recognition techniques so that the temperature measurement is performed only at the requested positions. However, no results are provided regarding the accuracy of the measurement. Other drawbacks include the large size of the image databases and poor reliability resulting from working with the image processing equipment.

Korukcu and Cilic [88] used an IR thermal camera for estimating the facial skin temperature of a driver during warm-up and cool-down trials. Facial skin temperature was also measured with thermocouples in order to evaluate the accuracy of the IR camera approach. The two results matched within a 2 ℃ RMSE.

Oliveira and Moreau [121] demonstrated the impact of local air flow on thermal comfort. An IR camera was used to obtain subjects' facial skin temperature distributions when different air temperatures and air flows were applied. Their results showed that local air flow temperature had a high impact on thermal comfort, whereas air flow had no significant impact.

Sabbatini [133] developed an IR-based measurement system for real-time estimation of thermal comfort in buildings. The system outputs mean surface temperatures, the number of occupants (using an IR camera combined with image processing techniques), as well as the PMV index based on the measured air temperature. Experimental results in an office showed average absolute errors of around 0.4 ℃ for the air temperature estimation, with a standard deviation of 0.8 ℃ for sensor measurement uncertainties. The estimated PMV index is not compared to subjective reports from the office occupants. Also, the system was deployed in a stable environment, with air temperature values close to each other (within a 1–2 ℃ range).

The method developed as part of this thesis has several advantages over the IR-based methods: i) lower cost, ii) less space occupied within the car cabin and iii) a small number of sensors can be used to predict the equivalent temperature at multiple locations, whereas more cameras would be needed to cover the whole human body for a more accurate prediction.

In summary, there are a number of tools for measuring thermal comfort in vehicular environments.

However, they all have disadvantages when considered for real-time comfort estimation. The disadvantages of measuring the basic climatic parameters individually, such as air flow, mean radiant temperature or humidity, for example, include the limited space available within the car cabin and the large amount of instrumentation needed. Moreover, it is impossible to place all the desired sensors at the exact measuring point required (particularly for production vehicles). The measurement accuracy decreases if sensors are placed at slightly different locations due to the car cabin inhomogeneity [32]. Also, Mayer and Schwab [105] observed a significant difference between computing equivalent temperature from the integrating parameters (air temperature, mean radiant temperature and air velocity) and measuring equivalent temperature using comfort meters or thermal manikins. This thesis solves these issues by presenting a method that estimates body equivalent temperature from a few sensors placed in convenient locations within the cabin.

2.3 Equivalent temperature

Cisternino [29] highlighted the need to develop new methods and instruments in order to estimate cabin thermal comfort for efficient automotive HVAC systems. The difficulty in achieving this goal lies in the non-uniform, transient nature of the automotive environment. Most journeys last between 15 and 30 minutes and passengers expect well balanced air flows at a low velocity, but also short heating and cooling times. The issue with thermal comfort models, such as PMV, is that even when overall thermal sensation is neutral, passengers can still feel uncomfortable because of local cooling or heating of individual body parts, a situation often encountered in car cabins. New standard measuring methods have to be developed for this specific type of environment and one of them is the equivalent temperature. The literature shows that equivalent temperature correlates well with the subjective responses of passengers [105, 110, 117]. Equivalent temperature also encapsulates PMV's advantage of being estimated from the basic climatic parameters (air temperature, mean radiant temperature and air velocity) using equation (2.24) on page 29.

2.3.1 Definition

Equivalent temperature is formally defined as the uniform temperature of an imaginary enclosure with air velocity equal to zero in which a person will exchange the same dry heat by radiation and convection as in the actual non-uniform environment [134]. Nilsson *et al.* [114] identified a series of expressions for the computation of equivalent temperature, as well as several measurement methods and calibration

procedures for the instruments used. Equivalent temperature can be referred to as whole body equivalent temperature (equivalent temperature for the whole body of a person), segmental equivalent temperature (equivalent temperature for one single body part), directional equivalent temperature (defined as a normal vector to every point of the measuring plane), or omni-directional equivalent temperature (equivalent temperature measured all around the whole body or one body part).

2.3.2 Calculation

Nilsson and Homer [113] offer an overview of ways to compute equivalent temperature. Firstly, equivalent temperature can be determined from the equations for radiative and convective heat transfer:

$$R = F_{cl} \times f_{cl} \times h_r \times (t_s - t_r) \tag{2.21}$$

$$C = F_{cl} \times f_{cl} \times h_c \times (t_s - t_a) \tag{2.22}$$

where R is the radiation heat exchange, C is the convective heat exchange, F_{cl} is the reduction factor for sensible heat exchange, f_{cl} is the clothing surface area factor, h_r is the radiation heat transfer coefficient, h_c is the convective heat transfer coefficient, t_s is the local surface temperature, t_r is the mean radiant temperature and t_a is the air temperature.

In this case, the equivalent temperature t_{eq} can be calculated as $R + C$ with no humidity influence. A different method for computing equivalent temperature is through the Resultant Surface Temperature (RST), as defined by Mayer [104]:

$$Q = h_c \times (\mathrm{RST} - t_a) + \varepsilon_s \times \varepsilon_a \times \sigma \times \left[(\mathrm{RST} + 273.2)^4 - (t_r + 273.2)^4\right] \tag{2.23}$$

where Q is the body heat gain or loss, ε_s is the sensor emissivity, ε_a is the emissivity of ambient air and σ is the Stefan-Boltzmann constant.

In homogeneous conditions ($Q = 85\,\mathrm{Wm^{-2}}$, $h_c = 1.6\,\mathrm{Wm^{-2}K^{-1}}$, $\varepsilon_s = 0.96$, $\varepsilon_a = 0.9$, $\sigma = 5.67 \times 10^{-8}\,\mathrm{Wm^{-2}K^{-4}}$) equivalent temperature can be calculated as:

$$t_{eq} = 1.1 \times \mathrm{RST} - 15.6 \tag{2.24}$$

An empirical equation for computing equivalent temperature (referring to sedentary conditions only, that is energy metabolism $< 70\,\mathrm{Wm^{-2}}$) is introduced by Madsen [98, 99], taking into consideration

the main elements that affect equivalent temperature (air temperature, mean radiant temperature, air velocity, and the clothing index):

$$t_{eq} = \begin{cases} 0.5 \times (t_a + t_r), & \text{for } v_a \leq 0.1\,\text{ms}^{-1} \\ 0.55 \times t_a + 0.45 \times t_r + \frac{0.24 - 0.75 \times \sqrt{v_a}}{1 + I_{cl}} \times (36.5 - t_a)\,, & \text{for } v_a > 0.1\,\text{ms}^{-1} \end{cases} \tag{2.25}$$

where v_a is the air velocity, t_a is the air temperature, t_r is the mean radiant temperature and I_{cl} is the clothing index factor.

2.3.3 Measurement

In addition to measuring the basic climatic parameters (air velocity, air temperature and mean radiant temperature), together with the clothing index and then applying the above formulas, equivalent temperature can be measured as follows:

- Using *ellipsoid sensors (*also called *comfort meters)*—the sensor's heat exchange corresponds to the total radiative and convective heat exchange.
- Using *heated, flat sensors*—give estimates of dry heat losses. Several flat sensors are needed in order to simulate the 3-dimensional human heat transfer.
- Using *local discomfort meters*—double-sided heated elements. The thermal asymmetry is the difference in mean heat flux between the two opposite element sides.
- Using *thermal manikins*—a thermal manikin is the most appropriate heat flux measurement tool (more details are provided in Section 2.2.3).

Holmer *et al.* [74] give recommendations for the equivalent temperature standard:

1. A heated sensor measuring heat flux is required for determining equivalent temperature. Equivalent temperature cannot be as accurately determined from individual measurements of air temperature, radiant temperature and air velocity as with thermal manikins, as shown through empirical evaluation.
2. Equivalent temperature can be calculated from the heat-loss (Q), surface temperature (t_s) of the real climate and the heat transfer coefficient (hcal) as:

$$\text{ET} = t_s - \frac{Q}{\text{hcal}} \tag{2.26}$$

3. Significant differences are introduced when measuring equivalent temperature with various instruments. In realistic vehicle cabins the differences can reach up to several degrees Celsius.

4. The most accurate equivalent temperature, according to its definition, will be obtained from measurements with a thermal manikin (same shape and size as a human being, with realistic clothing and surface temperatures).

5. Smaller, individual sensors can be more useful than thermal manikins in certain situations, for example in field testing, however, the measurement would not be as accurate.

2.3.4 Measured equivalent temperature in comparison to subjective responses

Several research case studies [105, 110, 117] have analysed how good the agreement between the measured equivalent temperature and the passengers' subjective responses is. To summarise, Nilsson *et al.* [117] found a high correlation between equivalent temperature and thermal sensation, with correlation indexes between 0.86 and 0.99, based on empirical data. Also, they developed a thermal comfort model mapping equivalent temperatures to thermal sensation that will be further evaluated in this thesis. Also, Mayer and Schwab [105] concluded that equivalent temperature was highly correlated with subjective thermal sensation responses, with a correlation index higher than 0.82. Mola *et al.* [110] found a correlation index between the combination of equivalent temperature and head air temperature and the subjective reports of 0.78. Finally, Curran *et al.* [31] concluded that an equivalent temperature set-point of 25.5 ℃ provides higher thermal comfort levels than an air temperature set-point of 25.5 ℃. In what follows, their works are presented in more detail.

Madsen *et al.* [100] used three different measurement methods for evaluating the thermal climate inside a car cabin, both at the driver and passenger locations: i) air temperature thermocouples at the foot and head level, ii) thermal comfort sensor measuring equivalent temperature and iii) a thermal manikin (as described in Section 2.2.3). The methods were evaluated within both steady-state and non-steady-state conditions (such as warm-ups and cool-downs) in a wind tunnel with temperatures between -18 ℃ and 40 ℃ and with simulated solar load. Madsen's investigation showed that it is insufficient to solely measure air temperature for an accurate representation of thermal comfort (that is, significant errors occur when the thermal sensation estimates are compared to the subjective reported sensation). Such errors are justified by not taking into account the solar radiation or the distribution of air coming from the vent. Comfort meters do not manifest this issue. Their main limitation is the measurement

at one point only, therefore several comfort meters would be needed for a good representation of the thermal environment. Madsen *et al.* concluded that thermal manikins are the best measuring instrument for equivalent temperatures.

Nilsson *et al.* [117] conducted two series of experiments, involving 20 subjects and 30 different climatic conditions. The measurements, performed in a vehicle cabin, were taken during winter conditions at −20 ℃ (corresponding to a passenger clothing index of 1.5) and during summer conditions at 30–35 ℃ (corresponding to a passenger clothing index of 1.2). The subjects sat in the cabin for 60 minutes, while their subjective responses were recorded every 30 minutes for 16 different body parts, together with the overall thermal sensation. The subjects' individual votes were averaged for each of the conditions and transformed into a Mean Thermal Vote (MTV) index. The scale used for MTV is the ASHRAE scale[3]. The overall and local heat fluxes from two manikins were also continuously measured. A regression analysis was used to compute the matching score. The correlation coefficients for individual segments ranged between 0.86 to 0.99, suggesting a strong dependence between the two. Nilsson *et al.* also provided, based on the experimental trials performed, ranges of body part equivalent temperature that correspond to the *too cold, cold, neutral, hot* and *too hot* thermal comfort indexes for both summer and winter conditions, as illustrated in Figure 2.1.

Mayer and Schwab [105] studied the correlation between subjective thermal response and measured equivalent temperature. A total of 50 subjects were used within the trials that consisted of 30 different thermal conditions. An additional goal of the trials was to observe the difference in measured equivalent temperature between different instruments. Seven instruments were used for measuring equivalent temperature: four manikins (Nille [107], Heatman [45], Aiman [107] and Eva [113]), a local discomfort meter, comfort meters (placed on the Flatman support manikin) and an artificial skin device. The Flatman, with the six comfort meters and the local discomfort meter attached, was positioned in the right front seat, as were each of the other four manikins in turn. The conditions were varied with regard to parameters such as radiation at the head level, ventilation rate, HVAC vent inlet and outlet temperature. Mayer and Schwab concluded that there is a significant difference in the measured equivalent temperature with different instruments (up to 7 ℃). Individually, the equivalent temperature measured by each instrument was highly correlated with the subjective responses (correlation index > 0.82 for any given combination of body part and instrument).

Mola *et al.* [110] performed road tests with over 100 people and 30 cars in order to find the parameters measured within the car that correlate best with people's judgement of thermal comfort. Performed both

[3]ASHRAE 2004 Standard—Thermal Environmental Conditions for Human Occupancy: `https://www.ashrae.org/resources--publications/bookstore/standard-55.html`

during winter and summer, the trials used the following instrumentation: an EVA3 thermal manikin [124] continuously measuring equivalent temperature at 18 different body parts; thermocouples at each of the air conditioning outlets, a thermocouple on the dashboard, a thermocouple on the windshield, and a thermocouple at the head level; an internal and an external humidity sensor; a thermocouple measuring ambient temperature, and a solar meter. Within the trials, two ways of using the air conditioning unit were defined: pre-determined settings (only the air flow could be modified by the passengers) and free settings (the passengers were allowed to modify any of the settings, including temperature set-point, compressor status, outlet opening and position). Passengers were provided with a questionnaire, requiring votes in the range of 0–10 for aspects such as overall thermal quality, air distribution homogeneity, perception of local discomfort due to solar radiation and level of noise coming from the air conditioning system. The measured quantities that related best to the subjective responses of the passengers were the equivalent temperature measured by the thermal manikin and the air temperature measured at the head level. Two linear regression formulas were applied (one for the summer and one for the winter) to express the perceived customer index. The correlation index between the combination of equivalent temperature and head air temperature and the subjective reports was 78%, which Mola *et al.* considered reasonable.

Curran *et al.* [31] provided further evidence that thermal comfort can be improved by controlling equivalent temperature rather than air temperature. In order to find the temperature set-point corresponding to maximum thermal comfort, Curran *et al.* placed a thermal manikin in a homogeneous environment varied over a range of temperatures. Curran *et al.* established that a value of 25.5 ℃ maximises comfort, therefore this set-point was used by the authors to control both the air temperature and the equivalent temperature. The experimental conditions consisted of a baseline condition (no solar load, while the floor and wall temperatures were equal to the air temperature), along with conditions consisting of added solar load, cold floor, cold floor with solar load and hot floor with cold walls. Curran *et al.* found that an equivalent temperature of 25.5 ℃ increased thermal comfort levels in all conditions, by an average of 0.38 on a -4 to 4 scale, when compared to an air temperature set-point of 25.5 ℃.

Based on the above, the author concludes that the existing literature does not provide a sufficiently detailed evaluation of the equivalent temperature-based thermal comfort estimation. Mayer and Schwab [105] and Nilsson *et al.* [117] provided a summarised evaluation of how equivalent temperature matched subjective sensation. Although the conditions were representative of the vehicular environment, the thermal sensation responses were reported only twice in the one hour interval, which may be misleading in terms of overall matching accuracy. Also, Mola *et al.* [110] did not specify the rate at which the responses were reported, however the questionnaire seemed to be given one per journey. Again, this

is not sufficient to understand in what conditions equivalent temperature may or may not be an accurate predictor for thermal comfort.

This thesis offers a more detailed evaluation of Nilsson's equivalent temperature-based thermal comfort model within various environmental conditions, as presented in Section 3.3.

2.4 Estimation methods for cabin parameters and thermal comfort

Measuring all parameters required as input for thermal comfort models is difficult, either due to impracticality or due to the complexity of the models themselves. This thesis, therefore, presents a method of estimating equivalent temperature based on fewer measurements. Other researchers [22, 87, 95, 151] have previously used learning techniques in order to estimate various parameters, ranging from cabin air temperature to passenger thermal sensation, as discussed in this section.

Similar to the work presented in this thesis, Mola *et al.* [109] developed an equivalent temperature estimation model for vehicular comfort-oriented HVAC control. They performed a series of trials in a controlled environment for developing the estimator, with a thermal manikin occupying the driver seat and measuring overall equivalent temperature. The cabin air temperature, HVAC outlet air temperature, external air temperature and mean radiant temperature were also recorded. Out of these measured parameters, mean radiant temperature, HVAC outlet air temperature and air velocity correlated best with the equivalent temperature. Based on their results, Mola *et al.* inferred a linear mathematical expression for estimating equivalent temperature. The method was only assessed qualitatively and it was concluded to provide successful HVAC control. A downside of this method is the fact that only one sensor was used to measure the cabin temperature, though different air temperature sensor locations within the cabin can increase the estimator's accuracy [73]. Moreover, the data used for training and testing the system was gathered within trials in stable conditions, leaving open the question of how well the system would perform in realistic driving scenarios.

MLRs were also used by Ibrahim *et al.* [78] for solar radiation estimation and by Shengxian *et al.* [138] and Wu *et al.* [163] for predicting indoor thermal sensation. Mehnert *et al.* [106], for example, estimated average skin temperatures from parameters such as air temperatures, mean radiant temperatures, air velocities, metabolic rates, rectal temperatures and partial vapour pressures. They developed linear relationships between these parameters and skin temperature for nude and clothed subjects and concluded that the models are valid for a wide range of hot and warm ambient steady-state conditions.

Freire *et al.* [55] also used a linear regression method for predicting indoor air temperature and relative humidity. The data used for training and validating the model was simulation-based and the RMSEs obtained were of 2.44×10^{-2} ℃ and 1.05×10^{-6} for temperature and humidity, respectively.

Adopting a different learning technique, Bin and Ke [14] presented a model to estimate the indoor PMV index using Least Squares Support Vector Machine (LS-SVM). The model consisted of a non-linear relationship between thermal comfort and its influencing factors. The parameters of the model were tuned using the Particle Swarm [85] algorithm, and then the relations between the six parameters (air temperature, air velocity, mean radiant temperature, relative humidity, metabolic rate and clothing index) and the PMV index were learnt through training. The experimental results showed that the PMV index was estimated with an average absolute error of 0.028 on a -3 to $+3$ scale, for 200 test samples.

Artificial Neural Network (ANN)s are also one of the most widely used machine learning techniques for estimation and prediction tasks. They are used in a variety of applications such as weather forecasting [10, 70, 101], frost prediction [129] and air temperature prediction [70, 141]. ANNs were also used to estimate thermal sensation from cabin environmental parameters and the details of these works are presented in what follows.

Kojima [87] described an ANN-based method for estimating human thermal sensation from several air temperature sensors, placed at the outlets of two Air Conditioning (AC) units and on the desks of room occupants. Thermal sensation was reported by the subjects on the ASHRAE scale, described in Section 2.1, Table 2.2. The ANN works on the basis of the correlations between the thermal sensation and the measured air temperature values and this method is capable of using the information acquired in order to update the network. The method was only qualitatively validated and Kojima concluded that the estimated thermal sensation is in good agreement with the thermal sensation reported by subjects. However, the conditions were stable throughout the experimentation, causing sensations only within the -1.5 to $+1$ interval.

Luo *et al.* [95] presented a fuzzy logic-based ANN for estimating thermal sensation. The model takes as input body part skin temperature, body core temperature and the rates of change of each and estimates local and overall thermal sensation. Evaluated on a range of warm and cold steady-state conditions, the model provided an RMSE of around 0.2 on the -4 to $+4$ scale.

Castilla *et al.* [22] developed an ANN-based model for estimating thermal sensation from air temperature, mean radiant temperature, indoor air velocity and relative humidity. The model obtained an RMSE of 0.0117 and 0.0079 on the -3 to $+3$ scale on two summer test data sets and 0.0145 and 0.0123 on two winter test data sets.

Within the car cabin environment, Ueda and Taniguchi [151] developed a method for estimating passengers' thermal sensation using an ANN. Thermal sensation was estimated from the cabin air temperature and facial skin temperature at 7 locations. A direct relationship was established between these parameters, instead of applying an existing thermal comfort model. Errors were within 0.5 of the comfort scale (−4=cold, −2=cool, 0=neutral, 2=warm, 4=hot) when compared to the passenger's reported sensations. However, the experimental trials were not conclusive, with data both for training and testing being collected in stable conditions (cabin set-point of 25 ℃), rather than conditions usually encountered in vehicles.

Although ANNs are a good approach for estimating thermal comfort, they have a number of disadvantages. For example, they are dependent on the training process, they require a high number of computations and they produce poor results if the network is not trained sufficiently.

Most estimation methods for environmental parameters or thermal sensation are designed for steady-state conditions. The methods are expected to produce higher estimation errors when applied to a car cabin's transient and non-uniform environment. As a solution, the method developed in this thesis estimates equivalent temperature from cheap air temperature sensors and can be used to infer passengers' thermal comfort or directly as the basis for HVAC control. This type of research is mostly performed through simulation in the literature. When research is based on experimental data the environment is usually stable, with controlled cool-downs and warm-ups and no driving involved. The experimental data sets gathered within this thesis include a wider range of conditions and thus the evaluation of the method is more thorough.

2.5 HVAC control methods

The development of comfort-based HVAC control algorithms represents a complex issue both in the automotive and buildings areas. A selection of the literature related to this topic is discussed in this section.

2.5.1 HVAC control in buildings

Buildings have benefited from 40 years of extensive thermal comfort research and therefore the state-of-the-art related to HVAC control in buildings has progressed significantly. There are fundamental differences between the building and vehicle environments, the latter consisting of more transient and inhomogeneous conditions. Despite these differences, some of the lessons learnt are transferable between

the HVAC control methods within these environments. The majority of controllers aim to maintain the PMV index within the comfortable range of ±0.5 using learning-based approaches. Hamdi *et al.* [66] and Nowak and Urbaniak [118] used fuzzy logic techniques in order to maintain the PMV level close to 0, while Egilegor *et al.* [44] and Torres and Martin [149] used ANNs to achieve the same goal. More details on these works are provided in the following.

Yang and Su [167] developed an intelligent HVAC controller for buildings that maintains the PMV index within the ±0.5 interval. A comparison between two identical rooms was performed: one equipped with a conventional AC system and the second equipped with the new controller, both aiming to maintain an average air temperature of 26 ℃ and humidity of 55%. By maintaining thermally comfortable PMV levels a total of 9.1 kWh (34.4%) energy was saved in the room equipped with the new controller.

Egilegor *et al.* [44] proposed a neuro-fuzzy method that controls fan air flow rate in a house to improve thermal comfort. The comfort variable used was PMV and the inputs were three zone temperatures and humidities. The building simulation was performed using the TRNSYS simulation program. Two computers were running the simulation and the control program, while a data acquisition card achieved the exchange of information between the building and control. The control program read the temperature and humidity inputs provided by the simulation program and calculated the PMV index. The air flow rate of the fan was then set by the fuzzy module as a function of the PMV value and the mean PMV rate of change. The simulation results were used to train an ANN to choose the optimum offset in each situation for improving the performance. Egilegor *et al.* validated the method in three winter and three summer climates and the results were compared to a traditional thermostatic control. The mean PMV values were improved between 50% and 90% for the winter climate. On the other hand, for one of summer climate test, the results obtained with thermostatic control were sufficiently good and the presented method does not improve them. In the other two summer tests the PMV values were improved between 50% and 90%.

Hamdi *et al.* [66] suggested the use of fuzzy modelling for minimising energy consumption while delivering occupant thermal comfort, with the advantage that no mathematical modelling is required for designing the controller. The fuzzy system evaluated the indoor thermal comfort level based on the six PMV inputs. If the estimated thermal comfort level was not achieved, the control algorithm would adjust the air temperature/velocity supplied by the HVAC system. In order to improve the occupant thermal comfort approximation on-line, the thermal comfort level computed was compared to the user's actual thermal sensation. An advantage is that each occupant's attributes were considered (metabolic rate and clothing insulation). Simulations of the environment (in TRNSYS and MATLAB) were used to verify the

effectiveness of the proposed system. Two conventional techniques were simulated for the same indoor and outdoor conditions: night setback (21.1 ℃ between 6 am and 10 pm and 15.6 ℃ between 10 pm and 6 am) and constant set-point (21.1 ℃) thermostat systems. The number of comfort hours were 5 for the conventional controller and 10 for the second, while the proposed controller offered 24 hours of thermal comfort. The night setback provided 14% energy saving, while the presented method saved 20% of the energy.

Freire *et al.* [54] developed an HVAC comfort control system for buildings. PMV was used as a comfort index and two strategies were presented: one consisting of thermal comfort optimisation and the second one consisting of energy consumption minimisation while thermal comfort is maintained (PMV maintained within the -0.5 to $+0.5$ range, rather than as close to 0 as possible). The methods were validated through simulation, along with additional studies of how different clothing insulations and metabolic rates impact on the results. Two occupants were considered inside the building environment within the simulation, with constant clothing index and metabolic rate (0.66 and 1.20, respectively). The energy usage of the HVAC system was reduced from 174.7 kWh to 98.6 kWh when the energy minimisation control strategy was applied.

Torres and Martin [149] presented an HVAC control technique based on modifying the set-point temperature of a Proportional Integral (PI) through an ANN. The objective was to keep the comfort level for the occupants within a predefined range (-0.5 to $+0.5$ on the PMV comfort scale) by only controlling the indoor temperature of an office space. The data set used for validation comprised the date and time, the geographical location (latitude, longitude and orientation) and the external weather variables (solar radiation, external temperature, relative humidity, wind speed and atmospheric pressure), obtained from a weather metering station installed in a room. The ANN was designed with one input layer consisting of the six parameters used for the PMV computation, and one output layer providing the desired temperature. Simulations were developed for validation, based on various conditions encountered over two consecutive days in April 2008. The described controller was compared to a conventional temperature controller (set-point fixed at 23 ℃). The temperature controller did not maintain the PMV index in the acceptable range, whereas the proposed controller maintained a PMV index very close to zero.

Feldmeier and Paradiso [50] developed an occupant focused thermal comfort control system. The system used wearable sensors to locate users within a building and to measure on-body temperature and humidity. Thermal comfort levels were thus inferred and used to control the AC system according to the needs of the occupants by using an ultra-low-power, wrist worn sensor node that allowed the

building occupants to express their thermal needs ('hot' and 'cold' buttons). A period of four weeks of the presented control strategy was compared in terms of energy and thermal comfort to the previous four weeks of standard control. Energy savings of up to 24% were achieved due to not cooling down areas when occupants are not present. Moreover, thermal comfort was maintained for more than of 80% of the time.

Nowak and Urbaniak [118] presented fuzzy and model predictive control algorithms that minimise the HVAC energy consumption while keeping occupants comfortable. A simulation model of a room was described, including physical parameters and construction parameters. The thermal comfort assessment is based on PMV and PPD. Fuzzy logic-based algorithms were used in the direct control layer, while predictive algorithms were used in the supervisory control layer. Optimising the PMV indexes was achieved by minimising an objective function and maintaining the PMV index between -0.5 and $+0.5$. Results showed that the controller maintained the PMV index within the desired limit, dropping around 0.2 on the thermal comfort scale when the energy consumption was further reduced.

Most comfort-oriented HVAC controllers within the state-of-the-art are intended for building environments. Although they are effective, the environment is milder and more stable than the car cabin environment. Thus, the suitability of such algorithms within vehicles is low. The next section describes methods of HVAC control in vehicles.

2.5.2 HVAC control in vehicles

Despite the large body of literature related to comfort-based HVAC control in buildings there is limited literature referring to comfort-oriented HVAC systems for vehicles.

The closest work in the state-of-the-art to this thesis belongs to Kranz [89] and his work will be, therefore, described in more detail. Kranz developed a thermal comfort-based control method for vehicles. He acknowledges the subjectivity of thermal comfort and the fact that thermal comfort models for transient environments have not yet been fully established. Kranz's work aims to apply artificial intelligence methods in order to extract thermal comfort knowledge from the interaction between the passengers and the HVAC controls. The method has the advantages of not requiring any prior knowledge and of adapting to each user. The measured parameters in the car were: sun azimuth angle, ambient temperature, standard deviation of the azimuth angle, sun elevation angle, standard deviation of the elevation, filtered ambient temperature, humidity, sun intensity, standard deviation of the sun intensity, air outlet temperature, cabin air temperature, driver foot and head temperature, passenger head and foot temperature, dashboard temperature, vehicle speed, cabin roof temperature and standard deviation of the

vehicle speed.

Kranz applied Principal Component Analysis (PCA) in combination with correlation analysis in order to reduce the dimensionality of the parameter space. Out of the above mentioned measured parameters, the ambient temperature, relative humidity, vehicle speed, in-cabin air temperature, dashboard temperature, sun intensity, sun azimuth angle and sun elevation angle were found to be the most relevant thermal comfort variables for the application. ANNs are used for predicting the blower level and flap position, respectively, with eight inputs each. Data was collected during spring, autumn and summer conditions in Southern Africa. The data set was split as 65% training data, 15% validation data and 20% test data. The results showed that the four different blower levels were estimated with 88.6%, 82.7%, 81.7% and 97.8% accuracy, respectively. The three different flap positions (corresponding to chest, head-chest and head) are predicted with 92.4%, 82.7% and 86.5% accuracy, respectively. Kranz concluded that the developed approach is a better substitute for psychological and physiological-based comfort models and aims to adapt to individual occupant thermal comfort preferences.

The work in this thesis uses, similarly to Kranz's, feature selection techniques in order to select the most suitable sensors for thermal comfort estimation, a mutual information-based method for the work here. Rather than collecting data from a variety of sensor types and selecting the most useful ones, as in Kranz's case, this thesis first establishes which thermal comfort model is the most suitable from the state-of-the-art and then finds the best sensors and corresponding best locations in order to accurately estimate the model's input parameters. Also, this thesis takes the learning-based approach adopted by Kranz to another level, by using a reinforcement learning method that gradually learns from interacting with the environment an optimum control policy that maximises occupant thermal comfort while minimising the energy consumption.

Different learning techniques have been adopted for thermal comfort user personalization in HVAC systems and, for the interested reader, the following works describe the works in more detail.

Ichishi *et al.* [79, 80] proposed an HVAC system consisting in a sensor-based unit (detecting values relevant to environmental conditions), an operating unit controlled by the passenger in order to set the air conditioning state, and a control unit that learns to correct the automatic control based on user manual changes. A stand-by Random Access Memory (RAM) was used to store the user preference related data learned. The environmental conditions, such as car cabin temperature, ambient temperature and solar load, were measured by sensors. A target blowing temperature (TAO) at the vent was computed using

the following formula:

$$\text{TAO} = \text{KSET} \times \text{TSET} + \text{KR} \times \text{TR} - \text{KAM} \times \text{TAM} - \text{KS} \times \text{TS} + \text{C} \tag{2.27}$$

where TSET (℃) is the car cabin set temperature, TR (℃) is the car cabin air temperature, TAM (℃) is the ambient air temperature, TS is the solar load in the cabin, KS, KAM, KR and KS are coefficients and C is a constant.

Goenka *et al.* [63] proposed a zonal HVAC system in which the pre-determined vehicle parameters are measured and sent to the controller. An occupant thermal comfort level was determined based on the sensor measurements (using thermal comfort charts, ASHRAE thermal scale, ISO 7730, the PMV index, the PPD index or any combination thereof). A desired level of the occupant comfort was established and the amount of HVAC work required to reach this level was computed. As a result, the flow rate and the fluid discharge temperature required were calculated.

Pham *et al.* [126] stated that current adaptive controllers can generate inaccurate control because of atypical, too frequent or over-exaggerated occupant manual adjustments. Also, some systems are too slow in creating a control characteristic because of infrequent occupant manual adjustments. There is a need to improve the response time and accuracy of such systems. Pham *et al.* proposed a control mechanism that allows the car cabin occupant to adjust either the manual temperature or the manual blower knob according to their preferences. When such a manual adjustment occurred, a signal was sent to the heater or cooler containing information regarding the time that the adjustment occurred at and the magnitude of the adjustment. An environmental sensor, measuring cabin air temperature, humidity, solar load and/or ambient air temperature, sent a signal to the controller at the time of the manual adjustment. Therefore, the controller would determine the occupant's preferred temperature and blower speed at those particular sensor readings and in the future it would automatically adjust the output based on earlier-determined user preferences. An example of a temperature learning rate used is:

$$\text{VLR} = k_1 \times (T_{\text{elapsed}} \times k_2 + \Delta N \times k_3) \tag{2.28}$$

where VLR is the temperature learning rate, k_1, k_2 and k_3 are constants determined during calibration, T_{elapsed} corresponds to the timing signal of the adjustment and ΔN corresponds to the magnitude signal of the adjustment.

Davis *et al.* [36, 37] suggested that fuzzy logic is a good approach in dealing with the imprecise nature of thermal comfort. The fuzzy logic controller proposed determined the difference between the cabin

temperature and the target temperature. Davis *et al.* defined membership functions and fuzzy rules between the difference signal and the control positions. The fuzzy logic-based control formula proposed in [36, 37] is defined as:

$$\text{FLValue} = \text{Offset} - G_1 \times \text{SUN} + G_2 \times (\text{SetPoint} - 75) + G_3 \times (75 - \text{Ambient}) + G_4 \times (\text{Target} - \text{InCar}) \quad (2.29)$$

where the coefficients G are fuzzy output variables calculated as functions of the sensor inputs. Examples of heuristic rules for the blower speed can be defined as follows:

- If the cabin temperature is close to the cabin set temperature, then the blower tends towards a low speed.
- If the cabin set temperature is high, then the blower tends toward a high speed.
- If the ambient temperature is very hot or very cold and the cabin temperature is close to the cabin set temperature, then the blower tends towards a minimum speed.
- If the ambient temperature is low and the engine coolant temperature is low, then the blower tends towards a low speed.

Kelly *et al.* [84] developed an HVAC system that learns user preferences. The values for the blower set temperature, blower mode and blower speed, manually selected by the driver, were stored in adaptive look-up tables or Cerebellar Model Articulation Controller (CMAC) neural networks [62]. The CMAC had an internal grid structure mapping input vectors into a single output value with stored weighting values deduced from an initial training data set. The table values do not need to be updated each time the driver performs a manual command. Instead, the new training example could be kept in a queue. Then, at an opportune timing, the training examples stored are submitted to the CMAC neural network for training.

Wei and Dage [159] presented an intelligent automotive HVAC control system driven by the passengers' thermal sensation. Previous to their research, air temperature was used as a predictor for subjective thermal sensation. However, newer research indicated that passengers' skin temperatures were a better predictor. Their own experiments consisted of passengers sitting in an idle car during different seasons (winter, spring, summer) with a traditional HVAC system ensuring a comfortable set-point temperature within the cabin. These experiments showed that a strong correlation exists between skin temperature and thermal sensation. Based on this result, Wei and Dage proposed the use of a passive remote IR sensor (placed on the ceiling in front of each passenger) to monitor skin temperature. Seven thermal sensation

labels were used (very hot, hot, warm, comfortable, cool, cold and very cold), with each corresponding to a certain range of skin temperature values. The HVAC control system proposed therefore integrated physiological states into the traditional climate system and used as inputs the outside temperature, the car cabin air temperature and the skin temperatures of the passengers. The control was driven by a linear proportional equation which incorporated these parameters and aimed to maintain skin temperatures within the comfort range by adjusting the blower speed, blend door position, and discharge mode position. The results improved the performance of the traditional controller, maintaining the thermal comfort of the occupants within the "comfortable" to "comfortable cool" range within the summer trials and within the "comfortable" to "comfortable warm" range within the winter trials.

Ueda and Taniguchi [151] previously discovered that facial skin temperature represents a good predictor for passengers' thermal sensation. Therefore they introduced a method based on ANNs to infer thermal sensation from facial skin temperature and car cabin air temperature. The ANN used as input the two parameter measurements during the past 30 seconds and predicted the thermal sensation 30 seconds into the future. The thermal sensation scale used consisted of: cold, cool, neutral, warm and hot. The number of data points used for training was 200, and the learning was performed using Vogl's method [155]. Experimental trials were performed in an environmental chamber with a vehicle controlled to 25 ℃ by a conventional air conditioner. The subjects had seven thermocouples taped to their faces, and the mean value from the seven points was used for the prediction. Another thermocouple was used for measuring the interior air temperature and the subjects were required to note down their subjective sensation readings. The thermal sensation prediction results had a mean error of 0.5 on the sensation scale. The HVAC control method consisted of the following steps: the target thermal sensation level was set based on outside and inside environmental information, then the temperature of the face and compartment were measured and the thermal sensation level was predicted by the ANN. Finally, the air-mixed damper and the air flow strength was determined by the difference between the predicted thermal sensation level and the target thermal sensation level. The controller was able to maintain the desired thermal sensation target for the occupant. The air conditioning level changed based on the subject's perception, treating differently subjects preconditioned at different temperatures—a major change compared to a conventional HVAC system controlled by air temperature alone.

Farzaneh and Tootoonchi [49] started from the premise that a temperature feedback-based controller cannot achieve efficient thermal comfort control due to the complexity of thermal comfort. Farzaneh and Tootoonchi therefore developed a fuzzy controller that used a simplified PMV index as the feedback variable. An evaluation was performed and the results showed that the PMV feedback system better

controlled thermal comfort and energy consumption than the system with temperature feedback. The performance was further improved when the parameters of the fuzzy controller were optimised using a genetic algorithm.

Stephen *et al.* [143] developed a fuzzy logic-based HVAC control mechanism for car cabins that uses PMV as the feedback variable. The controller performance was compared with another controller with solely air temperature as feedback. The results showed that the fuzzy PMV-based feedback controller was able to maintain the PMV level close to the 0 value, whereas the air temperature-based controller was not.

The majority of the HVAC control algorithms targeted at vehicular environments are focused on machine learning techniques that maintain the PMV index within the neutrality interval of ± 0.5 [49, 143, 151]. Recently, through works such as Kranz's [89], it has become clear that the future of HVAC control algorithms lies in personalization. Thermal comfort is a subjective measure and there is no fixed thermal comfort model that can match the personal preferences of individuals. As demonstrated in Chapter 3 of this thesis, none of the existing thermal models perfectly match the subjective responses of passengers in all conditions. Thus, there is a need for control algorithms that can learn user preferences. To fulfil this purpose, reinforcement learning is proposed as a control algorithm within this thesis, representing an innovation in the field of automotive control methods.

2.6 Reinforcement learning theory and applications

Machine learning algorithms can be grouped into three categories depending on the type of feedback the learner has access to. One of the categories is supervised learning, in which case for every input the learner is informed of the target (the correct value of the response). The learner then compares the target to its actual response and adjusts its internal memory so that it is more likely to reproduce the correct target next time it receives the same input. The second type of learning is unsupervised learning, where the learner receives no information about the correct output, but looks at similarities and differences among the input patterns.

Reinforcement learning belongs to a third learning category. It is closer to supervised learning because the learner receives feedback about the appropriateness of its response from the environment. The difference between supervised learning and reinforcement learning is that for the former the learner is told exactly what the outcome should have been, while for the latter the learner is only told whether the behaviour is inappropriate and how inappropriate.

Reinforcement learning is a widely used technique for optimal control [35, 94, 169]. In this thesis, reinforcement learning is considered to be an appropriate mechanism for comfort-oriented HVAC control due to the following factors:

1. Car cabin comfort is a non-linear problem with respect to the state of the cabin environment.

   The reason why designing comfort-oriented HVAC controllers is a challenging task is because cabin thermal comfort is non-linear with respect to the observable state. There is no linear formula that can relate occupant comfort to the measurements of various parameters within the cabin. Therefore, rather than using traditional linear controllers, more complex control strategies are required. Davis *et al.* [36, 37] argued the disadvantages of traditional controllers. For example, when the threshold engine coolant temperature is passed (on/off switch based controller) and the car is cold, the blower goes to its highest setting, therefore the noise level produced by the blower is very high and the residual cold air is blown directly to occupants' feet. Also, crisp logic in control is not a suitable solution because abrupt changes in the environment are not perceived favourably by most occupants.

   Fuzzy logic is a good approach for dealing with the imprecise nature of thermal comfort [13, 37, 49, 58, 139, 143, 148]. Membership functions and fuzzy rules can be defined, either for estimating the occupant thermal comfort level or for deciding the actions to be taken based on cabin sensor actuators. In these works, fuzzy logic controllers were found to perform better than traditional air temperature controllers. Fuzzy logic has, however, several disadvantages and it does not deal with the entire problem of ensuring occupant thermal comfort, namely it does not account for learning occupant preferences. Other disadvantages that can be argued are: i) it is very difficult to design accurate membership functions and rules (most of the time the rules are too simplified, for example: if the car cabin temperature is low and the sun load is low then the estimated equivalent temperature is low) and the control will only be as good as the defined rules; ii) the cohesion of the rules is not guaranteed, mismatches between the rules can occur and iii) the fuzzification and defuzzification operations are computationally expensive.

2. Comfort control involves multiple inputs and multiple outputs.

   Existing car cabin HVAC control systems include sensor measurements (such as cabin air temperature, ambient air temperature, humidity and solar load) for controlling occupant thermal comfort [37, 63]. However, the systems lack algorithms that translate these measurements to occupant comfort [63].

   Neural networks are a good approach in dealing with multiple input and output control problems

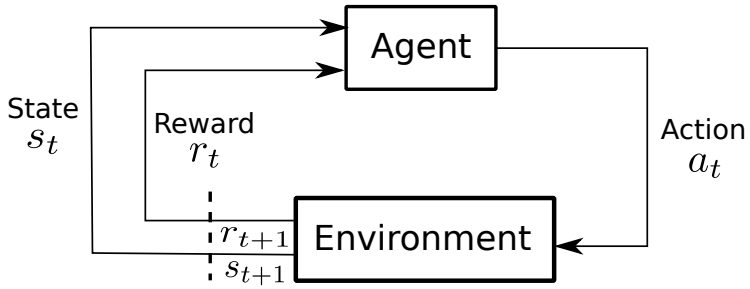

Figure 2.3: The interaction between the agent and environment in reinforcement learning.

and have been used in a variety of existing works [9, 22, 89, 151]. A disadvantage of neural networks is that in case of further online learning, retraining a neural network is a computationally expensive process.

3. Personalisation of control is appropriate and desirable.

   According to Fanger, the "optimal" environmental setting, which suits the widest audience, will still leave 5% dissatisfied. A system that can adjust according to preferences, however, may be able to do better than this. Moreover, no thermal comfort model based on mathematical or physical equations would be able to fully satisfy all car cabin occupants. This is due to the subjectivity factor of thermal comfort (for example, some people are more comfortable at a warmer temperature). Learning on top of the controller would improve occupant comfort by adapting to individual preferences [62, 79, 84, 126] .

Sutton and Barto [145] provide a detailed overview of reinforcement learning. In this section, the basic theory behind reinforcement learning is presented, together with the associated learning algorithm used in this thesis.

2.6.1 Agent-Environment interface

The main components of a reinforcement learning problem are the agent, the environment and the reward. The agent is the entity that learns and makes decisions, while the environment is what the agent interacts with. The two entities interact continuously as follows: the agent selects an action and the environment responds to that action and, also, provides new situations to the agent as a result. The reward is a numerical value that the environment provides to the agent after each action is performed. The agent's goal is to maximise the total amount of reward it receives over the long run. Figure 2.3 illustrates the interaction between the agent and the environment.

The interaction between the agent and environment takes place at discrete time steps ($t = 0, 1, 2, ..., N$).

A set of possible states S and a set of possible actions A available in those states are defined. At each time step, the environment sends the agent a representation of its state s_t. The agent then selects an action a_t and one time step later it receives a numerical reward r_{t+1} as a consequence of the action selected. A new state of the environment will be created as a result of applying the action, s_{t+1}. Also, at each time step, the agent implements a policy Π_t, where $\Pi_t(s, a)$ is the probability that $a_t = a$ if $s_t = s$. The policy represents a mapping from the states to the probabilities of selecting each possible action. The policy changes as a result of the agent's experience.

2.6.2 Markov property and Markov Decision Processes

In the reinforcement learning framework, the concept of "state" refers to the information available to the agent about its environment at that time. Roughly speaking, a state that retains all relevant information about the environment is said to be Markov or to have the Markov property. An example of a Markov state would be the current configuration of all pieces on a chess board, summarizing important information about the sequence of positions that led to that particular configuration.

Formally, the Markov property for reinforcement learning is defined below. The assumption is that there are a finite number of states and reward values. A state has the Markov property if, given the current state, the probability of an action causing a transition to a state is identical to the probability given all previous states including the current one:

$$Pr\{s_{t+1} = s', r_{t+1} = r \mid s_t, a_t\} = Pr\{s_{t+1} = s', r_{t+1} = r \mid s_t, a_t, r_t, \ldots, s_1, a_1, r_1, s_0, a_0\} \tag{2.30}$$

where s is the state, r is the reward and a is the action.

Note that the number of states has an effect on the complexity of the reinforcement learning problem. The state should be minimised without affecting the Markov property so that the reinforcement algorithm can produce a solution quicker and use less memory.

A Markov Decision Process (MDP) represents a reinforcement learning task that satisfies the Markov property. A finite MDP is a MDP in which the state and action spaces are finite. A finite MDP is defined by the state, action sets and the one-step dynamics of the environment.
The probability of each possible next state s', given any state and action, can be defined as:

$$P^a_{ss'} = Pr\{s_{t+1} = s' \mid s_t = s, a_t = a\} \tag{2.31}$$

The expected value of the next reward, given any current state, action and next state (s, a and s',

respectively), can be defined as:

$$R^a_{ss'} = E\left\{r_{t+1} \,|\, s_t = s, a_t = a, s_{t+1} = s'\right\} \tag{2.32}$$

2.6.3 Discounting

Reinforcement learning aims to maximise the expected return. The expected return R_t is defined as a function of the reward sequence:

$$R_t = r_{t+1} + r_{t+2} + r_{t+3} + \ldots + r_T \tag{2.33}$$

where T is the final time step.

There are two types of reinforcement learning applications that we can distinguish. The first type takes place when the agent-environment interaction can be split into episodes (for example the rounds of a game). Each episode then ends in a so called terminal state and the task is reset to a starting state. The second type of application involves a continuous interaction between the agent and the environment. The latter type applies to the problem presented in this thesis, of a comfort-oriented HVAC controller.

The concept of discounting is particularly useful in the non-episodic reinforcement learning problems in order to avoid the expected reward being infinite. The goal of the agent is to maximise the expected discounted return:

$$R_t = r_{t+1} + \gamma r_{t+2} + \gamma^2 r_{t+3} + \ldots = \sum_{k=0}^{\infty} \gamma^k r_{t+k+1} \tag{2.34}$$

where γ is the discount rate ($0 \leq \gamma \leq 1$).

The discount rate determines the value of future rewards: a reward that receives k time steps in the future is worth only γ^{k-1} times what it would be worth if received immediately. If $\gamma = 0$, the agent only aims to maximise immediate rewards, whereas as γ approaches 1, the agent takes more into account future rewards.

2.6.4 Value functions and optimal value functions

A value function is a fundamental aspect of a reinforcement learning problem and it estimates how useful it is for the agent to be in a certain state (value of the state) or how useful it is for the agent to perform a particular action in a given state (value of a state-action pair). Usefulness here corresponds to maximizing the total expected, discounted reward of being in that state with respect to a particular policy.

The value of a state s under a policy Π, denoted $V^{\Pi}(s)$, is the expected return when starting in state s and following the policy Π from there onwards. The value function is defined as:

$$V^{\Pi}(s) = E_{\Pi}\{R_t \,|\, s_t = s\} = E_{\Pi}\left\{\sum_{k=0}^{\infty} \gamma^k \times r_{t+k+1} \,|\, s_t = s\right\} \tag{2.35}$$

Similarly, we define the value of taking action a in state s under a policy Π, denoted $Q^{\Pi}(s,a)$, as the expected return starting from state s, taking the action a and following policy Π thereafter:

$$Q^{\Pi}(s,a) = E_{\Pi}\{R_t \,|\, s_t = s, a_t = a\} = E_{\Pi}\left\{\sum_{k=0}^{\infty} \gamma^k \times r_{t+k+1} \,|\, s_t = s, a_t = a\right\} \tag{2.36}$$

V^{Π} is called the state-value function for policy Π, while Q^{Π} is called the action-value function for policy Π. Solving a reinforcement learning problem involves finding an optimal policy, that is a policy better than or equal to all other policies.

Formally defined, a policy Π is better than or equal to a policy Π' if its expected return is greater than or equal to that of Π' for all states ($\Pi \geq \Pi'$ if and only if $V^{\Pi}(s) \geq V^{\Pi'}(s)$ for all $s \in S$). All optimal policies are denoted by $\Pi^{\star}$. Now the optimal state-value and the optimal action-value functions can be defined.

The optimal state-value function is denoted as $V^{\star}$ and is defined as:

$$V^{\star}(s) = \max_{\Pi} V^{\Pi}(s) \tag{2.37}$$

The optimal action-value function is denoted as $Q^{\star}$ and is defined as:

$$Q^{\star}(s,a) = \max_{\Pi} Q^{\Pi}(s,a) \tag{2.38}$$

$$Q^{\star}(s,a) = E\{r_{t+1} + \gamma \times V^{\star}(s_{t+1}) \,|\, s_t = s, a_t = a\} \tag{2.39}$$

2.6.5 Function approximation

Most applications require modelling the state using continuous values, rather than discrete values corresponding to finite MDPs. Function approximation can be used to overcome this problem. A function approximation is a function that, given a state or a state-action pair, returns the utility value. The CMAC [4] is a function approximation method commonly used in reinforcement learning problems. The specific form of a CMAC used in reinforcement learning is also called "tile coding". Tile coding represents

Algorithm 2.1 Linear, gradient descent Sarsa(λ) with eligibility traces.

1. Initialise $Q(s, a)$ arbitrarily and $e(s, a) = 0$, for all $s \in S$ and $a \in A$.
2. Repeat for each episode:
   (a) Initialise s with initial state of episode.
   (b) Choose a from s using policy derived from Q
   (c) Repeat for each step of episode until s' is terminal:
      i. Take action a, observe reward r and next state s'
      ii. Choose a' from s' using policy derived from Q
      iii. Update $\delta \leftarrow r + \gamma \times Q(s', a') - Q(s, a)$
      iv. Update $e(s, a) \leftarrow e(s, a) + 1$
      v. For all s, a
         A. $Q(s, a) \leftarrow Q(s, a) + \alpha \times \delta \times e(s, a)$
         B. $e(s, a) \leftarrow \gamma \times \lambda \times e(s, a)$
      vi. $s \leftarrow s'$and $a \leftarrow a'$

a grid and each location in that grid corresponds to a "tile". Each tile has a weight corresponding to the value that the point maps to. If multiple grids are used, the sum of the weights of relevant tiles is used to produce the value.

2.6.6 SARSA

Sarsa(λ) [145] is an on-policy (that is, the policy being followed is the one being evaluated) Temporal Difference (TD) learning algorithm. Off-policy algorithms, on the other hand, evaluate one policy while following another. Sarsa(λ) is an abbreviation from the State, Action, Reward, State, Action sequence. The symbol λ is the decay factor used (suggesting the use of an eligibility trace). An eligibility trace represents a temporary record of the occurrence of an event (for example visiting a state or taking an action). The decay of eligibility λ, where $0 \leq \lambda \leq 1$, has the following effect: when $\lambda = 0$, no credit is assigned to past state-action pairs, whereas when $\lambda = 1$, credit is assigned equally to all previously visited states. Eligibility traces can be combined with TD learning methods in order to perform a more efficient learning. Algorithm 2.1 reproduces the Sarsa(λ) algorithm used in this thesis.

There are a few studies referring to the convergence of the Sarsa(λ) algorithm. Sutton [144] concludes that Sarsa(λ) performs well often, however it has a tendency to oscillate rather than converge. Gordon [64] concludes that Sarsa(0) converges to a region and it does not diverge from that region. Singh [140] proved convergence for tabular Sarsa($\lambda = 0$).

The control method presented in this thesis combines the above Sarsa(λ) algorithm and tile coding-

based function approximation.

2.6.7 Reinforcement learning applications in HVAC control

Dalamagkidis *et al.* [35] appear to be the only authors to date looking at optimising HVAC thermal comfort-based control through a reinforcement learning-based technique. In their case, they looked at HVAC control in a building environment. They developed and simulated a reinforcement learning-based controller using the Matlab/Simulink environment. The reward is a function of the building occupants' thermal comfort, the energy consumption and the indoor air quality. The proposed controller was compared to a Fuzzy-PD controller and a traditional on/off controller. The results showed that, after a couple of simulated years of training, the reinforcement learning-based controller performed better in comparison to the other two controllers.

In terms of the system's design, two different environments were simulated: one that uses indoor air temperature, outdoor air temperature, relative humidity and CO_2 concentration as inputs and another that does not include the relative humidity input. Three control variables were used: the operating status of the heat pump (six settings: off and high, medium and low for heating and cooling, respectively), the air ventilation subsystem (three modes: off, low and high) and the window control (four states: closed, slightly open, open and wide open).
The reward function used is expressed as:

$$\text{Reward} = -w_1 \times \text{TCP} - w_2 \times \text{EP} - w_3 \times \text{IAQP} \tag{2.40}$$

where TCP is the thermal comfort penalty, EP is the energy penalty, IAQP is the indoor air quality penalty and w_1, w_2, w_3 are the weights associated with these parameters.

$$\text{TCP} = (\sum_{t=0}^{k} \text{PPD})/k \tag{2.41}$$

$$\text{EP} = (\sum_{t=0}^{k} \text{EC})/\max \text{EC} \tag{2.42}$$

$$\text{IAQP} = (\sum_{t=0}^{k} (1 + exp(-0.06 \times (\text{CO}_2 - 870)))^{-1})/k \tag{2.43}$$

where EC is the energy consumption and PPD is the percent of people dissatisfied as computed by Fanger's model [46].

Dalamagkidis *et al.* [35] highlight an issue with regard to reinforcement learning-based controllers—that of sufficient exploration. Taking random actions, even during short times, is unacceptable for a system deployed in a real environment and Dalamagkidis *et al.* recommend to exhaustively train the controller prior deployment and allow little exploratory actions or no exploration at all afterwards.

The work of Dalamagkidis *et al.* is presented in more detail due to its relevance to the work in this thesis. However, reinforcement learning is applied within a wide range of areas [75, 86, 94, 135].

2.7 Summary

The literature surveyed here included the areas of thermal comfort models, modalities of measuring thermal comfort in cars, learning-based estimation methods, HVAC control algorithms in both buildings and vehicular environments and reinforcement learning related theory and applications.

Automatic HVAC controllers are used in most vehicles nowadays. However, they do not offer maximum comfort levels, requiring user intervention often, especially at the beginning of journeys. Current controllers primarily use air temperature and/or humidity to actuate the control. However, the notion of thermal comfort is more complex, arising from both physiological and psychological conditions. Moreover, current controllers have no ability to automatically differentiate between different body parts of the passengers, whereas it is known that thermal sensation differs considerably within different body parts.

There is extensive research in the area of comfort-oriented HVAC control algorithms within the building environment, but considerably less in vehicular environments. The PMV thermal comfort model, for example, continues to be applied for vehicular HVAC control, despite the fact that it was not designed for transient environments. Also, there is a lack of empirical evaluation of thermal comfort models with regard to establishing whether any of them is suitable for vehicular control.

The work developed in this thesis fills in the state of the art gaps by:

1. Evaluating existing thermal comfort models on empirically derived car cabin data and establishing the most suitable model for vehicular control.

2. Developing a Virtual Thermal Comfort Sensing (VTCS) method that estimates occupant body part equivalent temperatures from cabin environmental sensors.

3. Developing and evaluating a novel method for vehicular HVAC control that outperforms the state-of-the-art methods—a reinforcement learning-based control policy that integrates in its reward

thermal occupant comfort and energy consumption.

The next chapter gives an overview of the work in this thesis, together with a discussion of a real-time system that could be implemented based on this work.

Chapter 3

Integrated HVAC System Overview

The previous chapter described the literature surveyed, including the areas of thermal comfort models, modalities of measuring thermal comfort in cars, learning-based estimation methods, Heating, Ventilation and Air Conditioning (HVAC) control algorithms in both buildings and vehicular environments and reinforcement learning related theory and applications.. This chapter gives an overview of the work in this thesis, together with a discussion of a real-time system that could be implemented based on this work.

3.1 Simulation-based system architecture

Figure 3.1 illustrates the overall architecture of the simulation-based car cabin heating and cooling control system proposed in this thesis. The components of the system are the following:

1. A one dimensional heat flux-based simulation of the car cabin environment that constitutes the platform for learning.

2. A cabin state vector integrating cabin environmental variables and the parameters desired to be controlled (the occupant equivalent temperature and the energy consumed for the work here).

3. A reward function scoring the desirability of the current car cabin state. The reward function takes as input a state and outputs a score that represents the desirability of that particular state. The reward function is expressed as a sum of several component functions related of parameters to control: $f(x) = w_c \times C(x) + w_e \times E(x)$, where $C(x)$ is the comfort factor, $E(x)$ is the energy consumption factor, and w_c, w_e are the weights associated with each of the factors. Other components could also be integrated in the function, such as window fogging. The weights associated with the components reflect their relative importance.

4. A reinforcement learning technique that finds an optimal policy mapping the states of the environment to actions to be taken when those states are encountered. Sarsa(λ) is used as a reinforcement

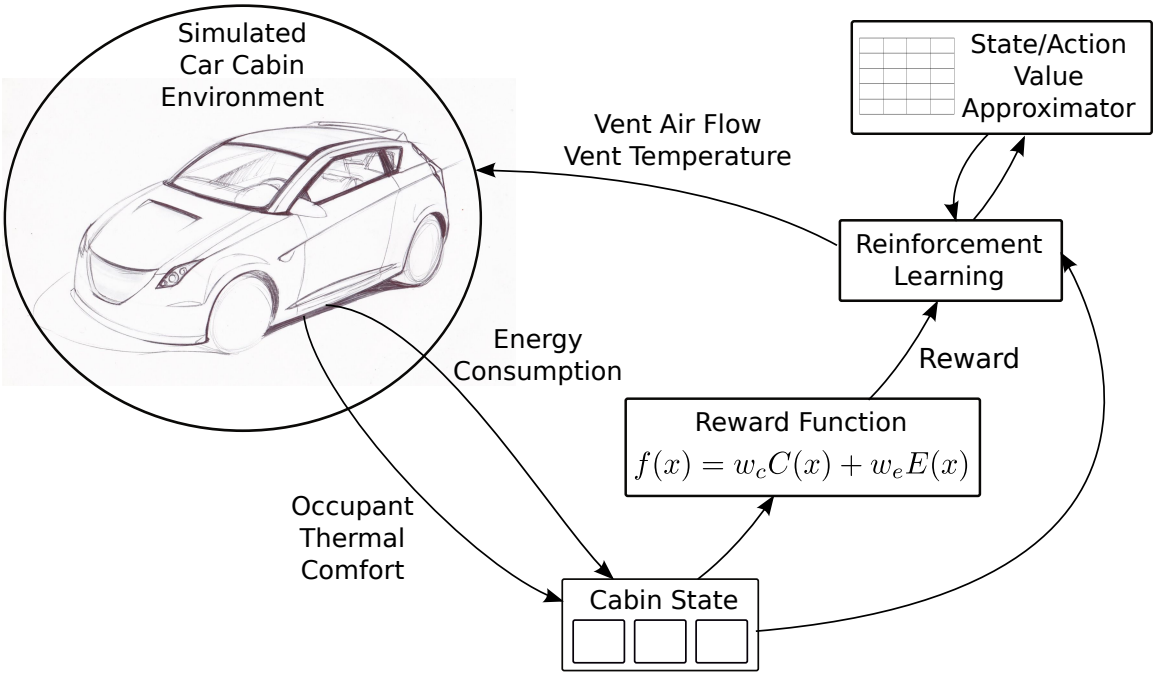

Figure 3.1: Overall simulation-based system architecture.

learning algorithm.

5. A state/action value approximator that provides an estimate of the value of each action for that particular cabin state.

The processing cycle of the system is as follows:

1. The reinforcement learning-based controller receives an initial state of the car cabin state.
2. The algorithm assesses the value of each possible action appropriate for that state and decides what action to take based on the current policy.
3. The action is then fed back to the simulation and a new cabin state is produced as a result.
4. The result is translated into features. For the work in this thesis the features are the passenger thermal comfort level (equivalent temperature) and the energy consumption. In general, however, additional features can be added such as air quality, screen clarity, etc.
5. These features, together with additional raw data, such as ambient temperature or solar load, are integrated into the cabin state vector.
6. Based on the cabin state vector, a numerical reward is computed as a weighted sum of its elements.

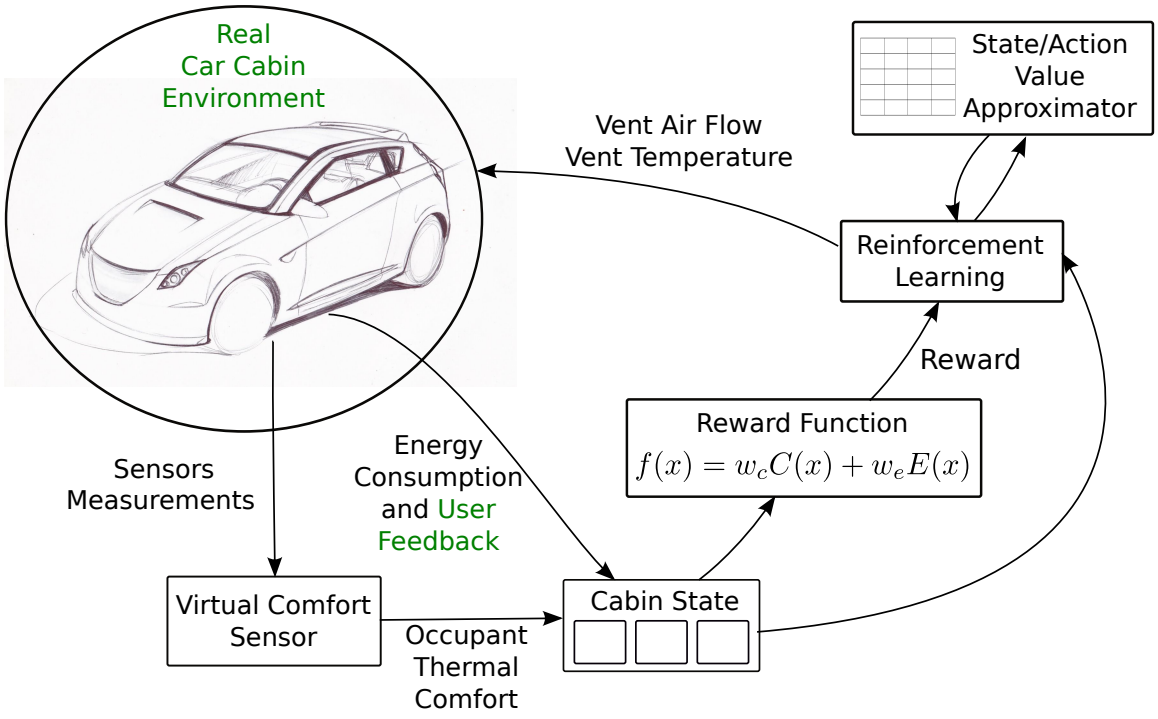

Figure 3.2: Potential real-time system architecture.

7. The reinforcement learning algorithm adjusts the parameters of the value function approximator or, in other words, adjusts the policy used to select the actions.

This process is then repeated.

3.2 Potential real-time system

Figure 3.2 shows the architecture of a potential real-time system based on the work in this thesis. Reinforcement learning takes a considerable number of learning cycles to learn an optimum policy, depending on the size and dimensionality of the state-action space. Moreover, at the start of the learning process, the actions are selected at random. As described in Section 2.6 on page 62, exploration is an important issue in reinforcement learning-based applications. Therefore, the solution consists of first learning an optimal policy through simulation. Then, the learnt policy would be installed within the HVAC controller.

There are two differences between the simulation-based system and the real-time one. First, occupant equivalent temperature cannot be feasibly measured in a real car cabin (as motivated in Sections 2.2 and 2.3), therefore a Virtual Thermal Comfort Sensing (VTCS) method is introduced in the loop. The role of the VTCS approach is to estimate occupant body part equivalent temperature from a minimal number

of inexpensive sensors in the cabin. Second, cabin occupants can freely override the learnt policy (by the adjustments they make to the vent air temperature and blower speed). As a result, user feedback is added as a feature of the reward function. Based on the actions performed (increasing the vent temperature, for example) further information is given regarding the comfort of the occupant and, therefore, the policy can improve accordingly. The user's feedback is thus able to manually override the learnt policy or directly intervene in control. When user feedback is given, the reward function will penalise this change heavily, therefore encouraging a policy well suited to the specific end-user.

The processing cycle of the system is as follows:

1. A number of sensors measuring raw parameters (such as air temperature and solar load) are placed within the car cabin. Along with offering valuable information about the car cabin environment, the sensor data is used as input to the VTCS method in order to estimate occupant thermal comfort. A minimum number of sensors should be used in order to reduce the production costs and complexity of the HVAC system. Therefore, they have to be selected in such a way that the information they share with the target (occupant thermal comfort in this case) is maximised. The sensor selection is performed offline, prior to the vehicle manufacturing, using the mutual information-based method proposed in Section 5.1.

2. Based on the cabin sensor measurements, the VTCS approach described in Section 5.2 will estimate occupant equivalent temperature in real-time within the cabin.

3. The system then performs similarly to the previously described simulation-based one. The reinforcement learning-based controller uses the existing policy to select an appropriate action for the current car cabin state. This action consists in adjusting air temperature set points, blower speeds, air distribution flaps, etc. The low-level control system then reacts to the control actions, resulting in heating-up or cooling-down the cabin correspondingly. As with simulated learning, the reward function provides feedback to the reinforcement learning-based controller, which then updates its policy accordingly. The difference in updating the policy is that the user feedback is included in the reward function.

For the real-time system, the following should be mentioned with regard to the flexibility of the proposed approach:

1. The comfort-oriented control approach presented in this thesis is generic. If a new thermal comfort model is developed that reflects vehicle occupant thermal comfort more accurately, then that model could be easily integrated into the system. For example, if the new thermal comfort model is skin

temperature-based, then a VTCS method that estimates occupant body skin temperature rather than equivalent temperature from a set of cabin environmental sensors can be implemented.

2. In order to redesign (tune for a particular cabin interior) the VTCS approach, a series of experimental trials have to be performed, similar to the ones described in Section 4.1. In the case of a VTCS method that estimates occupant skin temperatures from cabin environmental sensors, skin temperature at multiple occupant body sites should be collected in a variety of conditions (different HVAC start set-points, different rates of change of the HVAC set-point), together with numerous cabin environmental sensor data (air flow, solar load, mean radiant temperature, air temperature at multiple locations within the cabin). The method presented in Chapter 4 can be used to derive the optimum set of sensors and their associated locations for any particular application.

3. For the purpose of this thesis, the thermal comfort level of a single occupant was presented. However, the approach described here allows controlling the thermal comfort of a larger number of occupants. The reinforcement learning-based controller can be tuned to the preferences of each particular occupant and, therefore, N different control policies are generated (N = number of passengers). The occupant identification can be made based on in-seat weight sensors or personal Radio-Frequency IDentification (RFID) tags.

This chapter gave an overview of the work in this thesis. The next chapter describes the empirical data gathering process, an analysis of the factors related to car cabin occupant thermal comfort and an evaluation of the thermal comfort models presented in this chapter using empirical data.

Chapter 4

Car Cabin Environment and Thermal Comfort Models

In order to develop efficient Heating, Ventilation and Air Conditioning (HVAC) control algorithms, both in terms of occupant comfort and energy consumption, there is a need to estimate the thermal comfort level of the cabin occupants in real-time [110]. Existing thermal comfort models provide the capability of estimating thermal comfort. A key problem is that these thermal comfort models do not produce accurate thermal comfort estimates for the car cabin environment [152]. Reasons for this include: the car cabin environment is transient and non-uniform, the outside environment affects the cabin in a non-uniform way, radiant heat asymmetry occurs due to the close position of dashboard, windows and walls with respect to the body, and finally, the passenger is fixed in position, unlike, for example, in an office [29]. Therefore, an important stage of this work is to establish an understanding of car cabin thermal comfort and how subjective occupant thermal comfort reports relate to existing thermal comfort models.

The overarching research question this chapter poses is: Is there an existing thermal comfort model that is suitable for real-time use in an HVAC system and if so, which is it?

In order to answer this question gathered experimental data was used, representing an advantage in comparison to other works in the literature [28, 67, 68]. The experimental data was gathered from a number of trials that included both steady-state conditions and conditions normally expected while driving and in which subjective comfort measures were sought from human participants. The main aim of the work was to understand the limitations and usefulness of existing thermal comfort models when applied to realistic car cabin data.

Based on the analysis using empirical data, this chapter advances the state-of-the-art by:

1. Answering several questions related to vehicular thermal sensation and comfort characteristics:

   (a) Does thermal neutrality generally correspond to a cabin air temperature set-point, such as 22 ℃?

(b) Does neutral thermal sensation correspond to thermal comfort?

(c) What is the effect of occupant pre-conditioning and solar load on thermal comfort?

(d) Do people feel more thermally comfortable when manual control is used, rather than automatic?

2. Establishing which of the four thermal comfort models (namely Predicted Mean Vote (PMV), Taniguchi's model, Zhang's model and Nilsson's model) is a better match for cabin occupant thermal comfort in typical vehicular conditions.

3. Illustrating the range of conditions in which thermal comfort models could be applied to drive comfort-oriented HVAC control algorithms.

Section 4.1 describes the data gathering methodology, focusing on the instrumentation used, the participating subjects and the range of conditions encountered in the car cabin. Section 4.2 answers several questions related to vehicular thermal comfort, while Section 4.3 evaluates four existing thermal comfort models on the gathered data. Finally, Section 3.4 summarises the chapter.

4.1 Experimental data gathering

There are three main strands of work that are supported by the empirical data collected:

1. Answering questions related to vehicular thermal sensation and comfort.

2. Evaluating existing thermal comfort models in order to establish the most suitable model for control (namely PMV, Taniguchi's model, Zhang's model and Nilsson's model, all described in Section 2.1).

3. The offline development and evaluation of a Virtual Thermal Comfort Sensing (VTCS) approach that estimates occupant body part equivalent temperature from cabin environmental sensors (presented in Chapter 4).

The test car used for the experimental data gathering was a Jaguar XJ (2010 model year), shown in Figure 4.2 (left). In order to i) measure equivalent temperature for computing Nilsson's thermal sensation index and ii) calculate the PMV index, the INNOVA Flatman support manikin[1], shown in Figure 4.2 (right), was placed in the front passenger seat. Throughout the experimental trials, equivalent temperature was measured in real-time at eight locations (corresponding to head, chest, left lower arm,

[1]LumaSense Technologies The INNOVA "Flatman" Manikin: `http://www.lumasenseinc.com/EN/products/thermal-comfort/flatman/the-manikin-innova-flatman.html`

Table 4.1: Areas of individual body parts and their relative weightings .

Body segment	Skin area (m^2)	Relative area (%)
Head	0.180	10.3
Chest	0.544	31.1
Right arm	0.112	6.4
Left arm	0.112	6.4
Right thigh	0.200	11.4
Left thigh	0.200	11.4
Right foot	0.201	11.5
Left foot	0.201	11.5

right lower arm, left upper arm, right upper arm, thigh and calf) using dry heat loss sensors attached to the Flatman and connected to an INNOVA thermal comfort data logger[2]. A dry heat loss transducer is an ellipsoidal device that thermally simulates the human body and consists of a surface temperature sensor and a surface heating element. The element is powered automatically to bring the surface to a temperature similar to that of the skin of a clothed person. The rate of power consumption needed to reach this temperature is used as a measurement of a person's rate of heat loss/gain in that environment. The data logger then estimates individual segment equivalent temperatures from the measured dry heat loss values[3]. The weighted overall equivalent temperature is computed based on the relative areas of the body parts, as presented in Table 4.1, as follows:

$$ET_{ov} = \sum_{i=1}^{n} w_i \times ET_i \tag{4.1}$$

where ET_{ov} is the overall equivalent temperature over the eight body parts, ET_i is the equivalent temperature for one body segment, w_i is the weighting for each body segment (the corresponding relative area from Table 4.1 and n is the number of body segments, eight in this case). The areas and weightings corresponding to the body parts were taken from Flatman's manual[4]. The data logger then estimates the PMV thermal comfort index by replacing the air temperature and mean radiant temperature values with the overall equivalent temperature, while the air flow is set to 0 (as per the definition of equivalent temperature). The clothing index, metabolic rate and humidity values that are used by the logger to compute the PMV thermal comfort index are manually set within the software. In the case of the trials here, the settings were: metabolic value of 1.2, clothing value for the head of 0.05, clothing value for the

[2]Grant Instruments (Cambridge) Ltd. Squirrel SQ2040 Series Data Loggers: `http://www.grantinstruments.com/gb/products/data-loggers/squirrel-sq2040-series`

[3]LumaSense Technologies Dry Heat Loss Transducers: `http://lumasenseinc.com/EN/products/thermal-comfort/t-equivalent`

[4]Manual of INNOVA's Flatman Thermal Manikin: `http://www.lumasenseinc.com/EN/products/thermal-comfort/flatman/the-manikin-innova-flatman.html`

upper arms of 0.15, clothing value for the lower arms of 0.0, clothing value for the chest of 0.15, clothing value for the thigh of 0.23, clothing value for the calf of 0.25. The overall clothing value was of 0.67 based on weighting each body part. These values were set to correspond to what the subjects were wearing (long trousers and a short-sleeved, light-coloured shirt or blouse).

In order to compute Taniguchi's and Zhang's thermal sensation indexes, subject body part skin temperature was also measured at eight points (neck, left and right wrist, chest, left and right thigh, left and right calf—corresponding to the Flatman dry heat loss sensor locations) using Grant Instruments EUS-UU-VL2-0 thermistors[5].

For the development and evaluation of the VTCS method (presented in Chapter 4), cabin environmental parameters were also measured, as follows:

1. Air temperature and relative humidity at six points (head, chest and feet level of the occupants, both on the left and right side) using type T thermocouples and Honeywell S&C HIH-5031 humidity sensors[6].

2. Solar loading at the driver sunroof using automotive solar sensors. A portable array on the driver side was used for applying the solar load. The array consisted of 16 bulbs, each rated at 150 Watts. The bulbs were controlled based on temperature readings from remote thermocouples mounted on the outside surface of the driver door. The temperature thresholds were set such that an average load of 455 $W \times m^{-2}$ was applied. This level of solar loading is consistent with that which would be experienced at around 9 am to 10 am on a sunny day according to data from Motor Industry Research Association (MIRA).

3. Cabin air and surface temperatures at 19 points (shown in Figure 4.1) using type K thermocouples.

4. Driver centre and outboard face vent air temperatures using type K thermocouples (shown in Figure 4.1).

In order to support the work in this thesis, specifically the evaluation of selected thermal comfort models in the literature and the development of the VTCS method, subjective thermal comfort data was collected. There were a total of seven subjects (four males and three females) with ages between 24 and 56 years, heights between 1.57 cm and 1.78 cm, and weights between 48 kg and 78 kg, as listed in Table 4.2. The subject occupied the driver seat, while an observer sat in the right-hand rear passenger seat. Clothing

[5]Grant Instruments (Cambridge) Ltd. Temperature and Humidity: `http://www.grantinstruments.com/gb/products/data-logger-accessories/temperature-and-humidity-probes.html`

[6]Sensirion SHT75 - Digital Humidity Sensor (RH&T): `http://www.sensirion.com/en/01_humidity_sensors/06_humidity_sensor_sht75.html`

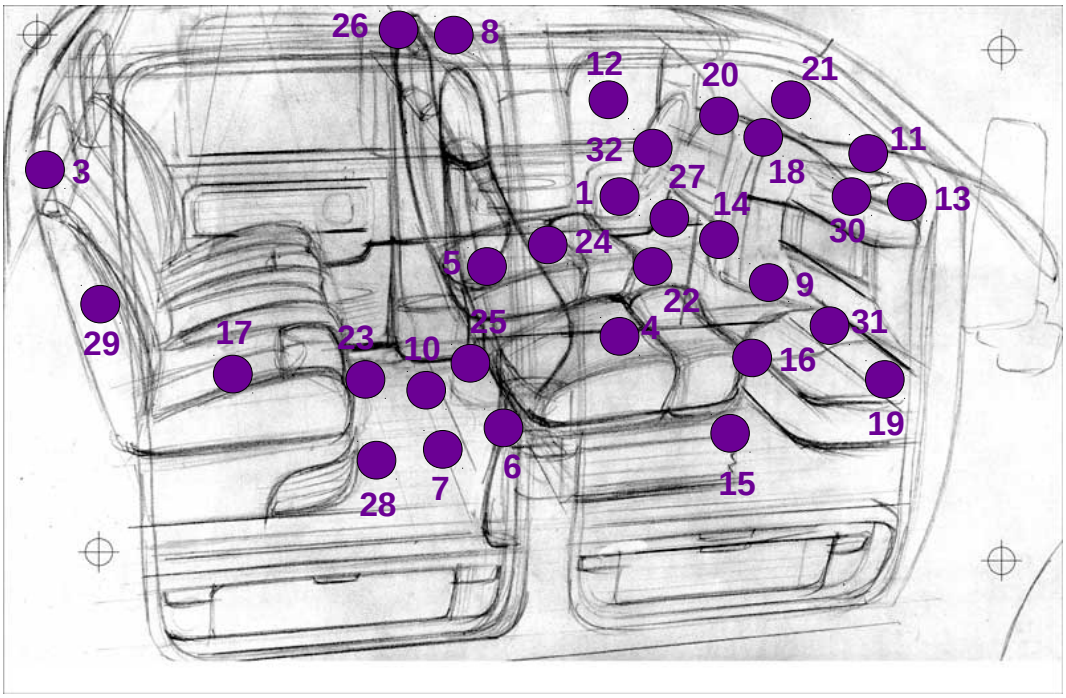

1 - Row 1 Discharge Outer Left
2 - Driver Seat Back
3 - Headliner Rear Pass Head
4 - Passenger Seat Cushion
5 - Passenger Seat Back
6 - Row 2 Foot Discharge Right
7 - Row 2 Discharge Right
8 - Panoramic Passenger Head
9 - Row 1 Discharge Inner Right
10 - Row 2 Discharge Left
11 - Front Screen Right Centre
12 - Front Side Glass Left Centre
13 - IP Top Right Centre
14 - Row 1 Discharge Inner Left
15 - Front Side Glass Right Centre
16 - Row 1 Foot Right
17 - Row 2 Right Seat Cushion
18 - Screen Defrost Left
19 - Row 1 Discharge Outer Right
20 - IP Top Left Centre
21 - Front Screen Left Centre
22 - Row 1 Foot Left
23 - Row 2 Foot Left
24 - Driver Seat Cushion
25 - Row 2 Foot Discharge Left
26 - Panoramic Driver Head
27 - Row 1 Foot Discharge Left
28 - Row 2 Foot Right
29 - Row 2 Right Seat Back
30 - Screen Defrost Right
31 - Row 1 Foot Discharge Right
32 - Steering Wheel

Figure 4.1: Air and surface temperature sensor locations within the car cabin.

Figure 4.2: Experimental data gathering. Left: Test car. Right: Flatman support manikin with dry heat loss sensors.

was standardised across all experiments and subjects, consisting of long trousers and a short-sleeved, light-coloured shirt or blouse.

Table 4.2: Experimental participant characteristics for trials *T1, T2* and *T3*.

Subject	Gender	Age (years)	Height (cm)	Weight (kg)
1	Male	46	173	78
2	Female	37	157	73
3	Male	56	166	70
4	Male	49	178	75
5	Female	24	162	48
6	Male	26	176	77
7	Female	34	160	55

Table 4.3: Experimental participant characteristics for trials $T4$.

Subject	Gender	Age (years)	Height (cm)	Weight (kg)
1	Male	50	178	81
2	Female	51	163	73
3	Male	56	166	70
4	Male	43	189	85
5	Female	28	165	64
6	Male	26	176	77
7	Female	47	150	47

Table 4.4: Thermal sensation scale.

4	Very hot
3	Hot
2	Warm
1	Slightly warm
0	Neutral
-1	Slightly cool
-2	Cool
-3	Cold
-4	Very cold

Table 4.5: Thermal comfort scale.

3	Very uncomfortable
2	Comfortable
1	Just uncomfortable
0	Neutral
-1	Just uncomfortable
-2	Uncomfortable
-3	Very uncomfortable

The subjects reported their overall thermal sensation and comfort to the observer throughout the trials, while local thermal sensation and comfort at the head, chest and foot level was reported only within one set of trials. Thermal sensation and comfort were collected using the scales given in Tables 4.4 and 4.5.

Four types of trials (a total of 96 individual trials) were performed, corresponding to two main categories, as described in Sections 4.1.1 and 4.1.2.

Technical considerations

1. Throughout the experimental trials, the Flatman occupied the front passenger seat, while the subject occupied the driver seat. As a result, the conditions could have varied between the two locations. In order to minimise the difference in conditions for the occupant and Flatman, the following were ensured throughout the trials:

   (a) The centre and outer vents for the driver and the front passenger were consistent in terms of orientation angle.

   (b) The HVAC mode was synchronised, ensuring that vents on both sides have the same set-point temperature and blower speed setting.

   (c) The subjects and cabin were pre-conditioned to the same temperature.

   Additionally, the trials with controlled solar radiation were eliminated from the evaluation of two thermal comfort models (PMV and Nilsson's model) due to the asymmetry of the solar array's position (driver side). They were, however, used in order to analyse the effect of solar radiation on subjects' thermal sensation.

2. The Flatman lacks a dry heat loss transducer corresponding to the foot location (the closest being the calf sensor), whereas the subjects reported thermal comfort and sensation at the foot level.

The influence of this aspect on the comparison between the subjective and Flatman reports is not expected to be significant.

3. For reasons of availability, the subjects who participated in trials *T1, T2* and *T3* are different from those who participated in trials *T4* (see Tables 4.2 and 4.3). Therefore, the analysis is conducted separately on the two groups.

4. The error associated with the Flatman's measured equivalent temperature is ±2%, while the error associated with the thermocouples measuring cabin air and surface temperature values is ±0.5 ℃[7].

4.1.1 Controlled environment trials

Two sets of trials, denoted *T1* and *T2,* involved a controlled steady-state external environment (solar load, ambient temperature, wind) with varying HVAC control set-point.

Variable cabin temperatures with steady state external conditions (T1)

The purpose of these trials was to record and analyse subject thermal comfort and sensation responses at various temperatures. In order to determine the comfortable range of temperatures for drivers in a stationary vehicle, the trials were performed within an enclosed space, characterised by stable ambient air temperature, in order to avoid the effects of wind and sun. The subjects were pre-conditioned to 22 ℃ in a separate room for 20 minutes. The test car cabin was also pre-conditioned to 22 ℃. The subject entered the car and remained in static conditions (HVAC set-point of 22 ℃ and air flow set on medium or high as per trial) for 10 minutes, reporting sensation and comfort scores after 5, 7 and 9 minutes. The HVAC set-point temperature was then increased by 1 ℃ every 3 minutes until it reached 28 ℃. During this process, the subject reported thermal sensation and comfort levels two minutes after each temperature change.

The subject then left the car and was again preconditioned to 22 ℃, as was the car cabin. The subject entered the car, again remaining in static conditions (HVAC set-point of 22 ℃) for 10 minutes. The HVAC set-point temperature was decreased by 1 ℃ every three minutes until it reached 16 ℃. This procedure was performed four times per subject, with each combination of medium and high air flow and with and without solar loading on the driver side of the car.

These trials are characterised by the following conditions: 1) absolute average car cabin temperature rates of change peaking at around 1.5 ℃ per minute, but usually under 1 ℃ per minute; 2) pre-conditioning

[7]Grant Instruments (Cambridge) Ltd. Temperature and Humidity: `http://www.grantinstruments.com/gb/products/data-logger-accessories/temperature-and-humidity-probes.html`

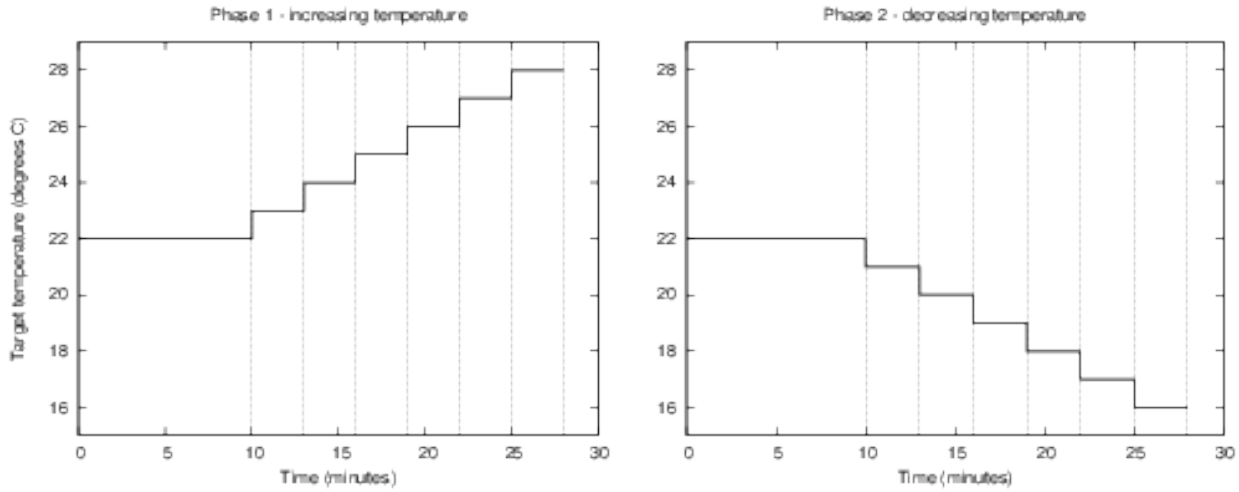

Figure 4.3: HVAC set-point step changes for the warm-up and cool-down trials.

of the cabin and subject at the same temperature; 3) no precipitation or wind effects; 4) steady ambient temperature between 19 ℃ and 24 ℃ and varying by less than 1 ℃ within an individual trial.

User control with steady state external conditions (T2)

The purpose of these trials was to gain knowledge of the HVAC inputs performed by the subjects in order to reach a comfortable temperature, starting with several pre-conditioning temperatures. As with trials *T1*, these trials were also performed with the vehicle in an enclosed space, characterised by stable ambient air temperature and shielded from the wind and sun. The car cabin and the subjects were pre-conditioned to a neutral (22 ℃), hot (28 ℃), or cold (16 ℃) temperature for 20 minutes prior to the trial. The subject entered the car and remained inside for 15 minutes, during which they were permitted to adjust the air conditioning at will in order to make themselves comfortable. The control adjustments performed were logged by the observer. These trials were performed both with and without simulated solar loading on the driver side of the car, with each condition tested once per subject. Thermal comfort and sensation were reported every two minutes.

These trials are characterised by the following conditions: 1) absolute average car cabin temperature rates of change peaking at 8 ℃ per minute; 2) pre-conditioning of the cabin and subject at the same temperature; 3) no precipitation or wind effects; 4) steady ambient temperature between 17 ℃ and 25 ℃ and varying by less than 1 ℃ within an individual trial.

The higher rates of change compared to trials *T1* are due to the driver controlling the HVAC compared to the prescribed steps defined for *T1.*

4.1.2 Realistic driving trials

Two sets of trials, denoted *T3* and *T4,* were aimed at providing realistic driving scenarios for both short and long trips. The trials involved actual driving and thus allowed no control over the external environment (solar load, ambient temperature, wind).

User control during short journeys (T3)

The purpose of these trials was to determine whether subjects select the HVAC inputs differently when driving, for example if the driver tolerates a wider range of temperature. The trials consisted of subjects driving the test car on private roads. The car and the subjects were pre-conditioned to a neutral (22 ℃), hot (28 ℃), or cold (16 ℃) temperature. The subjects entered the car and drove for 15 minutes, during which they were permitted to adjust the air conditioning at will in order to make themselves comfortable. The subjects were required to turn and change speed at frequent intervals in order to simulate daily driving routines. The hot and cold tests were performed twice per subject, while the neutral tests were performed once. Thermal comfort and sensation were reported every two minutes. The adjustments made to the HVAC inputs were also logged by the observer.

These trials are characterised by the following conditions: 1) absolute average car cabin temperature rates of change peaking at 10 ℃ per minute; 2) pre-conditioning of the cabin and subject at the same temperature; 3) uncontrolled ambient solar load and wind; 4) ambient outside temperature between 12 ℃ and 28 ℃ and varying by less than 2 ℃ within an individual trial.

Automatic and user control during long journeys (T4)

The purpose of these trials was to capture comfort in a variety of conditions, clothing types and HVAC settings. These trials consisted of a five day road-trip throughout the UK in a Jaguar XJ (2010 model year). On each day there were four trials, lasting around two hours each. The trials were differentiated by the HVAC control mode: automatic mode at 20 ℃, automatic mode at 22 ℃, automatic mode at 24 ℃ and manual mode. The car cabin instrumentation consisted of the sensors used for the previous three types of trials along with an additional set of sensors: mean radiant temperature collected at a centre ceiling location; solar load, collected at locations corresponding to dashboard left and right; air temperature, collected at locations corresponding to dashboard left and right. The experimental conditions encountered are characterised by interior temperature rates of change of up to 6 ℃ per minute and external temperature differences up to 6 ℃ per trial, along with varying ambient wind, solar load and precipitation.

Table 4.6: Summary of the experimental conditions in all trials, with the duration given per trial.

Type	Duration (mins)	Blower speed	Solar load	Driving	Pre-conditioning	Subjects
T1	56	High or Medium	Controlled	No	22 ℃	7
T2	15	User	Controlled	No	16 ℃, 22 ℃ or 28 ℃	7
T3	15	User	Ambient	Yes	16 ℃, 22 ℃ or 28 ℃	6
T4	120	User	Ambient	Yes	None	7

Seven subjects (three females and four males) took part in the trials, rotating within the driver, back left and back right passenger positions. There were three variations of upper-body clothing types for the subjects: light (t-shirt), medium (shirt) and heavy (jacket). The subject located in either the back right or back left position was also an observer who was required to collect subjective data from the driver every 15 minutes. Additional information referring to weather, window fogging, breaks, travel conditions and window opening was also recorded. Thermal sensation at the head, hands and foot level was collected (using the scale presented in Table 3.3), together with the overall thermal comfort score on a continuous scale ranging from -1 (very uncomfortable) to 1 (very comfortable).

Table 4.6 provides a summary of the experiments performed and the number of subjects involved in each.

4.1.3 Data pre-processing

Prior to the investigation, the collected data was pre-processed as follows:

1. Equivalent temperature and the PMV index were collected at a frequency of 0.2 Hz—the maximum possible frequency for the Flatman. Thermal sensation was collected at fixed intervals during the trips (every three minutes during trials *T1, T2* and *T3* and every 10 minutes during trials *T4*). In order to compare the two parameters the equivalent temperature corresponding to each nearest available thermal sensation report was used.

2. The Flatman's functioning includes a warming-up period (the time required for the dry heat loss transducers to warm-up in order to simulate the occupant skin temperature). Therefore, at the beginning of the first trial each day in *T4,* the initial data points were removed from the data set (until the first valid value was encountered).

3. The data corresponding to sensors with a yield of below 70% were eliminated from the data analysis and method validation (front vent air temperature and front passenger right footwell).

4. Faulty data were eliminated from the analysis. This was determined by the absolute difference

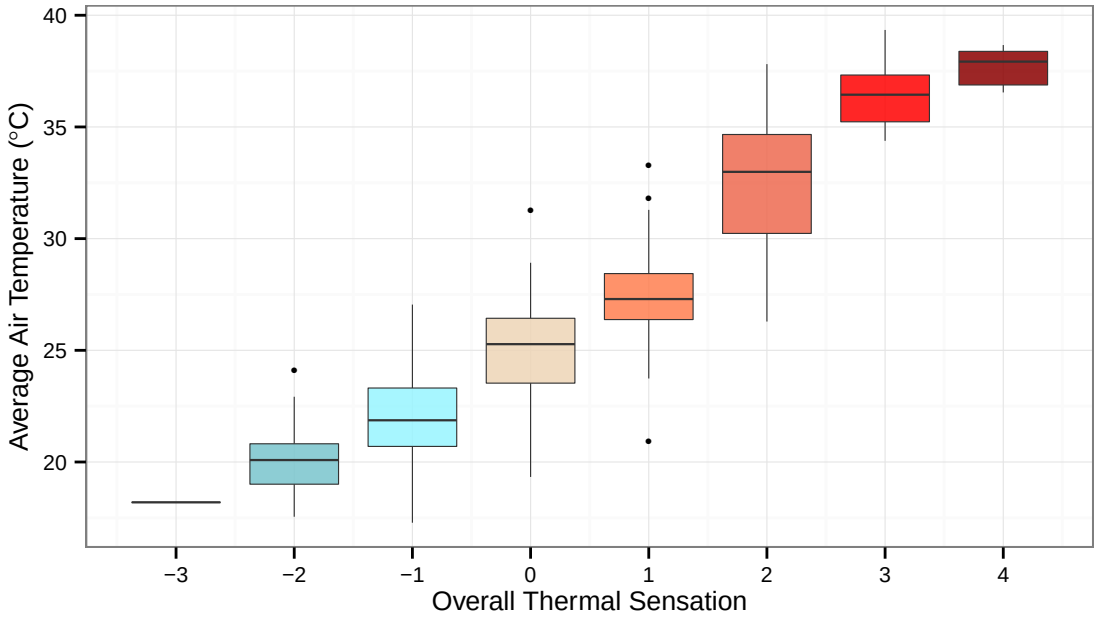

Figure 4.4: Overall thermal sensation versus average car cabin temperature.

between two consecutive sensor readings higher than 2 ℃.

4.2 Car cabin thermal comfort

This section investigates five thermal comfort related hypotheses in the literature.

H4.1: *Thermal neutrality does not generally correspond to a certain cabin air temperature set-point, such as 22* ℃.

In order to respond to **H4.1**, the cabin average air temperature ranges mapping to each thermal sensation index were plotted, aggregating the results from all the trials performed. Figure 4.5 shows that a thermal neutral sensation of 0 occurs at a range of cabin air temperature centred around 25 ℃. However, the range extends between 19 ℃ and 28 ℃ depending on factors such as pre-conditioning, solar load, gender and subjective preferences. Figure 4.5 depicts the average cabin air temperature ranges where individual subjects felt thermally neutral during all trials. The figure shows that the ranges differ considerably amongst the seven subjects. The widest range is encountered for subject 1, between 19 ℃ and 27 ℃, while the narrowest range is encountered for subject 6, between 23 ℃ and 27 ℃.

This experiment supports hypothesis **H4.1**. Figure 4.5 demonstrates that neutral thermal sensation does not occur at a certain single temperature, as traditionally assumed, but over a wide range of car

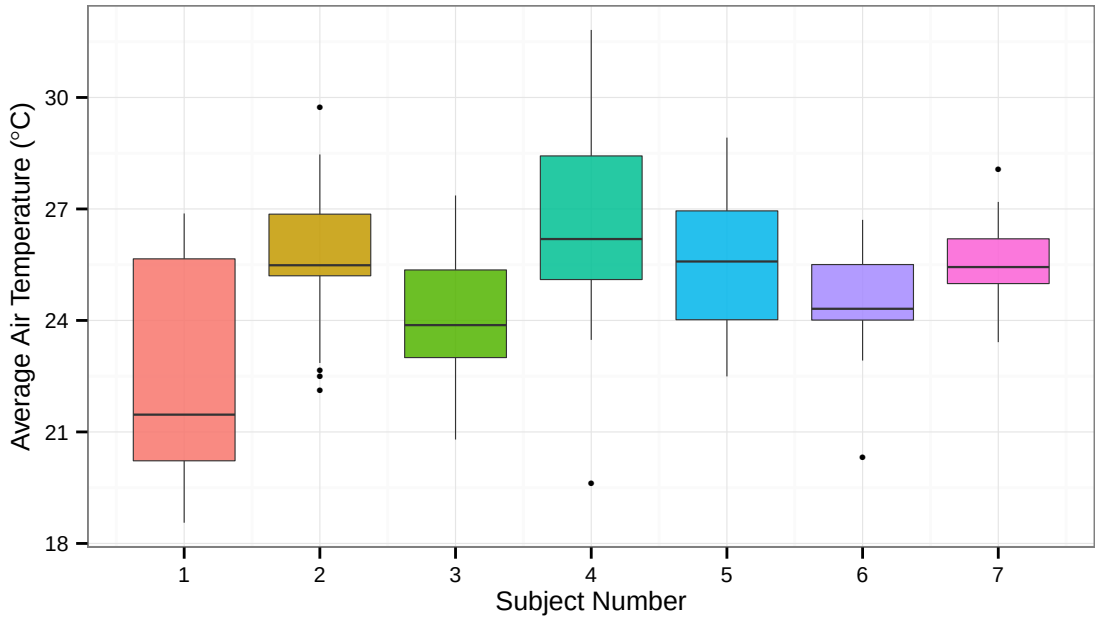

Figure 4.5: Neutral thermal sensation range for each of the seven subjects.

cabin temperatures.

This is the case for overall thermal comfort as well. Figure 4.6 presents the overall thermal comfort reported by the subjects versus the average air temperature across trials *T1, T2* and *T3*. The average air temperature that provides maximum comfort (corresponding to scale unit 3) is 25.5 ℃. However, as in the case of thermal sensation, comfort is achieved within a wider range of average temperatures (19 ℃ to 30 ℃) throughout different conditions and for different people. The same temperature also provides comfort values down to −1. Figure 4.7 shows the average air temperature ranges in which subjects felt comfortable (a comfort index of 2 corresponding to "comfortable"; the comfort index of 3 was not used because not all subjects reported this index within the trials). The figure shows that the ranges differ, like in the case of thermal sensation, amongst the seven subjects. The widest range is encountered for subject 5, between 23 ℃ and 30 ℃, while the narrowest range is encountered for subject 7, between 23 ℃ and 27 ℃.

H4.2: *Neutral thermal sensation corresponds to thermal comfort.*

The literature reports that thermal neutrality results in thermal comfort [47, 59]. This hypothesis is supported to an extent by the data gathered, with figure 4.8 illustrating that the thermal sensation of 0 provides the highest average comfort levels (2 corresponding to "comfortable"). Sensation levels of −1 (corresponding to a "slightly cool" sensation) and 1 (corresponding to a "slightly warm" sensation) also

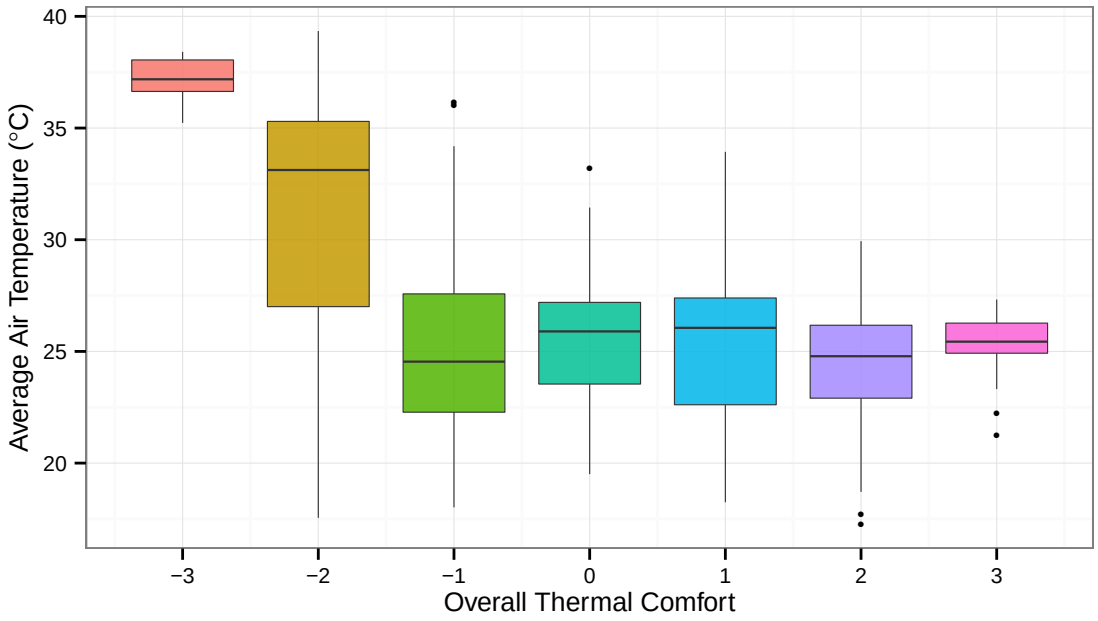

Figure 4.6: Overall thermal comfort versus average car cabin temperature.

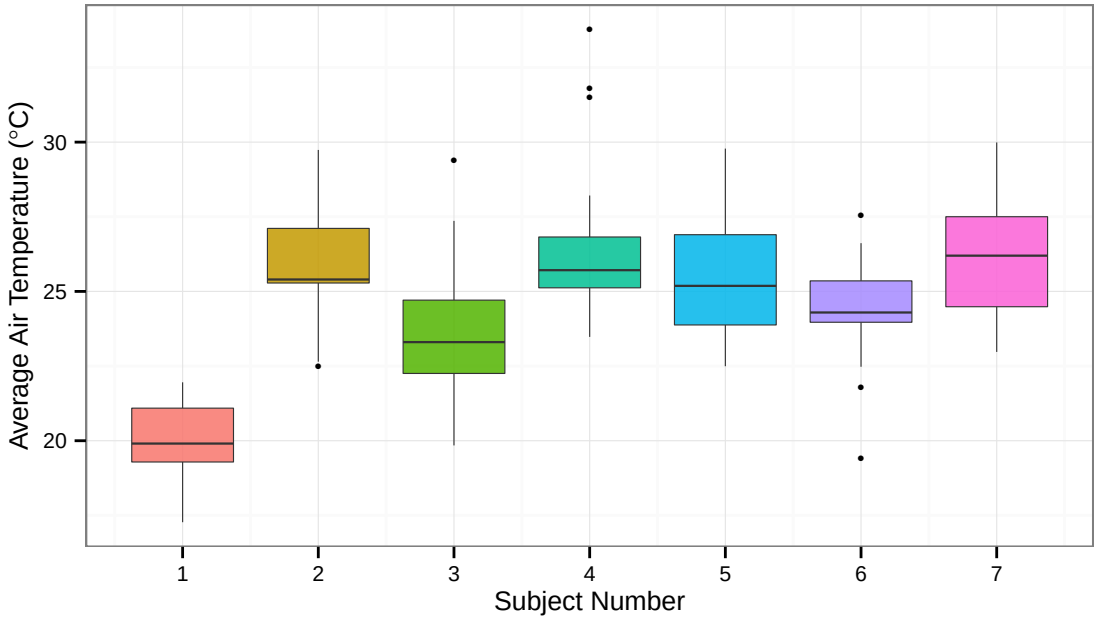

Figure 4.7: Comfortable range for each of the seven subjects.

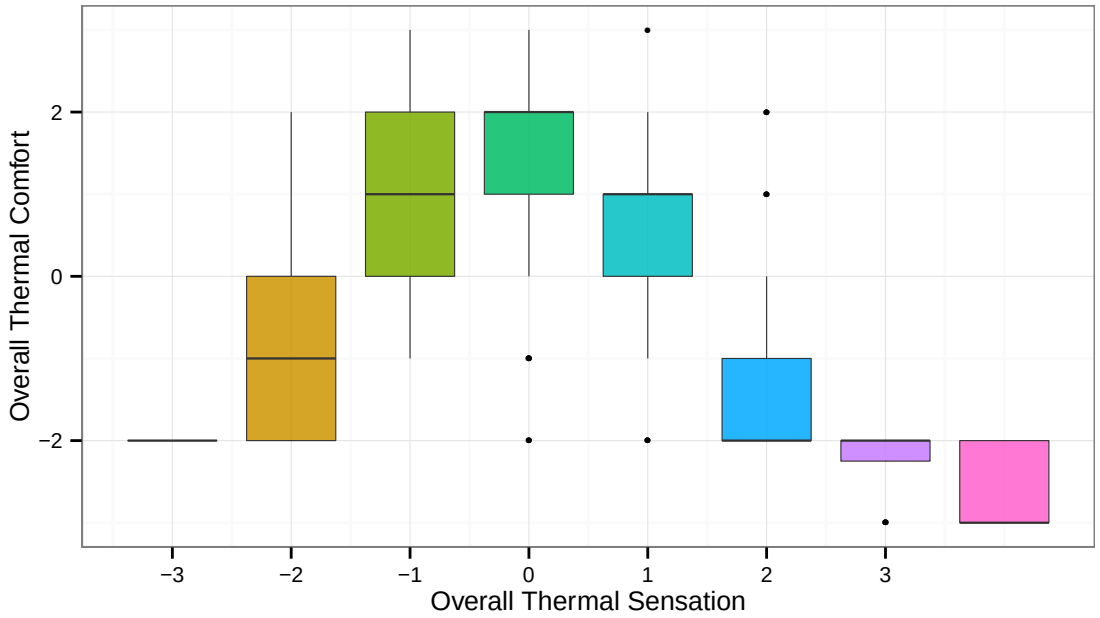

Figure 4.8: Overall thermal sensation versus overall thermal comfort.

provided reasonable comfort levels, averaging at 1 (corresponding to "just comfortable"). A considerable drop-off in comfort is encountered when thermal sensation goes beyond this range (at a thermal sensation level of -2 corresponding to "cool"). If the aim is to provide a comfort level of at least 0, then sensations between -1 and 1 would achieve this. As noted in the answer to the previous hypothesis, this can translate to temperatures anywhere in the 20 ℃ to 30 ℃ range depending on environmental conditions and personal preferences.

Hypothesis **H4.2** is confirmed, though with a caveat. Neutral thermal sensations can be linked to thermal comfort levels above 1, however, thermal comfort higher than 1 can also be experienced at sensations of -1 and 1.

H4.3: *Pre-conditioning a subject to a particular temperature affects the temperatures at which neutral thermal sensation is experienced.*

It is known that various factors influence occupant thermal comfort and sensation, with an important factor being pre-conditioning. If occupants are exposed to a certain temperature before entering the car cabin, then their perception of comfort will differ. In response to hypothesis **H4.3,** Figure 4.9 shows how occupant pre-conditioning affects the perception of thermal neutrality within trials *T1*. The analysis was performed on this type of trials because the environment was controlled and there were no external factors that could further affect the perception of sensation and comfort. Due to working with a discrete

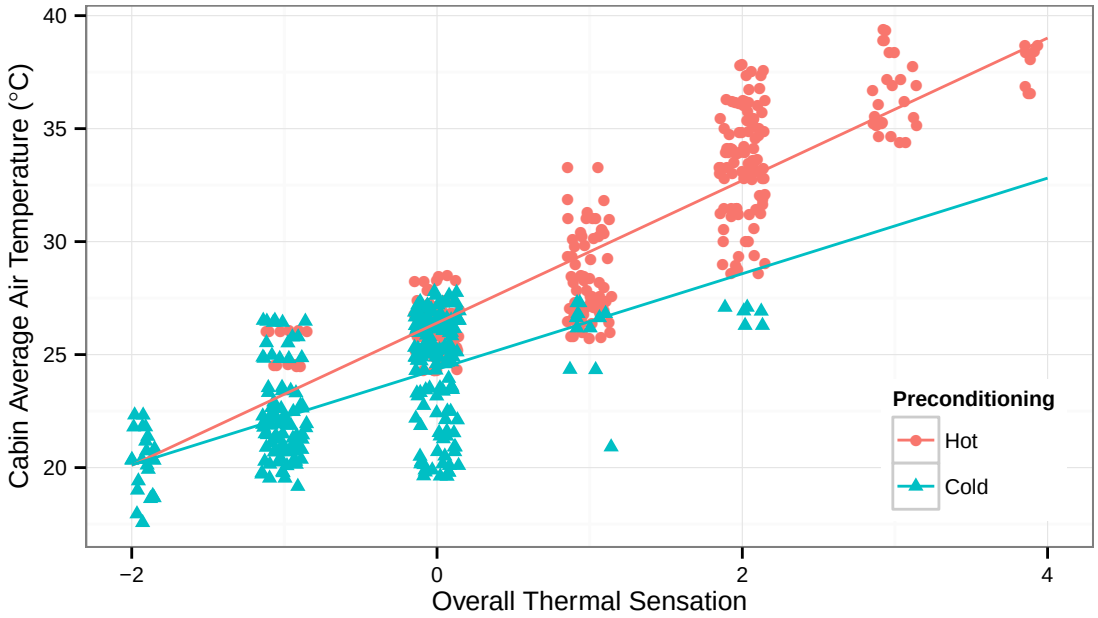

Figure 4.9: Overall thermal sensation versus average car cabin air temperature based on two different types of pre-conditioning: hot and cold.

scale, jittering (the act of adding random noise to data when plotting) is used in order to prevent groups of points obscuring each other.

Both linear regression-based models are statistically significant, with the p-value being smaller than the threshold of 0.001. Figure 4.9 shows that, for example, the "slightly warm" sensation occurs at lower temperatures in case of cold pre-conditioning (as low as 21 ℃). In case of hot pre-conditioning, the same thermal sensation index can be encountered up to 33 ℃. This pattern can be observed for sensation indexes −1 to 2.

Hypothesis **H4.3** is confirmed—pre-conditioning a subject to a particular temperature affects the temperatures at which neutral thermal sensation is experienced.

H4.4: *Solar loading causes a higher thermal sensation for a given cabin average air temperature.*

Another important factor that affects thermal comfort is solar radiation. Figure 4.10 depicts how subjects perceive thermal sensation with and without solar load after initially being neutrally pre-conditioned at 22 ℃. The analysis was performed on trials *T1, T2* and *T3* that involved neutral pre-conditioning. Trials involving cold or hot pre-conditioning have been excluded as pre-conditioning has already been shown to have an impact on thermal sensation. Figure 4.10 shows that when solar load is present subjects achieve similar thermal sensation indexes at lower average temperatures. Both linear regression-based models

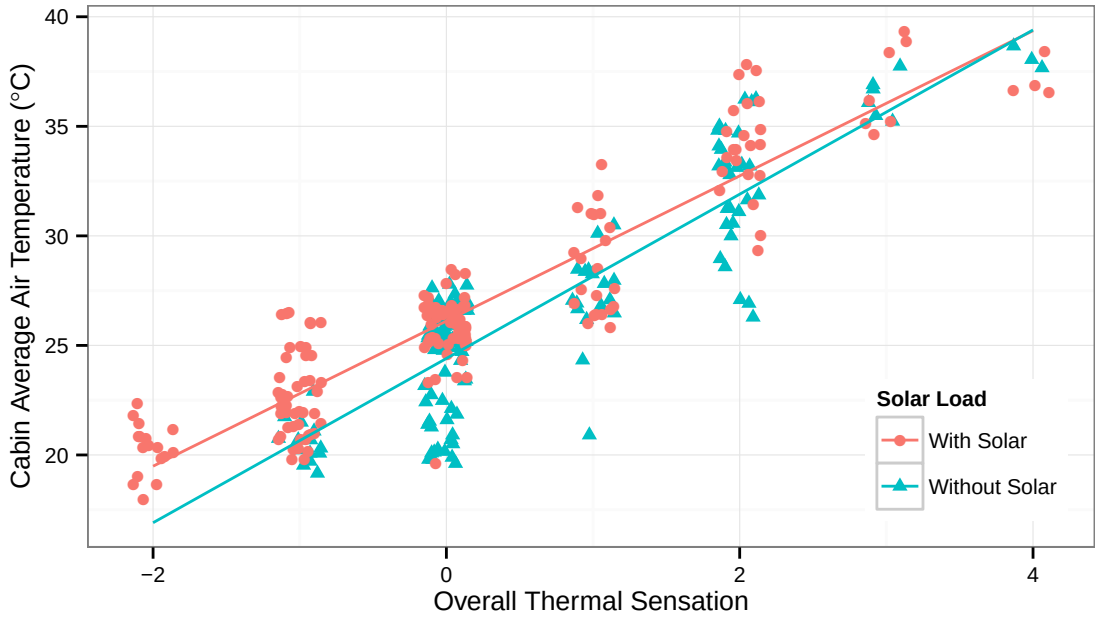

Figure 4.10: Overall thermal sensation versus average car cabin air temperature throughout trials that consist of neutral pre-conditioning.

are statistically significant, with the p-value being smaller than the threshold of 0.001. Other conclusions obtained are:

1. When no solar load was applied, participants experienced neutral thermal sensation at temperatures between 23.8 ℃ and 28.1 ℃. When solar loading was applied, the range was instead 19.9 ℃ to 27.8 ℃.

2. Without solar loading, the range of temperatures in which all subjects were experiencing thermal sensations between -1 and $+1$ was 19.9 ℃ to 26.4 ℃. When solar loading was applied, the range became 19.2 ℃ to 22.7 ℃.

3. It can be seen that solar loading generally decreases the temperature at which a given thermal sensation level will be experienced. Furthermore, when solar loading was applied, the minimum temperature at which neutral sensation was experienced and the minimum temperature at which all subjects experienced a thermal sensation of -1 were the same.

Hypothesis **H4.4** is confirmed—solar load causes a higher thermal sensation for a given temperature.

H4.5: *Manual control provides higher thermal comfort levels than automated control, highlighting the need for learning-based HVAC control.*

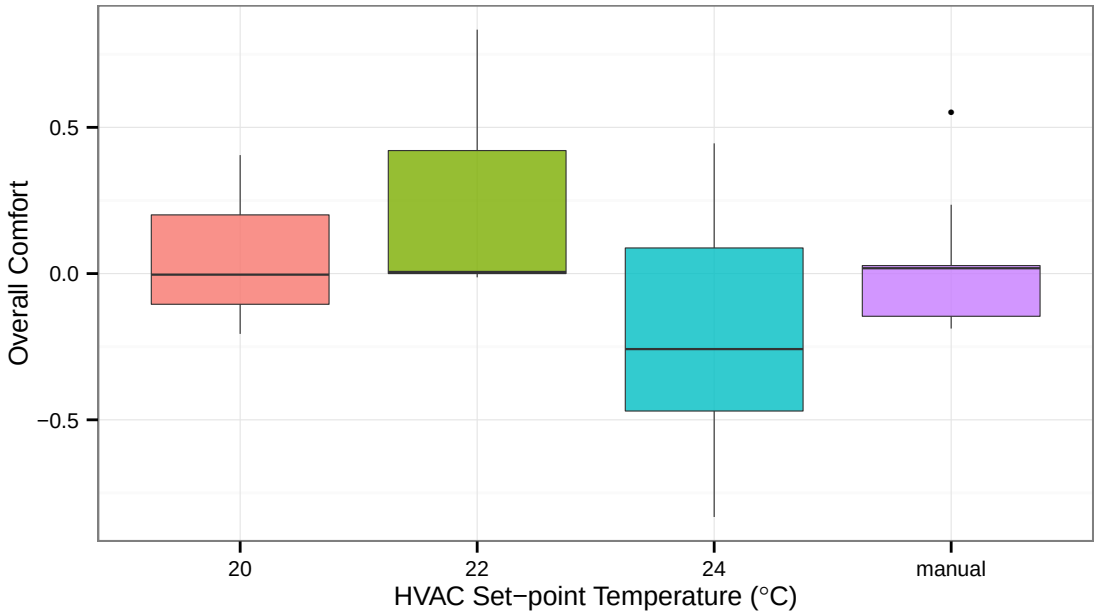

Figure 4.11: Overall reported comfort index by the driver against the HVAC set-point temperature.

In order to test this hypothesis, an analysis on trials *T4* was performed. The trials consisted of the HVAC temperature being set at 20 ℃, 22 ℃, 24 ℃, or manually controlled by the subjects. The purpose of the analysis was to see whether manual control offers passengers better comfort compared to automated control at commonly used set-points. The scale of the reported comfort ranged between -1 (very uncomfortable) and 1 (very comfortable), with 0 being comfortable.

Figures 4.11, 4.12 and 4.13 show the comfort level for each HVAC setting for the driver, left back passenger and right back passenger. As it can be observed, the manual setting offers the highest degree of comfort for all three passengers, with an average of 0.05 for the driver, 0.3 for the left back passenger and 0.2 for the right back passenger. In the case of the driver and left back passenger, the HVAC set-point of 22 ℃ provides a thermal comfort value around 0.05 less than the manual setting, whereas for the right back passenger the difference is more significant—around 0.35. The HVAC set-point of 24 ℃ provides the poorest comfort levels, between -0.25 and -0.4. The coldest setting, of 20 ℃, provides a reasonable comfort level solely for the driver.

This experiment has demonstrated that hypothesis **H4.5** is true—manual control provides higher thermal comfort levels for car cabin occupants.

With manual control offering the highest comfort ratings, learning-based HVAC is clearly needed within the automotive industry and this is a motivational aspect for the work in this thesis. In summary,

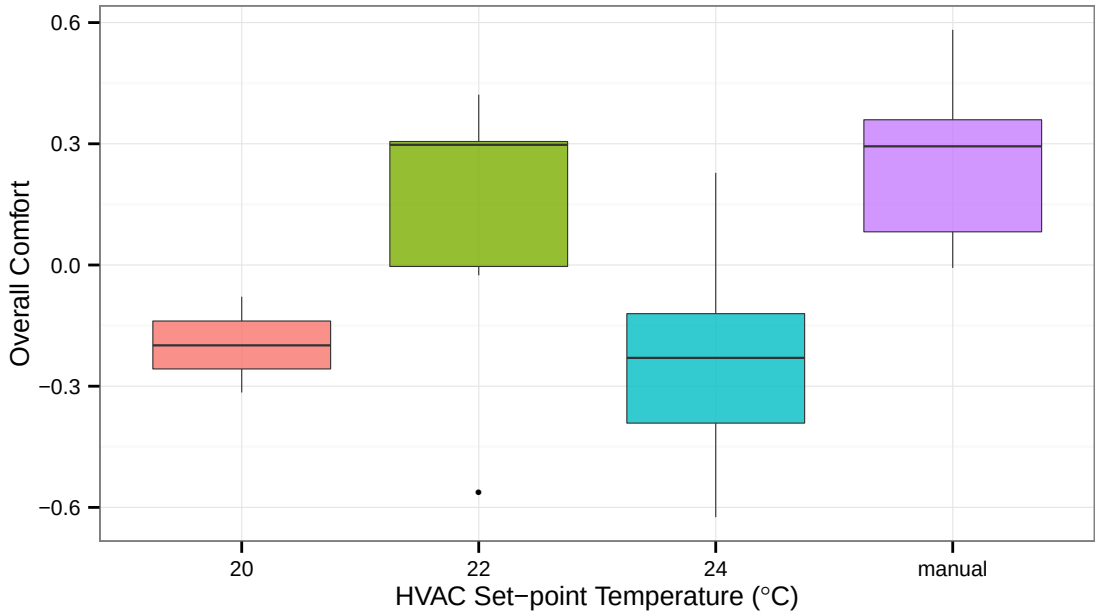

Figure 4.12: Overall reported comfort index by the left back passenger against the HVAC set-point temperature.

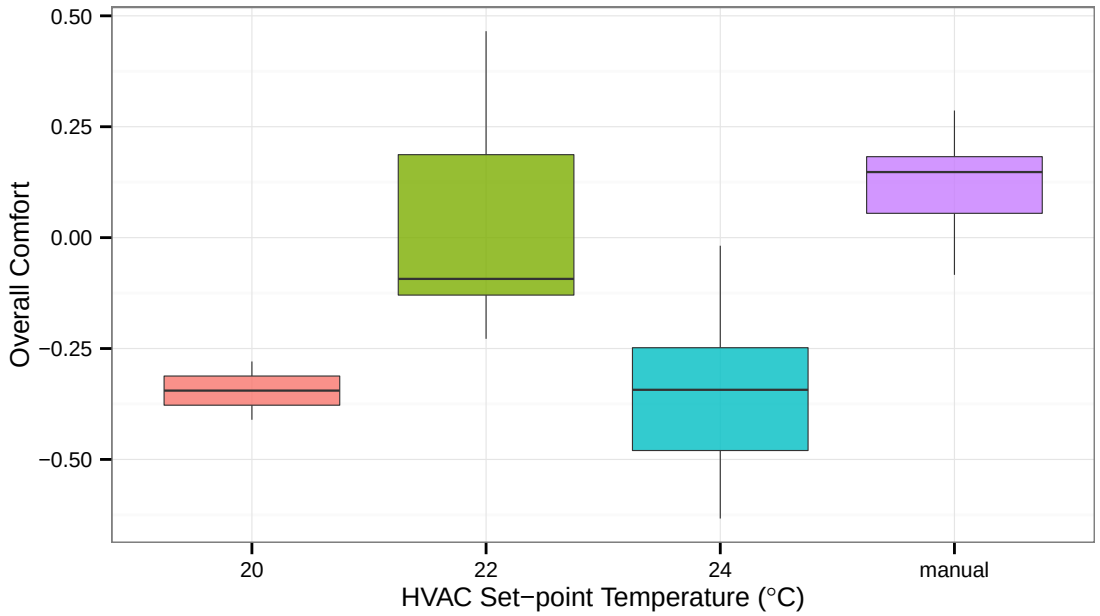

Figure 4.13: Overall reported comfort index by the right back passenger against the HVAC set-point temperature.

thermal comfort is a subjective parameter influenced by many factors including pre-conditioning and solar radiation, as demonstrated by the analysis presented in this section. In the next section, four thermal comfort models in the literature are evaluated based on the gathered data.

4.3 Evaluation of existing thermal comfort models

This section provides an evaluation of four thermal comfort models based on the gathered data described in Section 4.1. The purpose of the analysis is to establish whether they can accurately predict car cabin occupant thermal sensation in any of the conditions in order to be used for comfort-based HVAC control. For this purpose, the overall thermal sensation reports of the drivers were compared to i) the PMV index as computed by the Flatman, ii) Zhang's index computed from the measured skin temperatures, iii) Taniguchi's index computed from the measured facial skin temperature and iv) Nilsson's index computed from the measured average body equivalent temperature.

The following hypotheses are formulated:

H4.6: *The PMV model matches the thermal comfort subjective reports more accurately when the environmental conditions encountered in the car cabin are stable (low cabin air temperature rates of change over time).*

H4.7: *Zhang's model matches the thermal comfort subjective reports more accurately than Taniguchi's model due to it taking into account a higher number of body part skin temperatures.*

H4.8: *Nilsson's equivalent temperature-based thermal comfort model is the most suitable model for comfort-oriented HVAC control.*

PMV is widely used in research for car cabin comfort-based HVAC controllers [5, 13, 20, 44, 49, 63, 112, 143]. The reason is the simplicity of measuring air temperature and humidity, while in most cases the remaining parameters are estimated (for example, the mean radiant temperature is set equal to the air temperature). However, does PMV actually reflect the reported sensation levels of the occupants? Table 4.7 presents the correlation coefficient and the determination coefficient R^2 between the subjective and experimental data for all models. The correlation coefficient quantifies the degree of correlation between two variables, while the R^2 coefficient indicates how well data points fit the linear regression. The p-value for a regression gives the probability that the result is not derived by chance. For all results presented, the p-value is smaller than the threshold (p = 1.2e-0.09) and the results are, therefore, significant.

Table 4.7: Statistic metrics between the models' output and the reported sensation.

	PMV		Taniguchi		Zhang		Nilsson	
Type	Correlation	R^2	Correlation	R^2	Correlation	R^2	Correlation	R^2
T1	0.91	0.85	0.56	0.32	0.10	0.0001	0.93	0.86
T2	0.76	0.57	0.03	0.001	0.50	0.25	0.77	0.59
T3	0.78	0.61	0.15	0.02	0.60	0.35	0.79	0.62

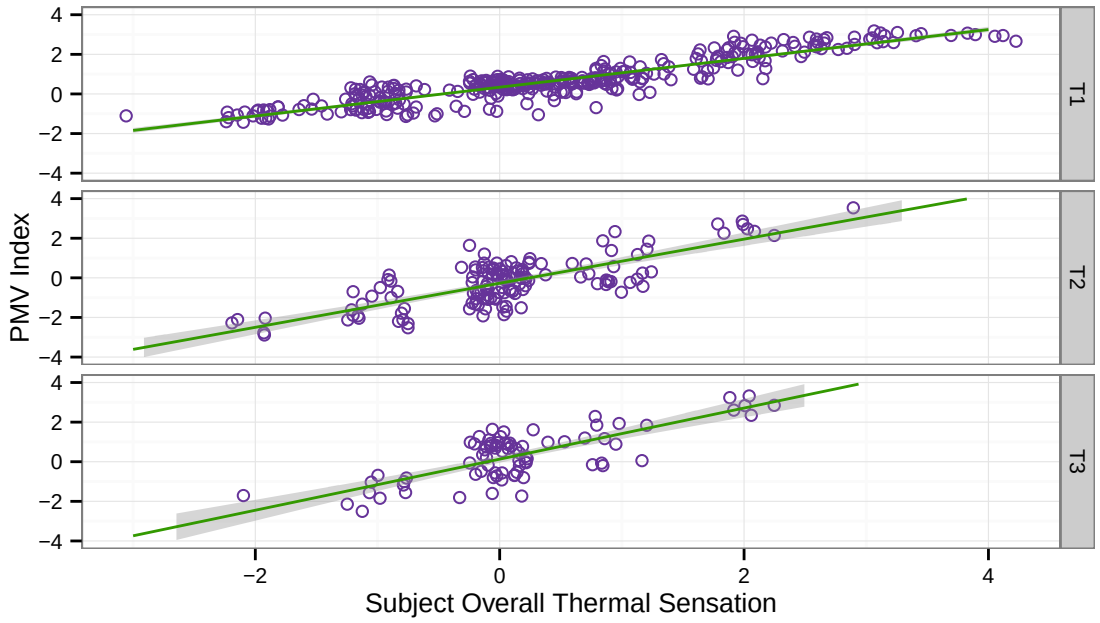

Figure 4.14: Flatman's PMV index versus overall thermal sensation reported by the subjects.

In the case of PMV, the highest level of agreement corresponds to trials *T1,* with a correlation index of 0.91. The high correlation is somewhat expected due to the stable conditions encountered throughout trials *T1* (interior temperature rates of change less than 1.5 ℃ per minute, stable outside temperature and no wind or precipitation). The experimental data matches less accurately the subjective reports in trials *T2* and *T*3. The correlation index between the two is 0.76 for *T2* and 0.78 for *T3.* Overall, Flatman's PMV tended towards colder reports than the subjective reports. For example, for *T1,* subjects reported thermal sensations of up to 4 (corresponding to "very hot"), whereas Flatman's PMV did not go beyond 3 (corresponding to "hot").

This experiment shows hypothesis **H4.6** to be true— the PMV model matches the thermal comfort subjective reports more accurately when the environmental conditions encountered in the car cabin are stable (air temperature rates of change lower than 1.5 ℃ per minute).

The results indicate that PMV can be applied in vehicle cabins to infer passenger comfort within

a limited set of conditions, however, the model brings forward another important issue in this type of environment, the inability to differentiate between different parts of the body. Due to the non-uniform nature of the environment, the difference in thermal sensation over small distances is considerable and so effective HVAC control should be able to warm-up or cool-down separately the feet and head for example.

With PMV's accuracy limited to a narrow range of conditions, the author further investigated two skin temperature-based models: Taniguchi's model and Zhang's model. For Taniguchi's model, as Table 4.7 illustrates, the highest level of agreement corresponds to trials *T1,* with a correlation index of 0.56. In trials *T2* and $T3$, on the other hand, the match is poor, with correlation indexes of 0.03 and 0.15, respectively. Facial skin temperature has a higher impact on overall thermal sensation when the rate of change of air temperature is low (less than 1.0 ℃ per minute), as suggested by the higher correlation for trials *T1.* As Taniguchi's model was developed only with respect to facial skin temperature, it is further interesting to see if Zhang's model improves on this by taking into consideration 8 different body parts.

Zhang's model was developed, like Taniguchi's, for transient environments such as car cabins. During experimentation, skin temperature was sampled at only 8 sites, compared to the 19 sites specified by Zhang. This is justified by the fact that within real-time vehicular comfort control, it would be infeasible to monitor skin temperature at all locations specified by Zhang. However, in order to ensure that the sum of skin temperature segment weightings is 1, the weightings for the contribution of local thermal sensations to the overall sensation were normalised. Mean skin temperature was calculated as a proxy for core temperature (this approach being suggested by Zhang). The body part skin temperatures recorded at the beginning of each trial were used as the set-point temperatures for the body segments in the model. As table 4.7 shows, the correlation levels are poor: 0.10 for *T1*, 0.50 for *T2* and 0.60 for *T3.* As the results show, for trials *T1,* facial skin temperature alone proved to be a better estimator than the combination of 8 different body parts. The performance of the two skin temperature-based models is not sufficient to support vehicular HVAC comfort control.

Table 4.7 shows hypothesis **H4.7** to be neither false nor true. Zhang's model matches the thermal comfort subjective reports more accurately than Taniguchi's model within two types of trials (*T2* and $T3$). However, Taniguchi's model is more suitable than Zhang's model for trials *T1*, suggesting that facial skin temperature is a reasonable thermal comfort predictor in stable conditions.

In order to compute the overall thermal sensation index of Nilsson's model, the equivalent temperature at 8 different body parts was averaged based on body area weightings. Once the average equivalent temperature was computed, the overall thermal sensation index was estimated from Figure 2.1 on page 21, using the diagram corresponding to light clothing (the participants wore light clothing throughout

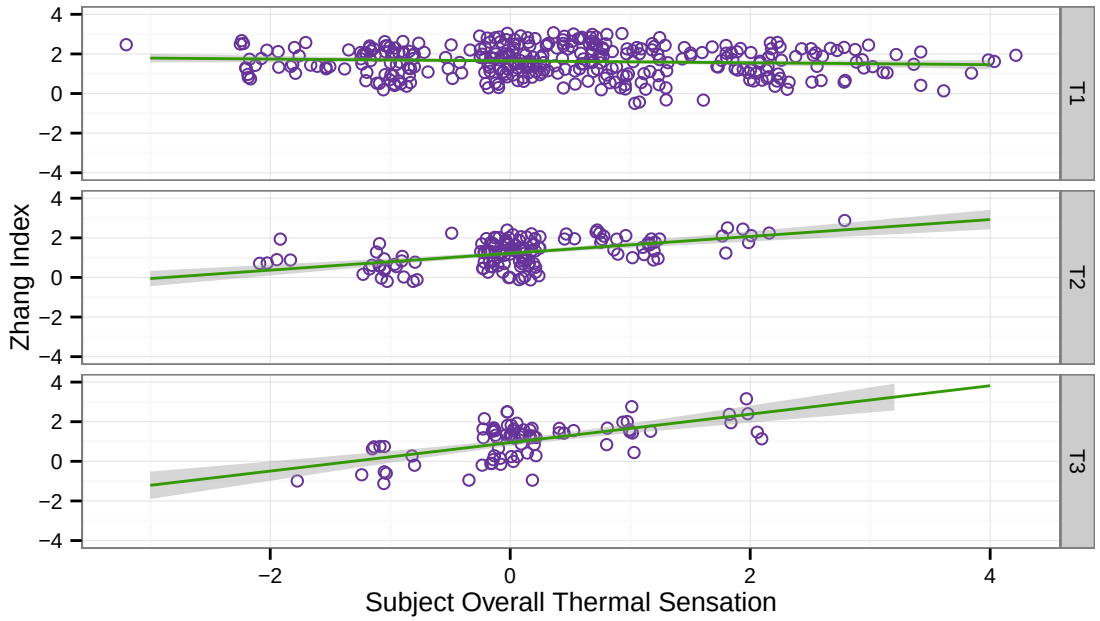

Figure 4.15: Zhang's sensation index versus overall thermal sensation reported by the subjects.

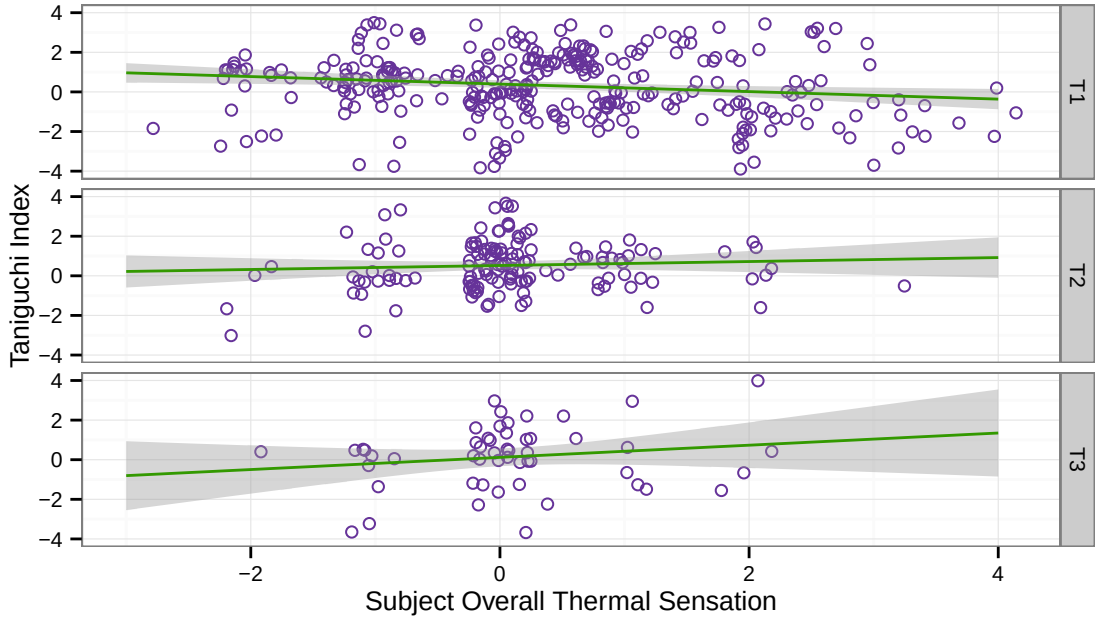

Figure 4.16: Taniguchi's sensation index versus overall thermal sensation reported by the subjects.

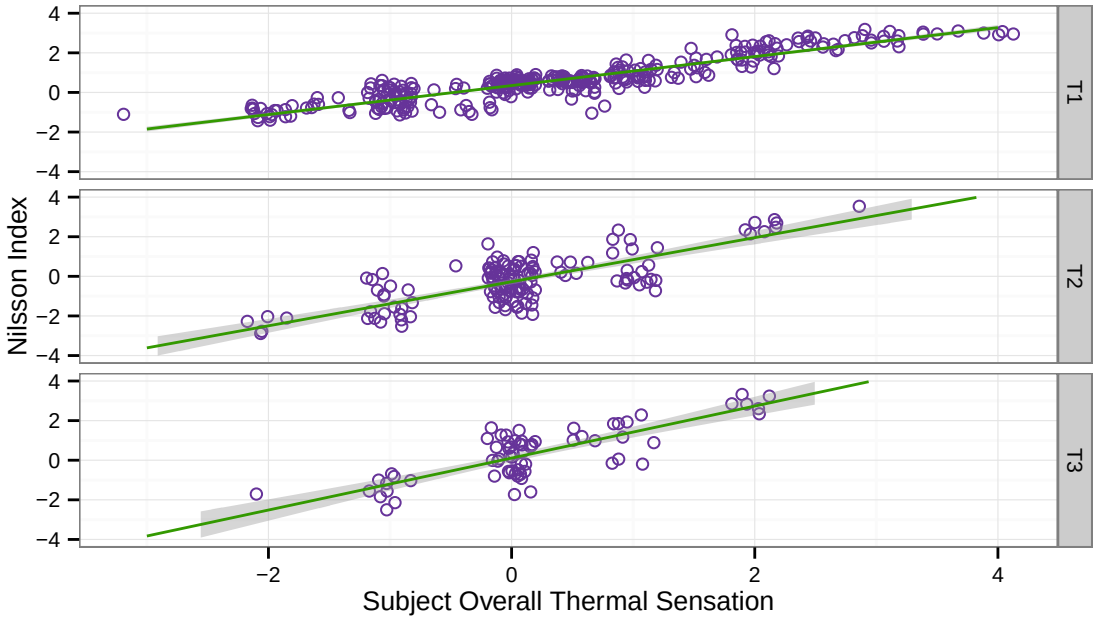

Figure 4.17: Nilsson's sensation index versus overall thermal sensation reported by the subjects.

the experiments).

This experiment shows hypothesis **H4.8** to be true—Nilsson's equivalent temperature-based thermal comfort model is the most suitable for comfort-oriented HVAC control out of the four models evaluated. Nilsson's model had a similar performance to the PMV model. The highest level of agreement with the subjective reports corresponds to trials *T1,* with a correlation index of 0.93. For trials *T2* and *T3*, the correlation index is lower, of 0.77 and 0.79, respectively. The similar performance is somewhat expected, because Flatman's PMV index is also based on the measured average equivalent temperature. The advantage Nilsson's model has over PMV is that local thermal sensation can also be estimated and that it requires less input parameters.

4.4 Summary

This chapter provided insight on the complexity of occupant thermal comfort based on empirical data. The first step was to design experimental trials covering a wide range of conditions: with preconditioning of the occupants and cabin at different temperatures, with or without ambient solar load, wind and precipitations, with steady or varying outside ambient temperature and with different temperature rates of change within the cabin. Then, an investigation related to vehicular thermal sensation and comfort in

vehicles was performed. The main findings related to cabin thermal comfort are:

1. Thermal neutrality does not generally correspond to a certain cabin air temperature set-point, such as 22 ℃.
2. Neutral thermal sensation corresponds, to a certain extent, to thermal comfort.
3. Pre-conditioning a subject to a particular temperature affects the temperatures at which neutral thermal sensation is experienced.
4. Solar loading causes a higher thermal sensation for a given cabin average air temperature.
5. Manual control provides higher thermal comfort levels than automated control, highlighting the need for learning-based HVAC control.

The chapter also evaluated four thermal comfort models, namely PMV, Taniguchi's model, Zhang's model and Nilsson's model in a variety of conditions in order to determine which one is the most suitable for vehicular HVAC control. A model is considered suitable if the correlation score with the subjective reports is higher than 0.70 for all experimental trial types and, also, if they have additional characteristics, such as if they are able to estimate local (not just overall) thermal sensation.

Based on the experimentally gathered data, the PMV index and Nilsson's index accurately matched (with correlations of 0.91 and 0.93, respectively) the occupant reported thermal sensation within a limited set of conditions: pre-conditioning of the passenger and the cabin at the same temperature, a steady outside temperature and low rates of change of the interior temperature (lower than 1.5 ℃ per minute). Higher interior temperature rates of change (up to 9 ℃ per minute), ambient solar load and wind leads to lower correlation factors, between 0.76 and 0.79. As presented earlier in the chapter, the results are significant (p-value = 1.2e-0.09).

The overall thermal sensation computed using the two skin temperature-based thermal comfort models (Taniguchi's model and Zhang's model) had a weak match with the subjective reports throughout all trial types (correlations between 0.10 and 0.60). Overall, based on the data gathered, the accuracy of these models is not sufficient to support vehicular HVAC comfort control.

Capitalizing on the findings, Nilsson's model is shown to be the most suitable thermal comfort model in the literature for vehicular comfort-oriented control. The model provided the highest correlations with subjective thermal sensation throughout the three trial types. An important advantage Nilsson's model has over PMV is its ability to estimate local thermal sensation, which the authors see as an important capability for the new generation vehicular HVAC control systems. Moreover, Nilsson's model

only requires two input parameters, rather than six parameters in PMV's case, some of which could not feasibly be determined by an automated system (for example the air flow at the occupant location).

It is known that no thermal comfort model can provide a perfect match for what people feel. One reason is the subjective nature of thermal sensation and comfort in terms of how comfort is felt and, also, how it is reported. However, adopting Nilsson's equivalent temperature-based model as a basis for estimating occupant comfort control and further integrating online learning within the car for tuning individual preferences would lead to a more thermally comfortable vehicular environment.

The next chapter presents the development and evaluation of a VTCS approach that estimates occupant body part equivalent temperatures from minimalistic, inexpensive cabin environmental sensors.

Chapter 5

Virtual Thermal Comfort Sensing

The previous chapter presented the data gathering trials performed and established the most suitable thermal comfort model to be used for vehicular Heating, Ventilation and Air Conditioning (HVAC) control. This chapter presents the development and evaluation of a vehicular Virtual Thermal Comfort Sensing (VTCS) approach that estimates occupant body part equivalent temperature from a minimalistic set of inexpensive cabin environmental sensors.

Virtual sensing is applied in a variety of domains [93, 142, 158, 160]. The idea behind the concept of vehicular VTCS is that, based on the data from a set of cabin environmental sensors, readings from virtual sensors are inferred. These virtual sensors are assigned to locations that are important in terms of estimating thermal sensation and comfort, but where real sensors cannot be placed due to reasons such as cost, inconvenience to the occupant, because the location is inaccessible or simply because the location provides no means of mounting the sensor.

With Nilsson's equivalent temperature-based model shown to be the most suitable thermal comfort model for HVAC control in the previous chapter, for the work here the virtual sensors are equivalent temperature sensors at eight driver body part locations (head, chest, left lower arm, left upper arm, right lower arm, right upper arm, thigh and calf). Although occupant equivalent temperature can be measured in a realistic end-user scenario, the approach is expensive, intrusive and bulky. Equivalent temperature can be, however, estimated from suitable cabin environmental data. The prerequisites are: i) a good understanding of the cabin environment and the relationships between various sensing locations within the cabin and ii) a machine learning-based method of estimating occupant body equivalent temperature in a variety of conditions based on cabin data.

The reinforcement learning-based control algorithm presented in the next chapter benefits from the use of VTCS due to the following reasons:

1. The occupant thermal comfort variable (in this case occupant equivalent temperature) needs to be integrated into a reward function. The reward function serves as an objective basis for comparing controllers. This particular aspect should be especially useful when making future improvements

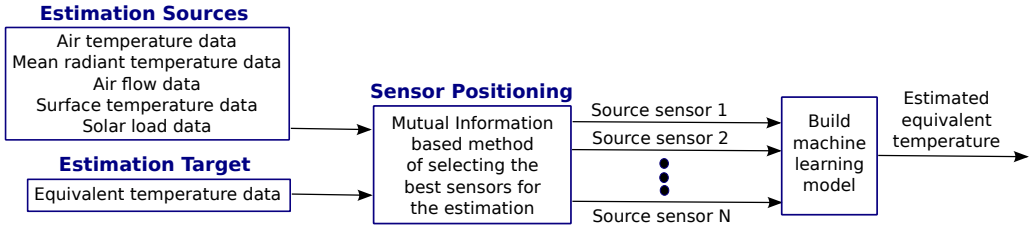

Figure 5.1: Development process for the VTCS approach.

to the developed controller.

2. The Markov property should be satisfied. As described in Section 2.6, the input state corresponding to the environment must ensure the Markov property, meaning that it has to retain all relevant information in order for the reinforcement learning algorithm to be applied.

3. To reduce the dimensionality of the learning problem, with one dimension corresponding to the comfort estimate rather than N dimensions corresponding to the N sensor inputs.

The VTCS-based control is innovative in the automotive field and represents a paradigm shift in the way HVAC control is developed. Moreover, the methods developed here are generic. They can be used in similar applications such as skin temperature driven control or for HVAC control in buildings. The method was successfully applied by the author for estimating cabin occupant skin temperature and for estimating building environmental sensor data at various locations in a room.

A summary of the VTCS development process is given in Figure 5.1. First, cabin environmental data (in this case air temperature, surface temperature, air flow, vent temperature, vent flow, solar load and mean radiant temperature) is collected in experimental trials, along with data for sensors that will later be replaced with virtual counterparts (in this case, equivalent temperature at various body locations). Then, the cabin environmental sensor locations are selected that correlate well with the body part equivalent temperature. A mutual information-based approach is used for this purpose, as described in Section 5.1. After the selection is performed, a machine learning technique infers the virtual equivalent temperatures from the selected cabin environmental sensors. This model, along with the cabin environmental sensor specifications, comprises the VTCS.

Seven learning approaches popular in the literature are investigated for the estimation of equivalent temperature:

1. Multiple Linear Regression (MLR).

2. Multilayer Perceptron (MLP).

3. K-Nearest Neighbour (KNN).
4. Multivariate Adaptive Regression Splines (MARS).
5. Radial Basis Function Network (RBF).
6. Reduced Error Pruning Tree (REPTree).
7. Random Forest (RF).

The research questions this chapter poses are:

1. Can an optimum set of cabin environmental sensors be defined for estimating occupant body part equivalent temperature, given realistic constraints?
2. Which is the most suitable machine learning technique, out of the seven implemented, for estimating occupant body part equivalent temperature from a set of cabin environmental sensors?

The contribution in this chapter is:

- A scheme for designing a VTCS approach, integrating:
    1. A mutual information-based sensor positioning method that selects the cabin environmental sensors (and their corresponding locations) best correlated with occupant body part equivalent temperature.
    2. A machine learning algorithm for estimating equivalent temperature (selected from seven different methods based on the estimation error and processing time required).

The VTCS method is developed and evaluated offline, on the real-world data sets described in Section 4.1.

This chapter is structured as follows: Section 5.1 describes the implementation and evaluation of the mutual information-based sensor positioning method. Section 5.2 describes the implementation and evaluation of the seven machine learning algorithms for equivalent temperature estimation, while Section 5.3 provides further analysis on the MLR-based equivalent temperature estimation. Finally, Section 5.4 presents a summary of the work in this chapter.

5.1 Sensor positioning through mutual information

Common sensor positioning approaches are driven by considerations such as cost or aesthetics, which may impact on the performance of the HVAC system and thus on occupant thermal comfort. Methods that

quantify the spatial-temporal variations in the car cabin environment by using similarity measures are needed in order to provide accurate estimates of virtual temperatures that would drive *occupant* rather than *cabin* focused HVAC control algorithms.

In the work here, the selection of the best cabin environmental sensors from those available is performed via a mutual information method based on entropy values. Mutual information is a quantitative measurement of how much one random variable tells us about another random variable. Mutual information is used as a feature selection technique in multiple works [11, 125, 136, 150, 157] and it performs similarly to a correlation analysis. Correlation measures linear relationships or monotonic relationships between two random variables. On the other hand, mutual information is a more general concept and measures the reduction of uncertainty in a random variable after observing another. Mutual information can therefore measure non-monotonic relationships and, in general, more complicated relationships. Within this thesis, the variables followed a normal distribution and therefore, using a correlation measure would have sufficed. However, if a non-linear variable is added, such as a binary variable specifying whether a control actuator is active or a binary variable specifying whether the window is open or not, mutual information represents a more reliable solution. Figure 5.2 shows a graphical representation of the mutual information between pairs of equivalent temperatures and potential cabin environmental sensors. The line thickness is directly proportional to the mutual information value.

The mutual information computation method follows the process shown in Figure 5.3 and is described in the following subsections.

5.1.1 Computing marginal entropies and mutual information

Given two sensors X and Y, let X be the equivalent temperature sensor data and Y the cabin environmental sensor data. Using the entropy concept, the mutual information between the two data streams, $I(X;Y)$, is:

$$I(X;Y) = H(X) - H(X \mid Y) \tag{5.1}$$

where $H(X)$ is the marginal entropy of X and $H(X \mid Y)$ is the conditional entropy of X given Y. Using the conditional entropy definition, $H(X \mid Y) = H(Y) - H(X,Y)$, mutual information can be computed as:

$$I(X;Y) = H(X) - H(Y) + H(X,Y) \tag{5.2}$$

where $H(X,Y)$ is the joint entropy of X and Y.

Both the marginal entropies and the joint entropy can be computed from the general joint entropy

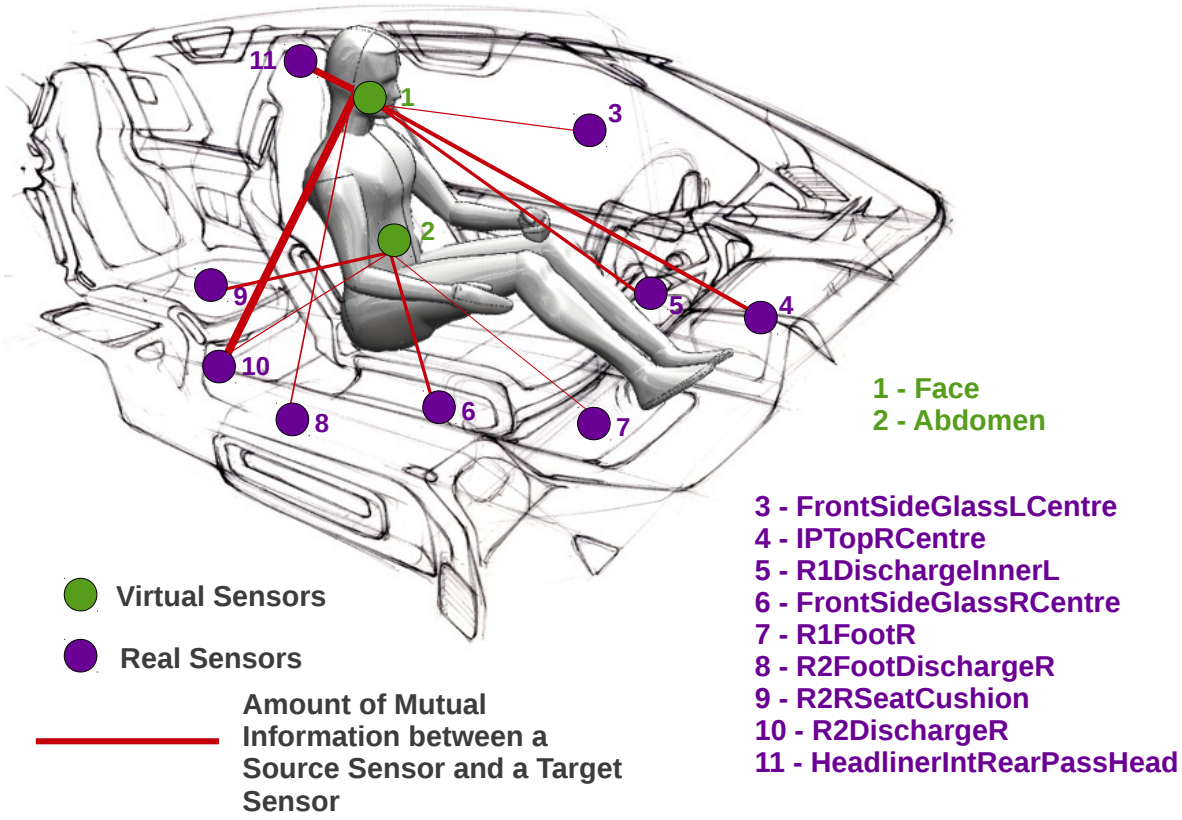

Figure 5.2: The mutual information concept.

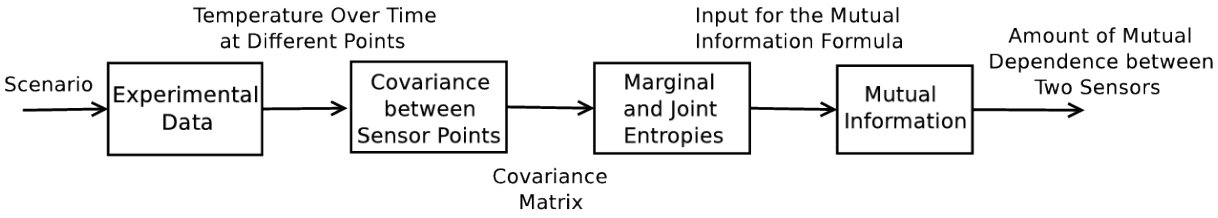

Figure 5.3: Entropy-based approach for computing mutual information.

formula for a multivariate normal distribution:

$$H(X_1, X_2, ..., X_k) = \frac{1}{2} \times \ln\left((2 \times \pi \times e)^k |\Sigma|\right) \tag{5.3}$$

where k represents the number of random variables forming the distribution and Σ is the covariance matrix of the variables.

5.1.2 Extending the mutual information concept for multiple cabin environmental sensors

Using several cabin environmental sensors in conjunction increases the mutual information shared with the equivalent temperatures, leading to a more accurate estimate of the latter. Computing the mutual information from multiple cabin environmental sensors is performed similarly to the previous case. Given $n+1$ sensors $X_1, ..., X_n$ and Y, let $X_1, ..., X_n$ be the cabin environmental sensors data and Y be the equivalent temperature data. Based on equation 4.1, the mutual information between the n cabin environmental sensors data and the equivalent temperature data is:

$$I(Y; X_1, ..., X_n) = H(Y) - H(Y|X_1, ..., X_n) \tag{5.4}$$

The conditional entropy is:

$$H(Y|X_1, ..., X_n) = H(Y, X_1, ..., X_n) - H(X_1, ..., X_n) \tag{5.5}$$

where $H(Y, X_1, ..., X_n)$ is the joint entropy for the $n+1$ sensors, while $H(X_1, ..., X_n)$ is the joint entropy for the n cabin environmental sensors. The mutual information is calculated as:

$$I(Y; X_1, ..., X_n) = H(Y) + H(X_1, ..., X_n) - H(Y, X_1, ..., X_n). \tag{5.6}$$

The marginal entropy $H(Y)$, as well as the joint entropies $H(X_1, ..., X_n)$ and $H(Y, X_1, ..., X_n)$, can be computed using equation (4.3).

5.1.3 Maximizing mutual information

If the best set of cabin environmental sensors for each body part equivalent temperature was selected then the total number of cabin environmental sensors to be placed within the car cabin would be relatively

Table 5.1: The five cabin environmental sensors sharing the highest mutual information for trials *T1*, *T2* and *T3*.

Cabin Environmental Sensor	Mutual Information
Air temperature row 2 right breath	0.88 nats
Air temperature row 2 left breath	0.82 nats
Air temperature row 2 belt	0.80 nats
Surface temperature row 2 left seat back	0.78 nats
Air temperature row 1 belt	0.76 nats

large. Therefore, the ultimate goal is to select the subset of cabin environmental sensors that provide the highest mutual information over all body part equivalent temperature. For convenience, the mutual information is denoted here with MI. The cabin environmental sensors data which maximise:

$$(MI_{\mathrm{H}} + MI_{\mathrm{CH}} + MI_{\mathrm{LAL}} + MI_{\mathrm{LAR}} + MI_{\mathrm{UAL}} + MI_{\mathrm{UAR}} + MI_{\mathrm{T}} + MI_{\mathrm{CA}}) \tag{5.7}$$

would be thus selected (Subscripts: H—head, CH—chest, LAL—lower arm left, LAR—lower arm right, UAL—upper arm left, UAR—upper arm right, T—thigh and CA—calf).

5.1.4 Variable normality

The mutual information computation method presented above, as well as some of the machine learning methods further used in estimating equivalent temperature, require normally distributed data as input. The normality of the data was, therefore, verified by applying D'agostino's normality test [34]. The normality hypothesis was confirmed for all variables.

5.1.5 Results

The results are presented separately for trials *T4* because the set of sensors used within the cabin was different. For trials *T1*, *T2* and *T3,* Table 5.1 lists the five cabin environmental sensors that shared the highest mutual information with the eight equivalent temperatures. The highest mutual information, of 0.88 nats (mutual information unit measure), was achieved with the air temperature sensor corresponding to the right breath level at the back row.

Table 5.2 shows the best five pairs of cabin environmental sensors that shared the highest mutual information with the eight body part equivalent temperature. The highest mutual information, of 1.39 nats, was achieved between the air temperature sensor corresponding to the right breath level at the back row and the surface temperature at the left seat back in the back row. Overall, the five pairs of sensors

Table 5.2: The five pairs of cabin environmental sensors sharing the highest mutual information for trials *T1*, *T2* and *T3*.

Cabin Environmental Sensor Pair	Mutual Information
Air temperature row 2 right breath + Surface temperature row 2 left seat back	1.39 nats
Vent temperature driver centre + Air temperature row 2 left breath	1.37 nats
Air temperature row 1 left foot + Air temperature row 1 belt	1.36 nats
Air temperature row 2 left breath + Surface temperature row 1 passenger seat back	1.35 nats
Vent temperature driver centre + Air temperature row 1 left breath	1.34 nats

Table 5.3: The five cabin environmental sensors sharing the highest mutual information for trials *T4*.

Cabin Environmental Sensor	Mutual Information
Mean radiant temperature	0.79 nats
Air temperature left seat belt left	0.48 nats
Air temperature right seat belt right	0.47 nats
Air temperature left seat belt right	0.41 nats
Air temperature right seat belt left	0.40 nats

included sensors measuring air temperature at the breath, chest or foot level of the occupants, together with humidities at the head or hand level, surface temperatures at the left seat back and centre vent air temperatures.

As individual sensors, the surface temperature, skin temperature and humidity sensors shared low mutual information values with the equivalent temperatures (as low as 0.001 nats). However, in combination with another sensor (usually an air temperature sensor), the mutual information increases considerably. The impact on the estimation accuracy when the number of cabin environmental sensors increases is further discussed in Section 5.2.

For trials *T4,* the most important addition to the set of sensors was the mean radiant temperature, a parameter used to calculate equivalent temperature. Table 5.3 shows the five cabin environmental sensors that shared the highest mutual information with the eight body part equivalent temperature. The highest mutual information, of 0.79 nats, was achieved with the mean radiant temperature measured at a central ceiling location.

Table 5.4 shows the five pairs of cabin environmental sensors that shared the highest mutual information with the eight body part equivalent temperature. The highest mutual information, of 0.86 nats, was achieved from the mean radiant temperature measured at a central ceiling location and the air temperature at the front left seat left head level. All five pairs of cabin environmental sensors included the mean radiant temperature as a component, suggesting the importance of including this parameter when estimating equivalent temperatures.

To note, the mutual information values corresponding to trials *T1*, *T2* and *T3* cannot be compared

Table 5.4: The five cabin environmental sensor pairs sharing the highest mutual information for trials *T4*.

Cabin Environmental Sensor Pair	Mutual Information
Mean radiant temperature + Air temperature left seat head left	0.86 nats
Mean radiant temperature + Solar load dashboard	0.84 nats
Mean radiant temperature + Air temperature right seat head right	0.83 nats
Mean radiant temperature + Air temperature left seat belt left	0.83 nats
Mean radiant temperature + Air temperature dashboard right	0.82 nats

to the mutual information values corresponding to trials *T4* due to different sensor input data.

5.2 Equivalent temperature estimation

Several machine learning methods were implemented and evaluated for estimating equivalent temperature, namely MLR, MLP, REPTree, KNN, MARS, RBF and RF. The following hypothesis is tested:

H5.1: *MLR will outperform the other estimation approaches with regard to fast processing time, however, it will not be the most accurate method.*

To implement the machine learning methods the author used Python [154], the Waikato Environment for Knowledge Analysis (WEKA) software libraries [65] (developed at the University of Waikato and consisting of a collection of machine learning algorithms for data mining tasks, including tools for data pre-processing, classification, regression, clustering, association rules, and visualisation) and the open-source Orange software libraries [39].

Cross-Validation (CV) was used to evaluate each estimator's performance on the full set of experimental data, indicating how well the algorithm generalised to unseen data. Both K-fold CV (presented in Algorithm 5.1) (with $k = 10$) and Leave-One-Trial-Out-Cross-Validation (LOTOCV) (presented in Algorithm 5.2) were applied. K-fold CV has the original data randomly partitioned into k subsets of equal size. Then, out of the k subsets, one subset is used for validating the model, while the remaining $k - 1$ subsets are used for training the model. The CV process is then repeated k times and the k results from the folds are averaged to produce a single estimation. On the other hand, LOTOCV has the original data partitioned into the 95 individual trials conducted. Then, out of the 95 trials, one trial is used for validating the model, while the remaining 94 trials are used for training the model. The LOTOCV process is then repeated 95 times and the 95 results from the folds are averaged to produce a single estimation. The author used LOTOCV to better cope with the tendency of autocorrelation for time series data and, also, with the existing trial-to-trial variation. The outputs of the estimators were compared to the original measured equivalent temperature and Root Mean Square Error (RMSE)

Algorithm 5.1 K-fold Cross-Validation process.

1. The whole dataset is randomly partitioned into k samples of equal size.
2. One sample out of the k is selected as the validation data.
3. The remaining $k-1$ samples are used as training data.
4. The process is repeated k times, with each sample set used once as validation data.
5. The k results are averaged to provide a mean error over the individual cross-validation processes.

Algorithm 5.2 Leave-One-Trial-Out-Cross-Validation process.

1. The whole dataset is partitioned into n individual experimental trials.
2. One trial out of the n is selected as the validation data.
3. The remaining $n-1$ trials are used as training data.
4. The process is repeated n times, with each trial set used once as validation data.
5. The n results are averaged to provide a mean error over the individual cross-validation processes.

was used as an accuracy measure. The estimation was performed using the best two sensors selected as described in Section 5.1 (Air temperature at row 2 right breath and Surface temperature row 2 left seat back).

The following subsections provide the results for each method, followed by a summary in Section 5.2.8. The most suitable method selected is further analysed in Section 5.3.

5.2.1 Multiple Linear Regression

MLR [43] models the relationship between a response variable (the variable we want to provide an estimate for) and two or more explanatory variables (the variables from which the estimate is performed) by fitting a linear equation to the observed data. Given $n+1$ observations Y, $X_1, ..., X_n$, let Y be the response variable and $X_1, ..., X_n$ be the explanatory variables. The estimate of a particular response variable value is:

$$Y_i = a + b_1 \times X_{1i} + b_2 \times X_{2i} + ... + b_n \times X_{ni} \tag{5.8}$$

where Y_i is the response variable estimate, a is the intercept of the regression line, $b_1, ..., b_n$ are the regression parameters and $X_{1i}, ..., X_{ni}$ are the explanatory variables values.

In the regression case with one explanatory variable the estimation is performed via:

$$\begin{aligned} Y_i &= a + b \times X_i \\ b &= \frac{\mathrm{Cov}_{XY}}{\mathrm{Var}_X} \\ a &= \overline{Y} - b \times \overline{X} \end{aligned} \tag{5.9}$$

where Cov_{XY} is the covariance between X and Y, Var_X is the variance of X, and $\overline{Y}$ and $\overline{X}$ are the means of Y and X respectively. Therefore, the estimated response variable value is:

$$Y_i = \overline{Y} - \frac{\mathrm{Cov}_{XY}}{\mathrm{Var}_X} \times \overline{X} + \frac{\mathrm{Cov}_{XY}}{\mathrm{Var}_X} \times X_i = \overline{Y} + \frac{\mathrm{Cov}_{XY}}{\mathrm{Var}_X} \times (X_i - \overline{X}) \tag{5.10}$$

The covariance matrix (a matrix whose element in the i, j position is the covariance between the i^{th} and j^{th} elements of a random vector) of X and Y is:

$$\mathrm{Cov} = \begin{pmatrix} \mathrm{Var}_X & \mathrm{Cov}_{XY} \\ \mathrm{Cov}_{YX} & \mathrm{Var}_Y \end{pmatrix} \tag{5.11}$$

Implementation

MLR was implemented in Python. Based on the principle described above, in the case of n regressors (the variables from which the prediction is performed) the covariance matrix can be partitioned as:

$$\mathrm{Cov} = \begin{pmatrix} \mathrm{Var}_{YY} & \mathrm{Cov}_{Y(X_1 \ldots X_n)} \\ \mathrm{Cov}_{(X_1 \ldots X_n)Y} & \mathrm{Var}_{(X_1 \ldots X_n)(X_1 \ldots X_n)} \end{pmatrix} \tag{5.12}$$

The estimated value is computed as:

$$Y_i = \overline{Y} + \mathrm{Cov}_{Y(X_1 \ldots, X)} \times \left(\mathrm{Cov}_{(X_1 \ldots X_n)(X_1 \ldots X_n)}\right)^{-1} \times \left(\begin{pmatrix} X1 \\ \vdots \\ X_n \end{pmatrix} - \begin{pmatrix} \overline{X}_1 \\ \vdots \\ \overline{X}_n \end{pmatrix} \right) \tag{5.13}$$

where y_1,...,y_n are particular values of Y_1,...,Y_n, respectively.

Table 5.5: Equivalent temperature estimation RMSE from the best two cabin environmental sensors using MLR.

	Estimation RMSE	
Body part	LOTOCV	10-fold CV
Head	1.91 ℃	1.81 ℃
Chest	1.41 ℃	1.42 ℃
Lower arm left	1.85 ℃	1.78 ℃
Lower arm right	1.59 ℃	1.49 ℃
Upper arm left	1.65 ℃	1.61 ℃
Upper arm right	1.77 ℃	1.70 ℃
Thighs	1.30 ℃	1.33 ℃
Calf	1.81 ℃	1.91 ℃
Average	1.66 ℃	1.63 ℃

Evaluation and results

For each of the 96 separate trials in turn, data from 95 trials were used for training and the remaining trial data were used for testing with LOTOCV. A 10-fold CV was used as an additional evaluation criteria. A summary of the result of applying a MLR approach on all datasets is given in Table 5.5. The results of the evaluation show that the RMSE varied between 1.30 ℃ and 1.91 ℃ (for the thigh and head, respectively) when LOTOCV was applied and between 1.33 ℃ and 1.81 ℃ (for the thigh and head, respectively) when 10-fold CV was applied.

5.2.2 Multilayer Perceptron

MLP [71] is a feed-forward artificial neural network model that consists of multiple layers of nodes and maps the input data onto an appropriate output. The back-propagation technique is used for training the network, as presented in Algorithm 5.3.

Implementation

The estimator was implemented in Python using WEKA libraries. The MLP parameters were set as: the number of hidden layers is 2, the learning rate is 0.2, the momentum is 0.2 and the training time corresponds to 500 epochs. The parameters were selected based on an initial empirical investigation.

Evaluation and results

For each of the 96 separate trials in turn, data from 95 trials were used for training and the remaining trials data were used for testing with LOTOCV. A 10-fold CV was used as an additional evaluation criteria. A summary of the result of applying a MLP approach on all datasets is given in Table 5.6.

Algorithm 5.3 Back-propagation algorithm for MLP [71].

1. A feed-forward network with n_{input} inputs, n_{hidden} hidden hidden units and n_{output} output units is created.
2. All network weights are initialised to small random numbers.
3. Until the terminal state is met do:
   (a) For each $< x, t >$ within the training samples do:
      i. Input x to the network and compute o_u of every unit u.
      ii. For each network output unit k, calculate its error term δ_k as follows: $\delta_k \leftarrow o_k(1-o_k)(t_k - o_k)$.
      iii. For each hidden unit h, calculate its error term δ_h as follows: $\delta_h \leftarrow o_h(1 - o_h)\sum_{k \epsilon outputs} w_{kh}\delta_k$.
      iv. Update each weight according to: $w_{ji} \leftarrow w_{ij} + \Delta w_{ji}$, where $\Delta w_{ji} = \eta \delta_j x_{ji}$.

Table 5.6: Equivalent temperature estimation RMSE from the best two cabin environmental sensors using MLP.

	Estimation RMSE	
Body part	LOTOCV	10-fold CV
Head	1.87 ℃	2.98 ℃
Chest	1.40 ℃	1.87 ℃
Lower arm left	1.56 ℃	2.23 ℃
Lower arm right	1.59 ℃	2.25 ℃
Upper arm left	1.48 ℃	2.08 ℃
Upper arm right	1.74 ℃	2.62 ℃
Thigh	1.18 ℃	1.76 ℃
Calf	1.48 ℃	2.48 ℃
Average	1.53 ℃	2.28 ℃

The results of the evaluation show that the RMSE varied between 1.40 ℃ and 1.87 ℃ (for the chest and head, respectively) when LOTOCV was applied and between 1.76 ℃ and 2.98 ℃ (for the thigh and head, respectively) when 10-fold CV was applied.

5.2.3 K-Nearest Neighbour

KNN [30] represents an instance-based lazy learning method considering the closest training examples in the feature space. The method relies in classifying an object by the majority vote of its neighbours. The object is assigned to the class most common amongst its k nearest neighbours, with k being a positive (typically small) integer. In the case of $k = 1$, the object is assigned to the class of the single nearest neighbour. The algorithm is presented in Algorithm 5.4.

Algorithm 5.4 KNN algorithm [30].

1. For each training sample $< x, f(x) >$ add it to the list of training samples.
2. Given a query instance x_q to be classified:
   (a) Let $x_1, x_2, \ldots, x_k$ denote the k instances from the training samples that are nearest to x_q.
   (b) Return the class that represents the maximum of the k instances.

Table 5.7: Equivalent temperature estimation RMSE from the best two cabin environmental sensors using KNN.

	Estimation RMSE	
Body part	LOTOCV	10-fold CV
Head	2.15 ℃	0.71 ℃
Chest	1.52 ℃	0.46 ℃
Lower arm left	2.08 ℃	0.59 ℃
Lower arm right	1.87 ℃	0.64 ℃
Upper arm left	1.76 ℃	0.46 ℃
Upper arm right	2.00 ℃	0.63 ℃
Thigh	1.58 ℃	0.42 ℃
Calf	1.88 ℃	0.58 ℃
Average	1.85 ℃	0.56 ℃

Implementation

The estimator was implemented in Python using the Orange software libraries. The KNN parameter were set as $k = 5$ as this is a commonly used value.

Evaluation and results

For each of the 96 separate trials in turn, data from 95 trials were used for training and the remaining trial data were used for testing with LOTOCV. A 10-fold CV was used as an additional evaluation criteria. A summary of the result of applying a KNN approach on all datasets is given in Table 5.7. The results of the evaluation show that the RMSE varied between 1.52 ℃ and 2.15 ℃ (for the chest and head, respectively) when LOTOCV was applied and between 0.42 ℃ and 0.71 ℃ (for the thigh and head, respectively) when 10-fold CV was applied. The results of the 10-fold CV are more accurate than the ones corresponding to LOTOCV due to over-fitting (results are not representative for unseen data) the model.

5.2.4 Multivariate Adaptive Regression Splines

MARS [56, 69] is a non-parametric regression technique that models non-linearities and interactions between variables. The basis functions, together with the model parameters (estimated with the least squares estimation method), are combined to predict the inputs. The general model equation is written as:

$$y = f(X) = \beta_o + \sum_{m=1}^{M} \beta_m \times h_m(X) \tag{5.14}$$

where y is the prediction as a function of the input variables X, β_o is an intercept parameter and $h_m(X)$ are the basis functions. The algorithm searches over the space of all inputs and predictor values as well as interactions between variables. Throughout this search a larger number of basis functions are added to the model in order to maximise an overall least squares goodness-of-fit criterion. As a result of these operations, MARS determines the most important independent variables as well as the most significant interactions among them.

Implementation

The estimator was implemented in Python using the Orange software libraries. The MARS parameters were set as: the maximum degree of the terms in the model is 2 and the maximum number of terms in the forward pass is 10. The values were set based on an initial empirical investigation.

Evaluation and results

For each of the 96 separate trials in turn, data from one trial was used for training and the remaining 95 trials used for testing with LOTOCV. A 10-fold CV was used as an additional evaluation criteria. A summary of the result of applying a MARS approach on all datasets is given in Table 5.8. The results of the evaluation show that the RMSE varied between 1.27 ℃ and 1.70 ℃ (for the thigh and head, respectively) when LOTOCV was applied and between 1.07 ℃ and 1.55 ℃ (for the thigh and head, respectively) when 10-fold CV was applied.

5.2.5 Radial Basis Function Network

RBF [71] is an Artificial Neural Network (ANN) that uses radial basis functions as activation functions. A RBF network consists of inputs, a hidden layer of basis functions and outputs. At the input of each neuron, the distance between the neuron centre and the input vector is calculated. The output of the neuron is then formed by applying the basis function to this distance. The RBF network output is formed

Table 5.8: Equivalent temperature estimation RMSE from the best two cabin environmental sensors using MARS.

	Estimation RMSE	
Body part	LOTOCV	10-fold CV
Head	1.70 ℃	1.55 ℃
Chest	1.37 ℃	1.20 ℃
Lower arm left	1.57 ℃	1.48 ℃
Lower arm right	1.54 ℃	1.41 ℃
Upper arm left	1.56 ℃	1.31 ℃
Upper arm right	1.56 ℃	1.47 ℃
Thigh	1.27 ℃	1.07 ℃
Calf	1.49 ℃	1.31 ℃
Average	1.51 ℃	1.35 ℃

by a weighted sum of the neuron outputs and the unity bias. Usually, RBF networks are complemented with a linear part. This corresponds to additional direct connections from the inputs to the output neuron. Mathematically, the RBF network produces an output given by:

$$\widehat{y}(\theta) = g(\theta, x) = \sum_{i=1}^{nb} w_i^2 e^{-\lambda_i^2 (x-\omega_i^1)^2} + w_{nb+1}^2 + \chi_1 x_1 + ... + \chi_n x_n \tag{5.15}$$

where nb is the number of neurons, each containing a basis function. The parameters of the RBF network consist of the positions of the basis functions ω_i^1, the inverse of the width of the basis functions λ_i, the weights in output sum w_i^2 and the parameters of the linear part $\chi_1 x_1, ..., \chi_n x_n$. The additional linear part can be excluded if desired.

Implementation

The estimator was implemented in Python using WEKA libraries. The values for the RBF parameters were set as: the minimum standard deviation for the clusters is 0.1, the learning rate is 0.2 and the number of clusters for K-Means corresponds to 2 epochs. The values were set based on an initial empirical investigation.

Evaluation and results

For each of the 96 separate trials in turn, data from 95 trials were used for training and the remaining trial data were used for testing with LOTOCV. A 10-fold CV was used as an additional evaluation criteria. A summary of the result of applying a RBF approach on all datasets is given in Table 5.9. The results of the evaluation show that the RMSE varied between 2.93 ℃ and 4.47 ℃ (for the chest and head, respectively) when LOTOCV was applied and between 3.09 ℃ and 4.54 ℃ (for the thigh and head,

Table 5.9: Equivalent temperature estimation RMSE from the best two cabin environmental sensors using RBF.

	Estimation RMSE	
Body part	LOTOCV	10-fold CV
Head	4.47 ℃	4.54 ℃
Chest	2.93 ℃	3.13 ℃
Lower arm left	3.15 ℃	3.36 ℃
Lower arm right	3.31 ℃	3.36 ℃
Upper arm left	3.26 ℃	3.22 ℃
Upper arm right	3.76 ℃	3.74 ℃
Thigh	3.01 ℃	3.09 ℃
Calf	3.08 ℃	3.48 ℃
Average	3.37 ℃	3.49 ℃

respectively) when 10-fold CV was applied. These results are worse than the ones produced by all other learning-based approaches.

5.2.6 Reduced Error Pruning Tree

REPTree [127, 162] is a fast decision tree learner that builds a regression tree using information gain reduction and pruning. Pruning is a technique that reduces the size of decision trees by removing sections of the tree that provide little power to classify instances, and, therefore, increases the detection rate when provided with noisy training data. Furthermore, pruning the tree speeds up the classification process. Generally speaking, pruning is used to find the best sub-tree of the initially grown tree with the minimum error for the test set. However, the number of sub-trees grows exponentially with the size of the initial tree. Thus, it is computationally impractical to search all sub-trees. REPTree yields a sub-optimal tree under the restriction that a sub-tree can only be pruned if it does not contain a sub-tree with a lower classification error than itself. More accurate performance can be obtained at a higher computation cost.

Implementation

The estimator was implemented in Python using WEKA libraries. REPTree is usually used as a classifier, however it allows the selection of numerical outputs and, therefore, be used as an estimator. The values for the parameters were set as: there is no restriction on the maximum depth, the minimum total weight of the instances in a leaf is 2 and the number of data folds used for pruning is 3. The values were set based on an initial empirical investigation.

Table 5.10: Equivalent temperature estimation RMSE from the best two cabin environmental sensors using REPTree.

	Estimation RMSE	
Body part	LOTOCV	10-fold CV
Head	2.09 ℃	1.91 ℃
Chest	1.47 ℃	1.03 ℃
Lower arm left	1.97 ℃	1.07 ℃
Lower arm right	2.01 ℃	1.43 ℃
Upper arm left	1.73 ℃	1.07 ℃
Upper arm right	1.67 ℃	1.61 ℃
Thigh	1.48 ℃	1.00 ℃
Calf	1.82 ℃	0.99 ℃
Average	1.78 ℃	1.26 ℃

Algorithm 5.5 Breiman's algorithm for constructing each tree in the random forests [16].

1. Let N be the number of training cases and M be the number of variables in the classifier.
2. Let m be the number of input variables used to determine the decision at a node of the tree (m should be much less than M).
3. Choose a training set for this tree by choosing n times with replacement from all N available training cases. Use the rest of the cases to estimate the error of the tree, by predicting their classes.
4. For each node of the tree, randomly choose m variables on which to base the decision at that node. Calculate the best split based on these m variables in the training set.
5. Each tree is fully grown and not pruned.

Evaluation and results

For each of the 96 separate trials in turn, data from 95 trials were used for training and the remaining trial were used for testing with LOTOCV. A 10-fold CV was used as an additional evaluation criteria. A summary of the result of applying a REPTree approach on all datasets is given in Table 5.10. The results of the evaluation show that the RMSE varied between 1.47 ℃ and 2.09 ℃ (for the chest and head, respectively) when LOTOCV was applied and between 0.99 ℃ and 1.91 ℃ (for the calf and head, respectively) when 10-fold CV was applied. The results of the 10-fold CV are significantly better than the ones corresponding to LOTOCV because of over-fitting (results are not representative for unseen data).

5.2.7 Random Forest

RF [16] is an ensemble classifier that consists of multiple decision trees and outputs the class produced by the largest number of individual trees. The algorithm that constructs the individual trees in the RF is presented in Algorithm 5.5 [16].

Table 5.11: Equivalent temperature estimation RMSE from the best two cabin environmental sensors using RF.

	Estimation RMSE	
Body part	LOTOCV	10-fold CV
Head	1.96 ℃	1.45 ℃
Chest	1.42 ℃	1.06 ℃
Lower arm left	1.79 ℃	1.20 ℃
Lower arm right	1.78 ℃	1.23 ℃
Upper arm left	1.67 ℃	1.12 ℃
Upper arm right	1.78 ℃	1.25 ℃
Thigh	1.40 ℃	0.95 ℃
Calf	1.39 ℃	1.20 ℃
Average	1.64 ℃	1.18 ℃

Implementation

The estimator was implemented in Python using the Orange software libraries. The values for the RF parameters were set as: the number of trees in the forest is 100.

Evaluation and results

For each of the 96 separate trials in turn, data from 95 trials were used for training and the remaining trial data were used for testing with LOTOCV. A 10-fold CV was used as an additional evaluation criteria. A summary of the result of applying a RF approach on all datasets is given in Table 5.11. The results of the evaluation show that the RMSE varied between 0.95 ℃ and 1.45 ℃ (for the thigh and head, respectively) when LOTOCV was applied and between 1.40 ℃ and 1.96 ℃ (for the thigh and head, respectively) when 10-fold CV was applied. The results of the 10-fold CV are significantly better than the ones corresponding to LOTOCV because of over-fitting (results are not representative for unseen data).

5.2.8 Conclusions

Table 5.12 provides a summary of accuracies of the equivalent temperature estimation methods, together with the processing time required. The processing time represents the time required to perform the estimation on an unseen data set. Each model receives data from two cabin environmental sensors as input (as described in Section 5.1), summing to approximately 100,000 training instances. The results obtained were similar for all methods, except for RBF, with average errors ranging between 1.51 ℃ for MARS and 1.85 ℃ for KNN. RBF performed the worst, with an average RMSE over the eight equivalent temperatures of 3.37 ℃.

Table 5.13 shows the p-values generated through paired t-tests for each combination of models. The

Table 5.12: Accuracy and classification time for all equivalent temperature estimators using LOTOCV.

Method	MARS	MLP	MLR	REPTree	KNN	RF	RBF
RMSE (℃)	1.51	1.53	1.66	1.78	1.85	1.91	3.37
Classification time (seconds)	3.06	18.16	0.23	7.45	64.34	59.11	4.12

Table 5.13: P-Values for each combination of models.

	MARS	MLP	MLR	KNN	RBF	REPTree	RF
MARS	–	0.07	0.08	0.34	0.019	0.934	8.91e-006
MLP	0.05	–	0.09	0.57	0.99	1.00	0.557
MLR	0.06	0.07	–	0.65	0.72	0.99	0.039
KNN	2.12e-008	1.56e-023	3.12e-023	–	1.48e-048	1.92e-039	3.83e-054
RBF	5.12e-034	6.38e-043	5.10e-009	0.12	–	0.99	1.48e-048
REPTree	6.12e-054	3.14e-034	6.82e-012	0.09	0.14	–	4.65e-009
RF	1.12e-001	2.92e-015	4.89e-078	0.21	0.21	0.08	–

meaning of the values is as follows:

- When $p \leq 0.01$ then the "column" model is significantly better (very strong confidence) than the "row" model.
- When $0.01 < p \leq 0.05$ then the "column" model is better (strong confidence) than the "row" model.
- When $0.05 < p \leq 0.1$ then the "column" is better (low confidence) than the "row" model.
- When $p > 0.1$ then the "column" is worse (strong confidence) than the "row" model.

In terms of estimation error, MLR is significantly better than KNN (p-value of 3.12e-023), RBF (p-value of 5.10e-009), REPTree (p-value of 6.82e-012) and RF (p-value of 4.89e-078). The models MLP and MARS are better than the MLR with low confidence (p-values of 0.08 and 0.09, respectively). However, the improvement of these models over MLR is of 0.13 ℃ average RMSE. At this stage, another factor to be taken into consideration is the processing time. This is an important factor to consider prior to integrating the VTCS method within a control unit. MLR provided the fastest processing time, of 0.23 seconds, outperforming all other methods (significance: p-value of around 2e-021 when combined with any of the other models). The MLR processing time was, therefore, the fastest for each individual trial. This evaluation has shown **H5.1** to be true. The classification time for MLR was lower than for all other estimation techniques, while the estimation error obtained was outperformed by two models, the MLP and MARS. The improvement in accuracy of the latter two methods is not significant, therefore the MLR approach is concluded to be the most suitable estimation approach.

5.3 Further analysis on Multiple Linear Regression

MLR is the most suitable equivalent temperature estimation method when taking into account both accuracy and processing time based on the previous results. This section provides a more detailed analysis of the method. The second hypothesis formulated is:

H5.2: *The number of cabin environmental sensor affects the accuracy of the equivalent temperature estimation. As the number of cabin environmental sensors increases, the accuracy of the estimation increases steadily, but with diminishing improvement.*

To test the hypothesis, the best one to five cabin environmental sensors for estimating each individual body part equivalent temperature were selected. The selection was performed by computing the mutual information between the group of sensors and the equivalent temperature of all body parts (as described in Section 5.1) for all possible combinations of one, two, three, four and five cabin environmental sensors. The best combination of sensors over the eight equivalent temperatures was:

1. One cabin environmental sensor: Air temperature row 2 left breath with an average mutual information of 0.85 nats over the eight body parts.

2. Two cabin environmental sensors: Surface temperature row 2 left seat back and Air temperature row 2 right breath with an average mutual information of 0.98 nats over the eight body parts.

3. Three cabin environmental sensors: Air temperature row 2 left breath, Surface temperature row 1 passenger seat cushion and Air temperature row 1 left foot with an average mutual information of 1.32 nats over the eight body parts.

4. Four cabin environmental sensors: Air temperature row 1 left foot, Air temperature row 2 right breath, Surface temperature row 1 passenger seat back and Air temperature row 2 belt with an average mutual information of 1.61 nats over the eight body parts.

5. Five cabin environmental sensors: Air temperature row 1 head, Air temperature row 1 belt, Air temperature row 1 right foot, Air temperature row 2 left breath and Surface temperature row 2 left seat back with an average mutual information of 1.75 nats over the eight body parts.

Figure 5.4 shows how the estimation accuracy changes when the number of cabin environmental sensors is varied. In order to avoid a crowded figure, only four out of the eight body parts were plotted. For all body parts, the error decreases gradually from the case when one cabin environmental sensor is used for the estimation to the case when five different sensors are used for the estimation. The most significant

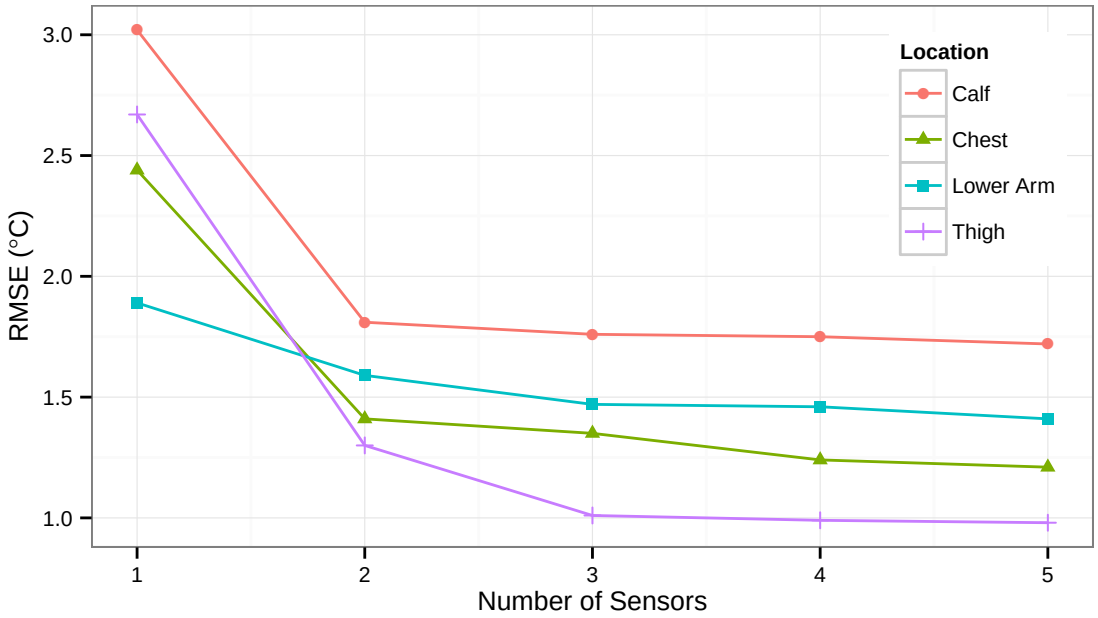

Figure 5.4: Decrease of estimated equivalent temperature RMSE when the number of cabin environmental sensors increases.

improvement takes place, in case of all body parts, when the second sensor is added, e.g. from a RMSE of 2.67 ℃ to a RMSE of 1.30 ℃ for the thigh. The accuracy improvement at the head level when the second sensor is added is of 0.03 ℃, the least of any body part equivalent temperature. The accuracy does not improve significantly when any of the remaining cabin environmental sensors are added. This implies that the estimation of head equivalent temperature can be best achieved using the air temperature at the head level and that other input data brings little accuracy improvement beyond that. There are body parts for which the third sensor brings significant improvement, such as the thigh (of up to 0.3 ℃). For all body parts, the improvement in accuracy when adding the fourth and fifth sensor is not substantial. The author concludes that a maximum of three cabin environmental sensors provide sufficient accuracy for the equivalent temperature estimation. This analysis has shown **H5.2** to be true to a certain extent—the accuracy of the estimation increases monotonically when additional estimation source sensors are added, however, the increase differs from body part to body part and diminishes fully when more than four cabin environmental sources are used.

Tables 5.14 and 5.15 show the estimation errors from the best one and two cabin environmental sensors, respectively. Here, the selection of cabin environmental sensors is optimised per body part. LOTOCV was used to evaluate the estimation accuracy.

Table 5.14: Equivalent temperature estimation results from the best cabin environmental sensor for each body part.

Temperature Sensors		Mutual Information	Estimation RMSE
Equivalent	Air/surface		
Head	Row 2 right breath	1.05 nats	2.05 ℃
Chest	Row 2 left seat back	0.95 nats	1.64 ℃
Lower arm	Row 2 left seat back	0.86 nats	1.95 ℃
Upper arm	Row 2 belt	0.84 nats	1.89 ℃
Thigh	Row 2 left seat back	1.00 nats	1.41 ℃
Calf	Row 2 left seat back	0.82 nats	2.02 ℃

Table 5.15: Equivalent temperature estimation results from the best two cabin environmental sensors for each body part.

Temperature Sensors			Mutual Information	Estimation RMSE
Equivalent	Air/surface 1	Air/surface 2		
Head	Row 2 right breath	Left upper IP	1.12 nats	1.84 ℃
Chest	Row 1 left foot	Row 2 left seat back	1.10 nats	1.37 ℃
Lower arm	Row 2 left seat back	Row 2 right foot	0.95 nats	1.74 ℃
Upper arm	Row 2 left seat back	Row 1 belt	1.04 nats	1.58 ℃
Thigh	Row 1 right foot	Row 2 left seat back	1.13 nats	1.35 ℃
Calf	Row 1 left foot	Row 1 passenger seat cushion	1.09 nats	1.57 ℃

Additional aspects of the MLR-based equivalent temperature estimation were investigated, such as whether the cabin environmental conditions impact on the estimation and whether integrating mean radiant temperature as a source sensor improves the accuracy of the estimation. The following hypotheses are formulated:

H5.3: *The environmental conditions affect the accuracy of the equivalent temperature estimation. When the cabin state is more transient (average cabin absolute temperature rates of change higher than 1.5* ℃ *per minute), the accuracy of the estimation is lower than in steady-state conditions (average cabin absolute temperature rates of change lower than 1.5* ℃ *per minute).*

H5.4: *Integrating mean radiant temperature as a cabin environmental sensor for the equivalent temperature estimation improves the accuracy of the estimation over air or surface temperature alone.*

Table 5.16 presents the equivalent temperature estimation results based on data from the experiments described in Section 4.1, when the two best sensors (Surface temperature row 2 left seat back and Air temperature row 2 right breath) were selected. Hypothesis **H5.3** is true—the lowest errors were obtained for trials *T1*, averaging at 1.01 ℃, while the highest errors were obtained for trials *T3*, averaging at 1.92 ℃. The higher error for the driving trials (*T3*) could be due to several factors, including the reduced quantity of data gathered and the influence of external factors such as varying position and intensity of

Table 5.16: Equivalent temperature estimation RMSE from the best two cabin environmental sensors on different experimental sets.

Target	*T1*	*T2*	*T3*	Average
Head	1.33 ℃	1.71 ℃	2.5 ℃	1.85 ℃
Chest	0.95 ℃	1.38 ℃	1.63 ℃	1.32 ℃
Lower arm left	1.05 ℃	1.59 ℃	2.32 ℃	1.65 ℃
Lower arm right	1.15 ℃	1.67 ℃	1.89 ℃	1.57 ℃
Upper arm left	0.96 ℃	1.92 ℃	2.01 ℃	1.63 ℃
Upper arm right	0.91 ℃	1.54 ℃	1.78 ℃	1.41 ℃
Thigh	0.53 ℃	1.51 ℃	1.63 ℃	1.22 ℃
Calf	1.28 ℃	1.44 ℃	1.47 ℃	1.40 ℃
Average	1.02 ℃	1.59 ℃	1.90 ℃	

Table 5.17: Equivalent temperature estimation RMSE from the best two cabin environmental sensors in trials $T4$.

Body part	With MRT	Without MRT	Difference
Head	1.44 ℃	2.69 ℃	1.25 ℃
Chest	1.42 ℃	2.03 ℃	0.61 ℃
Lower arm left	1.29 ℃	2.50 ℃	1.08 ℃
Upper arm left	1.37 ℃	2.34 ℃	0.97 ℃
Thigh	1.06 ℃	1.95 ℃	0.89 ℃
Calf	2.08 ℃	2.77 ℃	0.69 ℃
Average	**1.41 ℃**	**2.38 ℃**	**0.97** ℃

solar load. Also, the response of the Flatman manikin, in case of trials *T2* and *T3,* lagged behind the changes the user performed on the blower speed and temperature.

The data from trials *T4* (described in Section 4.1) allow testing the validity of hypothesis **H5.4**. Equivalent temperature integrates the effect of mean radiant temperature, air temperature and air flow. Mean radiant temperature was measured within trials *T4* and related very well to equivalent temperature. The pair of cabin environmental sensors providing the lowest estimation errors is the mean radiant temperature sensor and the air temperature sensor located at the front row right belt level. When the mean radiant temperature was not considered, the pair of sensors providing the lowest estimation errors were the air temperature sensor on the left hand side of the dashboard and the air temperature located at the left footwell. Table 5.17 shows the equivalent temperature estimation results in this scenario.

The average error, when the mean radiant temperature is integrated in the cabin environmental sensors subset, is of 1.41 ℃ over the eight body parts, with a minimum error of 1 ℃ for the thigh and a maximum error of 2 ℃ for the calf. On the other hand, when the mean radiant temperature is not integrated in the cabin environmental sensor subset, the average error is of 2.38 ℃ over the eight body parts, with a minimum error of 1.95 ℃ for the thigh and a maximum error of 2.77 ℃ for the calf. The

pair integrating mean radiant temperature outperformed the other pair over all trials, with a p-value of 1.45e-009. Hypothesis **H5.4** is thus confirmed, that is the integrating mean radiant temperature as a cabin environmental sensor significantly improves the equivalent temperature estimation accuracy.

Note that the VTCS approach was tested in real-time at a Jaguar Land Rover (JLR) event and the details are presented in Appendix A.

5.4 Summary

This chapter described the development and evaluation of a VTCS method that estimates occupant body part equivalent temperature from a minimalistic set of inexpensive cabin environmental sensors. Firstly, the cabin environmental sensors are selected that share the most information with the body part equivalent temperature. Mutual information was used to select the sensor types and corresponding locations. The method was applied to linear variables, but it has the potential to be further extended to non-linear variables. Seven different machine learning approaches were implemented for estimating body part equivalent temperature based on the measurements from the selected cabin environmental sensors: MLR, MLP, KNN, MARS, RBF, REPTree and RF.

Most learning tehniques provided a RMSE between 1.51 ℃ (for MARS) and 1.85 ℃ (for KNN). RBF performed the worst, with an average RMSE of 3.37 ℃. MLR had an average RMSE of 1.60 ℃ over the eight body part equivalent temperatures and also had the fastest processing time, enabling a straightforward real-time implementation in a car's engine control unit.

The main findings related to the VTCS approach designed are:

1. MLR outperforms all other estimation techniques with regard to fast processing time. In terms of accuracy, MARS and MLP improve on MLR with around 0.13 ℃ average RMSE, however the improvement is not significant at the cost of a higher processing time.

2. The number of cabin environmental sensors affects the accuracy of VTCS. As the number of cabin environmental sensors increases, the accuracy of VTCS increases monotonically, but with diminishing improvement.

3. The environmental conditions affect the accuracy of VTCS. When the cabin state is more transient (average cabin absolute temperature rates of change higher than 1.5 ℃ per minute), the accuracy of VTCS is lower than in steady-state conditions (average cabin absolute temperature rates of change lower than 1.5 ℃).

4. Integrating mean radiant temperature as a cabin environmental source for the VTCS approach improves the accuracy of the equivalent temperature estimation over air or surface temperature alone.

The next chapter describes the implementation of a reinforcement learning-based heating and cooling controller and evaluates it through simulation.

Chapter 6

Reinforcement Learning-based Heating and Cooling Controller

The previous chapter presented the development of a Virtual Thermal Comfort Sensing (VTCS) approach that estimates body part equivalent temperatures from a small set of cabin environmental sensors. With Nilsson's equivalent temperature-based model shown to be the most suitable thermal comfort model for Heating, Ventilation and Air Conditioning (HVAC) control (evaluated in Chapter 4), this chapter presents the development and evaluation of a reinforcement learning-based heating and cooling controller using the equivalent temperature as input. Two scenarios are designed and evaluated:

1. Single-zone scenario: The goal of the controller is to maintain the occupant overall equivalent temperature within a thermally neutral range, according to Nilsson's thermal comfort model (between 24 ℃ and 26 ℃ for a summer clothing index), while minimising the associated energy consumption.

2. Multi-zone scenario: The goal of the controller is to maintain the occupant head equivalent temperature within a thermally neutral range and the occupant foot equivalent temperature within a "slightly cool" range, according to Nilsson's thermal comfort model (between 24 ℃ and 26 ℃ for the head and between 17 ℃ and 19 ℃ for the foot, respectively).

The research questions this chapter poses are:

1. Is it possible to represent the state of the cabin environment in such a way that it fulfils the Markov Decision Process (MDP) criteria?

2. Can a reinforcement learning-based heating and cooling control policy provide performance beyond the current state-of-the-art?

The contribution in this chapter is the development of a reinforcement learning-based heating and cooling controller that outperforms state-of-the-art controllers. This reinforcement learning-based approach is innovative in the automotive field and represents a paradigm shift in the way HVAC control is developed.

Moreover, the control method can be extended to include additional HVAC control actuators, such as vent orientation, and to take into account additional zones. The algorithm is developed and evaluated offline through simulation.

This chapter is structured as follows: Section 6.1 describes the car cabin simulation environment that the reinforcement learning-based controller was evaluated through. Section 6.2 describes the mapping of the reinforcement learning components onto the problem of occupant overall equivalent temperature control, while Section 6.3 provides details regarding the implementation of a fuzzy logic-based controller that the reinforcement learning-based controller is compared against. Section 6.4 presents the results obtained for the single-zone scenario, while Section 6.5 provides a sensitivity analysis for the reinforcement learning parameters. Section 6.6 presents the results obtained for the multi-zone scenario. Finally, Section 6.7 presents a summary of the work in this chapter.

6.1 Simulation of the car cabin environment

A simulation of the car cabin environment was implemented in order to evaluate the reinforcement learning-based controller proposed in this chapter. The criteria for a valid simulation are:

1. Responding to control actions in an appropriate way.
2. Providing a means of integrating the state variables,the actions variables, and the reward.
3.

The cabin simulation described in this section is a one dimensional heat flux-based model specified by Jaguar Land Rover (JLR) and implemented by the author in Java. The simulation fulfils the criteria previously stated. Figure 6.1 gives a high-level view of the simulation. Due to the nature of the model, there are several assumptions:

1. There is no air leakage from the cabin.
2. Only one dimensional heat transfers are considered.
3. There is one main vent and its position does not change throughout the simulation.
4. Each simulation time step corresponds to one second.

The simulation is detailed in the remainder of this section. The update of the car cabin air temperature (after one second of simulation) is:

$$T_a^{'} \leftarrow T_a + \frac{Q_a}{C_a \times m_a} \tag{6.1}$$

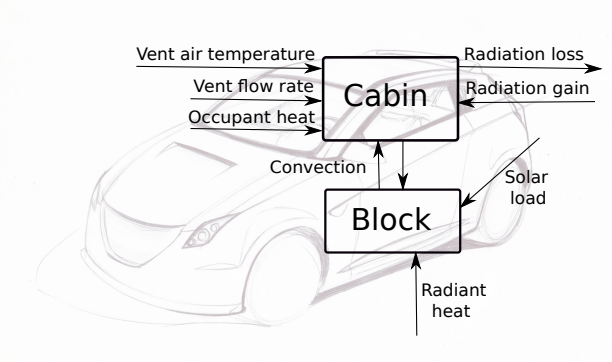

Figure 6.1: High-level diagram of the simulation.

where T_a is the current cabin air temperature, C_a is the specific heat capacity of air, m_a is the air mass and Q_a is the cabin heat energy sum.

The heat sum for cabin air Q_a is:

$$Q_a = Q_i + Q_{conv_{b\to a}} + Q_O - Q_{lg} \tag{6.2}$$

where Q_i is the energy input for heating, $Q_{conv_{b\to a}}$ is the heat energy transferred via convection from the block to the cabin, Q_O is the heat energy given off by the occupant and Q_{lg} is the ambient loss/gain load.

The input heat Q_i is:

$$Q_i = C_a \times m_i \times (T_i - T_a) \tag{6.3}$$

where C_a is the specific heat capacity of air, m_i is the mass of air at input, T_i is the vent air temperature and T_a is the cabin air temperature.

The input mass m_i is:

$$m_i = v_i \times \rho_a \times T_i \tag{6.4}$$

where v_i is the volume of air at input, ρ_a is the air density and T_i is the vent air temperature.

The heat energy transferred through convection between the block and the cabin air $Q_{c_{b\to a}}$ is:

$$Q_{c_{b\to a}} = h_c \times A \times (T_b - T_a) \tag{6.5}$$

where h_c is the heat transfer coefficient, A is the area of the material, T_b is the block temperature and T_a is the cabin air temperature.

The ambient loss Q_{lg} is:

$$Q_{lg} = l \times (T_a - T_o) \tag{6.6}$$

where l is the coefficient of thermal transfer loss, T_a is the cabin air temperature and T_o is the outside temperature.

For the block temperature, the temperature update at one moment in time is:

$$T_b' \leftarrow T_b + \frac{Q_b}{C_s \times m_s} \tag{6.7}$$

where T_b is the block temperature, Q_b is the block heat energy sum, C_s is the specific heat capacity of steel and m_s is the mass of steel.

The mass of steel m_s is:

$$m_s = \rho_s \times v_s \tag{6.8}$$

where ρ_s is the density of steel and v_s is the volume of the block structure.

The total heat energy transferred into the block Q_b is:

$$Q_b = Q_{r_{c\to b}} - Q_{cond_{b\to a}} + Q_R + Q_S \tag{6.9}$$

where $Q_{r_{c\to b}}$ is the heat energy transferred via radiation from the cabin to the block, $Q_{cond_{b\to a}}$ is the heat energy transferred via conduction from the block to the cabin, Q_R is the heat energy radiated by the road and Q_S is the heat energy absorbed from the sun.

The heat energy transferred due to thermal radiation Q_S together with the heat energy transferred from the road Q_R are constants set at the beginning of the simulation. The heat energy transferred due to thermal radiation $Q_{r_{c\to b}}$ is:

$$Q_{r_{c\to b}} = \varepsilon_g \times \sigma \times A \times \left(T_a^4 - T_b^4\right) \tag{6.10}$$

where ε_g is the emissivity of glass, σ is the Stefan-Boltzmann constant, A is the area of the material, T_a is the cabin air temperature and T_b is the block air temperature.

The energy consumed, part of the reinforcement learning reward component, is estimated within the simulation. When heating the cabin, the heat energy used Q is derived from the vent air temperature

T_i, the temperature of the air being heated T_a and the mass of the input air m_i:

$$Q = (T_i - T_a) \times C_a \times m_i \tag{6.11}$$

where T_i is the vent air temperature, T_a is the cabin air temperature, C_a is the specific capacity of air and m_i is the mass of air at input.

When cooling the cabin, the heat energy used Q is derived similarly:

$$Q = (T_a - T_i) \times C_a \times m_i \tag{6.12}$$

The cabin temperature when recirculation is considered is:

$$T_x = A_r \times T_a + (1 - A_r) \times T_o \tag{6.13}$$

where A_r is the air recirculation ratio, T_a is the cabin air temperature and T_o is the outside air temperature.

The simulation data was compared to the empirical data collected (described in Section 4.1). When the simulated average cabin air temperature was matched against the corresponding measured data, the Root Mean Square Error (RMSE) for the simulated temperature was between 0.86 ℃ and 2.21 ℃ for different warm-up and cool-down scenarios.

Figure 6.2 shows the simulated average cabin temperature using equations 6.1 to 6.10 compared with real data from a cool-down scenario. The conditions encountered within the trial are: ambient temperature between 21 ℃ and 23 ℃, solar load of 655 W $\times$ m^{-2} and a vehicle speed of 50 mph. Similarly, Figure 6.3 illustrates the simulated average cabin temperature against the real data from a warm-up scenario. The conditions encountered within the warm-up trial are: ambient temperature between 21.5 ℃ and 22.5 ℃, solar load of 515 W $\times$ m^{-2} and a vehicle speed of 50 mph. The errors were higher for the warm-up scenarios, with the actual average cabin temperature heating up at a faster pace. The errors obtained are considered acceptable given i) that some parameters within the simulation were estimated, such as the block temperature, solar load and vent air flow (the air flow setting was the only available information and it was mapped into litres per second) and ii) the assumptions described earlier in this section.

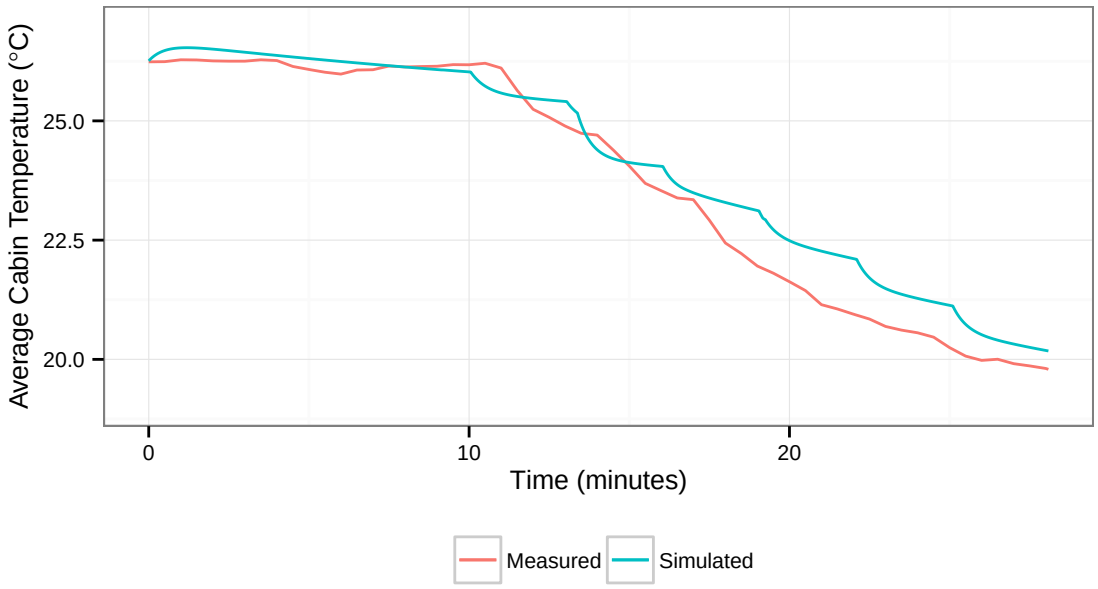

Figure 6.2: Simulated versus measured average cabin temperature during a cool-down scenario.

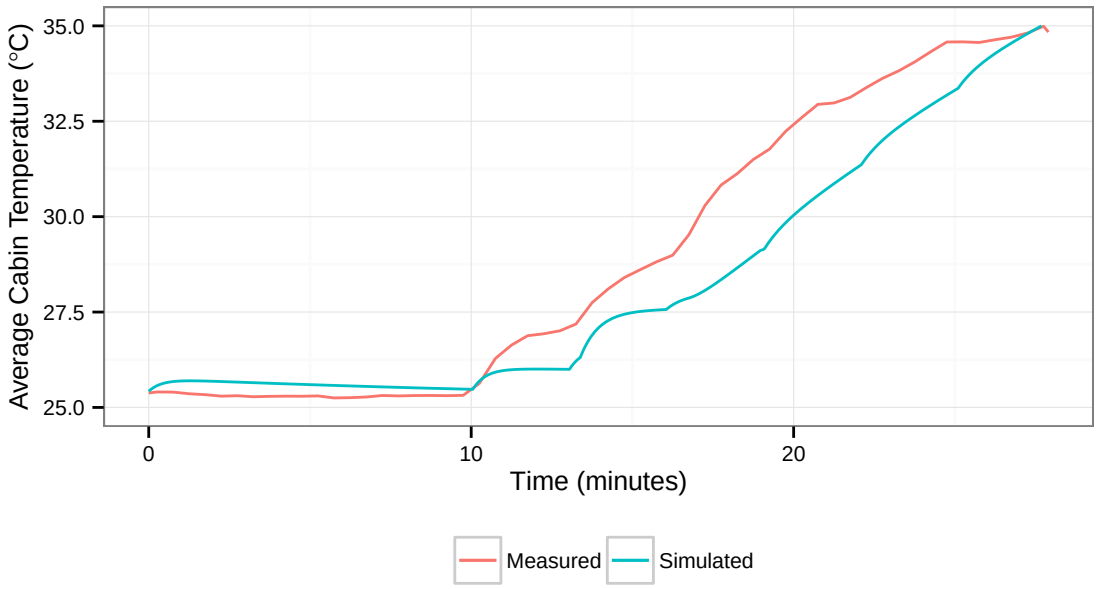

Figure 6.3: Simulated versus measured average cabin temperature within a warm-up scenario.

6.2 Reinforcement learning components

This section describes the reinforcement learning implementation.

6.2.1 State representation

The state of the environment is described by three variables, namely the occupant overall equivalent temperature T_e, the block temperature T_b and the outside air temperature T_o. The equivalent temperature is computed from the air temperature, air flow and mean radiant temperature variables within the simulation using equation 2.24 on page 29. The air flow corresponding to the cabin occupant is not directly available and it is estimated here by dividing the vent air flow V_i by 10. The value was selected based on cabin air flow measurements in the literature. Random continuous values are assigned to the state variables at the beginning of each learning episode in the following ranges:

- Block temperature T_b: [0,50] ℃.
- Outside temperature T_o: [0,30] ℃.
- Occupant equivalent temperature T_e: [0,40] ℃.

The representation of the state is minimalistic and fulfils the Markov property. For this task, a state has the Markovian property if it specifies exactly, or makes it possible to reconstruct exactly, the thermal comfort level of the occupant and the energy consumed by the HVAC (the components of the reward function). In an idealised control system, this information would be sufficient to exactly predict the future thermal comfort states of the occupants, given the actions taken by the controller. In practice, however, it is never possible to know this information exactly because any real sensor will introduce some distortion and delay in its measurements. Furthermore, in any real car cabin there are always other effects that were not considered in the simulation, such as leakage of air, that affect the behaviour of the system. For the simulation here, however, the combination of occupant equivalent temperature, block temperature and ambient temperature is expected to give acceptable results.

Numerous applications in reinforcement learning consist of episodic tasks, in which terminal states are defined. For example, if the reinforcement learning goal is for a robot to grasp an object then the terminal state occurs when the robot actually grasped the object. For the purpose of the comfort-oriented HVAC control here there is no need for a terminal state because once the optimum thermal comfort level is reached, the goal is to maintain it throughout the journey.

As noted previously, learning starts at different randomly generated states in each iteration of the simulation. In order to avoid cases in which, for example, the outside air temperature is 30 ℃ and the occupant equivalent temperature is 0 ℃ (such combinations are unlikely in a real world environment), a set of rules has been defined as follows:

$$\begin{cases} T_b \in [0, 20] \text{ ℃} \text{ and } T_o \in [0, 20] \text{ ℃}, & \text{for } T_e \leq 20 \text{ ℃} \\ T_b \in [20, 50] \text{ ℃ and } T_o \in [20, 30] \text{ ℃}, & \text{for } T_e > 20 \text{ ℃} \end{cases} \tag{6.14}$$

6.2.2 Action representation

A set of actions that can be taken by the agent is defined. The learning agent is able to control the vent air flow V_i, the vent air temperature T_i and the ratio of air to be recirculated A_r. For each action there is a discrete range of values available, as follows:

- Vent air flow: Four vent air flow set-points, evenly distributed over the $[0, 100]\ ls^{-1}$ range. The value of $100\, ls^{-1}$ was chosen because it is a common maximum value for the vent air flow in production vehicles.
- Vent air temperature: Five set-points, evenly distributed over the [−20,40] ℃ range.
- Recirculation: Three set-points—0 (no recirculation), 0.5 (partial recirculation) and 1 (full recirculation).

For this task there are, therefore, 61 different combinations of actions.

6.2.3 Reward function

The goal of the learning problem is to maintain the overall occupant equivalent temperature between $[24, 26]$ ℃ corresponding to thermal neutrality based on Nilsson's model for summer clothing conditions. The reward, therefore, firstly takes into account whether the thermal comfort criteria has been satisfied. The reward also takes into consideration the energy consumed and the vent flow rate. By penalizing a large consumption of energy, the agent will learn in time to select actions that would reduce the energy consumed. Controlling the occupant thermal comfort and the energy consumption are the two goals considered within the scope of this thesis. However, the reward function can be extended to integrate additional goals, such as avoiding window fogging. The current reward function was developed based on an empirical investigation and is expressed as:

$$R(s, a, s^{'}) = R_i(s^{'}) + R_c(s^{'}) + R_e(s^{'}) \tag{6.15}$$

$$R_i(s^{'}) = \begin{cases} -1000, & s^{'} \text{ is illegal} \\ 0, & \text{otherwise} \end{cases} \tag{6.16}$$

$$R_c(s^{'}) = \begin{cases} -1, & T_e \notin [24.0, 26.0] \\ 0, & \text{otherwise} \end{cases} \tag{6.17}$$

$$R_e(s^{'}) = -(Q + 2 \times V_i)/1500 \tag{6.18}$$

Equation 6.16 is the part of the reward that penalises illegal states. A state is considered illegal when its components (occupant equivalent temperature, block temperature and outside air temperature) go beyond the minimum or maximum possible value. For example, if the initial randomly generated occupant overall equivalent temperature is assigned the maximum value and, through the random actions the agent selects, the equivalent temperature goes beyond this value then a high penalty should be introduced. If the state is legal, then no penalty is introduced. The penalty for an illegal state is large so that the actions leading to these illegal states are quickly eliminated as a solution.

Equation 6.17 is the thermal comfort reward component. If the occupant equivalent temperature is within the desired limits, then no penalty is given, otherwise a penalty of -1 is introduced. Equation 6.18 is the energy consumption reward component. In all circumstances, a penalty is given directly proportional to the amount of heat coming into the cabin Q and the vent air flow setting V_i.

In order to reach the final reward function (illustrated in equation 6.15), a variety of approaches were tried to encourage learning a policy that balances well the optimisation of thermal comfort and the minimisation of consumed energy. If, for example, the $-(Q+2\times v_i)$ factor is divided by a value less than 1500, then the focus will be placed on reducing the energy consumption. The lower the dividing factor is, the slower thermal comfort will be achieved, if achieved at all. Therefore, for production vehicles, one needs to decide what the focus is placed on (occupant thermal comfort or consuming little energy) and what the weights of these components should be based on oberving the trial and error performance.

6.2.4 Policy

Sarsa(λ) is used to learn the optimum policy, together with a tile coding function approximator, both described in Section 2.6. The tile coding parameters used for this problem are presented in Table 6.1.

Table 6.1: Tile coding parameters used to learn the control policy.

Variable	Minimum	Maximum	Intervals
T_e	0	40	9
T_b	0	50	3
T_i	-20	40	3
V_i	1	100	3
A_r	0	1	3

The tile coding used to represent the action-values included 30 tiles, 10 tiles integrating variables $(T_e, T_b, T_i, V_i, V_r)$ and 20 tiles integrating variables (T_e, T_i, V_i, V_r). The outside air temperature variable T_o had little effect on the outcome, therefore it was left out from the tile coding process. In general, variables that have little effect on the performance of the learning should not be integrated in tile coding because the increasing dimensionality becomes computationally expensive, making the learning process more time consuming. The number of intervals for each variable was selected based on an initial empirical investigation.

6.2.5 Parameter values

There are a series of parameter values to be set prior to the learning process. Their role is described in Section 2.6 and their values were optimised for this particular application.

1. Number of steps per episode: A maximum number of steps per learning episode has to be set since a behaviour may never reach the target. For this problem 1000 steps are allowed because it is higher than the number of steps required based on trial and error. A smaller number can be selected in order to speed up the learning process.

2. Decay factor $\lambda = 0.6$: The decay of eligibility λ has the following effect: when $\lambda = 0$, no credit is assigned to past state-action pairs, whereas when $\lambda = 1$, credit is assigned equally to all previously visited states.

3. Reward discount factor $\gamma = 0.98$: A factor of 0 will make the agent "myopic" (or short-sighted) by only considering current rewards, while a factor approaching 1 will make it strive for a long-term high reward.

4. Learning rate $\alpha = 0.01$: A learning rate of 0 will make the agent not learn anything, while a learning rate of 1 would make the agent consider only the most recent information.

5. Exploration factor: $\varepsilon = 0$. Epsilon greedy is a learning policy and a greedy action implies that, for

the current state, the agent looks at the q-values for all actions and picks the one with the highest value. The ε in the epsilon greedy policy is the probability that the agent picks at random one of the non-greedy actions. And, thus, with probability (1-ε) the agent selects the greedy action.

A sensitivity analysis of the reinforcement learning controller's performance based on the values of these parameters is provided in Section 6.5.

6.3 Fuzzy logic-based controller

This section discusses the implementation of a fuzzy logic-based controller as an alternative for the performance comparison against the reinforcement learning-based controller.

The fuzzy logic-based controller is the most popular choice in terms of vehicular HVAC control algorithms in the literature [13, 37, 49, 58, 139, 143, 148]. For the evaluation here, a fuzzy logic controller was implemented in Java using the JFuzzyLite library version 1.0 [128]. There were two input variables defined: the occupant overall equivalent temperature T_e and the block temperature T_b. The two input variables were normalised (normalisation is defined as adjusting values measured on different scales to a notionally common scale) between 0 and 1 and three ranges were defined as follows: COLD between $[0.0, 0.5]$, NEUTRAL between $[0.5, 0.6]$ and HOT between $[0.6, 1.0]$. There were two output variables defined: the vent air temperature T_i and the vent flow V_i. The ranges for the output variables are identical to the ones in the reinforcement learning, namely $[-20, 40]$ ℃ for T_i and $[0, 100]$ ls^{-1} for V_i. The vent air temperature T_i is split into three ranges as follows: LOW between $[-20.0, 10.0]$ ℃, MEDIUM between $[10.0, 30.0]$ ℃ and HIGH between $[30.0, 40.0]$ ℃. The input air flow V_i is split into three ranges as follows: LOW between $[0.0, 30.0]$ ls^{-1}, MEDIUM between $[30.0, 70.0]$ ls^{-1} and HIGH between $[70.0, 100.0]$ ls^{-1}. Theoretical details about fuzzy logic parameters are given by Rada-Vilela [128]. For the controller here, all input and output variables are defined as Gaussian terms (illustrated by equation 6.19).

$$f(x|\mu, \sigma) = e^{(x-\mu)^2/2\sigma^2} \tag{6.19}$$

The defuzzifier used for the output variables is the Centroid (illustrated with formula 6.20), with a radius of 100.

$$\frac{\int x\mu(x)dx}{\mu(x)dx} \tag{6.20}$$

The type of terms and defuzzifier were selected based on an initial empirical evaluation. The conjunction between the rules is computed as an algebraic product, the disjunction between the rules is computed as a maximum and the rule activation is computed as an algebraic product.

In order to produce the fuzzy output values T_i and V_i, inference rules are constructed based on the fuzzy input values T_e and T_b as follows:

1. If T_e is COLD and T_b is COLD then T_i is HIGH and V_i is HIGH.
2. If T_e is COLD and T_b is NEUTRAL then T_i is HIGH and V_i is HIGH.
3. If T_e is COLD and T_b is HOT then T_i is HIGH and V_i is MEDIUM.
4. If T_e is NEUTRAL and T_b is COLD then T_i is MEDIUM and V_i is LOW.
5. If T_e is NEUTRAL and T_b is NEUTRAL then T_i is MEDIUM and V_i is LOW.
6. If T_e is NEUTRAL and T_b is HOT then T_i is MEDIUM and V_i is LOW.
7. If T_e is HOT and T_b is COLD then T_i is LOW and V_i is MEDIUM.
8. If T_e is HOT and T_b is NEUTRAL then T_i is LOW and V_i is HIGH.
9. If T_e is HOT and T_b is HOT then T_i is LOW and V_i is HIGH.

The rules were developed based on the works of Dalamagkidis [35] and Kelly [84].

The simulation described in Section 6.1 is used in order to provide an estimate of the next car cabin state based on the actions chosen by the fuzzy logic controller. The performance function used is the same as the reward function in Section 6.2.3 in order to perform a meaningful comparison of the two controllers.

Generally, designing a fuzzy logic-based controller either relies on previously acquired human knowledge or can be derived from data. Therefore, fuzzy controllers could be further tuned by optimising the set of fuzzy rules (Figure 6.4). There are three popular techniques of optimising the fuzzy rules, namely reinforcement learning, stocchastic oprimisation, such as genetic algorithms or connectionist methods. Optimising the fuzzy logic-based controller, however, goes beyond the scope of this thesis.

6.4 Results

In this section, the performance of the reinforcement learning-based controller (described in Section 6.2) is compared to the performance obtained by a fuzzy logic-based controller (described in Section 6.3) and

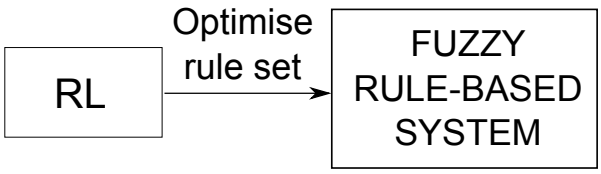

Figure 6.4: Reinforcement learning for optimising a fuzzy controller.

a basic heating and cooling controller. The basic controller blows the coldest vent temperature at the fastest vent speed in order to cool down the cabin and blows the hottest vent temperature at the fastest vent speed in order to warm up the cabin. Once the comfortable temperature is reached, the controller maintains it by setting the air flow on a minimum value and the vent air temperature at 25 ℃. This represents a baseline that the other controllers should be fully capable of out-performing. The fuzzy logic-based controller aims to maintain the overall occupant equivalent temperature between 24 ℃ and 26 ℃. The hypothesis that can be formulated is:

H6.1: *The reinforcement learning-based controller will outperform both the basic controller and the fuzzy logic-based controller.*

To test this hypothesis, the relative performance during learning of the Sarsa(λ) algorithm was compared to that of the fuzzy logic-based controller and basic controller, shown in Figure 6.5. The reward is averaged over a standard set of 100 randomly generated test cases (referred to as one learning trial). The same set of generated test cases are used each time the performance is evaluated. The reinforcement learning-based controller achieves an average reward of -29.16 over 1,000,000 trials. Learning a good policy is achieved quickly (in around 1,500 trials) and the improvement of the policy stops after around 150,000 trials. Learning for the SARSA(λ) algorithm, corresponding to 1,000,000 trials, completed in 35 minutes. As illustrated by Figure 6.5, the algorithm does not converge to a precise value. This result is expected, as the algorithm is known to converge to a region [64].

Intuitively, the basic controller should have the poorest performance. Even though its behaviour is optimum in terms of time-to-comfort, by cooling-down or warming-up the cabin on maximum vent temperature and maximum flow until the desired temperature is reached, this approach is energy wasteful and, therefore, the energy component of the performance function is greatly penalised. The reward of the basic controller was -62.70.

The fuzzy logic-based controller is expected to perform better than the basic controller in terms of energy consumption because the energy consumption factor was indirectly integrated in the design of the

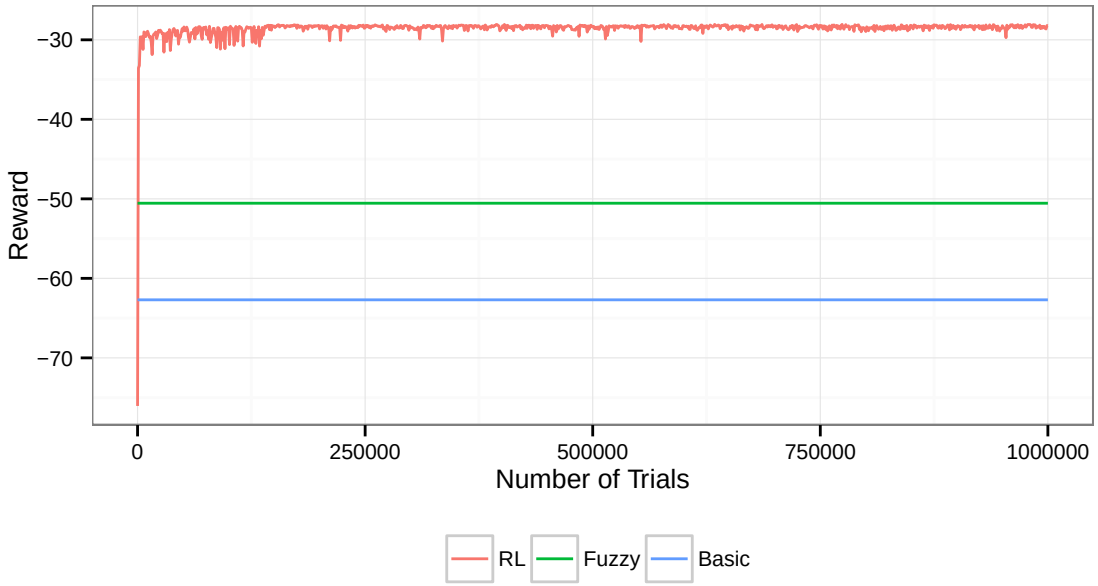

Figure 6.5: Policy performance during learning for Sarsa(λ) compared to the basic and fuzzy logic-based controllers.

fuzzy rules. For example, in the case of rule number 3 "If T_e is COLD and T_b is HOT then T_i is HIGH and v_i is MEDIUM", it is taken into consideration that if the cabin block temperature is hot then the cabin temperature would also increase naturally and therefore the vent flow is set on medium rather than high. This approach improves the performance of the basic controller, however, it does not benefit from the reinforcement learning approach of receiving feedback. With the latter, higher energy use is proportionally penalised, while for the fuzzy logic approach the controller will perform based on the defined rules. The performance of the fuzzy logic-based controller is -50.55. The improvement is reasonable, but lower than expected by the author when compared to the basic controller. The reinforcement learning-based controller performs better due to directly including the energy consumption in its performance function and being able to learn an optimum policy. These results translate into an average of 27.05% energy saving (corresponding to 129.85 J) over 200 testing scenarios when compared to the fuzzy logic-based controller, while thermal comfort was achieved and maintained successfully. This analysis has shown **H6.1** to be true.

Figure 6.6 shows how the optimum policy is learnt by the Sarsa(λ) algorithm trial by trial, up to 2,000 trials. Most of the learning occurs in the first 500 trials. The oscillation is present throughout the trials, reducing in size with the increasing number of training trials.

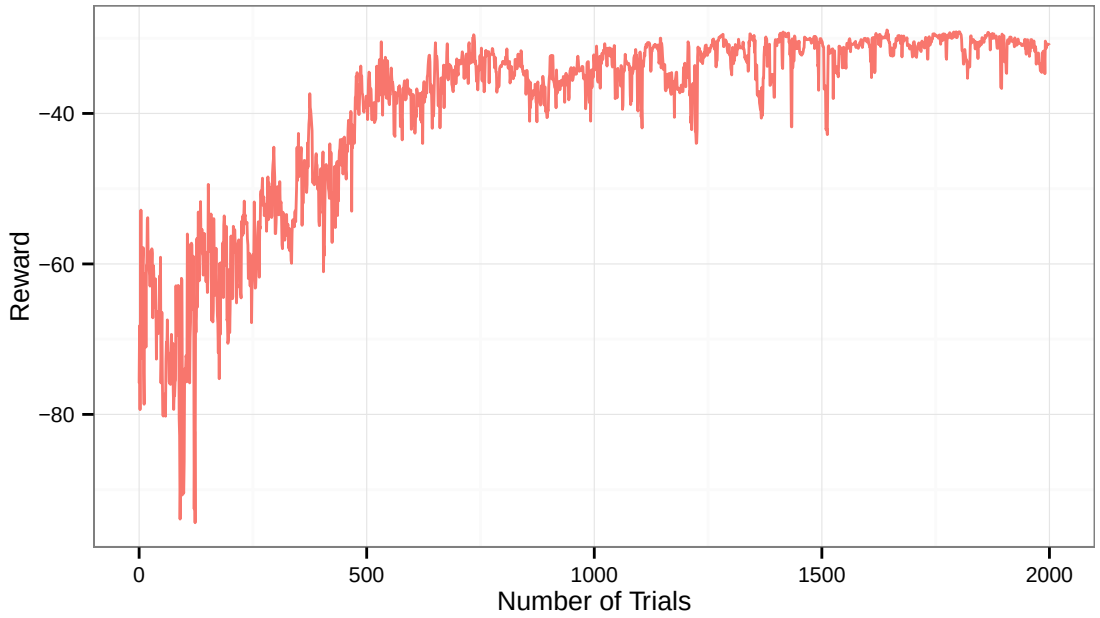

Figure 6.6: Policy performance during learning for Sarsa(λ).

Figure 6.7 shows how the Sarsa(λ) policy controls the occupant equivalent temperature starting with a random state (32.7 ℃ overall occupant equivalent temperature, 28.5 ℃ block temperature and 30.1 ℃ outside temperature). As the figure shows, the desired temperature is reached in about 6 steps (6 seconds for the purpose of this simulation). Then, the occupant equivalent temperature is maintained between the upper and lower limits of the desired interval (24 ℃ and 26 ℃).

6.5 Sensitivity analysis

The number of potential actions the controller can take and the value of the learning parameters (such as α, γ, and λ) impact on the performance of the reinforcement learning-based controller. This section analyses the effect of these parameters on the performance of the system.

Figure 6.8 shows how the average reward over 1,000 trials changes with the number of vent flow set-points available. The lowest average reward (of -65.54) accumulates when only two vent flow set-points are available to the agent while the highest average reward (of-31.61) accumulates when four vent flow set-points are available to the agent. However, the average reward is very similar between three and ten set-points (not all values were plotted in order to avoid crowded figures). The space of state-action pairs the algorithm uses grows with every possible action set-point added. Therefore, choosing a large

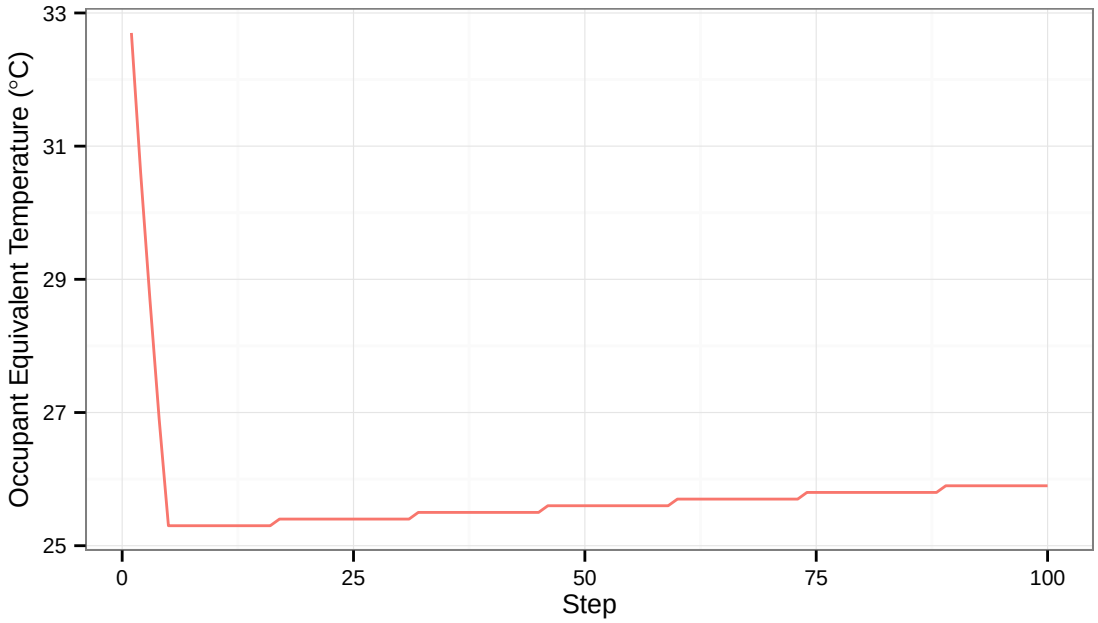

Figure 6.7: Cooling down scenario using Sarsa(λ).

number of action set-points when the performance is not significantly increased should be avoided. With only two vent flow set-points available (vent flow of 0.0 and 100.0) the equivalent temperature would not be smooth, but with significant transitions between each step (with one step corresponding to one second), a case not desirable for cabin occupants. The use of 4 possible vent flow set-points was selected as optimum, being small enough in terms of space complexity while smoothing the transitions between steps (maximum 0.2 ℃ occupant equivalent temperature rate of change).

The outcome is similar for the vent air temperature action. Figure 6.9 shows how the average reward over 1,000 trials changes with the number of vent air temperature set-points available. The lowest average reward (of -51.23) accumulates when only two vent air temperature set-points are available to the agent while the highest average reward (of-31.61) accumulates when five vent air temperature set-points are available to the agent. Similarly with the vent flow action, the average reward shows little change between three and ten set-points (as observed by the author when all values were plotted). The use of five possible vent air temperature set-points was selected as optimum, for similar reasons with the vent air flow scenario.

Figure 6.10 shows how the average reward over 1,000 trials changes with the value λ. Parameter λ is the decay factor with the following effect: when $\lambda = 0$ no credit is assigned to past state-action pairs, whereas when $\lambda = 1$ credit is assigned equally to all previously visited states. The highest reward

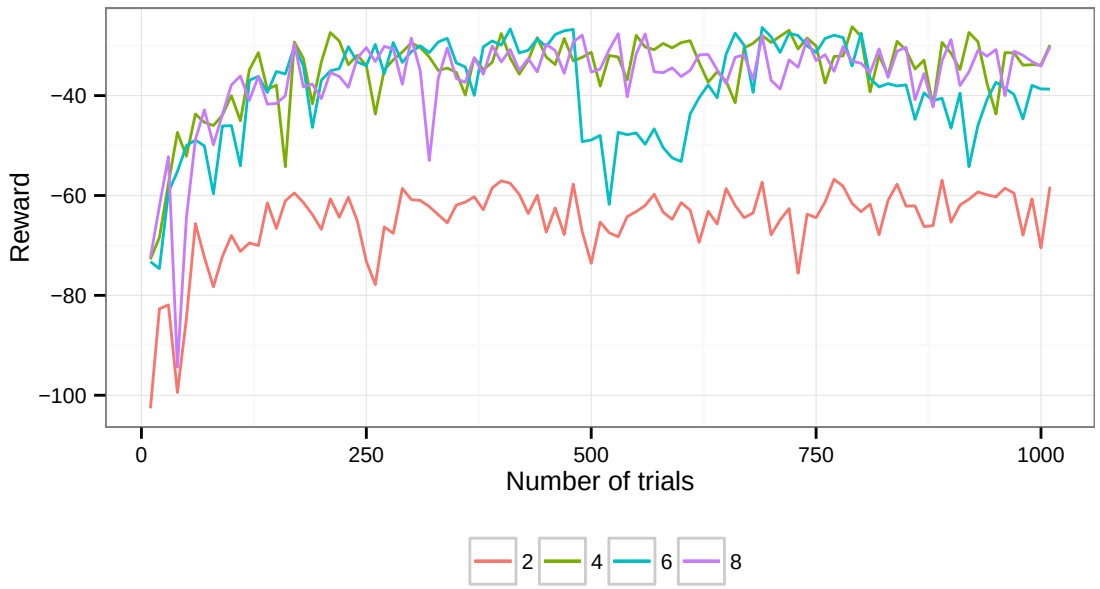

Figure 6.8: Sensitivity analysis on the number of vent air flow set-points (values of 2, 4, 6 and 8, respectively) on the controller's performance over 1,000 trials.

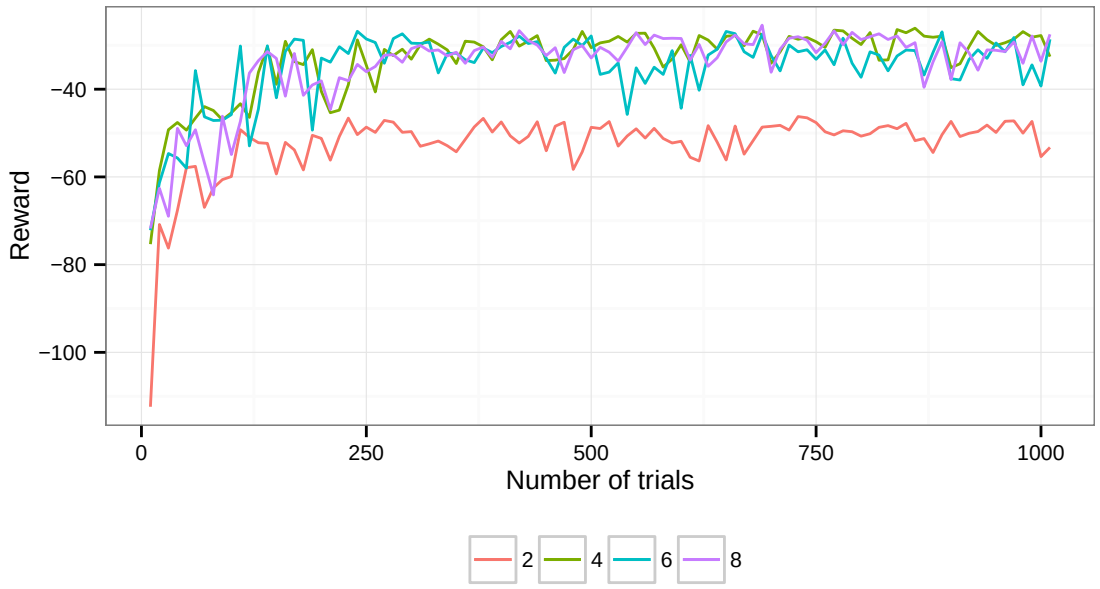

Figure 6.9: Sensitivity analysis on the number of vent air temperature set-points (values of 2, 4, 6 and 8, respectively) on the controller's performance over 1,000 trials.

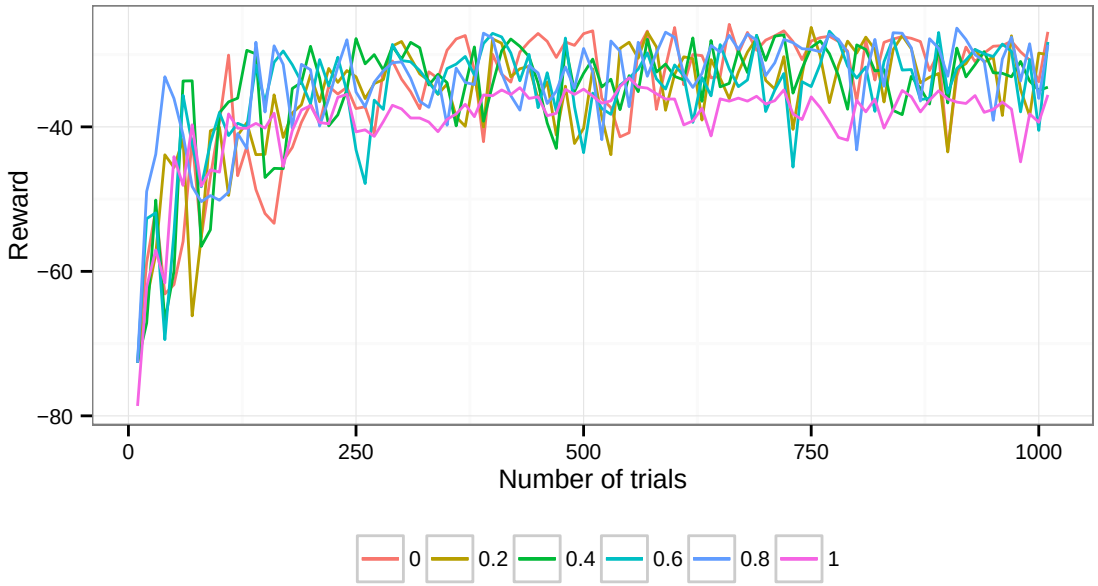

Figure 6.10: Sensitivity analysis on the λ parameter (values of 0, 0.2, 0.4, 0.6, 0.8 and 1, respectively) on the controller's performance over 1,000 trials.

accumulates when λ is 0.6 (reward of -31.61), while the lowest reward accumulates when λ is 1.0 (reward of -41.16). However, the results showed that the average reward is close between the λ values of 0.0 and 0.9. Therefore, it is concluded that the maximum value for λ, when equal credit is allocated to all previously visited states does not lead to an optimum performance, whereas all other values lead to a similar performance.

The γ parameter is directly used for computing the reward, therefore an analysis based on its values is not useful because the smaller γ becomes, the lower the reward. A common value of 1 is usually assigned to γ for episodic tasks. For this task, however, based on criteria such as whether the goal is reached from all random starting states and how quickly the goal is reached, the most suitable value for γ (that gives the best performance on the criteria mentioned) is 0.98.

Figure 6.11 shows how the average reward over 1,000 trials changes with the value of α, the learning rate. The learning rate controls the learning step size, that is, how fast learning takes place. A learning rate of 0 will make the agent not learn anything, while a learning rate of 1 would make the agent consider only the most recent information. The lowest reward (of -72.61) accumulates when α is 0, while the highest reward (of -31.61) accumulates when α is 0.01. Therefore, it is concluded that a low learning rate (in the 0.005–0.05 range) leads to the best performance of the controller.

Figure 6.12 shows how the average reward over 1,000 trials changes with the value of ε, the exploration

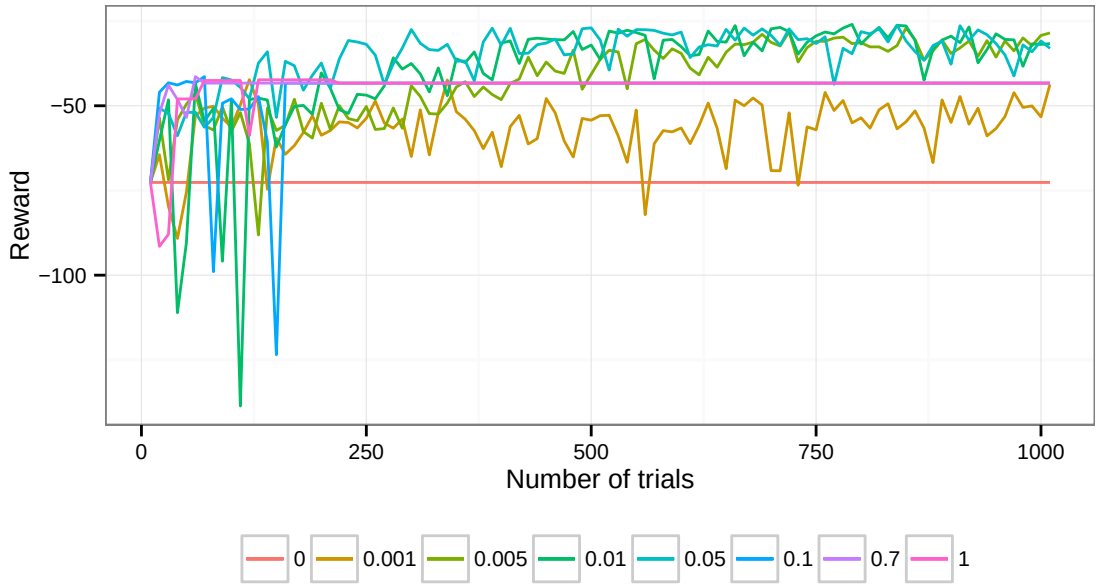

Figure 6.11: Sensitivity analysis on the α parameter (values of 0, 0.001, 0.005, 0.01, 0.05, 0.1, 0.7 and 1, respectively) on the controller's performance over 1,000 trials.

factor. The learning policy used here is an epsilon greedy policy, meaning that it does not always takes the best actions, but sometimes tries something else. The ε parameter is the probability that the agent picks, at random, one of the non-greedy actions. And, thus, with probability (1-ε) the agent selects the greedy action. For the scenario here, the highest reward (of -31.61) accumulates when ε is 0, while the lowest reward accumulates when ε is 1 (of -76.42). Therefore, it is concluded that less exploration leads to a better performance of the controller.

Figure 6.13 shows how the average reward over 1,000 trials changes with the number of tiles used for the function approximation. A higher number of tiles is equivalent to a more time consuming learning process. The highest reward (of -31.61) accumulates when 30 tiles are used, while the lowest reward (of -74.47) accumulates when 80 tiles are used. Therefore, it is concluded that a large number of tiles leads to a worse performance of the controller, and also a longer run-time (approximately 3 times longer for 80 tiles, compared to 30). For this reason, 30 tiles were used in the work here.

6.6 Reinforcement learning-based multi-zone control

Another test scenario evaluated is a reinforcement learning-based multi-zone control. Rather than controlling the whole occupant equivalent temperature, the multi-zone control aims to control independently

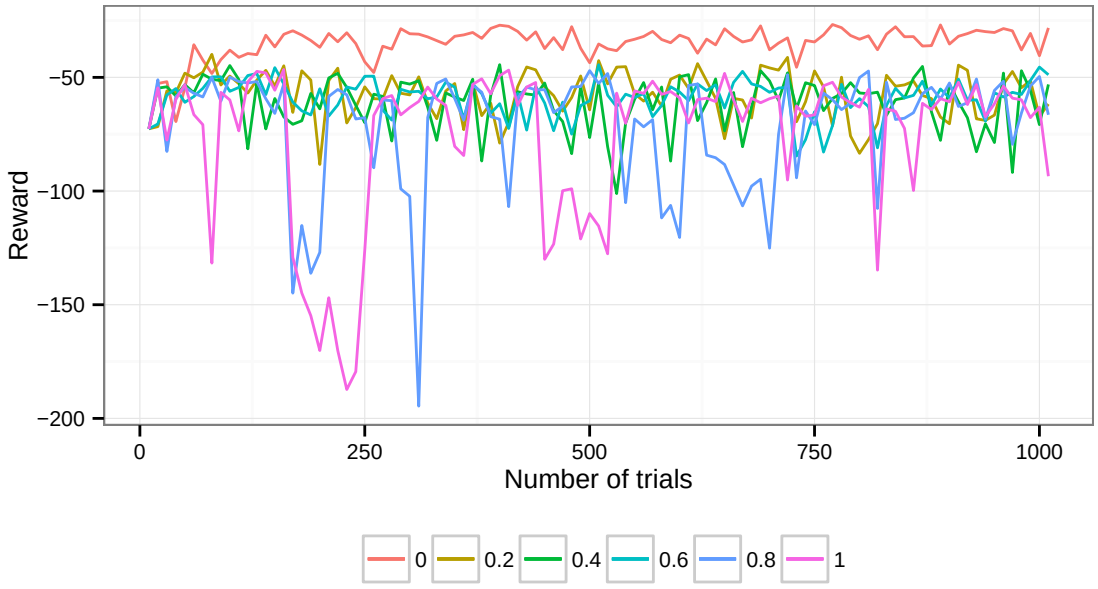

Figure 6.12: Sensitivity analysis on the ε parameter (values of 0, 0.2, 0.4, 0.6, 0.8 and 1, respectively) on the controller's performance over 1,000 trials.

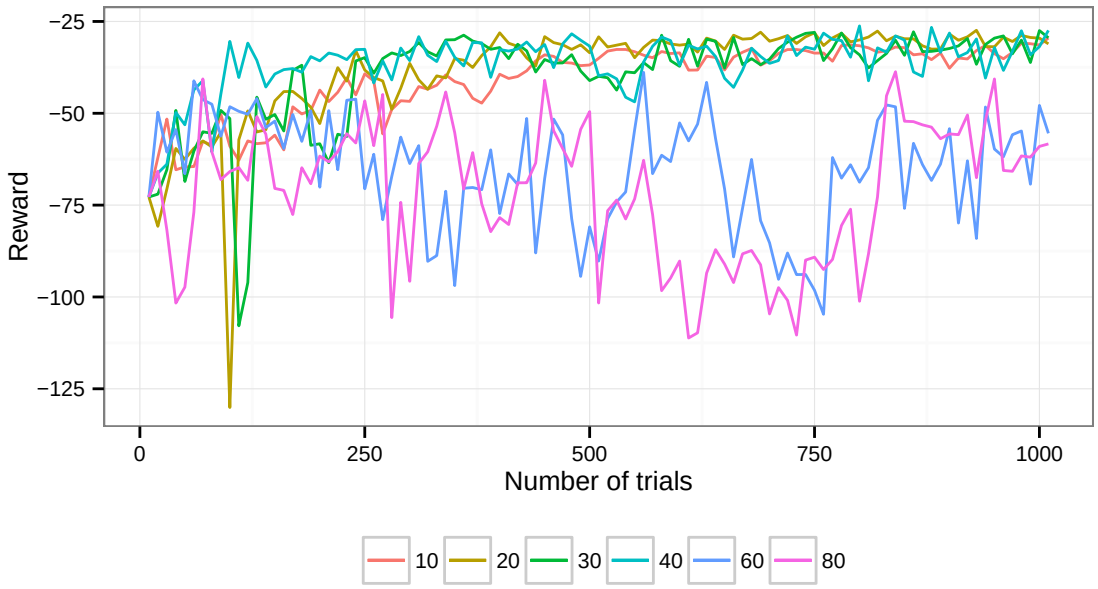

Figure 6.13: Sensitivity analysis on the number of tiles (values of 10, 20, 30, 40, 60 and 80, respectively) on the controller's performance over 1,000 trials.

two separate body parts, the head and feet of the cabin occupant. The reinforcement learning components are described in the following subsections.

6.6.1 Simulation

A simulation was created based on equations 6.1 to 6.12 with the addition of multiple zones. The relationship between the zones is illustrated in Figure 6.14. Two vents are considered in this simulation, one oriented towards the head and one oriented towards the feet, both with fixed position throughout the simulation. The simulation assumptions presented in the previous scenario, in Section 6.1, also apply for this simulation.

6.6.2 State representation

The state of the environment is described by four variables, namely the head equivalent temperature T_H, the foot equivalent temperature T_F, the block temperature T_b and the outside air temperature T_o. The equivalent temperature of a body part can be computed, as in the previous scenario, from the body part air temperature, air flow at that particular body part, mean radiant temperature at that particular body part and the clothing index at that particular body part.
Random continuous values are assigned to the state variables at the beginning of each learning episode in the following ranges:

- Head equivalent temperature T_H: [0,40] ℃.
- Foot equivalent temperature T_F: [0,40] ℃.
- Outside temperature T_o: [0,30] ℃.
- Block temperature T_b: [0,50] ℃.

As with the previous scenario, in order to avoid combinations of temperatures that are not likely to be encountered in a real environment, a set of rules similar to the one in 6.15 has been developed.

6.6.3 Action representation

A set of actions that can be taken by the agent is defined. The learning agent is able to control the head vent air flow V_h, the foot vent air flow V_f, the head vent air temperature T_h, the foot vent air temperature T_f, and the amount of air to be recirculated A_r. For each action there is a discrete range of values available, as follows:

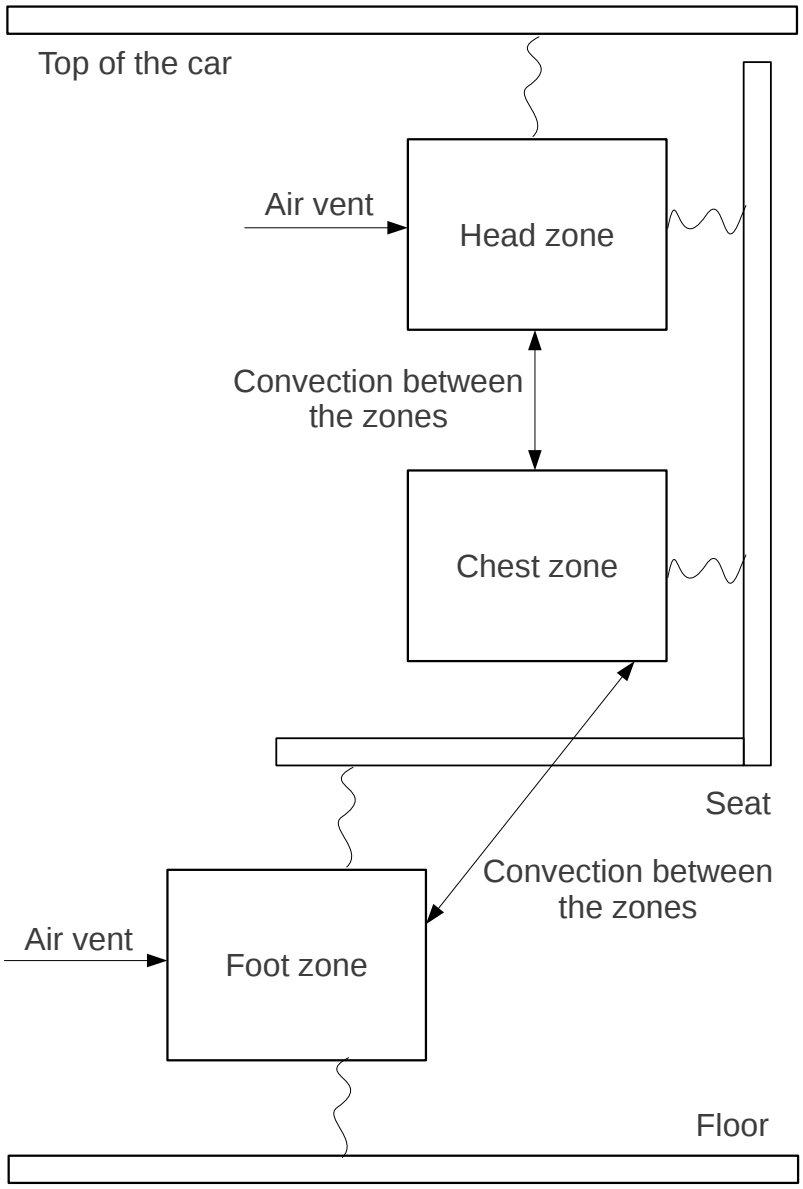

Figure 6.14: Multi-zonal simulation.

- Head and foot vents air flow: Three vent air flow set-points, evenly distributed over the $[0, 100]$ ls^{-1} range.
- Head and foot vents air temperature: Four set-points, evenly distributed over the [−20,40] ℃ range.
- Recirculation: Three set-points: 0 (no recirculation), 0.5 (partial recirculation) and 1 (full recirculation).

For this task there are, therefore, 434 different combinations of actions.

6.6.4 Reward

The goal of the learning problem is to maintain the equivalent temperature of the occupant's head between $[24, 26]$ ℃, corresponding to thermal neutrality based on Nilsson's model for summer clothing conditions, and the foot equivalent temperature between $[17, 19]$ ℃, corresponding to the "slightly cool" thermal sensation based on the same model. The reward, therefore, firstly takes into account whether the thermal comfort criteria has been satisfied. The reward also takes into consideration the energy consumed and the vent flow rate. The current reward function was developed based on an empirical investigation and is expressed as:

$$R(s, a, s^{'}) = R_i(s^{'}) + R_c(s^{'}) + R_e(s^{'}) \tag{6.21}$$

$$R_i(s^{'}) = \begin{cases} -1000, & s^{'} \text{ is illegal} \\ 0, & \text{otherwise} \end{cases} \tag{6.22}$$

$$R_c(s^{'}) = \begin{cases} 1, & T_H \in [24.0, 26.0] \text{ and } T_F \in [17.0, 19.0] \\ 0, & T_H \in [24.0, 26.0] \text{ or } T_F \in [17.0, 19.0] \\ -1, & \text{otherwise} \end{cases} \tag{6.23}$$

$$R_e(s^{'}) = -(Q + V_h + V_f)/1500 \tag{6.24}$$

Equation 6.20 is the part of the reward dealing with illegal states and shows how these illegal states are penalised. A state is considered illegal when its components (the head equivalent temperature, the foot equivalent temperature, the block temperature and the outside air temperature) go beyond the minimum or maximum possible value. If the state is legal, then no penalty is introduced. The penalty for an illegal state is large so that the actions leading to these illegal states are quickly eliminated as a solution.

Table 6.2: Tile coding parameters used to learn the control policy.

Variable	Minimum	Maximum	Intervals
T_H	0	40	9
T_F	0	40	9
T_b	0	50	3
T_h	-20	40	3
T_f	-20	40	3
V_h	1	100	3
V_f	1	100	3
A_r	0	1	3

Equation 6.21 is the thermal comfort reward component. If both body part equivalent temperatures (head and foot) are within the desired limits, then a reward of 1 is given. If only one of the body part equivalent temperatures is within the desired limits, then no penalty is given, otherwise, if none of the body part equivalent temperatures are within the desired range, a penalty of -1 is introduced. Equation 6.22 is the energy consumption reward component. In all circumstances, a penalty is given directly proportional to the amount of heat entering the cabin Q and the two vent air flow setting, V_h and V_f.

6.6.5 Parameter values

As in the previous scenario, the parameter values were optimised for this particular application.

1. Number of steps per episode: 1000.
2. Decay factor: $\lambda = 0.3$.
3. Reward discount factor: $\gamma = 0.99$.
4. Learning rate: $\alpha = 0.005$.
5. Exploration factor: $\varepsilon = 0$.

6.6.6 Policy

As with the previous scenario, Sarsa(λ) is used to learn the optimum policy, together with a tile coding function approximator. The tile coding parameters used for this problem are presented in Table 6.2. The tile coding used to represent the action-values included 50 tiles, 30 tiles integrating the variables $(T_H, T_h, T_f, V_h, V_f, A_r)$ and 20 tiles integrating the variables $(T_H, T_{F,} T_h, T_f, V_h, V_f, A_r)$. The number of intervals for each variable was selected based on an initial empirical investigation.

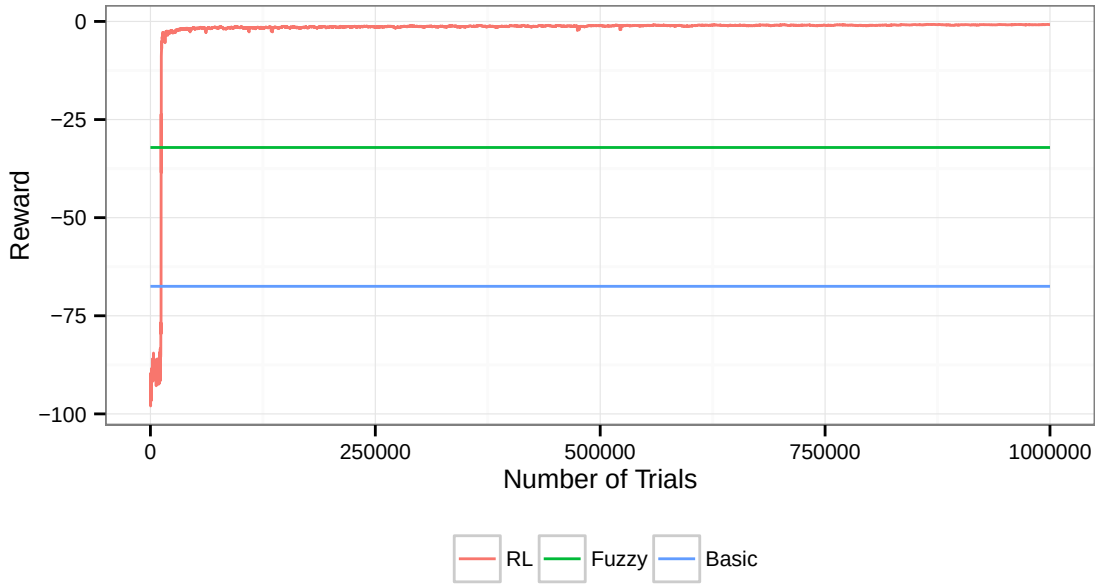

Figure 6.15: Policy performance during learning for Sarsa(λ) compared to the basic and fuzzy logic-based controllers.

6.6.7 Results

In this section, the performance of the reinforcement learning-based controller is compared to the performance obtained by a fuzzy logic-based controller (developed similarly to the one described in Section 6.3) and a basic heating and cooling controller. As in the previous scenario, the basic controller blows the coldest vent temperature at the fastest vent speed in order to cool down the cabin and blows the hottest vent temperature at the fastest vent speed in order to warm up the cabin.

Figure 6.15 shows the relative performance of the reinforcement learning-based controller compared to the fuzzy logic-based controller and the basic controller. The reward is averaged over a standard set of 100 randomly generated test cases (referred to as one learning trial). The same set of generated test cases are used each time the performance is evaluated. The reinforcement learning controller achieves an average reward of -2.24 over 1,000,000 trials. Learning a good policy is achieved slower than for the previous scenario due to the more complex environment representation (in around 15,000 trials). As for the single-zone case, the algorithm does not converge to a particular value, but to a region.

Intuitively, the basic controller should have the poorest performance. Even though its behaviour is optimum in terms of time-to-comfort, by cooling-down or warming-up the cabin on maximum vent temperature and maximum flow until the desired temperature is reached, this approach is energy wasteful

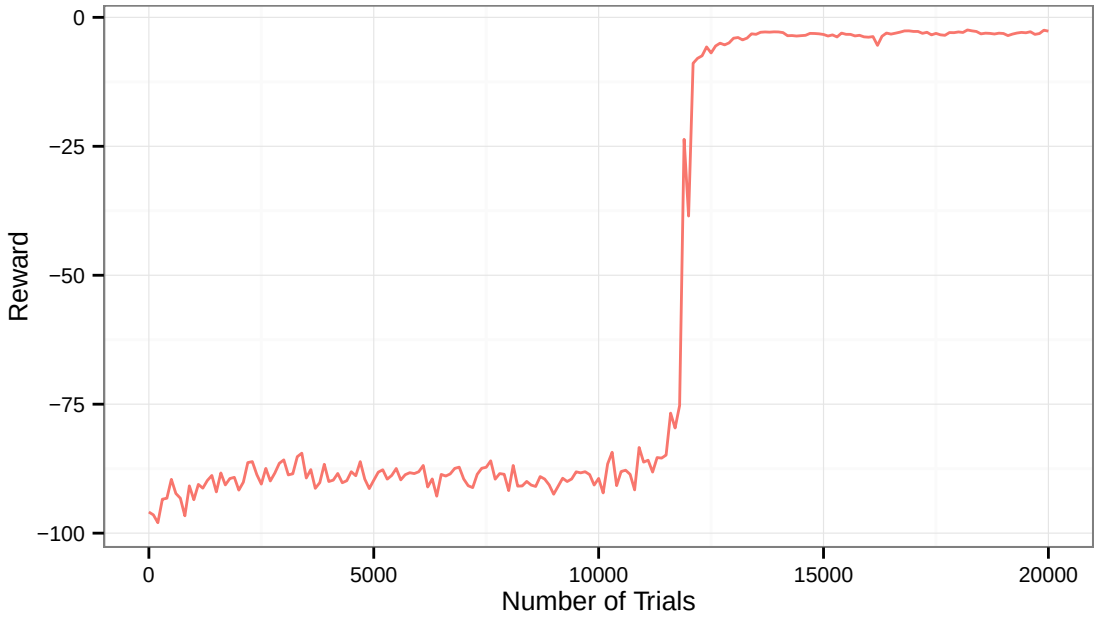

Figure 6.16: Policy performance during learning for Sarsa(λ).

and, therefore, the energy component of the performance function is greatly penalised. The performance of the basic controller was of -67.85, while the performance of the fuzzy controller-based controller was of -32.12.

These results translate into an average of 29.87.1% energy saving (corresponding to a 156.43 J) when using the reinforcement learning-based controller over 200 testing scenarios when compared to the fuzzy logic-based controller, while thermal comfort was achieved and maintained successfully.

Figure 6.16 shows that the optimum policy is learnt by the Sarsa(λ) algorithm within the first 20,000 trials. It is interesting to observe that the learning process is slower within the first 11,000 trials, followed by a sharp increase. The reward continues to increase gradually within the 1,000,000 trials, reaching up to -0.82.

Figure 6.16 shows how the Sarsa(λ) policy controls the occupant head and foot equivalent temperatures starting with a random state (38.7 ℃ head equivalent temperature, 31.2 ℃ foot equivalent temperature, 28.5 ℃ block temperature and 30.1 ℃ outside temperature). Then, the head and foot equivalent temperature are maintained between the upper and lower limits of the desired interval (24 ℃ and 26 ℃ for the head and 17 ℃ and 19 ℃ for the foot).

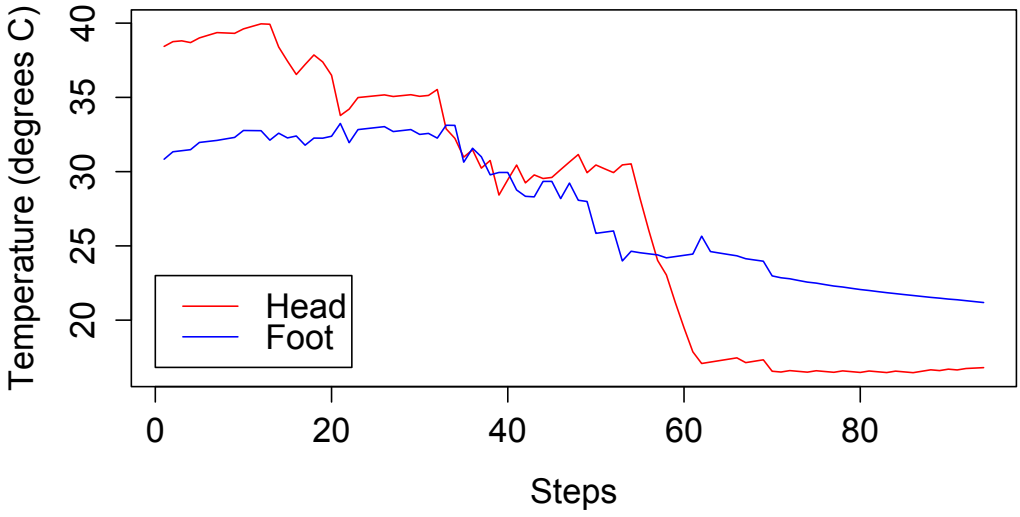

Figure 6.17: Cooling down scenario using Sarsa(λ).

6.7 Summary

This chapter described the development and evaluation of a reinforcement learning-based heating and cooling controller that learns an optimum policy of maintaining occupant equivalent temperature within thermally comfortable ranges, while minimising the energy consumption. The reinforcement learning-based controller used the Sarsa(λ) algorithm and its parameters were optimised for this particular application. The controller's performance was evaluated on a one dimensional heat flux-based car cabin simulation and compared to the performance of two other controllers: a basic one and a fuzzy logic-based one.

For the single-zone scenario, the results show that the reinforcement learning-based controller brings considerable performance improvement when compared to the other two controllers: an average reward of -29.16, compared to a reward of -62.70 achieved by the basic controller and a reward of -50.55 achieved by the fuzzy logic-based controller. The same takes place in the multi-zone scenario. The reinforcement learning-based controller maximised the reward to -2.24. The basic controller had, as in the single-zone scenario, the poorest performance (a reward of -67.85), while the performance of the fuzzy logic-based controller was a reward of-32.12.

For the single-zone scenario the reinforcement learning-based controller saved an average of 27.05% energy over 200 testing scenarios when compared to the fuzzy logic-based controller, while thermal com-

fort was achieved and maintained successfully. On the other hand, for the multi-zone scenario the reinforcement learning-based controller saved an average of 29.87% energy over 200 testing scenarios when compared to the fuzzy logic-based controller, while thermal comfort was achieved and maintained successfully.

The next chapter presents an overview of the work presented in this thesis and the way the individual components work together. It also gives an insight into a potential real-time system that can be developed based on this work.

Chapter 7

Conclusions and Future Work

The work in this thesis focused on developing a reinforcement learning-based Heating, Ventilation and Air Conditioning (HVAC) controller that maximises occupant thermal comfort while minimising energy consumption. First, in order to efficiently control occupant comfort, a model relating measurable parameters, such as air temperature, to human thermal comfort is needed. Based on an empirical data analysis, Nilsson's equivalent temperature-based thermal comfort model was shown to be the most suitable model for vehicular comfort-oriented control due to the following reasons:

1. The model provided high correlations with subjective thermal sensation throughout the experimental trials (between 0.78 and 0.92).

2. The model has the advantages of estimating local thermal sensation and requiring only two input parameters.

In order to apply Nilsson's thermal comfort model to actuate the HVAC controller, equivalent temperature has to be measured in real-time. Direct real-time measurement of equivalent temperature is, however, not feasible. Therefore, this thesis further focuses on an innovative way to actuate the HVAC controller—through a Virtual Thermal Comfort Sensing (VTCS) approach. The VTCS method estimates body part equivalent temperature from a minimalistic set of inexpensive cabin environmental sensors. First, VTCS requires a mechanism for selecting the optimal sensors and their associated locations for the estimation, achieved in this thesis through a mutual information-based method. Based on empirical cabin data, the optimal set of sensors selected were a mean radiant temperature sensor placed at a central ceiling location and an air temperature sensor placed in the front row at the belt level of the driver. Second, the actual estimation is performed using Multiple Linear Regression (MLR)—a learning approach selected as the most suitable out of seven different techniques examined based on two metrics: the estimation Root Mean Square Error (RMSE) and the processing time required for the estimation.

The final component of this thesis consists of the high-level reinforcement learning-based HVAC controller that maximises occupant thermal comfort while minimising the energy consumed. Two evaluation scenarios are proposed:

1. A single-zone scenario that aims to maintain the overall equivalent temperature of a cabin occupant within a thermally comfortable range based on Nilsson's thermal comfort model.

2. A multi-zone scenario that aims to maintain the occupant head and foot equivalent temperatures within different ranges.

The performance of the reinforcement learning-based controller was compared to that of a basic controller (blows the coldest vent temperature at the fastest vent speed in order to cool-down the cabin and blows the hottest vent temperature at the fastest vent speed in order to warm-up the cabin, respectively) and a fuzzy logic-based controller. The performance metric is the *reward* (a number that translates into whether the thermal comfort criteria is satisfied and how much energy is consumed), allowing a meaningful comparison between the controllers. For the single-zone scenario, the performance for the basic controller was the lowest (reward of -62.70). The fuzzy logic-based controller improved on this performance (reward of -50.55). However, the reinforcement learning-based controller managed to achieve a significantly better performance (reward of -29.16).

The performance ranking from above held also for the multi-zone scenario. The reinforcement learning-based controller achieved the highest performance (reward of -2.24). The basic controller had, as in the single-zone scenario, the poorest performance (a reward of -67.85), while the performance of the fuzzy logic-based controller, again, improved on the basic controller (reward of-32.12).

The work presented in this thesis resulted in the following contributions to knowledge:

1. The identification and evaluation (based on gathered empirical data) of the most suitable existing thermal comfort model to be used for vehicular heating and cooling control.

2. A method for developing VTCS to actuate the heating and cooling control. The method consists of:

   (a) A method that selects the optimum set of cabin environmental sensors and their associated locations for estimating occupant body part equivalent temperature.

   (b) An equivalent temperature estimation machine learning-based method. The method was selected out of seven different approaches based on accuracy and processing time.

3. A reinforcement learning-based policy design for producing an energy efficient comfort-oriented heating and cooling controller, which outperforms current state-of-the-art methods.

This chapter is structured as follows: Section 7.1 provides answers to the research questions posed in Chapter 1. Section 7.2 proposes future research topics. Finally, Section 7.3 concludes this thesis.

7.1 Answers to research questions

This thesis has answered the following research questions:

7.1.1 Is there an existing thermal comfort model that is suitable for real-time use in an HVAC system and if so, which is it?

Yes—Nilsson's equivalent temperature-based thermal comfort model is the most suitable model for comfort-oriented HVAC control.

To answer this question, an empirical analysis was conducted investigating four existing thermal comfort models: Predicted Mean Vote (PMV), Zhang's model, Taniguchi's model and Nilsson's model (all described in Section 2.1). In order to conduct this analysis, experimental data was gathered from a number of trials that included both steady-state conditions and conditions normally expected while driving and in which subjective comfort measures were sought from human participants.

The main criteria for selecting the most suitable thermal comfort model was the correlation index between the model output and the subjective thermal comfort reports. Additional characteristics of the models are also considered. Based on the experimentally gathered data, the PMV index and Nilsson's index accurately matched (with correlations of 0.91 and 0.93, respectively) the occupant reported thermal sensation within a limited set of conditions: pre-conditioning of the passenger and the cabin at the same temperature, a steady outside temperature and low rates of change of the interior temperature (lower than 1.5 ℃ per minute). High cabin average temperature rates of change (up to 9 ℃ per minute), ambient solar load and wind led to lower correlation factors, between 0.76 and 0.79.

On the other hand, the overall sensation computed using the two skin temperature-based thermal comfort models (Taniguchi's model and Zhang's model) matched the subjective reports with low correlation levels throughout all trial types (correlation indexes between 0.10 and 0.60). Overall, the accuracy of the two skin temperature-based models is not sufficient to support vehicular HVAC comfort control.

Based on the findings, Nilsson's model was shown to be the most suitable model for vehicular comfort-oriented control out of the four thermal comfort models evaluated. The model matched the subjective reports with a correlation index similar to PMV. However, an important advantage Nilsson's model has over PMV is its ability to estimate local thermal sensation, which is an important capability for the new generation of vehicular HVAC control systems. Moreover, Nilsson's model only requires two input parameters—equivalent temperature and the clothing index—rather than six parameters in PMV's case, some of which could not feasibly be determined by an automated system.

More details regarding the investigations performed are given in Section 4.3.

7.1.2 Can an optimum set of cabin environmental sensors be defined for estimating occupant body part equivalent temperature, given realistic constraints?

Yes—an optimum set of cabin environmental sensors for estimating occupant body part equivalent temperature can be selected using a mutual information-based feature selection mechanism.

Common sensor positioning approaches are driven by considerations such as cost or aesthetics, which may impact on the performance of the HVAC system and thus on occupant comfort. This thesis presented a generic method of improving the location of sensors in order to more accurately estimate occupant body part equivalent temperature and thus thermal sensation.

In order to answer this research question, an analysis was conducted based on experimental data. Data was gathered from a number of trials that included both steady-state conditions and conditions normally expected while driving, and from both cabin environmental data and equivalent temperature measured by dry heat loss transducers attached to a support manikin. The selection of the best cabin environmental sensors from the available set is performed via a mutual information method based on entropy values. Two cabin environmental sensors, a mean radiant temperature sensor placed at a central ceiling location and an air temperature sensor located at the front row right belt level, sharing a mutual information of 1.56 nats with the body part equivalent temperatures, were shown to provide an average equivalent temperature estimation RMSE of 1.41 ℃ in highly-transient vehicular environment conditions. The cabin environmental sensor selection can be optimised for a different number of passengers and for estimating different parameters. Also, the method can be applied in a variety of other applications.

More details regarding this work are given in Section 5.1.

7.1.3 Is MLR the most suitable machine learning technique for estimating occupant body part equivalent temperature from a set of cabin environmental sensors?

Yes—MLR is the most suitable machine learning approach out of seven different methods examined for estimating occupant body part equivalent temperature.

To answer this question, seven different machine learning approaches were implemented for estimating body part equivalent temperature based on the measurements from the selected cabin environmental

sensors: MLR, Multilayer Perceptron (MLP), K-Nearest Neighbour (KNN), Multivariate Adaptive Regression Splines (MARS), Radial Basis Function Network (RBF), Reduced Error Pruning Tree (REPTree) and Random Forest (RF). Most algorithms provided a RMSE between 1.51 ℃ (for MARS) and 1.85 ℃ (for KNN). RBF performed the worst, with an average RMSE of 3.37 ℃. MLR had an average RMSE of 1.60 ℃ over the eight body part equivalent temperatures. MLR requires the least computational power (after KNN) and had the fastest processing time out of the seven methods examined, a factor important to take into account when integrating the VTCS approach in a car's engine control unit.

More details regarding the investigation performed are given in Section 5.2.

7.1.4 Is it possible to represent the state of the cabin environment in such a way that it fulfils the Markov Decision Process (MDP) criteria?

Yes—the state for the car cabin environment in two different scenarios (one controlling the overall occupant equivalent temperature and one controlling occupant head and foot equivalent temperature) was represented such that it fulfils the MDP criteria.

In order for an environment to fulfil the MDP criteria, the representation of the state needs to be Markovian (that is, the state comprises all the necessary information and this information suffices in order to decide the next action). In general, the aim is to express the state in a compact way, so that the complexity of the reinforcement learning problem is significantly reduced.

For the scenarios presented within this thesis, it was possible to gather enough information to form a state signal with the Markov property that fully observed the environment. For the single-zone scenario, the state consisted of the occupant overall equivalent temperature, block temperature and outside air temperature. For the multi-zone scenario, the state consisted of the occupant head equivalent temperature, occupant foot equivalent temperature, block temperature and outside temperature.

More details regarding this work are given in Chapter 6.

7.1.5 Can a reinforcement learning-based heating and cooling control policy provide performance beyond the current state-of-the-art?

Yes—the reinforcement learning-based control policy was compared with two other controllers and it outperformed them with a factor of 2.15 and 1.73, respectively in simulation trials.

To answer this question, the Sarsa(λ) algorithm was implemented and two evaluation scenarios were proposed: i) a single-zone scenario that aims to maintain the overall equivalent temperature of a cabin

occupant within a thermally comfortable range based on Nilsson's thermal comfort model and ii) a multi-zone scenario that aims to maintain the occupant head and foot equivalent temperatures within different ranges. A basic controller and a fuzzy logic-based controller were also implemented in order to provide a performance comparison. The performance metric used was the *reward*—a numerical index expressing whether the occupant thermal comfort criteria is achieved and the amount of energy consumed.

For the single-zone scenario, intuitively, the basic controller should have the poorest performance. Even though its behaviour is optimum in terms of achieving comfort, by cooling-down or warming-up the cabin on maximum vent temperature and maximum flow until the desired temperature is reached, this approach is very energy wasteful and, therefore, the energy component of the reward function is greatly penalised. The reward for the basic controller was of -62.70. On the other hand, the fuzzy logic-based controller is expected to perform better. This approach improves over the basic controller, however, it does not benefit from the reinforcement learning approach of receiving feedback. The performance for the fuzzy logic-based controller was a reward of-50.55. The reinforcement learning algorithm, by including energy consumption in its reward function, managed to achieve a significantly better performance, with a reward of -29.16. These results translate into an average of 27.05% energy saving over 200 testing scenarios when compared to the fuzzy logic-based controller, while thermal comfort was achieved and maintained successfully.

For the multi-zone scenario, the reinforcement learning-based controller maximised the reward to -2.24. The basic controller had, as in the single-zone scenario, the poorest performance (a reward of -67.85), while the performance of the fuzzy logic-based controller was a reward of -32.12. These results translate into an average of 29.87.1% energy saving over 200 testing scenarios when compared to the fuzzy logic-based controller, while thermal comfort was achieved and maintained successfully.

By outperforming the fuzzy logic-based controller, which is the most used type of controller in the literature, the author has shown that the reinforcement learning-based controller improves the state-of-the-art in the area of thermal comfort-oriented vehicular HVAC control.

More details regarding this work are given in Chapter 6.

7.2 Future work

There are several areas of potential future work. This section presents three such areas that would improve the system functionality and provide additional evaluation of its performance.

7.2.1 Further improvement on the thermal comfort model

The work in this thesis focused on evaluating several hypotheses related to vehicle thermal comfort and existing thermal comfort models. A related avenue for future work is with regard to heated/cooled seats and steering wheels. These are becoming more widespread and will clearly have an impact on local thermal sensation and comfort, which should be evaluated through empirical work. Examples of questions that would be interesting to answer are:

1. Identify the separate contributions of heated seats and heated steering wheels to skin temperature, thermal sensation and time to thermal comfort after entering the vehicle at a range of cool temperatures in comparison to that achieved through the HVAC system alone.

2. Identify the separate contributions of cooled seats and cooled steering wheels on skin temperature, thermal sensation and time to thermal comfort after entering the vehicle at a range of hot temperatures in comparison to that achieved through the HVAC system alone.

3. Determine the optimal combination of heating and cooling actuation of seats/steering wheels required to achieve thermal comfort in the shortest possible time in hot and cold conditions, respectively.

Also, as a related issue, the deviation between the Flatman's PMV output and the subjective responses may be because the subjects were in contact with the seat and the steering wheel whereas the Flatman's dry heat loss sensors were not. This could be confirmed via further experimentation.

7.2.2 Extend the VTCS approach to include additional sensor types

The work in Chapter 4 of this thesis focused on developing a VTCS method that estimates occupant body part equivalent temperature from cabin environmental sensors. The method developed allows the selection of the optimum cabin sensors and their associated locations estimating equivalent temperatures. The best cabin environmental sensors were the mean radiant temperature sensor and the air temperature sensor located at the front row right belt level. Since equivalent temperature integrates the effect of air flow, future work should examine the impact of this on the estimation error and find optimal air flow sensor locations using the methodology presented in Chapter 4.

7.2.3 Extend the reinforcement learning work

The reinforcement learning-based controller developed is dependent on the simulation of the car cabin environments used for learning. There is, therefore, scope for improvement beyond the work on this thesis. An important avenue for this improvement is designing a more complex, multiple dimensional simulation using a software tool such as Dymola. This would allow a more thorough evaluation of multi-zone control. An improved simulation should also incorporate elements such as heated/cooled seats and steering wheels. These could be effectively controlled in order to improve comfort and minimise overall energy consumption.

Also, the simulation-based controller could be integrated in progressive stages within the car cabin and its thermal management actuators and sensors. At this stage, the user's feedback, in terms of manually overriding the learnt policy or intervening in the control, provides an additional cabin state element and the reward function will penalise this heavily—thus encouraging a policy well suited to the specific end-user.

Another venue for future work consists in identifying a feasible time constant. A key component of the learning approach is the identification of the most appropriate time-scale for the system. This time-scale is essentially the simulation sample rate, however it will also become the cycle time for the final controller. If this rate is set too low (long periods between each actuation change), then the learnt system may lag the environmental change in a noticeable way. If the rate is set too high, then the actions will have had little time to take effect and the learning algorithm will have difficulty in converging on a solution.

There are a few other questions related to the reinforcement learning-based controller that future work aims to answer, such as:

1. How frequently should the reinforcement learning-based control act throughout a journey?
2. Which is the optimal way for the controller to learn from manual user overrides?
3. How to design the state space for a real-time use of the system in an optimal way?

7.3 Summary

This thesis set out to demonstrate that vehicle HVAC comfort control can be improved beyond the current state-of-the-art. A strength of this work comes from the fact that the thermal comfort related analysis conducted is based on gathered empirical data—both cabin environmental sensor data and subjective occupant reports. This data was used to determine that Nilsson's equivalent temperature-based model

is the most suitable for vehicular HVAC control, by considering the correlation score with subjective occupant comfort data and additional characteristics of the models, such as ability to estimate local thermal sensation and number of input parameters.

Further to selecting the most suitable thermal comfort model, the development of a VTCS method that estimates occupant body part equivalent temperatures is proposed. First, using a mutual information-based approach, the subset of cabin environmental sensors that correlate well with the body part equivalent temperatures are selected. Second, MLR is used to infer the occupant body part equivalent temperatures from the selected cabin environmental sensors. The equivalent temperature estimation RMSE are on average around 1.41 ℃ across environmental conditions characterised by cabin interior temperature rates of change of up to 6 ℃ per minute, ambient temperature differences up to 6 ℃ per experimental trial, varying ambient wind, solar load and precipitation.

Finally, this thesis proposes an innovative reinforcement learning-based controller that phrases the control specification in terms of an overall objective function based on the thermal comfort of the passengers and the energy consumption. The performance metric used in evaluating the controllers was the *reward*—a measure quantifying whether occupant thermal comfort was achieved and the amount of energy consumed. The proposed controller was evaluated through simulation within both single-zone and multi-zone scenarios and it exceeded the performance of a basic controller and a fuzzy logic-based controller by a factor of 2.15 and 1.7, respectively. These results translate into an average of 32.5% energy saving over 100 testing scenarios when compared to the fuzzy logic-based controller, while thermal comfort was achieved and maintained successfully.

The learning-based control method presented sets the benchmark for future vehicular HVAC systems. Furthermore, the underlying approaches can be applied to existing techniques and instantiated for a wide variety of applications.

References

[1] Ali Alahmer, Mahmoud Abdelhamid, and Mohammed Omar. Design for Thermal Sensation and Comfort States in Vehicles Cabins. *Journal of Applied Thermal Engineering*, 36:126–140, 2012.

[2] Ali Alahmer, Ahmed Mayyas, Abed Mayyas, Mohammed Omar, and Dongri Shan. Vehicular Thermal Comfort Models - a Comprehensive Review. *Journal of Applied Thermal Engineering*, 31:995–1002, 2011.

[3] Ali Alahmer, Mohammed Omar, Abed Mayyas, and Dongri Shan. Effect of Relative Humidity and Temperature Control on In-Cabin Thermal Comfort State: Thermodynamic and Psychometric Analyses. *Journal of Applied Thermal Engineering*, 31:2636–2644, 2011.

[4] James Albus. A New Approach to Manipulator Control: The Cerebellar Model Articulation Controller (CMAC). *Journal of Dynamic Systems, Measurement and Control*, 97:220–227, 1975.

[5] Rafael Alcala, Jose M. Benitez, Jorge Casillas, Oscar Cordon, and Raul Perez. Fuzzy Control of HVAC Systems Optimized by Genetic Algorithms. *Journal of Applied Intelligence*, 18:155–177, 2003.

[6] A. Alexandrov, V. Kudriavtsev, and M. Reggio. Analysis of Flow Patterns and Heat Transfer in Generic Passenger Car Mini-Environment. In *Proceedings of the 9th Annual Conference of the CFD Society of Canada*, 2001.

[7] Edward Arens, Hui Zhang, and Charlie Huizenga. Partial and Whole-Body Thermal Sensation and Comfort, Part I: Uniform Environmental Conditions. *Journal of Thermal Biology*, 31:53–59, 2006.

[8] Edward Arens, Hui Zhang, and Charlie Huizenga. Partial and Whole-Body Thermal Sensation and Comfort, Part II: Non-uniform Environmental Conditions. *Journal of Thermal Biology*, 31:60–66, 2006.

[9] S. Atthajariyakul and T. Leephakpreeda. Neural Computing Thermal Comfort Index for HVAC Systems. *Journal of Energy Conversion and Management*, 46:2553–2565, 2005.

[10] Santhosh Baboo and Kadar Shereef. An Efficient Weather Forecasting System using Artificial Neural Network. *International Journal of Environmental Science and Development*, 1:321–326, 2010.

[11] Roberto Battiti. Using Mutual Information for Selecting Features in Supervised Neural Net Learning. *IEEE Transactions on Neural Networks*, 5(4):537–550, 1994.

[12] T. Bedford. Skin Temperature in Relation to the Warmth of the Environment. *Journal of Hygiene*, 35:307–317, 1935.

[13] Ivars Beinarts and Anatoly Levchenkov. Fuzzy Logic Controller Support to Passengers' Comfort for Electric Train Coach Heating System. In *Proceedings of the International Conference on Computer as a Tool*, pages 1–4, 2011.

[14] Sun Bin and Han Ke. Indoor Thermal Comfort PMV Index Prediction based on Particle Swarm Algorithm and Least Square Support Vector Machine. In *Proceedings of the International Conference on Intelligent System Design and Engineering Application*, volume 1, pages 857–860, 2010.

[15] Anna Bogdan. Case Study Assessment of Local and General Thermal Comfort by Means of Local Skin Temperature. *International Journal of Ventilation*, 10(3):291–300, 2011.

[16] Leo Breiman. Random Forests. Technical report, University of California Berkeley, 2001.

[17] Christian F. Bulcao, Steven M. Frank, Srinivasa N. Raja, Kha M. Tran, and Davis S. Goldstein. Relative Contribution of Core and Skin Temperatures to Thermal Comfort in Humans. *Journal of Thermal Biology*, 25:147–150, 2000.

[18] S.D. Burch, J.T. Pearson, and S. Ramadhyani. Experimental Study of Passenger Thermal Comfort in an Automobile Under Severe Winter Conditioning. *Journal of ASHRAE Transactions*, 97:239–246, 1991.

[19] Richard Burke, Allen Curan, and Mark Hepokoski. Integrating an Active Physiological and Comfort Model to the Newton Sweating Thermal Manikin. Technical report, Measurement Technology NorthWest, ThermoAnalytics Inc., 2008.

[20] Matthias Busl. Design of an Energy-Efficient Climate Control Algorithm for Electric Cars. Master's thesis, Lund University, 2011.

[21] V. Candas. The Thermal Environemnt and Its Effects on Human. In *CABCLI Consortium*, 1999.

[22] Maria Castilla, Jose Domingo Alvarez, M.G. Ortega, and Manuel Arahal. Neural Network and Polynomial Approximated Thermal Comfort Models for HVAC Systems. *Journal of Building and Environment*, 59:107–115, 2013.

[23] Tulin Gunduz Cengiz. A Field Study on Drivers' Thermal Comfort with Road Trials. *G. U. Journal of Science*, 22:301–311, 2009.

[24] Kate E. Charles. Fanger's Thermal Comfort and Draught Models. Technical report, Institute for Research in Construction, National Research Council of Canada, 2003.

[25] Chen-Peng Chen, Ruey-Lung Hwang, Shih-Yin Chang, and Yu-Ting Lu. Effects of Temperature Steps on Human Skin Physiology and Thermal Sensation Response. *Journal of Building and Environment*, 46:2387–2397, 2011.

[26] Yuanda Cheng, Jianlei Niu, and Naiping Gao. Thermal Comfort Models: A Review and Numerical Investigation. *Journal of Building and Environment*, 47:13–22, 2012.

[27] Stephen Cheung. *Advanced Environmental Exercise Physiology.* Advanced Exercise Physiology Series, 2010.

[28] C.H. Chien, J.Y. Jang, Y.H. Chen, and S.C. Wu. 3-D Numerical and Experimental Analysis for Airflow within a Passenger Compartment. *International Journal of Automotive Technology*, 9:437–445, 2008.

[29] Maurizio Cisternino. Thermal Climate in Cabs and Measurement Problems. In *Proceedings of the CABCLI Consortium*, 1999.

[30] T. Cover and P. Hart. Nearest Neighbor Pattern Classification. *Journal of IEE Transactions on Information Theory*, 13:21–27, 1967.

[31] Allen Curran, Scott Peck, and Mark Hepokoski. Improving Passenger Compartment Thermal Comfort by Measuring and Controlling Equivalent Temperature. In *Proceedings of the FISITA World Automotive Congress*, 2010.

[32] Manuel Gameiro da Silva. Measurements of Comfort in Vehicles. *Journal of Measurement Science and Technology*, 13:41–60, 2002.

[33] Hein A.M. Daanen, Evert van de Vliert, and Xu Huang. Driving Performance in Cold, Warm and Thermoneutral Environments. *Journal of Applied Ergonomics*, 34:597–602, 2003.

[34] Ralph D'Agostino, Albert Belanger, and Ralph D'Agostino Jr. A Suggestion for Using Powerful and Informative Tests of Normality. *Journal of The American Statistician*, 44:316–321, 1990.

[35] Konstantinos Dalamagkidis, Dionysia Kolokotsa, K. Kalaitzakis, and G. Stavrakakis. Reinforcement Learning for Energy Conservation and Comfort in Buildings. *Journal of Building and Environment*, 42:2686–2698, 2007.

[36] Leighton Ira Davis, Robert Wayne Matteson, and Gerhard Allan Dage. Method and Control System for Controlling an Automotive HVAC System for Increased Occupant Comfort. US Patent 5570838, November 1996.

[37] Leighton Ira Davis, Thomas Francis Sieja, Gerhard Allan Dage, and Robert Wayne Matteson. Method and Control System for Controlling an Automotive HVAC System. European Patent 0739507 B1, September 1998.

[38] Richard de Dear and Gail Brager. Developing an Adaptive Model of Thermal Comfort and Preference. *Journal of ASHRAE Transactions*, 104:549–561, 1998.

[39] Janez Demsar, Tomaz Curk, Ales Erjavec, Crt Gorup, Tomaz Hocevar, Mitar Milutinovic, Martin Mozina, Matija Polajnar, Marko Toplak, Anze Staric, Miha Stajdohar, Lan Umek, Lan Zagar, Jure Zbontar, Marinka Zitnik, and Blaz Zupan. Orange: Data Mining Toolbox in Python. *Journal of Machine Learning Research*, 14:2349–2353, 2013.

[40] Joel M. Devonshire and James R. Sayer. Radiant Heat and Thermal Comfort in Vehicles. *Journal of Human Factors*, 47(4):827–839, 2005.

[41] Noel Djongyang, Rene Tchinda, and Donatien Njomo. Thermal Comfort: A Review Paper. *Journal of Renewable and Sustainable Energy Reviews*, 14:2626–2640, 2010.

[42] T. Doherty and Edward Arens. Evaluation of the Physiological Bases of Thermal Comfort Models. *Journal of ASHRAE Transactions*, 94, 1988.

[43] Norman R. Draper and Harry Smith. *Applied Regression Analysis*. Wiley, 1981.

[44] B. Egilegor, J. Uribe, G. Arregi, E. Pradilla, and L. Susperregi. A Fuzzy Control Adapted by a Neural Network to Mantain a Dwelling within Thermal Comfort. In *Proceedings of the 5th International IBPSA Conference*, 1997.

[45] Sture Elnaes. Thermal Climate in Confined Spaces - Measurement and Assessment Using a Thermal Manikin. In *Proceedings of SAE International*, 1988.

[46] Povl Ole Fanger. *Thermal Comfort*. Danish Technical Press, 1970.

[47] Povl Ole Fanger. Assessment of Man's Thermal Comfort in Practice. *British Journal of Industrial Medicine*, 30:313–324, 1973.

[48] Povl Ole Fanger and Jorn Toftum. Extension of the PMV Model to Non-Air-Conditioned Buildings in Warm Climates. *Journal of Energy Buildings*, 34:533–536, 2002.

[49] Yadollah Farzaneh and Ali A. Tootoonchi. Controlling Automobile Thermal Comfort using Optimized Fuzzy Controller. *Journal of Applied Thermal Engineering*, 28:1906–1917, 2008.

[50] Mark Feldmeier and Joseph A. Paradiso. Personalized HVAC Control System. In *Proceedings of the International Conference on Internet of Things*, pages 1–8, 2010.

[51] Marcio Alves Ferreira and Arlindo Tribess. Users Perception of Thermal Comfort in Ventilated Automotive Seats. In *Proceedings of the SAE International*, 2009.

[52] Dusan Fiala, Agnes Psikuta, Gerd Jendritzky, Stefan Paulke, David A. Nelson, Wouter D. van Marken Lichtenbelt, and Arjan J.H.Frijns. Physiological Modeling for Technical, Clinical and Research Applications. *Journal of Frontiers in Bioscience*, 2:939–968, 2010.

[53] Marc Fountain, Gail Brager, and Richard de Dear. Expectations of Indoor Climate Control. *Journal of Energy and Buildings*, 24:179–182, 1996.

[54] R. Freire, G. Oliveira, and N. Mendes. Predictive Controllers for Thermal Comfort Optimization and Energy Savings. *ABCM Symposium Series in Mechatronics*, 3:839–848, 2008.

[55] Roberto Z. Freire, Gustavo H.C. Oliveira, and Nathan Mendes. Development of Regression Equations for Predicting Energy and Hygrothermal Performance of Buildings. *Journal of Energy and Buildings*, 40:810–820, 2008.

[56] Jerome H. Friedman. Multivariate Adaptive Regression Splines. *Annals of Statistics Journal*, 19:1–67, 1991.

[57] Ming Fu, Tiefeng Yu, Hui Zhang, Edward Arens, Wenguo Weng, and Hongyong Yuan. A Model of Heat and Moisture Transfer Through Clothing Integrated with the UC Berkeley Comfort Model. *Journal of Building and Environment*, 80:96–104, 2014.

[58] Beatrice Gach, Michael Lang, and Jean-Christophe Riat. Fuzzy Controller for Thermal Comfort in a Car Cabin. In *Proceedings of SAE International*, 1997.

[59] A.P. Gagge, J.A.J. Stolwijk, and J.D. Hardy. Comfort and Thermal Sensations and Associated Physiological Responses at Various Ambient Temperatures. *Journal of Environmental Research*, 1:1–20, 1967.

[60] Guohui Gan. Analysis of Mean Radiant Temperature and Thermal Comfort. *Journal of Building Services Engineering Research and Technology*, 2:95–101, 2001.

[61] Hirokazu Genno, Atsuo Saijo, Hiroyuki Yoshida, Ryuuzi Suzuki, and Masato Osumi. Non-Contact Method for Measuring Facial Skin Temperature. *International Journal of Industrial Ergonomics*, 19:147–159, 1997.

[62] F.H. Glanz, W.T. Miller, and L.G. Kraft. An Overview of the CMAC Neural Network. In *Proceedings of the International Conference on Neural Networks for Ocean Engineering*, pages 301–308, 1991.

[63] Lakhi Nandlal Goenka and Clay Maranville. Control Strategy for a Zonal Heating, Ventilating and Air Conditioning System of a Vehicle. US Patent 0232996 A1, September 2013.

[64] Geo J. Gordon. Reinforcement Learning with Function Approximation Converges to a Region. *Journal of Neural Information Processing Systems*, pages 1040–1046, 2000.

[65] Mark Hall, Eibe Frank, Geoffrey Holmes, Bernhard Pfahringer, Peter Reutemann, and Ian Witten. The WEKA Data Mining Software: An Update. *Journal of SIGKDD Explorations*, 11, 2009.

[66] Maher Hamdi, Gerard Lachiver, and Francois Michaud. A New Predictive Thermal Sensation Index of Human Response. *Journal of Energy and Buildings*, 29:167–178, 1999.

[67] Taeyoung Han, Kuo-Huey Chen, Bahram Khalighi, Allen Curran, Joshua Pryor, and Mark Hepokoski. Assessment of Various Environmental Thermal Loads on Passenger Thermal Comfort. In *Proceedings of SAE International*, 2010.

[68] Taeyoung Han and Linjie Huang. A Sensitivity Study of Occupant Thermal Comfort in a Cabin Using Virtual Thermal Comfort Engineering. In *Proceedings of SAE International*, 2005.

[69] Trevor Hastie, Robert Tibshirani, and Jerome Friedman. *The Elements of Statistical Learning*. Springer, 2009.

[70] Mohsen Hayati and Zahra Mohebi. Temperature Forecasting Based on Neural Network Approach. *Journal of World Applied Sciences*, 6:613–620, 2007.

[71] Simon S. Haykin. *Neural Networks: A Comprehensive Foundation*. Prentice Hall, 1998.

[72] J.L.M. Hensen. Literature Review on Thermal Comfort in Transient Conditions. *Journal of Building and Environment*, 25:309–316, 1990.

[73] Diana Hintea, James Brusey, Elena Gaura, Neil Beloe, and David Bridge. Mutual Information-based Sensor Positioning for Car Cabin Comfort Control. In *Proceedings of the 15th International Conference on Knowledge-based and Intelligent Information and Engineering Systems*, volume III, pages 483–492, 2011.

[74] I. Holmer, Hakan Nilsson, M. Bohm, and O. Noren. Equivalent Temperature in Vehicles - Conclusions and Recommendations for Standard. In *Proceedings of the CABCLI Consortium*, 1999.

[75] M.N. Howell, G.P. Frost, T.J. Gordon, and Q.H. Wu. Continuous Action Reinforcement Learning Applied to Vehicle Suspension Control.

[76] Michael Humphreys and Mary Hancock. Do People Like to Feel 'Neutral'?: Exploring the Variation of the Desired Thermal Sensation on the ASHRAE Scale. *Journal of Energy and Buildings*, 39:867–874, 2007.

[77] Michael Humpreys and J.. Fergus Nicol. The Validity of ISO-PMV for Predicting Comfort Votes in Every-Day Thermal Environments. *Journal of Energy and Buildings*, 34:667–684, 2002.

[78] S. Ibrahim, I. Daut, Y. Irwan, M. Irwanto, N. Gomesh, and Z. Farhana. Linear Regression Model in Estimating Solar Radiation in Perlis. *Journal of Energy Procedia*, 18:1402–1412, 2012.

[79] Yoshinori Ichishi and Tatsumi Kumada. Vehicle Air Conditioner Having Learning Function and Correcting Function. US Patent 7346440 B2, March 2008.

[80] Yoshinori Ichishi, Akira Ohga, and Tatsumi Kawai. Vehicle Air Conditioner With Automatic Air-Conditioning Control Having Learning Function of Manual Operation. US Patent 6669101 B2, December 2003.

[81] B. Jones, K. Hsieh, and M. Hashinaga. The Effect of Air Velocity on Thermal Comfort at Moderate Activity Levels. *Journal of ASHRAE Transactions*, 92, 1986.

[82] Byron W. Jones. Capabilities and Limitations of Thermal Models for Use in Thermal Comfort Standards. *Journal of Energy and Buildings*, 34:653–659, 2002.

[83] G. Karimi, E. Chan, J. Culham, I. Linjacki, and L. Brennan. Thermal Comfort Analysis of an Automobile Driver with Heated and Ventilated Seat. In *Proceedings of SAE International*, 2002.

[84] Sean Michael Kelly and John Lawrence Pawlak. Adaptive Automatic Climate Control Method for a Motor Vehicle. European Patent 1340635 A2, September 2003.

[85] James Kennedy and Russell Eberhart. Particle Swarm Optimization. In *Proceedings of IEEE International Conference on Neural Networks*, volume IV, pages 1942–1948, 1995.

[86] Theresa J. Klein, Devika Subramanian, David Kortenkamp, and Scott Bell. Using Reinforcement Learning to Control Life Support Systems. In *Proceedings of SAE International*, 2004.

[87] Kazuyuki Kojima. Prediction of Individual Thermal Sensation using Unspecified Sensors in Sensor Networks. In *Proceedings of the International Conference on Control, Automation and Systems*, 2008.

[88] M.Ozgun Korukcu and Muhsin Kilic. The Usage of IR Thermography for the Temperature Measurements Inside an Automobile Cabin. *International Journal on Communications in Heat and Mass Transfer*, 36:872–877, 2009.

[89] Jurgen Kranz. *Intelligent Automotive Thermal Comfort Control*. PhD thesis, Nelson Mandela Metropolitan University, Port Elizabeth, 2011.

[90] Anuj Kumar, I.P. Singh, and S.K. Sud. An Approach Towards Development of PMV Based Thermal Comfort Smart Sensor. *International Journal on Smart Sensing and Intelligent Systems*, 3(4):621–642, 2010.

[91] Paul A. Lebbin and Mohammad H. Hosni. Automobile Climate Measurement using Two Thermal Observations Manikins. In *Proceedings of SAE International*, 2005.

[92] Tien-Yun Lee. Prediction of Car Cabin Temperature using Artificial Neural Network. Master's thesis, Technische Universitat Munchen, 2007.

[93] Lichuan Liu, Sen M. Kuo, and Meng Chu Zhou. Virtual Sensing Techniques and Their Applications. In *Proceedings of the IEEE International Conference on Networking, Sensing and Control*, 2009.

[94] Simeng Liu and Gregor P. Henze. Evaluation of Reinforcement Learning for Optimal Control of Building Active and Passive Thermal Storage Inventory. *Journal of Solar Energy Engineering*, 129:215–225, 2006.

[95] Xiaonan Luo, Wenbang Hou, Yi Li, and Zhong Wang. A Fuzzy Neural Network Model for Predicting Clothing Thermal Comfort. *Journal of Computers and Mathematics with Applications*, 53:1840–1846, 2007.

[96] H.N. Maaijen. People-Oriented Comfort Control and Energy Saving by Tracking the Building Users' Position and Electrical Appliance Use. Master's thesis, TU Eindhoven, 2012.

[97] Thomas Lund Madsen. *Thermal Environment Parameters and Their Measurement.* Technical University of Denmark, 1976.

[98] Thomas Lund Madsen. Measurement of Thermal Comfort and Discomfort. Technical report, Thermal Insulation Laboratory, Technical University of Denmark, 1978.

[99] Thomas Lund Madsen, Bjarne W. Olesen, and N. Kristensen. Comparison between Operative and Equivalent Temperature under Typical Indoor Conditions. In *Proceedings of ASHRAE*, 1984.

[100] Thomas Lund Madsen, Bjarne W. Olesen, and K. Reid. New Methods for Evaluation of the Thermal Environment in Automotive Vehicles. Technical report, Thermal Insulation Laboratory , Technical University of Denmark, January 1986.

[101] Imran Maqsood, Muhammad Riaz Khan, and Ajith Abraham. An ensemble of neural networks for weather forecasting. *Journal of Neural Computing and Applications*, 13:112–122, 2004.

[102] N.A.G. Martinho, Manuel Gameiro da Silva, and Joao Esteves Ramos. Evaluation of Thermal Comfort in a Vehicle Cabin. *Journal of Automobile Engineering*, 218:159–166, 2004.

[103] Kazuhiko Matsunaga, Fujio Sudo, Shin ichi Tanabe, and Thomas Lund Madsen. Evaluation and Measurement of Thermal Comfort in the Vehicles with a New Thermal Manikin. In *Proceedings of SAE International*, 1993.

[104] E. Mayer. Objective Criteria for Thermal Comfort. *Journal of Building and Environment*, 28:399–403, 1993.

[105] E. Mayer and R. Schwab. Correlation between Thermal Response and Equivalent Temperature. In *Proceedings of CABCLI Consortium*, 1999.

[106] Peter Mehnert, Jacques Malchaire, Bernhard Kampmann, Alain Piette, Barbara Griefahn, and Hansjurgen Gebhardt. Prediction of the Average Skin Temperature in Warm and Hot Environments. *European Journal of Applied Physiology*, 82:52–60, 2000.

[107] A. Melikov and H. Zhou. Comparison of Methods for Determining Equivalent Termperature under Well-Defined Conditions. In *Proceedings of the CABCLI Consortium*, 1999.

[108] Stefano Mola. Climate Control: Comfort Assessment and Energy Saving. Technical report, Centro Ricerche Fiat, 2010.

[109] Stefano Mola, Massimo Magini, and Carloandrea Malvicino. Equivalent Temperature Estimator using Mean Radiant Temperature Sensor. *Journal of Measurement and Control*, 34:167–170, 2001.

[110] Stefano Mola, Giulio Lo Presti, R. Ardusso, Carloandrea Malvicino, Andrea Zussino, and Guglielmo Caviasso. Measuring Customer Perceived Thermal Comfort in Car Cabin Compartment: Index of Perceived Thermal Comfort. In *Proceedings of FISITA World Automotive Congress*, 2004.

[111] M. Nakamura, T. Yoda, L. Crawshaw, S. Yasuhara, Y. Saito, M. Kasuga, K. Nagashima, and K. Kanosue. Regional Differences in Temperature Sensation and Thermal Comfort in Humans. *Journal of Applied Physiology*, 105:1897–1906, 2008.

[112] Henry Nasution. Development of Fuzzy Logic Control for Vehicle Air Conditioning System. *Telkomnika Journal*, 6:73–82, 2008.

[113] H. Nilsson and I. Holmer. Definitions and Measurements of Equivalent Temperature. Technical report, The Climate Group, National Institute for Working Life, Solna, Sweden, 2002.

[114] H. Nilsson, I. Holmer, M. Bohm, and O. Noren. Definition and Theoretical Background of the Equivalent Temperature. In *Proceedings of the CABCLI Consortium*, 1999.

[115] Hakan Nilsson. *Comfort Climate Evaluation with Thermal Manikin Methods and Computer Simulation Models*. PhD thesis, Royal Institute of Technology, 2004.

[116] Hakan Nilsson. Thermal Comfort Evaluation with Virtual Manikin Methods. *Journal of Building and Environment*, 42:4000–4005, 2007.

[117] Hakan Nilsson, I. Holmer, M. Bohm, and O. Noren. Equivalent Temperature and Thermal Sensation - Comparison with Subjective Responses. In *Proceedings of the International Conference on Comfort in the Automotive Industry*, 1997.

[118] M. Nowak and A. Urbaniak. Utilization of Intelligent Control Algorithms for Thermal Comfort Optimization. In *Proceedings of the International Carpathian Control Conference*, 2011.

[119] Hajime Oi, Koji Tabata, Yasuhito Naka, Akira Takeda, and Yutaka Tochihara. Effects of Heated Seats in Vehicles on Thermal Comfort During the Initial Warm-up Period. *Journal of Applied Ergonomics*, 43:360–367, 2012.

[120] B.W. Olesen. Measurement of Thermal Comfort in Vehicles. Application Notes, 1988.

[121] F. De Oliveira and S. Moreau. Assessment of Thermal Environment Sensation for Various Climatic Conditions and Fluctuating Air Flow. In *Proceedings of the Indo-French Indoor Air Quality Seminar*, 2009.

[122] Jose A. Orosa. Research on General Thermal Comfort Models. *European Journal of Scientific Research*, 2:217–227, 2009.

[123] N.A. Oseland. Thermal Comfort in Naturally Ventilated Versus Air-Conditioned Offices. In *Proceedings of the International Conference on Indoor Air Quality and Climate*, 1996.

[124] M. Palazzetti, M. Cisternino, and M. Giordana. EVA3: The Virtual Sensor Thermal Manikin. Technical report, Fiat Research Center, 1996.

[125] H. Peng, Fulmi Long, and C. Ding. Feature Selection based on Mutual Information Criteria of Max-Dependency, Max-Relevance, and Min-Redundancy. *IEEE Transactions on Pattern Analysis and Machine Intelligence*, 27(8):1226–1238, 2005.

[126] Chuck Pham, Peter Gawthrop, and Aaron Tweadey. Adaptive Automotive Climate Control with Variable Learning Rate. US Patent 7246499 B2, July 2007.

[127] John Ross Quinlan. Introduction of Decision Trees. *Journal of Machine Learning*, 1:81–106, 1986.

[128] Juan Rada-Vilela. Fuzzylite - A Fuzzy Logic Control Library in C++. Technical report, 2007.

[129] R. Ramyaa. Frost Prediction Using Artificial Neural Networks: A Classification Approach. Master's thesis, Madurai Kamaraj University, 2004.

[130] John P. Rugh and Desikan Bharathan. Predicting Human Thermal Comfort in Automobiles. In *Proceedings of the Vehicle Thermal Management Systems Conference and Exhibition*, 2005.

[131] John P. Rugh, Robert B. Farrington, Desikan Bharathan, Andreas Vlahinos, Richard Burke, Charlie Huizenga, and Hui Zhang. Predicting Human Thermal Comfort in a Transient Nonuniform Thermal Environment. *Journal of Applied Physiology*, 92(6):721–727, 2004.

[132] Paul M. Rutkowski. Thermal Comfort Modeling of Cooled Automotive Seats. In *Proceedings of SAE International*, 2010.

[133] Enrico Sabbatini. An Innovative IR Camera Monitoring System for Energy Fluxes and Comfort Estimation in Built Environment. Technical report, University Politecnica delle Marche, 2012.

[134] SAE Journal. Equivalent Temperature: Truck and Bus. 2012.

[135] Tsuyoshi Sakuma, Toshiyuki Shimizu, Yonosuke Miki, Kenji Doya, and Eiji Uchibe. Computation of Driving Pleasure based on Driver's Learning Process Simulation by Reinforcement Learning. In *Proceedings of SAE International*, 2013.

[136] Luciano Sanchez, M. Rosario Suarez, J.R. Villar, and Ines Couso. Mutual Information-based Feature Selection and Partition Design in Fuzzy Rule-based classifiers from Vague Data. *International Journal of Approximate Reasoning*, 49(3):607–622, 2008.

[137] G.E. Schiller. A Comparison of Measured and Predicted Comfort in Office Buildings. *Journal of ASHRAE Transactions*, 96:609–622, 1990.

[138] Wei Shengxian, Li Ming, H. Fene, and Sun Yanlin. New Correlations for Predicting Indoor Thermal Environment in Yunnan-Guizhou Plateau Climate. In *Proceedings of Power and Energy Engineering Conference*, 2010.

[139] Jagdev Singh, Nirmal Singh, and J.K. Sharma. Fuzzy Modeling and Control of HVAC Systems - A Review. *Journal of Scientific & Industrial Research*, 65:470–476, 2006.

[140] Satinder Singh, Tommi Jaakkola, Michael L. Littman, and Csaba Szepesvari. Convergence Results for Single-Step On-Policy Reinforcement-Learning Algorithms. *Journal of Machine Learning*, 38:287–308, 2000.

[141] Brian Smith, Ronald W. McClendon, and Gerrit Hoogenboom. Improving Air Temperature Prediction with Artificial Neural Networks. *Journal of World Academy of Science, Engineering and Technology*, 1(10):3155–3162, 2007.

[142] Ashok N. Srivastava, Nikunj C. Oza, and Julienne Stroeve. Virtual Sensors: Using Data Mining Techniques to Efficiently Estimate Remote Sensing Spectra. *IEEE Transactions on Geoscience and Remote Sensing*, 43, 2005.

[143] Elizabeth Amudhini Stephen, Mercy Shnathi, P. Rajalakshmy, and Melbern M. Parthido. Application of Fuzzy Logic in Control of Thermal Comfort. *International Journal of Computational and Applied Mathematics*, 5:289–300, 2010.

[144] Richard Sutton. Open Theoretical Questions in Reinforcement Learning. *Lecture Notes in Computer Science*, 1572:11–17, 1999.

[145] Richard S. Sutton and Andrew Barto. *Reinforcement Learning: An Introduction*. MIT Press, 1998.

[146] S. Tanabe, Edward Arens, F. Bauman, Hui Zhang, and Thomas Lund Madsen. Evaluating Thermal Environments by Using a Thermal Manikin with Controlled Skin Surface Temperature. *Journal of ASHRAE Transactions*, 100(1):39–48, 1994.

[147] Yousuke Taniguchi, Hiroshi Aoki, and Kenji Fujikake. Study on Car Air Conditioning System Controlled by Car Occupants Skin Temperatures - Part 1: Research on a Method of Quantitative Evaluation of Car Occupants' Thermal Sensations by Skin Temperature. In *Proceedings of SAE International*, 1992.

[148] Richard Thompson and Arthur Dexter. Thermal Comfort Control Based on Fuzzy Decision-Making.

[149] Jose Luis Torres and Marcelo Luis Martin. Adaptive Control of Thermal Comfort Using Neural Networks.

[150] Georgia D. Tourassi, Erik D. Frederik, Mia K. Markey, and Carey E. Floyd Jr. Application of the Mutual Information Criterion for Feature Selection in Computer-Aided Diagnosis. *Journal of Medical Physics*, 28(12):2394–2402, 2001.

[151] M. Ueda and Y. Taniguchi. The Prediction of the Passenger's Thermal Sensation Level Using a Neural Network and Its Application to the Automobile HVAC Control. In *Proceedings of IEEE Systems, Man and Cybernetics*, volume 4, pages 623–634, 1999.

[152] Joost van Hoof. Forty Years of Fanger's Model of Thermal Comfort: Comfort for All? *Indoor Air Journal*, 18:182–201, 2008.

[153] Joost van Hoof and J.L.M. Hensen. Quantifying of Relevance of Adaptive Thermal Comfort Models in Moderate Thermal Climate Zones. *Journal of Building Environment*, 42:156–170, 2007.

[154] G. van Rossum and F. Drake. *Python Reference Manual*. PythonLabs, 2001.

[155] T. Vogl, J. Mangis, A. Rigler, W. Zink, and D. Alkon. Accelerating the Convergence of the Back-Propagation Method. *Journal of Biological Cybernetics*, 59:257–263, 1988.

[156] Danni Wang, Hui Zhang, Edward Arens, and Charlie Huizenga. Observations of Upper-Extremity Skin Temperature and Corresponding Overall-Body Thermal Sensations and Comfort. *Journal of Building and Environment*, 42:3933–3943, 2007.

[157] X. Rosalind Wang, Joseph T. Lizier, Thomas Nowotny, Amalia Z. Berna, Mikhail Prokopenko, and Stephen C. Trowell. Feature Selection for Chemical Sensor Arrays Using Mutual Information. *PLoS ONE Journal*, 9(3), 2014.

[158] M. Way and A. Srivastava. Novel Methods for Predicting Photometric Redshifts from Broadband Photometry using Virtual Sensors. *The Astrophysical Journal*, 647:102–115, 2006.

[159] K.C. Wei and G.A. Dage. An Intelligent Automotive Climate Control System. In *Proceedings of the IEEE International Conference on Systems, Man and Cybernetics*, 1995.

[160] T. Wenzel, Keith Burnham, Mike Blundell, and R. Williams. Kalman Filter as a Virtual Sensor: Applied to Automotive Stability Systems. *Transactions of the Institute of Measurement and Control*, 29, 2007.

[161] R.N. Williams. A Field Investigation of Thermal Comfort, Environmental Satisfaction and Perceived Control Levels in UK Office Buildings. *Journal of Healthy Buildings*, 3:1181–1186, 1995.

[162] Ian H. Witten and Eibe Frank. *Data Mining: Practical Machine Learning Tools and Techniques*. Morgan Kaufmann, 2005.

[163] Siyu Wu and Jian-Qiao Sun. Two-Stage Regression Model of Thermal Comfort in Office Buildings. *Journal of Building and Environment*, 57:88–96, 2012.

[164] David P. Wyon, Christer Tennstedt, Inger Lundgren, and Stefan Larsson. A New Method for the Detailed Assessment of Human Heat Balance in Vehicles - Volvo's Thermal Manikin, VOLTMAN. In *Proceedings of SAE International*, 1985.

[165] Wang XL. *Thermal Comfort and Sensation under Transient Conditions*. PhD thesis, The Royal Institute of Technology, Sweden, 1994.

[166] Kazuaki Yamashita, Juntaro Matsuo, Yutaka Tochihara Tochihara, Youichiro Kondo, Shizuka Takayama, and Hiroki Nagayama. Thermal Sensation and Comfort during Exposure to Local Air-

flow to Face or Legs. *Journal of Physiological Anthropology and Applied Human Science*, 24:61–66, 2005.

[167] K.H. Yang and C.H. Su. An Approach to Building Energy Savings Using the PMV Index. *Journal of Building and Environment*, 32:25–30, 1997.

[168] Ye Yao, Zhiwei Lian, Weiwei Liu, and Qi Shen. Experimental Study on Skin Temperature and Thermal Comfort of the Human Body in a Recumbent Posture under Uniform Thermal Environments. *Journal of Indoor and Built Environment*, 16, 2007.

[169] Alexander Zenger, Jochen Schmidt, and Michael Krodel. Towards the Intelligent Home: Using Reinforcement-Learning for Optimal Heating Control. *Lecture Notes in Computer Science*, 8077:304–307, 2013.

[170] Huajun Zhang, Lan Dai, Guoquan Xu, Yong Li, Wei Chen, and Wenquan Tao. Studies of Air-Flow and Temperature Fields Inside a Passenger Compartment for Improving Thermal Comfort and Saving Energy. Part I: Test/Numerical Model and Validation. *Journal of Applied Thermal Engineering*, 29:2022–2027, 2009.

[171] Huanjun Zhang, Lan Dai, Guoquan Xu, Yong Li, Wei Chen, and Wenquan Tao. Studies of Airflow and Temperature Fields Inside a Passenger Compartment for Improving Thermal Comfort and Saving Energy. Part II: Simulation Results and Discussion. *Journal of Applied Thermal Engineering*, 29:2028–2036, 2009.

[172] Hui Zhang. *Human Thermal Sensation and Comfort in Transient and Non-Uniform Thermal Environments*. PhD thesis, University of California Berkeley, 2003.

[173] Hui Zhang, Edward Arens, Charlie Huizenga, and Taeyoung Han. Thermal Sensation and Comfort Models for Non-Uniform and Transient Environments, part I: Local Sensation of Individual Body Parts. *Journal of Building and Environment*, 45:380–388, 2010.

[174] Hui Zhang, Edward Arens, Charlie Huizenga, and Taeyoung Han. Thermal Sensation and Comfort Models for Non-Uniform and Transient Environments, part II: Local Comfort of Individual Body Parts. *Journal of Building and Environment*, 45:389–398, 2010.

[175] Hui Zhang, Edward Arens, Charlie Huizenga, and Taeyoung Han. Thermal Sensation and Comfort Models for Non-Uniform and Transient Environments, part III: Whole-Body Sensation and Comfort. *Journal of Building and Environment*, 45:399–410, 2010.

Appendix A

Demo

The Virtual Thermal Comfort Sensing (VTCS) presented in Chapter 5 was tested within a real-time demo for a Jaguar Land Rover (JLR) TechFair, described in this Appendix.

For the demo, the VTCS was trained with data gathered in a series of experiments performed in steady-state controlled conditions. The cabin locations suitable for estimation were selected prior to the event using the mutual information-based sensor positioning method detailed in Chapter 4. The two best air temperature sensor locations selected were the back seat of the back passenger and the front row left footwell. Two LM35CAZ air temperature sensors were placed in those particular positions and wired each to a TelosB sensor node. The TelosB nodes sampled every second and sent the values to another TelosB node that further transmitted the values to the base station laptop through a USB. Furthermore, the values were transmitted to another laptop that had the estimation processing and visualiser (see Figure A.1). Based on each of the samples coming from the two air temperature sensors in the car, the equivalent temperature at six locations (head, chest, lower arm, upper arm, thigh and calf) was estimated. A Multiple Linear Regression (MLR) equation was used for estimating the equivalent temperatures at the six locations.

The Predicted Mean Vote (PMV) comfort model was applied to the estimated equivalent temperature values, outputting a thermal comfort index (a real number between -3 and 3). In order to assess the accuracy of both the equivalent temperature and PMV estimation, the INNOVA Flatman manikin was installed in the car cabin in the front passenger seat. The manikin was wired to a data logger that stored the equivalent temperatures and comfort index measured in a database format. The visualiser queries the database to extract the manikin values and further introduce them into the visualiser code.

The visualiser consisted in an user interface that allows an end-user to select which equivalent temperature body part target to estimate and the number of sensors to be used for the estimation (one or two in order to see how the accuracy of the estimation increases if two sensors are used, rather than one). The visualiser displayed two graphs: one showing the estimated equivalent temperature at the selected body part versus the equivalent temperature measured by the Flatman, the accuracy of which

Figure A.1: Test car and laptop with the demo visualiser.

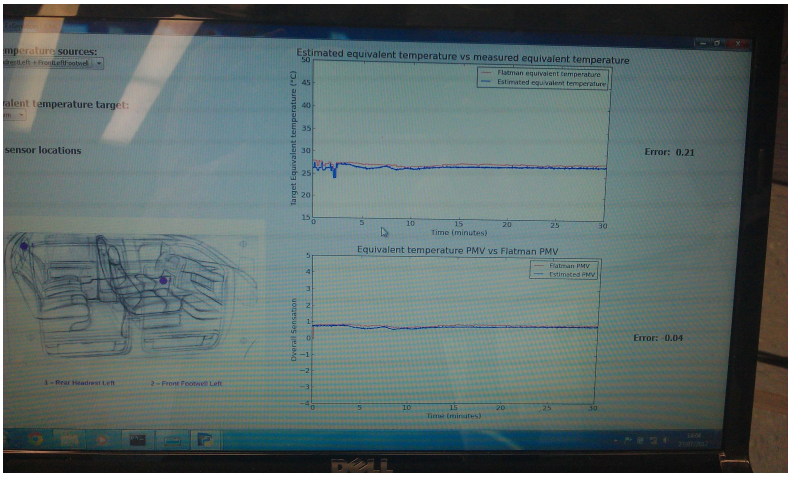

Figure A.2: Demo visualiser.

is calculated using Root Mean Square Error (RMSE) and the second showing the estimated PMV index (overall sensation of the passenger) versus the PMV index measured by the Flatman and outputting the RMSE (see Figure A.2). The equivalent temperatures were estimated within 0.5 ℃ RMSE, while the PMV index was estimated within 0.1 RMSE on the comfort scale (-3 to 3) throughout the day. The car was inside for the event and so the Air Conditioning (AC) was not used. Even though the conditions were rather stable (ambient temperature, changes in temperatures only due to people going inside/outside the car, opening doors, etc), the real-time results were promising, showing that the VTCS is a useful tool for deriving passenger thermal comfort.

Appendix B

Scripts Exemplification

Below are some examples of coded scripts for the work presented in Chapter 5.

B.1 Multiple Linear Regression implementation

```
  from learner import Learner
from numpy import * import unittest
def mcov(vlist):
    m = [mean(v) for v in vlist]
    l = len(vlist)
    ll = len(vlist[0])
    cov_array = zeros((l,l),dtype=float64)
    for i in range(l):
        for j in range(i,l):
            assert len(vlist[i]) == len(vlist[j])
            z = zip(vlist[i],vlist[j])
            cov_array[i,j] = sum([(a - m[i]) * (b - m[j]) for a,b in z]) / (ll-1)
            cov_array[j,i] = cov_array[i,j]
    return cov_array
class GaussianLearner(Learner):
    def __init__(self, inputlen=1, inputnames=[]):
        self.source = []
        for i in range(inputlen):
            self.source.append([])
        self.targetA = []
        self.input_len = inputlen
        self.smean = [0.] * inputlen
```

```
    def learnPairs(self, pairs):
        for s,t in pairs:
        assert len(s) == self.input_len
        for i in range(self.input_len):
            self.source[i].append(s[i])
        self.targetA.append(t)
        for i in range(self.input_len):
            self.smean[i] = mean(self.source[i])
        self.smean = matrix(self.smean).T
        self.tmean = mean(self.targetA)
        a = [self.targetA]
        a.extend(self.source)
        ll = len(a)
        covar = mcov(a)
        s12 = covar[0:1,1:ll]
        s22Inv = linalg.inv(covar[1:ll,1:ll])
        self.matr = matrix(s12) * matrix(s22Inv)
    def estimate(self, source):
        s = matrix(source).T
        self.vbl = s - self.smean
        meanCX = self.tmean + self.matr * self.vbl
        return meanCX[0,0]
```

B.2 Learning process

```
  from optparse import OptionParser
import csv
import glob
import math
import sys
from GaussianLearner import GaussianLearner
methods = { "GaussianLearner" : GaussianLearner}
```

```
    def train_test(learner, testfn, trainfn, source, target):
        global methods testf = csv.DictReader(open(testfn, "rb"))
        trainf = csv.DictReader(open(trainfn, "rb"))
        trainset = []
        dropped_rows = 0
        for row in trainf:
            ss = [row[s] for s in source]
            ts = row[target]
            if "NA" in ss or ts == "NA": dropped_rows += 1
            else: trainset.append(([float(s) for s in ss], float(ts)))
        learner.learnPairs(trainset)
        if (target=='eqt-d(calf)'):
            sse = 0.
            count = 0
            f = open("temp/estim-calf.csv",'w')
            f.write("real-calf,estimated-calf\n")
            outStr=""
            for row in testf:
                ss = [row[s] for s in source]
                ts = row[target]
                if not ("NA" in ss or ts == "NA"):
                    err = float(ts) - learner.estimate([float(s) for s in ss])
                    est = learner.estimate([float(s) for s in ss])
                    outStr=str(ts)+","+str(est)+"\n"
                    f.write(outStr)
                    sse += err * err
                    count += 1
            f.close()
            return math.sqrt(sse / count)
    def run_method(p, method, source, target, outf):
        result = train_test(methods[method](inputlen=len(source),inputnames=source), "temp/TestData.csv",
"temp/TrainData.csv", source, target)
```

```
        outf.writerow([method + "_" + '-'.join(source) + "_" + target, result])
    if __name__ == "__main__": parser = OptionParser()
       parser.add_option("-p", "–prefix", default="rows", help="Prefix for training and test data [default:
rows]")
        parser.add_option("-o", "–output", default=None, help="Output filename [required]")
        parser.add_option("-m", "–method", default="simple", help="Learning method to trial [default:
simple]")
        parser.add_option("-x", "–expfile", default=None, help="Filename containing target and source
sensors")
        parser.add_option("-s", "–source", default=None, help="Comma separated list of source column
name(s) [required]")
        parser.add_option("-t", "–target", default=None, help="Target column name [required]")
        (opts, args) = parser.parse_args()
        if opts.expfile is None:
            assert opts.source is not None
            assert opts.target is not None
        else:
            assert opts.source is None
            assert opts.target is None
        assert opts.output is not None
        assert len(args) == 0
        outf = csv.writer(open(opts.output, "w"))
        outf.writerow(["method", "trial", "result"])
        if opts.expfile is not None:
            ff = open(opts.expfile,"r")
            for exp in ff.readlines():
                exp = exp.rstrip()
                if exp != '' and exp[0] != '#':
                    print "running:", exp
                    srclist = exp.split(",")
                    tgt = srclist.pop(0)
                    run_method(opts.prefix, opts.method, srclist, tgt, outf)
```

else: run_method(opts.prefix, opts.method, opts.source.split(","), opts.target, outf)

B.3 WEKA library integration in Python

Makefile

TEMPDIR = temp

TRAINDIR = train

TESTDIR = test

RESULTS = results

WEKAJAR=/home/dianah/Desktop/WorkStuff/weka-3-6-6/weka.jar

EXP_NUMS=2 3 4 5 6 7 8 9 10 11 12 13 14 15 16 17 18 19 20 21 22 23 24 25 26 27 29 30 31 32 35 36 37 38 39 40 41 42 43 45 46 49 52 53 54 55 56 57 58 59 61 62 63 64 65 67 68 70 71 72 73 74 75 79 82 83 85 86 88 90 91 92 93 94 95 96

RESULTS_FILES=$(foreach t,$(EXP_NUMS),results/$(t).csv)

RESULTS_FILESF=$(foreach t,$(EXP_NUMS),results/$(t)F.csv)

all: $(TEMPDIR) $(RESULTS) $(RESULTS_FILES) $(RESULTS_FILESF) $(RESULTS)/all.csv

$(TEMPDIR): mkdir $(TEMPDIR)

$(RESULTS): mkdir $(RESULTS)

$(TEMPDIR)/test_%.csv: $(TESTDIR)/test_%.csv reorderTest.py python reorderTest.py $< $@

$(TEMPDIR)/train_%.csv: $(TRAINDIR)/train_%.csv reorderTrain.py python reorderTrain.py $< $@

$(TEMPDIR)/test_%.arff: $(TEMPDIR)/test_%.csv create_arff.py python create_arff.py $< > $@

$(TEMPDIR)/train_%.arff: $(TEMPDIR)/train_%.csv create_arff.py python create_arff.py $< > $@

#$(TEMPDIR)/weka.model.%: $(TEMPDIR)/train_%.arff # java -cp $(WEKAJAR) -Xmx1024m weka.classifiers.functions.MultilayerPerceptron -d $@ -L 0.2 -M 0.1 -N 20 -V 0 -S 0 -E 20 -H 3 -t $<

#results/%.csv: $(TEMPDIR)/weka.model.% $(TEMPDIR)/test_%.arff # java -cp $(WEKAJAR) -Xmx1024m weka.classifiers.functions.MultilayerPerceptron -l $< -T $(TEMPDIR)/test_$*.arff -i > $@

#$(TEMPDIR)/weka.model.%: $(TEMPDIR)/train_%.arff # java -cp $(WEKAJAR) -Xmx1024m weka.classifiers.functions.LinearRegression -d $@ -S 0 -R 1.0E-8 -t $<

#results/%.csv: $(TEMPDIR)/weka.model.% $(TEMPDIR)/test_%.arff # java -cp $(WEKAJAR) -Xmx1024m weka.classifiers.functions.LinearRegression -l $< -T $(TEMPDIR)/test_$*.arff -i > $@

$(TEMPDIR)/weka.model.%: $(TEMPDIR)/train_%.arff java -cp $(WEKAJAR) -Xmx1024m weka.classifiers.trees.I

-d $@ -M 2 -V 0.001 -N 3 -S 1 -L -1 -t $<

results/%.csv: $(TEMPDIR)/weka.model.% $(TEMPDIR)/test_%.arff java -cp $(WEKAJAR) -Xmx1024m weka.classifiers.trees.REPTree -l $< -T $(TEMPDIR)/test_$*.arff -i > $@

#$(TEMPDIR)/weka.model.%: $(TEMPDIR)/train_%.arff # java -cp $(WEKAJAR) -Xmx1024m weka.classifiers.functions.RBFNetwork -d $@ -B 2 -S 1 -R 1.0E-8 -M -1 -W 0.1 -t $<

#results/%.csv: $(TEMPDIR)/weka.model.% $(TEMPDIR)/test_%.arff # java -cp $(WEKAJAR) -Xmx1024m weka.classifiers.functions.RBFNetwork -l $< -T $(TEMPDIR)/test_$*.arff -i > $@

results/%F.csv: $(RESULTS)/%.csv cleanRes.py python cleanRes.py $(RESULTS)/$*.csv > $@

results/all.csv: mergeAll.py python mergeAll.py $< $@

clean: -rm -rf $(TEMPDIR) -rm -rf $(RESULTS)

Create file format for WEKA in Python import sys import csv

infile = open(sys.argv[1], 'r') csvfile = csv.reader(infile, delimiter=',', quotechar='"')

header = csvfile.next() cols = range(len(header))

col_names = map(header.__getitem__, cols)

arff_header = "@relation estimation\n\n\n"

for col in col_names:

arff_header += "@attribute %s real\n" % (col.replace('_', '')) arff_header += "@data"

print arff_header

for line in csvfile:

try:

row = map(line.__getitem__, cols)

except:

print >> sys.stderr, 'Cols:', cols

print >> sys.stderr, 'Row:', line

print ','.join(row)

infile.close()

B.4 Computing the PMV index

from pmv import calc_pmvEqTemp

from pmv import calc_pmvAir import sys import csv

met = 1.2

```
clo = 0.66689
vel = 0.0
rh = 50.
in_filename = sys.argv[1]
infile = csv.reader(open(in_filename, 'r'), delimiter=',', quotechar='"')
header = infile.next()
flatman_nr = int(sys.argv[2])
mean_weight_est_eq_temp_nr = int(sys.argv[3])
avg_interior_nr = int(sys.argv[4])
sens_nr = int(sys.argv[5])
outfile = csv.writer(sys.stdout, delimiter=',', quotechar='"')
outfile.writerow(["time","pmv-air","pmv-eq-temp","pmv-flatman","sensation"])
i = 1
for row in infile:
    ta = float(row[avg_interior_nr])
    eq = float(row[mean_weight_est_eq_temp_nr])
    pmv_flatman = float(row[flatman_nr])
    sens = row[sens_nr]
    pmv_air = calc_pmvAir(clo, ta, ta, met, vel, rh)
    pmv_eq_temp = calc_pmvEqTemp(clo, eq, eq, met, vel, rh)
    outfile.writerow([i,pmv_air,pmv_eq_temp,pmv_flatman,sens])
    i = i+1
```

Appendix C

Publications, Presentations and Attended Conferences

The work in this thesis has resulted in the following peer-reviewed publications, presentations, and technical reports.

C.1 Conference proceedings

Mutual Information-based Sensor Positioning for Car Cabin Comfort Control

Diana Hintea, James Brusey, Elena Gaura, Neil Beloe and David Bridge. Mutual Information-based Sensor Positioning for Car Cabin Comfort Control. In *Proceedings* of *KES 2011*, 15th international conference on Knowledge-based and intelligent information and engineering systems, Volume Part III, pages 483-492, Kaiserslautern, Germany, September 13-15 2011. ISBN: 978-3-642-23853-6 521–525.

Car cabins are transient, non-uniform thermal environments, both with respect to time and space. Identifying representative locations for the Heating, Ventilation and Air Conditioning (HVAC) system sensors is an open research problem. Common sensor positioning approaches are driven by considerations such as cost or aesthetics, which may impact on the performance/outputs of the HVAC system and thus occupants' comfort. Based on experimental data, this paper quantifies the spacial-temporal variations in the cabin's environment by using Mutual Information (MI) as a similarity measure. The overarching aim for the work is to find optimal (but practical) locations for sensors that: i) can produce accurate estimates of temperature at locations where sensors would be difficult to place, such as on an occupant's face or abdomen and ii) thus, support the development of occupant rather than cabin focused HVAC control algorithms. When applied to experimental data from stable and hot/cold soaking scenarios, the method proposed successfully identified practical sensor locations which estimate face and abdomen temperatures of an occupant with less than 0.7 ℃ and 0.5 ℃ error, respectively.

Comfort in Cars: Estimating Equivalent Temperature for Comfort Driven Heating, Ventilation and Air Conditioning (HVAC) Control

Diana Hintea, James Brusey, Elena Gaura, John Kemp and Neil Beloe. Comfort in Cars: Estimating Equivalent Temperature for Comfort Driven Heating, Ventilation and Air Conditioning (HVAC) Control. In *Proceedings of ICINCO* 2013, International Conference on Informatics in Control, Automation and Robotics, Volume I, pages 507-513, Reykjavik, Iceland, July 28-31, 2013. ISBN: 978-989-8565-70-9.

Equivalent Temperature is generally considered an accurate predictor for thermal comfort in car cabins. However, direct measurement of this parameter is impractical in fielded applications. The paper presents an empirical, multiple linear regression based approach for estimating body segment equivalent temperatures for car cabin occupants from different sensors within the car. Body part equivalent temperature at eight segments and cabin sensor data (air temperature, surface temperature, mean radiant temperature, humidity and solar load) was gathered in a variety of environmental and cabin conditions. 38 experimental hours of trials in a controlled environment and 26 experimental hours of realistic driving trials were used for training and evaluating the estimator's performance. The estimation errors were on average between 0.5 ℃ and 1.9 ℃ for different body parts for trials within a controlled environment, while for trials in realistic driving scenarios they ranged between 1 ℃ and 2 ℃. This demonstrates that passenger body part equivalent temperature can be estimated using a multiple linear regression from environmental sensors and leads the way to comfort driven Heating, Ventilation and Air Conditioning control.

Applicability of Thermal Comfort Models in Car Cabin Environments

Diana Hintea, John Kemp, James Brusey, Elena Gaura and Neil Beloe. Applicability of Thermal Comfort Models in Car Cabin Environments. In *Proceedings of ICINCO* 2014, International Conference on Informatics in Control, Automation and Robotics, Volume I, pages 769-776, Vienna, Austria, September 1-3, 2014. ISBN: 978-989-758-039-0..

Car cabins are non-uniform and asymmetric environments in relation to both air velocity and temperature. Estimating and controlling vehicle occupant thermal comfort is therefore a challenging task. This paper focuses on evaluating the suitability of four existing thermal comfort models, namely the Predicted Mean Vote (PMV), Taniguchi's model, Zhang's model and Nilsson's model in a variety of car cabin conditions. A series of comfort trials were performed ranging from controlled indoor trials to on-road driving trials. The outputs of all four models were compared to the sensation index reported by the subjects situated in the driver seat. The results show that PMV and Nilsson's model are generally applicable for the car cabin environment, but that they are most accurate when there is a small air temperature

rate of change (of under 1.5 ℃ per minute), giving correlation levels of 0.91 and 0.93 for the two models respectively. Taniguchi's and Zhang's models were found unsuitable for all conditions, with correlation levels ranging between 0.03 and 0.60. Nilsson's model is recommended by the authors based on the level of agreement with the subjective reports, its ability to estimate both local and overall thermal sensation and the smaller number of input parameters.

C.2 Technical reports

Mutual Information-based Sensor Positioning for Car Cabin Comfort Monitoring

Diana Hintea, James Brusey and Elena Gaura. Mutual Information-based Sensor Positioning for Car Cabin Comfort Monitoring. Technical Report COGENT, Coventry University, 20010.

This report summarises work so far in developing a generic method for optimizing the sensor positions within a car cabin. The work is closely related to efforts in WP9.9 towards the development of effective HVAC control algorithms which enhance passengers and driver comfort. In this context, such a generic positioning method is necessary as: i) cabins present a highly variable environment, particularly with respect to temperature, thus sensor readings vary considerably from one point in the cabin to the next; ii) sensors are usually placed within the cabin as dictated by opportunity, aesthetic or cost reasons, thus control algorithms driven by their data might not be optimal. The initial focus of the work is on temperature, however the approach is applicable to other sensor modalities.

To date, the work on this strand took a theoretic approach to potential methods definition and optimal method selection. Validation was performed using RadTherm cabin data to determine the mutual information content of pairs of cabin sensors. A key novel element in this work comes from the need, within the car-cabin thermal sensing problem, to estimate the temperature at the one location that will be difficult to directly sense: on the skin of the passenger. Indeed, it may be the case that no single feasible sensor location will provide accurate information about the skin temperature and that instead a number of sensors are needed. An advantage of this approach is that it offers the possibility of meaningfully comparing the information value of, say, one expensive sensor compared with two inexpensive sensors. Furthermore, it does so in the context of the target application of the sensors. This report covers the development and testing of a variety of methods of finding the mutual information or correlation associated with two sensor positions. The method found to be most useful is based on finding the entropy based on a multivariate Gaussian assumption over the two sensors. Specifically, it is assumed that probability

distribution for any pair of sensors is a multivariate Gaussian.

Skin Temperature Estimation Method for Car Cabin Comfort Control

Diana Hintea, James Brusey and Elena Gaura. Skin Temperature Estimation Method for Car Cabin Comfort Control. Technical Report COGENT, Coventry University, 2011.

Car cabins are transient, non-uniform thermal environments, both with respect to time and space. Identifying representative locations for the Heating, Ventilation and Air Conditioning (HVAC) system sensors is an open research problem. Common sensor positioning approaches are driven by considerations such as cost or aesthetics, which may impact on the performance/outputs of the HVAC system and thus occupants' comfort. Based on experimental data, this report quantifies the spacial-temporal variations in the cabin's environment by using Mutual Information (MI) as a similarity measure. Accurate estimates of temperature at locations where sensors would be difficult to place, such as on an occupant's face or abdomen, are then computed. These estimations are produced from optimal (but practical) locations for sensors that support the development of *occupant* rather than *cabin* focused HVAC control algorithms. When applied to experimental data from stable and hot/cold soaking scenarios, the method proposed successfully identifies practical sensor locations which estimate face and chest temperatures of an occupant with less than 0.7 ℃ and 0.4 ℃ error, respectively.

Skin Temperature Estimation Method for Car Cabin Comfort Control

Diana Hintea, James Brusey and Elena Gaura. Skin Temperature Estimation Method for Car Cabin Comfort Control. Technical Report COGENT, Coventry University, 2011.

Car cabins are transient, non-uniform thermal environments, both with respect to time and space. Identifying representative locations for the HVAC system sensors is an open research problem. Common sensor positioning approaches are driven by considerations such as cost or aesthetics, which may impact on the performance / outputs of the HVAC system and thus occupants' comfort. Based on experimental data, this report quantifies the spatial-temporal variations in the cabin's environment by using **MI!** (**MI!**) as a similarity measure. Accurate estimates of temperature at locations where sensors would be difficult to place, such as on an occupant's face or abdomen, are then computed. These estimations are produced from optimal (but practical) locations for sensors that support the development of *occupant* rather than *cabin* focused HVAC control algorithms. When applied to experimental data from two trials, the first involving one subject and the second involving 7 subjects, the method proposed successfully identifies practical

sensor locations that estimate face, chest, right hand, right thigh and right lower leg temperatures of an occupant with errors of 0.50 ℃, 0.27 ℃, 0.68 ℃, 0.32 ℃ and 0.25 ℃, respectively, when the training and testing were performed on the same subject. On the other hand, when Leave-One-Subject-Out-Cross-Validation (LOSOCV) was used, the method estimated the face, chest, right hand, right thigh and right lower leg temperatures of an occupant with errors of 1.11 ℃, 0.96 ℃, 1.29 ℃, 0.90 ℃ and 1.09 ℃, respectively.

Whole Vehicle Thermal Efficiency WS9

James Brusey, Diana Hintea, John Kemp and Doug Thake. Skin Temperature Estimation Method for Car Cabin Comfort Control. Technical Report COGENT, Coventry University, 2014.

This report describes progress on STRIVE workstream 9 for the six month period from the start of the project (September 2013) to date. In brief, progress has been as initially expected: a thorough literature search has been performed on the topic area and initial progress has been made towards setting up the interfaces to the machine learning algorithm to enable the use of Modelica simulation. The overall aim of the work is to develop a car cabin comfort control system that, through machine learning, is optimised to provide a balance of thermal comfort and energy efficiency in the context of a physical thermal management system that not only blows hot and cold air but also heats and cools various surfaces including seats and the steering wheel.

C.3 Publications in progress

Patent: Reinforcement Learning-based Vehicle Thermal Comfort Control: Diana Hintea, James Brusey, Elena Gaura and Neil Beloe - approved.

Journal: Reinforcement Learning-based Thermal Comfort Control for Car Cabins: Diana Hintea, James Brusey and Elena Gaura - to be sumitted to Applied Thermal Engineering.

C.4 Presentations and demos

- **Skin Temperature Estimation Method for Car Cabin Comfort Control** (September 2014) – ICINCO 2014 International Conference – Vienna, Austria
- **Comfort in Cars - Estimating Equivalent Temperature for Comfort Driven Heating, Ventilation and Air Conditioning (HVAC) Control** (July 2013) – ICINCO 2013 International

Conference – Reykjavik, Iceland

- **Estimating Equivalent Temperature for Comfort Driven Heating, Ventilation and Air Conditioning (HVAC) Control** (July 2013) – Coventry University Research Symposium (won 2nd prize at the poster section) – Coventry, UK
- **Comfort in Cars: Estimating Comfort from Equivalent Temperatures** (September 2012) – Southampton, Cambridge and Coventry Research Exchange – Coventry University, UK
- **Estimating Equivalent Temperature for Comfort Driven Heating, Ventilation and Air Conditioning (HVAC) Control** (July 2012) – Demo and Poster at Jaguar Land Rover TechFair – Coventry, UK
- **Comfort in Cars: Estimating Comfort from Equivalent Temperatures** (May 2012) – The Polish-British Workshop (won best paper award) – Wroclaw, Poland
- **Mutual Information based Sensor Positioning for Car Cabin Comfort** (September 2011) – KES 2011 International Conference– Kaiserslautern, Germany
- **Mutual Information based Sensor Positioning for Car Cabin Comfort** (September 2011) – Southampton, Cambridge and Coventry Research Exchange – Coventry University, UK
- **Skin Temperature Estimation Method for Car Cabin Comfort Control** (May 2011) – Coventry Cambridge Research Exchange – Coventry, UK

C.5 Conferences attended

- **11th International Conference on Informatics in Control, Automation and Robotics (ICINCO)** (September 2014) – Vienna, Austria
- **10th International Conference on Informatics in Control, Automation and Robotics (ICINCO)** (July 2013) – Reykjavik, Iceland
- **WiSIG: Advances in Wireless Sensor Networks for Hostile Environments** (May 2012) – Derby, UK
- **The Polish-British Workshop** (May 2012) – Wroclaw, Poland
- **15th International Conference on Knowledge-Based and Intelligent Information & Engineering Systems (KES)** (September 2011) – Kaiserslautern, Germanys

- **WiSIG: Wireless Sensing for Smart Buildings** (February 2011) – Coventry University, UK
- **WiSIG: Sensing Technology 2010** (September 2010) – Birmingham, UK

Selected publications follow.

Applicability of Thermal Comfort Models to Car Cabin Environments

Diana Hintea[1], John Kemp[1], James Brusey[1], Elena Gaura[1] and Neil Beloe[2]
[1]*Coventry University, Priory Lane, Coventry, CV1 5FB, UK*
[2]*Jaguar Land Rover Ltd, Abbey Road, Whitley, Coventry, CV3 4LF, UK*
{hintead, aa9384, j.brusey, e.gaura}@coventry.ac.uk, nbeloe@jaguarlandrover.com

Keywords: PMV, Thermal Comfort Model, HVAC Control, Skin Temperature

Abstract: Car cabins are non-uniform and asymmetric environments in relation to both air velocity and temperature. Estimating and controlling vehicle occupant thermal comfort is therefore a challenging task. This paper focuses on evaluating the suitability of four existing thermal comfort models, namely the Predicted Mean Vote (PMV), Taniguchi's model, Zhang's model and Nilsson's model in a variety of car cabin conditions. A series of comfort trials were performed ranging from controlled indoor trials to on-road driving trials. The outputs of all four models were compared to the sensation index reported by the subjects situated in the driver seat. The results show that PMV and Nilsson's model are generally applicable for the car cabin environment, but that they are most accurate when there is a small air temperature rate of change (of under 1.5 °C per minute), giving correlation levels of 0.91 and 0.93 for the two models respectively. Taniguchi's and Zhang's models were found unsuitable for all conditions, with correlation levels ranging between 0.03 and 0.60. Nilsson's model is recommended by the authors based on the level of agreement with the subjective reports, its ability to estimate both local and overall thermal sensation and the smaller number of input parameters.

1 Introduction

Car cabins are environments with inherent non-uniformity and asymmetry in both air velocity and temperature fields. Steady-state trends can be encountered for journeys in excess of 15-20 minutes, however 85% of journeys are of shorter duration (Cisternino, 1999). Predicting passengers' thermal comfort for efficient Heating, Ventilation and Air Conditioning (HVAC) control is therefore a complex problem.

More than forty years after its development, Fanger's Predicted Mean Vote (PMV) (Fanger, 1973) remains the most used method for assessing occupant thermal comfort in a range of environments. Although designed specifically for use in buildings, PMV continues to drive research into vehicle HVAC control algorithms (Ueda and Taniguchi, 2000; Busl, 2011; Farzaneh and Tootoonchi, 2008). The main reasons are the simplicity of measuring the air temperature and humidity parameters, combined with the ability to estimate the remaining parameters within controlled tests. Nilsson (Nilsson, 2004) proposed thermal comfort zones for 18 different body parts and overall based on equivalent temperatures. Nilsson's model uses similar parameters with PMV (air temperature, air flow, mean radiant temperature and clothing index). However, the model has the advantage of estimating local thermal sensation, as well as overall.

Skin temperature is shown to be a good predictor of local and overall thermal sensation in the state of art (Bogdan, 2011; Wang et al., 2007). Taniguchi's model (Taniguchi et al., 1992) was designed for vehicular applications and is based on face skin temperature only. Zhang's thermal sensation and comfort model (Zhang, 2003), on the other hand, is a more recent model developed with transient, inhomogeneous environments in mind. The model, however, has been criticized in the literature for having too many coefficients, for the limitations of the experimentation and for the body part set-point temperature approach (Luo et al., 2007). Moreover, no validation of these two skin temperature based models within daily driving scenarios or other typical conditions encountered in vehicular environments exists in the literature.

Considering the above, this paper evaluates PMV, Taniguchi's model, Zhang's model and Nilsson's model on empirical data gathered in a variety of car cabin conditions, establishing whether they are suitable for comfort-oriented vehicular control.

The main contributions of this paper are: 1) illustrating the range of conditions in which these models could be applied to drive comfort-oriented HVAC

control algorithms and 2) establishing which of the four thermal comfort models is a better match of cabin occupant thermal comfort in typical vehicular conditions based on gathered empirical data.

The paper is structured as follows: Section 2 presents an overview of the the four thermal comfort models. Section 3 describes the data gathering methodology, focusing on the instrumentation used, the participating subjects and the range of conditions encountered in the car cabin. Section 4 presents the results obtained when comparing the sensation index corresponding to the four models with the subjects' reported sensation. Finally, Section 5 concludes the paper.

2 Background

Based on the review provided by Cheng *et al.* (Cheng et al., 2012), the following thermal comfort models were implemented and evaluated on the data gathered: PMV, Taniguchi's model, Nilsson's model and Zhang's model. These thermal comfort models are reviewed in (Alahmer et al., 2011; Cheng et al., 2012; Orosa, 2009) and discussed in the following subsections.

With regard to other models, Matsunaga *et al.* (Matsunaga et al., 1993) adopted, for example, the concept of Average Equivalent Temperature (AET) in order to compute the PMV sensation index. The AET is a surface area-weighted value for three body parts: the head with a weight of 0.1, the abdomen with a weight of 0.7 and the feet with a weight of 0.2. Because the end product is the PMV index, this technique is not evaluated in this paper. Also, the Berkeley advanced human thermal comfort model (Arens et al., 2006) is used as a cabin occupant comfort estimator in multiple works. The virtual manikin in the software model estimates occupant skin temperatures and Zhang's model uses the latter to calculate thermal sensation and thermal comfort. As this paper is concerned with empirical results rather than simulation, only Zhang's model is evaluated.

2.1 Predicted Mean Vote (PMV)

Fanger (Fanger, 1970) developed the PMV model in 1967 based on thermo-regulation and heat balance theories. These theories are based on human bodies employing physiological processes in order to maintain a balance between the heat produced by metabolism and the heat lost from the body. The PMV index provides a score that corresponds to the American Society of Heating, Refrigerating and Air Conditioning Engineers (ASHRAE) thermal sensation scale shown in Table 1 and it is defined as the average thermal sensation felt by a large group of people in a space. The PMV model combines four physical variables (air temperature, air velocity, mean radiant temperature and relative humidity) and two personal variables (clothing insulation and activity level). The mathematical equations used to derive the PMV index are given in the ISO 7730 standard (ISO, 2005).

Table 1: PMV thermal sensation index.

3	Hot
2	Warm
1	Slightly warm
0	Neutral
-1	Slightly cool
-2	Cool
-3	Cold

Fanger validated and refined the comfort equation with data from other previous thermal comfort studies combined with his own, summing to approximately 1400 participants. Fanger stated that the PMV model should be used with care for indexes below -2 and above $+2$ and that significant errors can appear in hot environments. PMV's main advantages are the standardisation of the implementation and that if some of the constituent parameters cannot be measured, they can be approximated without introducing a significant error in the outputted PMV index.

However, PMV was never intended to be applied in transient, inhomogeneous conditions. Van Hoof (van Hoof, 2008) discussed PMV's applicability to transient conditions, concluding that there is a lack of PMV assessment in transient environments and that extensive research is still required. Also, body parts experience local discomfort and thermal sensation levels differ from each other and from the overall sensation (Arens et al., 2006; Nakamura et al., 2008). With the introduction of heated/cooled seats and steering wheels the impact on individual body part sensation is even higher. Therefore, a big disadvantage of the PMV model is that it is unable to differentiate between sensations at different body parts, which is an important capability in the case of vehicular HVAC control systems.

2.2 Taniguchi's model

Skin temperature is shown to be a good predictor of local and overall thermal sensation in the state of art (Bogdan, 2011; Wang et al., 2007), especially in case of extremities such as face and hands. Taniguchi *et al.* (Taniguchi et al., 1992) developed a multiple linear regression model relating the average facial skin tem-

perature and its rate of change to the Overall Thermal Sensation (OTS) in a vehicle environment. The model was proposed based on a series of human subject tests and OTS is calculated as:

$$OTS = 0.81\,(T_f - 33.9) + 39.1\frac{dT_f}{dt}$$

where T_f is the face skin temperature and $\frac{dT_f}{dt}$ is the face skin temperature rate of change.

A significant disadvantage of this model is not taking into account that the thermal sensation of body segments other than the face also impact the overall body thermal sensation. Moreover, it does not allow the computation of local thermal sensation.

2.3 Zhang's model

Zhang (Zhang, 2003) developed local and overall thermal sensation and comfort models targeted at transient, non-uniform conditions. Unlike Taniguchi's model, Zhang's models are based on skin temperatures at multiple sites along with core temperature, if available. A nine point analogue scale (shown in Table 2) is used for expressing thermal sensation. Experimental tests were carried out at UC Berkeley, with subjects placed into chambers of uniform temperature and with heated or cooled air applied individually to 19 separate body areas. The tests were carried out in a climate-controlled chamber, consisting of both cold and hot test cases. Throughout these tests, subjects were allowed to adjust the HVAC settings to their preference. Skin temperature was measured at 19 locations using thermocouples, while core temperature was measured using an ingestible temperature device. Local and overall sensation equations were developed, using the measured skin temperature, mean skin temperature and core temperature along with subjective reports. Zhang validated the model against subjective reports and acceptable results were obtained. The coefficient of determination (R^2) for the overall sensation model was 0.95 and the standard deviation of residuals was 0.54.

Luo *et al.* (Luo et al., 2007) criticize the model, citing that "the mathematical model is not practicable as it is limited by having too many coefficients, and because of the experiment's limitation, the regression analysis result cannot be assured either". Furthermore, they criticize the body part set-point temperature approach of the model. Also, Cheng *et al.* (Cheng et al., 2012) points out that during the experiments, they focused more on cooling local body parts in warm environments than on warming local body parts in cool environments. In addition, the influence of local stimulation duration and intensity were not varied in the test. Moreover, no validation of the model within daily driving scenarios or other typical conditions encountered in vehicular environments exists in the literature. The main advantage of Zhang's model over PMV is its ability to determine local sensation indexes.

Table 2: Zhang's thermal sensation scale.

4	Very Hot
3	Hot
2	Warm
1	Slightly Warm
0	Neutral
-1	Slightly Cool
-2	Cool
-3	Cold
-4	Very Cold

2.4 Nilsson's model

Nilsson (Nilsson, 2004) proposed clothing independent thermal comfort zones for 18 different body parts based on equivalent temperatures. Equivalent temperature is formally defined as the uniform temperature of an imaginary enclosure with air velocity equal to zero in which a person will exchange the same dry heat by radiation and convection as in the actual non-uniform environment (Nilsson and Holmer, 2002). Equivalent temperature can be computed based on environmental parameters such as air temperature, mean radiant temperature, air flow and clothing index or it can be directly measured with appropriate instruments, such as dry heat loss transducers for example (Nilsson and Holmer, 2002). Once the equivalent temperature is calculated, the local or overall thermal sensation level can be estimated using the diagrams in Figure 1. Nilsson developed this model through experimentation.

A gap in the literature that this paper responds to is the lack of empirical evaluation of the thermal comfort models presented within vehicular environments in order to establish whether any of them is suitable for comfort-oriented HVAC control. According to the authors' knowledge, no empirical data based evaluation of these models in vehicular environments exists in the state of art.

3 Methodology

In order to address this lack of empirical evaluation, car cabin data and subjective comfort readings were gathered over a wide range of experimental con-

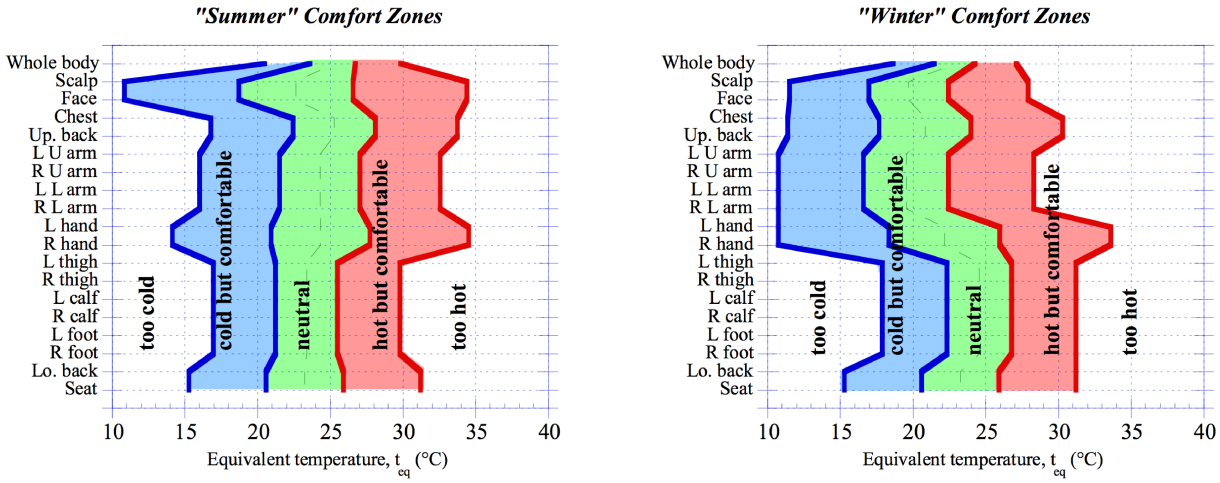

Figure 1: Nilsson's clothing independent thermal sensation diagrams (Nilsson, 2004).

Table 3: Subject details.

Subject	Gender	Age	Height (cm)	Weight (kg)
1	Male	46	173	78
2	Female	37	157	73
3	Male	56	166	70
4	Male	49	178	75
5	Female	24	162	48
6	Male	26	176	77
7	Female	34	160	55

ditions. This section provides a description of the participating subjects in the comfort trials, the instrumentation used and the variety of conditions encountered throughout the trials.

3.1 Participating subjects

Seven adults (four males and three females) were selected as experimental subjects. Their ages were between 24 and 56 years old, with heights between 1.57 cm and 1.78 cm and weights between 48 kg and 78 kg, as presented in Table 3. The subjects occupied the driver seat and were asked by the observer in the right-hand rear passenger seat for their overall thermal sensation throughout the experimental trials (as detailed in Section 3.3). The thermal sensation scale used was the ASHRAE seven point scale (coincides with the PMV scale) shown in Table 1. Clothing was standardised across all trials and subjects, consisting of long trousers and a short-sleeved, light-coloured shirt or blouse, corresponding to a clothing index value of 0.7.

3.2 Measured variables

Throughout all trials, equivalent temperature was monitored at eight locations (corresponding to head, chest, left lower arm, right lower arm, left upper arm, right upper arm, thigh and calf) using the INNOVA Flatman support manikin, shown in Figure 2 (right) and the associated INNOVA 1221 thermal comfort data-logger. Throughout the trials, the Flatman was positioned in the front passenger seat, continuously calculating equivalent temperature via the dry heat loss sensors and computing the PMV thermal sensation level. Cabin air and surface temperature data was gathered from 19 points using type K thermocouples and was recorded by a Grant Instruments DataTaker DT85 data logger. Near-body air temperature and relative humidity were measured at eight points (close to the neck, wrist, chest, thigh and calf locations) using type T thermocouples and Honeywell S&C HIH-5031 humidity sensors and also recorded by a SQ2040 data-logger. Solar loading at the driver sunroof location was measured using automotive solar sensors and recorded by a Grant Instruments Squirrel SQ2040 data-logger. The driver's center and outboard face vent air temperatures were monitored using type K thermocouples and recorded by the SQ2040 data-logger. Finally, subject skin temperature was also monitored at eight points (neck, left and right wrist, chest, left and right thigh and left and right calf) using Grant Instruments EUS-UU-VL2-0 thermistors and recorded by the SQ2040 data-logger.

3.3 Experimental procedure

The trials were performed from the 8th to the 29th of August 2011. The test car used was a Jaguar XJ (2010

Figure 2: Experimental data gathering. Left: Mean radiant temperature sensor. Right: Upper body of the Flatman thermal manikin.

model year). Three types of trials were performed, with 78 trials in total, as described in the following sections.

3.3.1 *Variable cabin temperatures within steady state external conditions (T1)*

These trials were performed within an enclosed space in order to eliminate wind and precipitation effects. Both the subjects and the test car were preconditioned for 20 minutes to 22 °C. At the outset of the experiment the subject, occupying the driver seat, remained in static conditions for 10 minutes. The temperature was then increased by 1 °C every 3 minutes until it reached 28 °C. The subject then left the car, which was again conditioned to 22 °C. After the subject returned, they again remained in static conditions for 10 minutes. Then the temperature was decreased by 1 °C every 3 minutes until it reached 16 °C. The air flow from the HVAC system was set to high or medium settings. During the static conditions, the subject reported thermal sensation and comfort at the 5, 7, and 9 minute marks and one minute before each temperature change when the HVAC set point was varied.

These trials are characterized by the following conditions: 1) absolute average car cabin temperature rates of change peaking at around 1.5 °C per minute, but usually under 1 °C per minute; 2) preconditioning of the cabin and subject at the same temperature; 3) no precipitation or wind effects; 4) steady ambient temperature (between 19 °C and 24 °C) varying by less than 1 °C within an individual trial.

3.3.2 *User control with steady state external conditions (T2)*

These trials were performed within an enclosed space. The car and the subjects were preconditioned to a neutral (22 °C), hot (28 °C), or cold (16 °C) temperature. The subjects entered the car and remained inside for 15 minutes time, during which they were permitted to adjust the air conditioning at will in order to make themselves more comfortable. The control adjustments they made were logged in addition to the previously described parameters. Thermal comfort and sensation was reported every two minutes, with the first report being at the start of the test.

These trials are characterized by the following conditions: 1) absolute average car cabin temperature rates of change peaking at 8 °C per minute; 2) preconditioning of the cabin and subject at the same temperature; 3) no precipitation or wind effects; 4) steady outside temperature (between 17 °C and 25 °C) varying by less than 1 °C within an individual trial.

3.3.3 *User control in driving conditions (T3)*

These trials are similar to the previous ones (*T2*), except that the subjects drove the car on private roads and there was no additional solar loading applied beyond that naturally falling on the car. Drivers were required to turn and change speed at frequent intervals in order to simulate to an extent the daily driving routine. This provided a comparison against the baseline established in the previous type of trials, as it was expected that the acceptable temperature range would widen as the driver was required to concentrate on driving. Thermal comfort and sensation was reported every two minutes, with the first report being at the start of the test.

These trials are characterized by the following conditions: 1) absolute average car cabin temperature rates of change peaking at 10 °C per minute; 2) preconditioning of the cabin and subject at the same temperature; 3) ambient solar load and wind; 4) ambient outside temperature (between 12 °C and 28 °C) varying by less than 2 °C within an individual trial.

The first set of trials were aimed at determining the extents of passenger thermal comfort with no extreme conditions, while the second set offered information on what control adjustments were required in order for the cabin occupants to feel comfortable and how quickly thermal neutrality was reached. The third set of trials aimed to capture the comfort ranges during daily driving and therefore with the subject less focused on their comfort. Altogether, the multitude of conditions (solar load, stationary or driving, different blower speeds, different initial temperatures) allowed a thorough evaluation of the validity of the selected thermal comfort models. Table 4 provides a summary of the trials performed.

Throughout the three sets of trials, the Flatman was positioned in the front passenger seat, with the subject occupying the driver seat. In order to ensure a valid comparison between the thermal sensation computed/reported by the two sides the following were ensured: 1) the front passenger vent and driver vent

Table 4: Summary of the experimental conditions in all trials.

Trial	Duration (mins)	Blower speed	Solar load	Driving	Pre-conditioning	Subjects
T1	56	High or Medium	Controlled	No	22 °C	7
T2	15	User	Controlled	No	16 °C, 22 °C or 28 °C	7
T3	15	User	Ambient	Yes	16 °C, 22 °C or 28 °C	6

had the same orientation and delivered the same set-point temperature; 2) both the test car (with the Flatman inside) and the driver were preconditioned to the same temperature prior to each trial.

4 Results

This section provides an evaluation of the four thermal comfort models based on the gathered data described in Section 3. The purpose is to establish whether they can accurately predict car cabin occupant thermal sensation in any of the conditions in order to be used for comfort based HVAC control. For this purpose the overall thermal sensation reports of the drivers were compared to i) the PMV index as computed by the Flatman, ii) Zhang's index computed from the measured skin temperatures, iii) Taniguchi's index computed from the measured facial skin temperature and iv) Nilsson's index computed from the measured average body equivalent temperature.

PMV is widely used for car cabin comfort based HVAC controllers (Busl, 2011; Farzaneh and Tootoonchi, 2008). The reason is the simplicity of estimating the PMV index. However, does PMV actually reflect the reported sensation levels of the occupants? Table 5 presents the correlation coefficient and the determination coefficient R^2 between the subjective and experimental data for all models. The correlation coefficient quantifies the degree of correlation between two variables, while the R^2 coefficient indicates how well data points fit the linear regression. The p-value for a regression gives the probability that the result is not derived by chance. For all results presented, the p-value is smaller than the threshold ($p < 0.001$) and the results are therefore significant.

In the case of PMV, the highest level of agreement corresponds to trials *T1*, with a correlation index of 0.91. The high correlation is somewhat expected due to the stable conditions encountered throughout trials *T1* (interior temperature rates of change less than 1.5 °C per minute, stable outside temperature and no wind or precipitation). The experimental data matches less accurately the subjective reports in trials *T2* and *T*3. The correlation index between the two is 0.76 for *T2* and 0.78 for *T3*. Overall Flatman's PMV tended towards colder reports than the subjective reports. For example, for *T1*, drivers reported thermal sensations of up to 4 (corresponding to "very hot"), whereas Flatman's PMV did not go beyond 3 (corresponding to "hot").

The results indicate that PMV can be applied in vehicle cabins to infer passenger comfort within a limited set of conditions, however the model brings forward another important issue in this type of environment, the inability to differentiate between different parts of the body. Due to the non-uniform nature of the environment, the difference in thermal sensation over small distances is considerable and so effective HVAC control should be able to warm up or cool down separately different body parts.

With PMV's accuracy limited to a narrow range of conditions, the authors further investigated two skin temperature based models: Taniguchi's model and Zhang's model. For Taniguchi's model, as Table 5 illustrates, the highest level of agreement corresponds to trials *T1*, with a correlation index of 0.56, while in trials *T2* and *T*3 the match is poor, with correlation indexes of 0.03 and 0.15, respectively. Face skin temperature seems to have a higher impact on overall thermal sensation when the rate of change of air temperature is low (less than 1.5 °C per minute), as suggested by the higher correlation for trials *T1*. As Taniguchi's model was developed only with respect to facial skin temperature, it is further interesting to see if Zhang's model improves on this by taking into consideration 8 different body parts.

Zhang's model was developed, like Taniguchi's, for transient environments such as car cabins. During experimentation, skin temperature was sampled at only 8 sites, compared to the 19 sites specified by Zhang. This is justified by the fact that within real-time vehicular comfort control, it would be infeasible to monitor skin temperature at all locations specified by Zhang. However, in order to ensure that the sum of skin temperature segment weights is 1, the weights for the contribution of local thermal sensations to the overall sensation were normalised. Mean skin temperature was calculated as a proxy for core temperature (this approach being suggested by Zhang). The body part skin temperatures recorded at the beginning of each trial were used as the set point temperatures of the body segments in the model. As table 5 shows, the correlation levels are poor: 0.10 for *T1*, 0.50 for *T2* and 0.60 for *T3*. As it stands, for trials *T1*, facial skin

Table 5: Statistic metrics between the models' thermal sensation index and the reported sensation.

	PMV		Taniguchi		Zhang		Nilsson	
Type	Correlation	R^2	Correlation	R^2	Correlation	R^2	Correlation	R^2
T1	0.91	0.85	0.56	0.32	0.10	0.0001	0.93	0.86
T2	0.76	0.57	0.03	0.001	0.50	0.25	0.77	0.59
T3	0.78	0.61	0.15	0.02	0.60	0.35	0.79	0.62

temperature alone proved to be a better estimator than the combination of 8 different body parts. The performance of the two skin temperature based models does not appear to be sufficient to support vehicular HVAC comfort control.

In order to compute the overall thermal sensation index of Nilsson's model, the equivalent temperature at 8 different body parts was averaged based on body area weights. Once the average equivalent temperature is computed, the overall thermal sensation index can be found from Figure 1, using the diagram corresponding to light clothing (the participants wore light clothing throughout the experiments). Nilsson's model had a similar performance to the PMV model. The highest level of agreement with the subjective reports corresponds to trials *T1*, with a correlation index of 0.93. For trials *T2* and *T3*, the correlation index is lower, of 0.77 and 0.79, respectively. The similar performance is somewhat expected, because Flatman's PMV index is also based on the measured average equivalent temperature. The advantage Nilsson's model has over PMV is that local thermal sensation can also be computed and used for control.

5 Conclusions and discussion

In this paper we evaluated the applicability of four thermal comfort models, namely PMV, Taniguchi's model, Zhang's model and Nilsson's model in a range of conditions specific to cars. A first step towards this aim was to design experimental trials covering a wide range of conditions: with preconditioning of the occupants and cabin at different temperatures, with or without ambient solar load, wind and precipitations, with steady or varying outside ambient temperature and with different temperature rates of change within the cabin.

Based on the experimentally gathered data, the PMV index and Nilsson's index accurately matched (with correlations of 0.91 and 0.93, respectively) the occupant reported thermal sensation within a limited set of conditions: preconditioning of the passenger and the cabin at the same temperature, a steady outside temperature and low rates of change of the interior temperature (lower than 1.5 °C per minute). Higher interior temperature rates of change (up to 9 °C per minute), ambient solar load and wind leads to lower correlation factors, between 0.76 and 0.79.

The overall sensation computed using the two skin temperature based thermal comfort models (Taniguchi's model and Zhang's model) poorly matched the subjective reports throughout all trial types (correlations between 0.10 and 0.60). Overall, the two skin temperature based models appear to have little success and their accuracy is not sufficient to support vehicular HVAC comfort control.

Capitalizing on our findings, Nilsson's model is recommended by the authors in preference to the other three models for vehicular comfort oriented control. The model provided similar results to PMV. However, an important advantage Nilsson's model has over PMV is its ability to estimate local thermal sensation, which the authors see as an important capability for the new generation of vehicular HVAC control systems. Moreover, Nilsson's model only requires two input parameters—equivalent temperature and clothing index—rather than six parameters in PMV's case, some of which could not feasibly be determined by an automated system.

The deviation between the Flatman's PMV output and the subjective responses may be because the subjects were in contact with the seat and the steering wheel whereas the Flatman's dry heat loss sensors were not. This could be confirmed via further experimentation. Another related avenue for future work is in regard to heated/cooled seats and steering wheels. These are becoming more widespread and will clearly have an impact on thermal sensation and comfort, which should be evaluated through empirical work.

It is known that no thermal comfort model can provide a perfect match for what people feel. The description of PMV, for example, acknowledges that any given environment will leave at least 5% of people dissatisfied. One reason is the subjective nature of thermal sensation and comfort in terms of how they are felt and, also, how they are reported. However, adopting Nilsson's model as a basis for estimating occupant comfort control and further integrating online learning within the car for tuning individual preferences would lead to a more thermally comfortable vehicular environment.

Acknowledgements

The Low Carbon Vehicle Technology Project (LCVTP) was a collaborative research project between leading automotive companies and research partners, revolutionising the way vehicles are powered and manufactured. The project partners included Jaguar Land Rover, Tata Motors European Technical Centre, Ricardo, MIRA LTD., Zytek, WMG and Coventry University. The project included 15 automotive technology development work-streams that will deliver technological and socio-economic outputs that will benefit the West Midlands Region. The £19 million project was funded by Advantage West Midlands (AWM) and the European Regional Development Fund (ERDF).

The authors would like to thank the anonymous reviewers for their insightful comments.

REFERENCES

Alahmer, A., Mayyas, A., Mayyas, A., Omar, M., and Shan, D. (2011). Vehicular thermal comfort models; a comprehensive review. *Applied Thermal Engineering*, 31:995–1002.

Arens, E., Zhang, H., and Huizenga, C. (2006). Partial and whole-body thermal sensation and comfort, part ii: Non-uniform environmental conditio. *Journal of Thermal Biology*, 31:60–66.

Bogdan, A. (2011). Case study assessment of local and general thermal comfort by means of local skin temperature. *International Journal of Ventilation*, 10:291–300.

Busl, M. (2011). Design of an energy-efficient climate control algorithm for electric cars. Master's thesis, Lund University.

Cheng, Y., Niu, J., and Gao, N. (2012). Thermal comfort models: A review and numerical investigation. *Building and Environment*, 47:13–22.

Cisternino, M. (1999). Thermal climate in cabs and measurement problems. In *CABCLI Consortium*.

Fanger, P. (1970). *Thermal Comfort*. Danish Technical Press.

Fanger, P. (1973). Assessment of man's thermal comfort in practice. *British Journal of Industrial Medicine*, 30:313–324.

Farzaneh, Y. and Tootoonchi, A. (2008). Controlling automobile thermal comfort using optimized fuzzy controller. *Applied Thermal Engineering*, 28:1906–1917.

ISO (2005). *Ergonomics of the Thermal Environment*.

Luo, X., Hou, W., Li, Y., and Wang, Z. (2007). A fuzzy neural network model for predicting clothing thermal comfort. *Computers and Mathematics with Applications*, 53:1840–1846.

Matsunaga, K., Sudo, F., Tanabe, S., and Madsen, T. (1993). Evaluation and measurement of thermal comfort in the vehicles with a new thermal manikin. Technical report, SAE Paper.

Nakamura, M., Yoda, T., Crawshaw, L., Yasuhara, S., Saito, Y., Kasuga, M., Nagashima, K., and Kanosue, K. (2008). Regional differences in temperature sensation and thermal comfort in humans. *Journal of Applied Physiology*, 105:1897–1906.

Nilsson, H. (2004). *Comfort Climate Evaluation with Thermal Manikin Methods and Computer Simulation Models*. PhD thesis, Royal Institute of Technology.

Nilsson, H. and Holmer, I. (2002). Definitions and measurements of equivalent temperature. Technical report, The Climate Group, National Institute for Working Life, Solna, Sweden.

Orosa, J. (2009). Research on general thermal comfort models. *European Journal of Scientific Research*, 2:217–227.

Taniguchi, Y., Hiroshi, A., and Kenji, F. (1992). Study on car air conditioning system controlled by car occupants' skin temperatures - part 1: research on a method of quantitative evaluation of car occupants. Technical report, SAE Paper.

Ueda, M. and Taniguchi, Y. (2000). The prediction of the passenger's thermal sensation level using a neural network and its application to the automobile hvac control.

van Hoof, J. (2008). Forty years of fanger's model of thermal comfort:l comfort for all? *Indoor Air Journal*, 18:182–201.

Wang, D., Zhang, H., Arens, E., and Huizenga, C. (2007). Observations of upper-extremity skin temperature and corresponding overall-body thermal sensations and comfort. *Building and Environment*, 42:3933–3943.

Zhang, H. (2003). *Human Thermal Sensation and Comfort in Transient and Non-Uniform Thermal Environments*. PhD thesis, University of California, Berkeley.

Comfort in Cars:
Estimating Equivalent Temperature for Comfort Driven Heating, Ventilation and Air Conditioning (HVAC) Control

Diana Hintea[1], James Brusey[1], Elena Gaura[1], John Kemp[1] and Neil Beloe[2]
[1]*Coventry University, Priory Lane, Coventry, CV1 5FB, UK*
[2]*Jaguar Land Rover Ltd, Abbey Road, Whitley, Coventry, CV3 4LF, UK*
{hintead, j.brusey, e.gaura, aa9384}@coventry.ac.uk, nbeloe@jaguarlandrover.com

Keywords: Equivalent Temperature, Multiple Linear Regression, Thermal Comfort, HVAC

Abstract: Equivalent Temperature is generally considered an accurate predictor for thermal comfort in car cabins. However, direct measurement of this parameter is impractical in fielded applications. The paper presents an empirical, multiple linear regression based approach for estimating body segment equivalent temperatures for car cabin occupants from different sensors within the car. Body part equivalent temperature at eight segments and cabin sensor data (air temperature, surface temperature, mean radiant temperature, humidity and solar load) was gathered in a variety of environmental and cabin conditions. 38 experimental hours of trials in a controlled environment and 26 experimental hours of realistic driving trials were used for training and evaluating the estimator's performance. The estimation errors were on average between 0.5 °C and 1.9 °C for different body parts for trials within a controlled environment, while for trials in realistic driving scenarios they ranged between 1 °C and 2 °C. This demonstrates that passenger body part equivalent temperature can be estimated using a multiple linear regression from environmental sensors and leads the way to comfort driven Heating, Ventilation and Air Conditioning control.

1 Introduction

Car buyers expect that climate control systems will make them comfortable. In order to control comfort and not merely climate temperature, one must first be able to estimate it. Estimating comfort, however, is acknowledged to be a difficult task given that the cabin is a rapidly changing environment, non-uniform with respect to parameters such as air temperature, air velocity and solar load. Furthermore, current Heating, Ventilation and Air Conditioning (HVAC) systems are power hungry and thus not well suited to electric vehicles as they may substantially reduce the vehicle's range.

In order to enable efficient control we need a better understanding of the relationships between environments and perceived comfort levels. Prior work established that Equivalent Temperature (ET) can be an accurate predictor for comfort (Mayer and Schwab, 1999), (Curran *et al*., 2010), (Mola *et al*., 2004). Dry heat loss transducers allow in-field calculation of ET (Madsen *et al*., 1986), however they are too large and costly to be used in a production car. An alternative approach is clearly needed.

In this paper, we propose a method for estimating ET at several body locations for cabin occupants, based on easily measured cabin variables, such as air temperature and mean radiant temperature. The method requires only a small number of cheap sensors placed within the car and accounts for the dynamic nature of the cabin environment. The method can be used to perform estimation in real-time and is intended to lead to high performance HVAC control systems which can be optimized for energy usage in low carbon vehicles.

The main contributions of this paper are: 1) to demonstrate an ET estimation method that requires non-expensive and non-intrusive sensors, 2) optimisation of the estimation method through sensor location selection based on Mutual Information and 3) validation of the method on data gathered in a variety of conditions, from controlled trials in stable environments to daily driving trials. Although the results here are specific to environmental conditions found within car cabins, the method itself is applicable to other environments, given appropriate empirical data.

The paper is structured as follows: Section 2 reviews related work in the area of remote estimation

of a range of parameters. Section 3 describes the experimental data sets gathered for evaluation purposes, while Section 4 presents the multiple linear regression ET estimation method. Section 5 presents the results obtained through training and testing the estimator. Finally, Section 6 concludes the paper.

2 Related Work

Traditionally, vehicle HVAC systems control cabin air temperature and humidity to a target set-point. However, it has long been established that thermal comfort is influenced by a variety of factors in addition to air temperature, such as mean radiant temperature, relative air velocity, relative humidity, metabolic rate and clothing thermal resistance (Fanger, 1973), (Gagge *et al*., 1967). Moreover, it is known that occupants feel comfortable over a range of temperatures rather than at one specific temperature (Fanger, 1973), (ANSI/ASHRAE, 2004), (Singh *et al*., 2010). Estimating the level of passenger comfort allows generating the exact amount of energy needed, instead of wasting additional energy by warming-up or cooling-down the whole cabin to a certain set-point temperature. It can therefore be concluded that the traditional approach is not optimal with regards to ensuring comfort and energy efficiency. This indicates that in order to develop improved HVAC control algorithms, there is a need to 1) sense more than just air temperature and 2) utilise thermal comfort estimates for cabin occupants in the control feedback loop.

ET is formally defined as the uniform temperature of the imaginary enclosure with air velocity equal to zero in which a person will exchange the same dry heat by radiation and convection as in the actual non-uniform environment (SAE Journal, 2012). Intuitively, ET corresponds more closely to the human sensation of environmental temperature than air temperature alone. ET is an accurate predictor for thermal comfort (Mayer and Schwab, 1999), (Curran *et al*., 2010), (Mola *et al*., 2004), which integrates the effect of air temperature, mean radiant temperature and relative air velocity. However, its direct measurement can be intrusive, expensive and bulky. An alternative to measuring ET is to estimate it from measurements made at more convenient locations.

A variety of learning based models have been created for the remote estimation of several parameters in different environments. Mehnert *et al*. (2000), for example, used a multiple linear regression to estimate average skin temperature from parameters such as air temperature, mean radiant temperature, air velocity, metabolic rate, rectal temperature and partial vapour pressure. Buller *et al*. (2010) developed an estimator of human core body temperature using Kalman filters, with only heart rate as input. Lee (2007) developed an artificial neural network for car cabin air temperature prediction from 17 inputs, such as direct sun intensity, air temperature outside the car, outside air velocity and ventilation temperature.

Similar to the work presented in this paper, Mola *et al*. (2001) developed an ET estimation model that can be used to control the car cabin environment. A series of trials in a controlled environment were performed to identify the estimator, during which a thermal manikin occupied the driver seat and measured overall ET. The cabin air temperature, HVAC outlet air temperature, external air temperature and mean radiant temperature were also recorded. Of these measured parameters, mean radiant temperature, HVAC outlet air temperature and air velocity were found to allow the best estimate of ET. A linear mathematical expression was inferred for estimating ET. The method was only assessed qualitatively and it was concluded to successfully drive HVAC control. A downside of this method is the fact that only one sensor was used to measure the cabin temperature, while different air temperature sensor locations within the cabin can increase the estimator's accuracy (Hintea *et al*., 2011). Moreover, the data used for training and testing the system came from controlled trials, leaving open the question of how well it would perform in realistic driving scenarios.

There are several gaps in the state of the art that this paper tries to fill: 1) using a large number of sensors for data gathering as this enables optimisation of sensor location (Hintea *et al.,* 2011) and leads to a more efficient estimator, 2) validating the estimator on data gathered in a variety of conditions, not only in stable, controlled environments and 3) quantifying the ET estimation error for multiple occupant body parts, rather than overall.

3 Experimental Data Gathering

The training and testing of the algorithm implemented here was based on experimentally gathered car cabin data within a variety of conditions. Throughout all 113 trials, ET was monitored at eight locations (corresponding to head, chest, left lower arm, right lower arm, left upper arm, right upper arm, thigh and calf) using the INNOVA Flatman thermal manikin, shown in Figure 1 (right), positioned in the front passenger seat of the test car. Cabin air and surface temperature data was gathered using type K ther-


Figure 1: Experimental data gathering. Left: Mean radiant temperature sensor. Right: Upper body of the Flatman thermal manikin.

mocouples and was recorded by a Grant Instruments DataTaker DT85 data logger.

Surface temperature was collected at the following locations: left and right instrumentation panel, steering wheel, front row passenger seat back and seat cushion, back row left seat back and seat cushion, left and right windscreen, front row left and right side glazing and back row left side glazing. Air temperature was collected at the following locations: external temperature, front row left and right headrest, front row belt, front row left and right foot, back row left and right headrest, back row belt, back row left and right foot. HVAC vent discharge temperature was collected at the following locations: front row left inner face vent, front row left out face vent, back row left face vent. A total of seven subjects (four males and three females) occupied the driver seat in turn and an observer occupied the rear right seat.

Four types of trials were performed corresponding to two main categories, as described in Sections 3.1 and 3.2.

3.1 *Controlled environment trials*

The trials described in Sections 3.1.1 and 3.1.2 involve controlling the external environment (solar load, ambient temperature, wind) while varying the HVAC control.

3.1.1 *Variable cabin temperatures within steady state external conditions (T1)*

These trials were performed within an enclosed space, characterized by stable ambient air temperature. Both the subjects and the test car cabin were preconditioned to 22 °C. At the outset of the experiment the subject entered the car and remained in static conditions (same HVAC set-point) for 10 minutes. The temperature was then increased by 1 °C every 3 minutes until it reached 28 °C. The same trial was performed with the HVAC set-point decreased by 1 °C every 3 minutes until it reached 16 °C. The air flow from the HVAC system was set to high or medium settings and trials with and without simulated solar loading on the driver side of the car were performed. The conditions are characterized by interior temperature rates of change less than 1.5 °C per minute, stable outside temperature (less than 1 °C difference per trial) and no wind or precipitation.

3.1.2 *User control within steady state external conditions (T2)*

These trials were performed within an enclosed space, characterized by stable ambient air temperature. The car cabin and the subjects were preconditioned to a neutral (22 °C), hot (28 °C), or cold (16 °C) temperature. The subjects entered the car and remained inside for 15 minutes, during which they were permitted to adjust the air conditioning at will in order to make themselves more comfortable. These trials were performed both with and without simulated solar loading on the driver side of the car. Higher car cabin interior temperature rates of change were encountered (up to 7 °C per minute) with stable outside temperature (less than 1 °C difference per trial) and no wind or precipitation.

3.2 *Realistic driving trials*

The trials described in Sections 3.2.1 and 3.2.2 were aimed at providing realistic driving scenarios within both short and long trips. They involve no control over the external environment (solar load, ambient temperature, wind) while varying the HVAC control.

3.2.1 *User control during driving within short trips (T3)*

These trials consisted of subjects driving the test car on private roads. The car and the subjects were preconditioned to a neutral (22 °C), hot (28 °C), or cold (16 °C) temperature. The subjects entered the car and drove for 15 minutes, during which they were permitted to adjust the air conditioning at will in order to make themselves more comfortable. The subjects were required to turn and change speed at frequent intervals in order to simulate to an extent the daily driving routine. These trials were characterized by interior temperature rates of change of up to 6 °C per minute and less stable outside temperature (up to 3 °C difference per trial), alone with ambient wind, solar load and precipitation.

3.2.2 *Automatic and user control during driving within long trips (T4)*

These trials consisted of a five day road-trip throughout the UK in a test vehicle. On each day there were

four trials, lasting around 2 hours each and differentiated by the HVAC control mode: automatic mode at 20 °C, automatic mode at 22 °C, automatic mode at 24 °C and manual mode. The car cabin instrumentation consisted of the sensors used for the previous three types of trials and an additional set of sensors: mean radiant temperature collected at a center ceiling location, shown in Figure 1 (left); solar load, collected at locations corresponding to dashboard left and right and at the car centre; air temperature, collected at locations corresponding to dashboard left and right. The experimental conditions encountered are characterized by interior temperature rates of change of up to 5 °C per minute and external temperature differences up to 5 °C per trial, along with ambient wind, solar load and precipitation.

Experiment types will be referred in the paper by the *T1, T2, T3* and *T4* abbreviations.

4 Equivalent Temperature Estimation Method

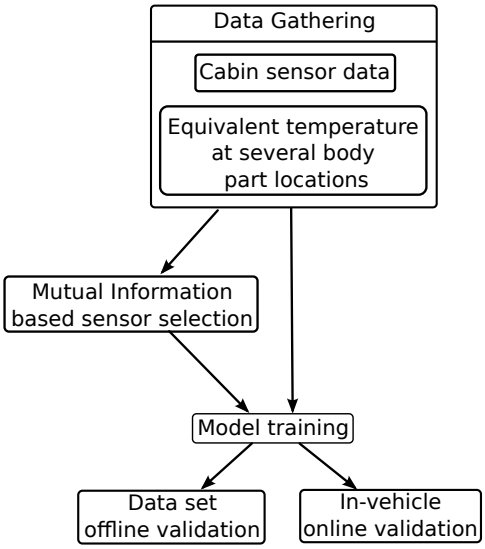

Figure 2: Equivalent temperature estimation method training and validation.

This section describes the method developed to estimate ET at different body part locations from one or more sensors located within the cabin (shown in Figure 2). The first step of the method consists of data gathering (described in detail in Section 3). Building an accurate ET estimation model also relies on the selection of an appropriate set of sensors within the car cabin. Here the sensors are selected through a Mutual Information (MI) based method (described in more detail in Hintea *et al*., 2011).

Given n sensors within the cabin, $S_1, S_2, ..., S_n$, and T_{eq} the ET to be estimated, the MI between them, $I(T_{eq}; S_1, ..., S_n)$, can be written as:

$$I(T_{eq}; S_1, ..., S_n) = H(T_{eq}) - H(T_{eq}|S_1, ..., S_n).$$

The conditional entropy $H(T_{eq}|S_1, ..., S_n)$ can be computed as following:

$$H(T_{eq}|S_1, ..., S_n) = H(T_{eq}, S_1, ..., S_n) - H(S_1, ..., S_n),$$

where $H(T_{eq}, S_1, ..., S_n)$ is the joint entropy for the $n+1$ sensors, while $H(S_1, ..., S_n)$ is the joint entropy for the n sensors used for the estimation.

Finally, MI can be defined as:

$$I(T_{eq}; S_1, ..., S_n) = H(T_{eq}) + H(S_1, ..., S_n) - H(T_{eq}, S_1, ..., S_n)$$

The group of m sensors ($m = 2$ within this paper) that shares the highest MI with the ET over all body parts is selected by maximising the MI over the eight body parts. It should be noted that the sensor locations selected may vary from one vehicle to another.

Multiple Linear Regression (MLR, Draper and Smith, 1981) lies at the core of the ET estimator. The MLR model suitable for this application can be written as:

$T_{eq} = \alpha_0 + \alpha_1 S_1 + \alpha_2 S_2 + ... + \alpha_m S_m$, where T_{eq} is the body part ET being estimated, $\alpha_0, ..., \alpha_m$ are the regression coefficients and $S_1, ..., S_m$ are the sensors previously selected. Training data gathered from the experimental trials described in Section 3 is used to compute the regression coefficients. Due to using k-fold cross validation to evaluate the performance of the estimator, training was performed on k-1 data chunks of the input data set, while testing was performed on the remaining data chunk. This model can be used in a deployed system by continuously estimating the T_{eq} values from real-time measured sensor values $S_1, ..., S_m$.

Several other estimation methods have been applied, such as Multilayer Perceptron (Haykin, 1998), REPTree (Witten and Frank, 2005), K-Nearest Neighbour (Cover and Hart, 1967), Multivariate Adaptive Regression Splines (Friedman, 1991), Radial Basis Function network (Haykin, 1998) and Random Forest (Breiman, 2001). MLR was the third in terms of accuracy, after the Multilayer Perceptron and Multivariate Adaptive Regression Splines methods, however, MLR outperformed the latter in terms of modeling and processing time, while the extra small gain in accuracy is not of significant impact (a lower average error of 0.10 °C on a 5 °C to 35 °C range) .

5 Evaluation of the Method on Experimental Data

K-fold cross validation was used to evaluate the estimator's performance, both on the full set of experimental data and on separate sets of trials in order to observe the best/worst scenario, indicating how well the algorithm generalizes to unseen data. The outputs of the estimator were compared to the original measured ET and the Root Mean Square Error (RMSE) was used as an accuracy measure.

5.1 *Controlled environment trials*

The MI sensor selection procedure was performed to determine the pair of sensors giving the lowest ET estimation errors over all body parts for trial sets *T1* and *T2*. The sensors selected were the surface temperature sensor located at the back row left seat back and the air temperature sensor located at the back row right headrest level.

As Table 1 shows, the lowest estimation errors were obtained for the trial set *T1*, ranging from 0.5 °C for the thigh to 1.3 °C for the head, averaging 1 °C over all eight body parts. The estimation errors were higher for the trial set *T2*, averaging 1.5 °C and ranging from 1.3 °C for the chest to 1.9 °C for the upper arm. The higher error for the latter could be due to significantly higher car cabin temperature rates of change (up to 7 °C per minute). Figures 3 and 4 show the measured versus estimated ET at the head and thigh level within one trial of *T1* and *T2* (starting from 28 °C and with the HVAC flow set on medium).

Table 1: Equivalent temperature estimation results (RMSE) from the best two sensors in trials *T1* and *T2*.

Equivalent temperature	Trial type *T1*	*T2*
head	1.33 °C	1.71 °C
chest	0.95 °C	1.38 °C
lower arm	1.05 °C	1.59 °C
upper arm	0.96 °C	1.92 °C
thigh	0.53 °C	1.51 °C
calf	1.28 °C	1.44 °C
average	1.02 °C	1.59 °C

5.2 *Realistic driving trials*

The pair of sensors corresponding to the lowest estimation errors for trial set *T3* was the same as for *T1*

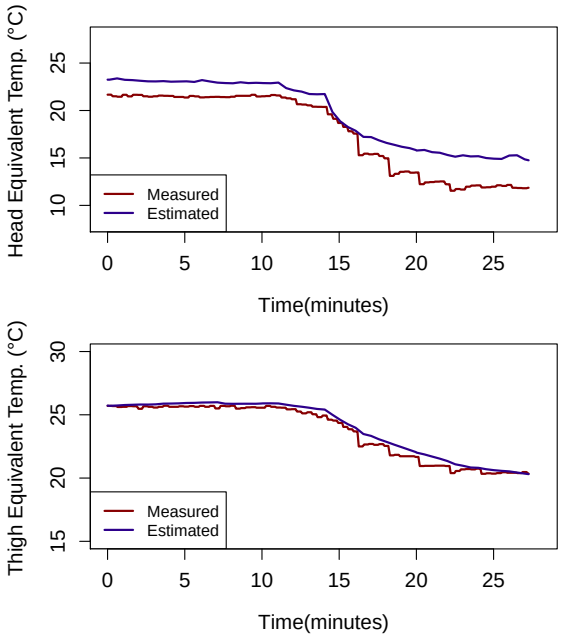

Figure 3: Estimated versus measured equivalent temperature at the head and thigh level during one trial of *T1*.

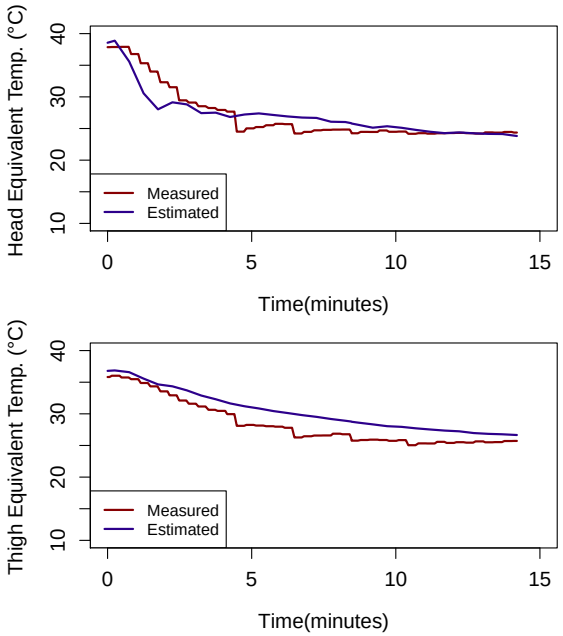

Figure 4: Estimated versus measured equivalent temperature at the head and thigh level during one trial of *T2*.

and *T2*. However, as Table 2 shows, the estimation errors were higher than for the previous types of trials, averaging 1.9 °C over all body parts and ranging from 1.4 °C for the calf to 2.5 °C for the head. The reasons for this could be the high car cabin temperature rates of change (up to 6 °C per minute) and variable external conditions, such as solar load, precipitation

Table 2: Equivalent temperature estimation results (RMSE) from the best two sensors in trials *T3* and *T*4.

Equivalent temperature	Trial type *T3*	*T4*
head	2.5 °C	1.44 °C
chest	1.63 °C	1.42 °C
lower arm	2.32 °C	1.29 °C
upper arm	2.01 °C	1.37 °C
thigh	1.63 °C	1.06 °C
calf	1.47 °C	2.08 °C
average	1.93 °C	1.44 °C

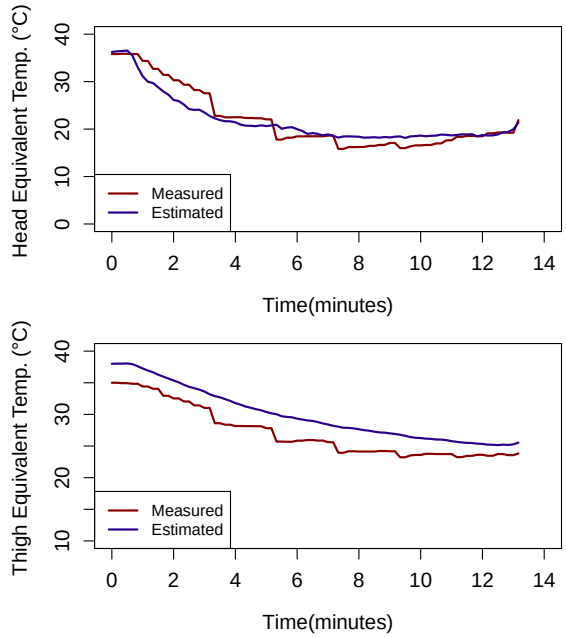

Figure 5: Estimated versus measured equivalent temperature at the head and thigh level during one trial of *T3*.

and air temperature.

Among other parameters, ET integrates the effect of mean radiant temperature. The latter was measured within trial set *T4* and was found to relate best to ET. The pair of sensors giving the lowest estimation errors were the mean radiant temperature sensor and the air temperature sensor located at the front row right belt level. The estimation errors for *T4* were lower than for *T3*, most likely due to using the mean radiant temperature as an estimation source. They average 1.4 °C over all body parts, with a minimum error of 1 °C for the thigh and a maximum error of 2 °C for the calf. Interesting to note is that throughout most experiment types the body parts directly exposed to the vent air flows (head, calf and arms) were estimated with the largest error. Figure 5 show the measured versus estimated ET at the head and thigh level within one trial of *T3* (starting from 28 °C and with the HVAC flow set on medium).

Nilsson *et al*. (1999) conducted empirical trials to find the ET ranges for 16 body parts that would correspond to thermal comfort. They found that both in winter and summer conditions, the comfortable range for each of the body parts was covering up to 7 °C (for example, for the head the comfortable range was between 18 °C to 25 °C in the winter and between 20 °C to 26 °C in the summer), therefore the maximum 2 °C error introduced by the estimation method here appears to be low enough to deliver sufficient accuracy for HVAC control.

6 Conclusion

A multiple linear regression model that estimates equivalent temperature at several body parts of the occupant has been derived. When applying k-fold cross validation on trials in a controlled environment, equivalent temperature is predicted with average errors between 0.5 °C and 1.9 °C for various body parts while using only two sensors as input previously selected. On the trials in realistic driving scenarios errors between 1 °C and 2 °C were achieved. The equivalent temperature estimation method provides sufficient accuracy for controlling the HVAC system.

Since equivalent temperature integrates the effect of air flow, in future work we will examine the latter's impact on the estimation error and find optimal air flow sensor locations.

Acknowledgements

The Low Carbon Vehicle Technology Project (LCVTP) was a collaborative research project between leading automotive companies and research partners, revolutionising the way vehicles are powered and manufactured. The project partners included Jaguar Land Rover, Tata Motors European Technical Centre, Ricardo, MIRA LTD., Zytek, WMG and Coventry University. The project included 15 automotive technology development work-streams that will deliver technological and socio-economic outputs that will benefit the West Midlands Region. The £19 million project was funded by Advantage West Midlands (AWM) and the European Regional Development Fund (ERDF).

The authors would like to thank the anonymous reviewers for their insightful comments.

References

ANSI/ASHRAE (2004). Thermal environmental conditions for human occupancy. Technical Report 55-2010, American Society of Heating, Refrigerating and Air-conditioning Engineers.

Breiman, L. (2001). Random forests. *Machine Learning*, 45:5–32.

Buller, M., Tharion, W., Hoyt, R., and Jenkins, O. (2010). Estimation of human internal temperature from wearable physiological sensors. In *Proc. of the 22nd Conf. on Innovative Applications of Artificial Intelligence (IAAI)*. AAAI Press.

Cover, T. and Hart, P. (1967). Nearest neighbor pattern classification. *IEEE Transactions on Information Theory*, 13:21–27.

Curran, A., Peck, S., Schwenn, T., and Hepokoski, M. (2010). Improving cabin thermal comfort by controlling equivalent temperature. *SAE International Journal Aerospace*, 2:263–267.

Draper, N. and Smith, H. (1981). *Applied Regression Analysis*. Wiley.

Fanger, P. O. (1973). Assessment of man's thermal comfort in practice. *British Journal of Industrial Medicine*, 30:313–324.

Friedman, J. H. (1991). Multivariate adaptive regression splines. *Annals of Statistics*, 19:1–67.

Gagge, A., Stolwijk, J., and Hardy, J. (1967). Comfort and thermal sensations and associated physiological responses at various ambient temperatures. *Environmental Research*, 1:1–20.

Haykin, S. (1998). *Neural Networks: A Comprehensive Foundation*. Prentice Hall.

Hintea, D., Brusey, J., Gaura, E., Beloe, N., and Bridge, D. (2011). Mutual information-based sensor positioning for car cabin comfort control. In *Proceedings of the 15th KES International Conference*, KES'11, pages 483–492. Springer.

Lee, T. Y. (2007). Prediction of car cabin temperature using artificial neural network. Master's thesis, Technische Universitat Munchen.

Madsen, T., Olesen, B., and Reid, K. (1986). New methods for evaluation of the thermal environment in automotive vehicles. Report.

Mayer, E. and Schwab, R. (1999). Correlation between thermal response and equivalent temperature. In *CABCLI Consortium*, pages 63–70. ISSN 1401-4963.

Mehnert, P., Malchaire, J., Kampmann, B., Piette, A., Griefahn, B., and Gebhardt, H. (2000). Prediction of the average skin temperature in warm and hot environments. *European Journal of Applied Physiology*, 82:52–60.

Mola, S., Magini, M., and Malvicino, C. (2001). Equivalent temperature estimator using mean radiant temperature sensor. *Measurement and Control*, 34:167–169.

Mola, S., Presti, G. L., Ardusso, R., Malvicino, C., Zussino, A., and Caviasso, G. (2004). Measuring customer perceived thermal comfort in car cabin compartment: Index of perceived thermal comfort. In *FISITA World Automotive Congress*. STA.

Nilsson, H., Holmer, I., Bohm, M., and Noren, O. (1999). Equivalent temperature and thermal sensation - comparison with subjective responses. In *Comfort in the Automotive Industry, Bologna, ATA*, pages 157–162.

SAE Journal (2012). Equivalent temperature: Truck and bus. Technical report, SAE International.

Singh, M., Mahapatra, S., and Atreya, S. (2010). Thermal performance study and evaluation of comfort temperatures in vernacular buildings of north-east India. *Building and Environment*, 45:320–329.

Witten, I. and Frank, E. (2005). *Data Mining: Practical Machine Learning Tools and Techniques*. Morgan Kaufmann.

Mutual Information-based Sensor Positioning for Car Cabin Comfort Control

Diana Hintea[1], James Brusey[1], Elena Gaura[1], Neil Beloe[2], and David Bridge[3]

[1] Coventry University, Priory Lane, Coventry, CV1 5FB, UK
[2] Jaguar Land Rover Ltd, Abbey Road, Whitley, Coventry, CV3 4LF, UK
[3] MIRA Ltd, Watling Street, Nuneaton, CV10 0TU, UK

Abstract. Car cabins are transient, non-uniform thermal environments, both with respect to time and space. Identifying representative locations for the Heating, Ventilation and Air Conditioning (HVAC) system sensors is an open research problem. Common sensor positioning approaches are driven by considerations such as cost or aesthetics, which may impact on the performance/outputs of the HVAC system and thus occupants' comfort. Based on experimental data, this paper quantifies the spacial-temporal variations in the cabin's environment by using Mutual Information (MI) as a similarity measure. The overarching aim for the work is to find optimal (but practical) locations for sensors that: i) can produce accurate estimates of temperature at locations where sensors would be difficult to place, such as on an occupant's face or abdomen and ii) thus, support the development of *occupant* rather than *cabin* focused HVAC control algorithms. When applied to experimental data from stable and hot/cold soaking scenarios, the method proposed successfully identified practical sensor locations which estimate face and abdomen temperatures of an occupant with less than 0.7 ℃ and 0.5 ℃ error, respectively.

1 Introduction

The role of Heating, Ventilation and Air Conditioning (HVAC) in cars is to keep passengers comfortable or, more correctly, to avoid their discomfort. Traditionally, the HVAC energy budget has been generous. However, with the introduction of electric and hybrid electric vehicles, any additional energy usage by the HVAC system reduces the range, and thus, the usefulness of the car. Energy efficient approaches to control are called for, potentially based on local conditioning of occupied cabin areas and driven by occupants' perceptions of the environment rather than set-point temperatures.

Several novel approaches to HVAC control have been presented in the literature. Generally, such approaches are concerned with directly controlling the comfort of the cabin occupants. Comfort is estimated by applying a model, such as Predicted Mean Value (PMV) [3], to the cabin sensed data. The success of such control algorithms heavily relies on an accurate representation of the sensed phenomena at specific points, i.e in the immediate vicinity of the occupant, and also presume the cabin environment to be relatively stable.

A parallel line of work in the domain takes advantage of enhanced understanding of human physiology and proposes models for estimating the occupant's thermal sensation and, with it, thermal comfort. Thermal sensation can be predicted either for the whole body or for individual body parts and common model inputs are local skin temperature, mean skin temperature and core body temperature, together reflecting the overall thermal state of the body. The Berkeley Comfort Model [6] and Zhang's Model [14] are the best empirical models to date and are used by most advanced automotive simulators such as RadTherm [10] for evaluating cabin environments.

Whilst expected to deliver a more accurate representation of the comfort experienced by occupants, physiological comfort models can not be directly used for HVAC control as it is impractical to acquire the necessary inputs (i.e. skin temperature at various points). The inputs could, however, be estimated from suitable cabin data. The prerequisites are: i) a good understanding of the cabin environment and the relationships between various sensing locations within the cabin and ii) a method of estimating with sufficient accuracy human skin temperature in a variety of conditions, from cabin data.

The work here proposes a Mutual Information (MI) based method as an aid to understanding the cabin environment and the spacial relationships between temperatures within the cabin. MI quantifies the shared informational content between a source sensor location and a target virtual location (such as various occupant skin sites). Within an experimental set-up which makes available not only cabin data at multiple points, but also occupant skin temperature data, the method allows the selection of practical cabin sensor locations best suited for estimating skin temperatures.

The paper is structured as follows. Section 2 presents related work in the areas of HVAC control and sensor positioning. Section 3 describes the methods developed for calculating the MI between sensor locations within a car cabin environment. Section 4 presents the results obtained when applying the MI methods to experimental data and Section 5 concludes the paper.

2 Related Work

Numerous attempts exist in the literature towards developing comfort control algorithms. Torres *et al.* [13] designed and implemented a neural network based control algorithm, using a back-propagation learning method. Though good results were achieved based on a simple neural network, a disadvantage is represented by the network's long training duration. In order to make the learning process less time consuming, Luo *et al.* [7] worked on a Fuzzy Neural Network (FNN) model for predicting clothing thermal functions, based on body core and skin temperatures. Another fuzzy logic-based control algorithm was presented by Stephen *et al.* [12]. The method simplified and converted Fanger's [3] PMV equations into fuzzy rules. However, the results were simulation-based and the controller's effectiveness was not clear from the results.

The works described above assume that the sensor data driving the control algorithms is a perfect representation of the cabin environment. The complexity and dynamics of the cabin are not considered. Spacial-temporal thermal variations in the cabin are however significant, as observed experimentally by the authors here in a variety of controlled tests.

Although not specifically dealing with cabin environments, a number of works in the literature are concerned with strategies for finding optimal sensor locations in similar complex environments. Guestrin *et al.* [4] chose a MI criteria (a measure of the amount of shared information between two random variables [2,8]) and implemented a polynomial-time approximation for maximizing the MI, leading to better sensor placements. A Bayesian approach used for optimally locating a sensor with respect to the others was described by Cameron *et al.* [1]. In this method the expectations regarding the sensing environment were updated based on the acquired sensor data and the next sensor locations were chosen by taking into account this prior information. Shah *et al.* [11] dealt with the problem of optimally positioning sensors in lumped and distributed parameter dynamic systems. The covariance of the parameter estimates was computed and the sensor locations were found by minimizing the covariance matrix. Using the concept of entropy, Papadimitriou *et al.* [9] illustrated a method for optimally locating the sensors in a structure in order to extract from the measured data the most valuable information about the model's parameters. Another entropy-based sensor placement method was developed by Gutierrez *et al.* [5]. A maximum entropy approach for selecting the corresponding probability distributions was used with the purpose of minimizing the average detection error for fault locations.

A MI based approach has been adopted in this work and is further presented in the next section.

3 Mutual Information-based Method

The MI computation method described here is based on finding entropies, leading to a multivariate Gaussian assumption over the variables. The normal distribution hypothesis was confirmed by applying the D'Agostino normality test on the experimental data sets.

A series of methods were researched towards the purpose of computing the MI. The first belongs to the discrete case and consists of sampling the raw data, the second one derives an approximate continuous curve that matches the probability distribution observed in the raw data. A third method implemented belongs to the continuous case and it consists of a numerical approximation to the integral definition of MI. The method presented further on was selected over the above described methods since it gave results consistent with expectations for all experimental data.

The MI computation method contains the steps in Figure 1, described in what follows.

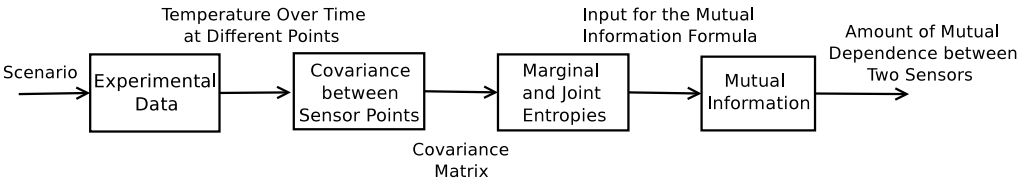

Fig. 1. Flow chart of the entropy-based approach of computing the mutual information

3.1 Gathering the Experimental Data

A series of experiments were performed in a climatic wind tunnel with a state of the art vehicle, as follows:

- Five 54 minutes long steady state experiments, each with three occupants in the car. The car cabin air temperature was initially set to 22 ℃, and increased by 1 ℃ per minute, towards a final temperature of 26 ℃. For the second part of the experiment, the temperature was gradually decreased to 16 ℃, and finally brought back to 22 ℃. The car was in idle state during the initial, middle and final parts of the experiment when the temperatures were maintained at 22 ℃, 16 ℃ and 22 ℃, respectively and driven at a constant speed of 50 km/h when the temperature increments were performed.
- Two warm-up experiments, each 70 minutes long. The car was initially soaked to -18 ℃. The experiments began by setting the cabin's thermostat to the highest possible temperature (first experiment), and 22 ℃, respectively (second experiment). There were two cabin occupants each time and the car was driven at a constant speed of 50 km/h for the first 30 minutes, and 100 km/h for the rest of each experiment.

The cabin and occupant sensor data was acquired with a frequency of 0.1Hz. The sensorized occupant was in the front passenger seat for all above experiments. 4 skin sensors were used: face, upper arm, chest and abdomen. The cabin had standard instrumentation consisting of a thermocouple harness with 32 sensors (locations shown in Figure 2). The abbreviations used in Figure 2 are: L = left, R = right, R1 = row containing the front seats, R2 = row containing the back seats, while the discharge sensors are the sensors placed at the air conditioning vent outlets.

In what follows, skin temperature is referred to as the *target variable* (or simply target). Similarly, the locations of sensors that can be practically considered for HVAC control are referred to as *source variables* (or sources).

3.2 Computing the Marginal Entropies and the Mutual Information

Given two sensors X and Y, let X be the target location and Y the source location. Using the entropy concept, the MI between the source and target can be expressed as:

$$I(X;Y) = H(X) - H(X \mid Y), \tag{1}$$

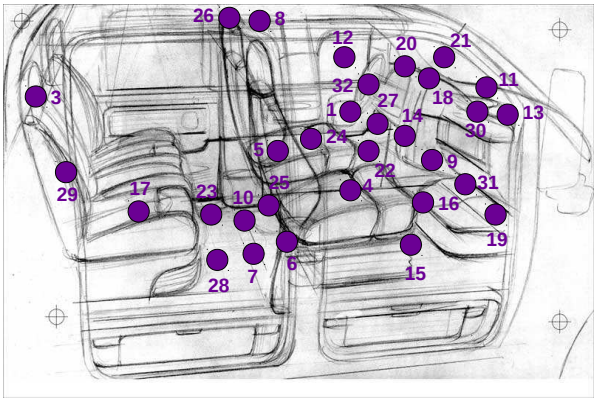

1 - R1DischargeOuterL
2 - DriverSeatBack
3 - HeadlinerIntRearPassHead
4 - PassengerSeatCushion
5 - PassengerSeatBack
6 - R2FootDischargeR
7 - R2DischargeR
8 - PanoramicPassengerHead
9 - R1DischargeInnerR
10 - R2DischargeL
11 - FrontScreenRCentre
12 - FrontSideGlassLCentre
13 - IPTopRCentre
14 - R1DischargeInnerL
15 - FrontSideGlassRCentre
16 - R1FootR
17 - R2RSeatCushion
18 - ScreenDefrostL
19 - R1DischargeOuterR
20 - IPTopLCentre
21 - FrontScreenLCentre
22 - R1FootL
23 - R2FootL
24 - DriverSeatCushion
25 - R2FootDischargeL
26 - PanoramicDriverHead
27 - R1FootDischargeL
28 - R2FootR
29 - R2RSeatBack
30 - ScreenDefrostR
31 - R1FootDischargeR
32 - SteeringWheel

Fig. 2. Source sensor locations

where $H(X), H(Y)$ denote the marginal entropies of the two random variables and $H(X \mid Y)$ is the conditional entropy of X knowing Y.

Using the conditional entropy definition, MI can be written as:

$$I(X;Y) = H(X) - H(Y) + H(X,Y).$$

Both the marginal entropies $H(X), H(Y)$ and the joint entropy $H(X,Y)$ can be computed from the general joint entropy formula for a multivariate normal distribution:

$$H(X_1, X_2, ..., X_k) = \frac{1}{2} \ln \left((2\pi e)^{\,k} \, |\Sigma| \right), \tag{2}$$

where k represents the number of random variables forming the distribution and Σ is the covariance matrix of the variables.

3.3 Extending the Mutual Information Concept for Multiple Sources

In order to represent more accurately the point of interest, namely the target location, computing the MI from multiple source sensors is considered.

Given three sensors X, Y and Z, let X be the target location and Y and Z be the source locations. Based on equation 1, the MI between the two sources and the target can be written as:

$$I\left(X;Y,Z\right)=H\left(X\right)-H\left(X|Y,Z\right).$$

The conditional entropy can be written as following:

$$H(X|Y,Z)=H(X,Y,Z)-H(Y,Z),$$

where $H(X,Y,Z)$ is the joint entropy for the three sensors, while $H(Y,Z)$ is the joint entropy for the two sensor sources.

Finally, MI can be defined as:

$$I(X;Y,Z)=H(X)+H(Y,Z)-H(X,Y,Z)$$

The marginal entropy $H(X)$, as well as the multiple joint entropies ($H(Y,Z)$ and $H(X,Y,Z)$), can be computed using equation 2.

4 Evaluation of the Method on Experimental Data

4.1 Mutual Information Outcomes between a Source Sensor and a Target Sensor

The MI values between source sensors (32 cabin locations as per Figure 2) and two target locations (face and abdomen of the front row passenger) were calculated, over the whole experimental data bank. MI values for the FACE target varied between 0.0003 and 1.05, with the highest MI obtained from the "R2DischargeR" sensor. For the ABDOMEN target, the lowest MI value was 0.0001 and the highest 0.67, obtained from the "R2RSeatCushion" sensor. Table 1 shows a sample of source locations and their respective MI values for FACE and ABDOMEN targets. The table also presents results for the estimation accuracy which would be achieved by using the respective source - target pair. (This estimation method is presented elsewhere.)

For both target locations, as the MI values decrease, the estimation accuracy decreases too, as expected. However, no direct relationship was observed here between the MI value and the estimation accuracy across the two targets (Figure 3).

Figure 4 represents graphically the MI between pairs of target sensors and potential source sensors. The line thickness is directly proportional to the MI value.

4.2 Mutual Information Outcomes between Two Source Sensors and a Target Sensor

Table 2 illustrates how MI changes when two source sensors are considered jointly. The use of two source sensors resulted in higher MI values throughout the source and target pairs considered. The highest MI value for the FACE target was 1.19, obtained from the "R2DischargeR" and "R2FootR" combination of sensors. For the ABDOMEN target, the highest MI value was 0.76, obtained from the "DriverSeatCushion" and "PassengerSeatCushion" combination of sensors.

Target Sensor: Face Source Sensor	MI	Temperature Estimation RMSE(℃)(mean±std)
R2DischargeR	1.05	0.7±0.08
HeadlinerIntRearPassHead	0.86	0.86±0.09
SteeringWheel	0.67	1.05±0.1
R2FootR	0.64	1.06±0.16
IPTopRCentre	0.48	1.2±0.09
R1DischargeInnerL	0.37	1.4±0.14
FrontSideGlassLCentre	0.09	1.9±0.2
Target Sensor: Abdomen **Source Sensor**	**MI**	**Temperature Estimation** **RMSE(℃)(mean±std)**
R2RSeatCushion	0.67	0.52±0.06
IPTopRCentre	0.61	0.55±0.06
PassengerSeatBack	0.59	0.56±0.06
PassengerSeatCushion	0.56	0.58±0.05
PanoramicDriverHead	0.36	0.72±0.06
FrontSideGlassRCentre	0.27	0.8±0.03
R1FootR	0.05	1.0±0.02

Table 1. MI results for face and abdomen selected as target sensors

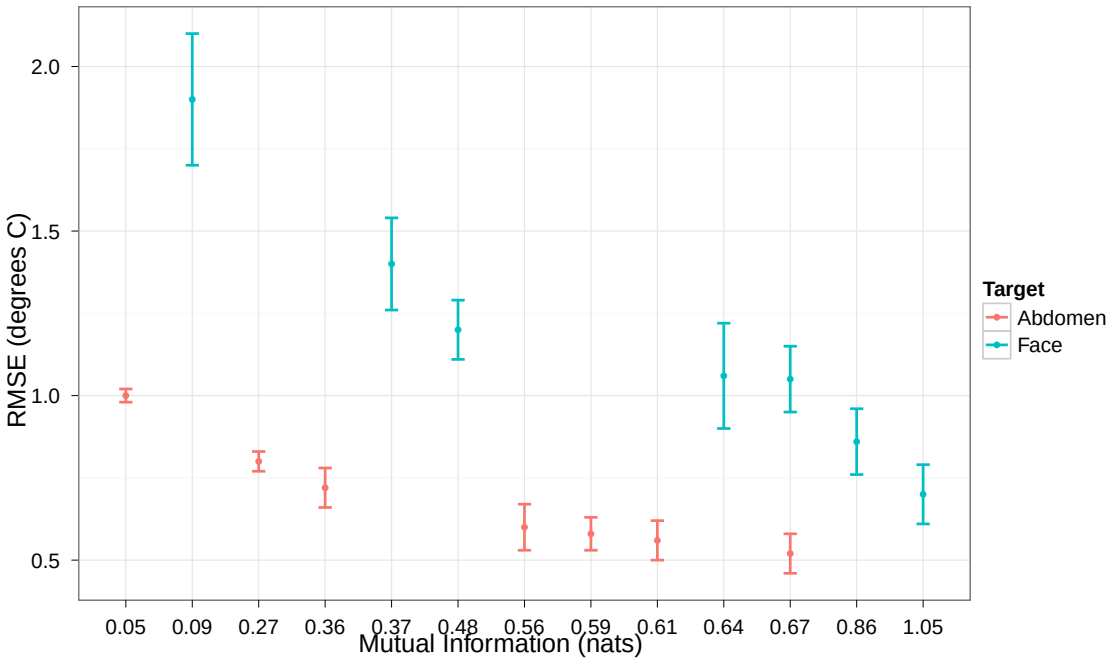

Fig. 3. MI values and their corresponding estimation accuracy

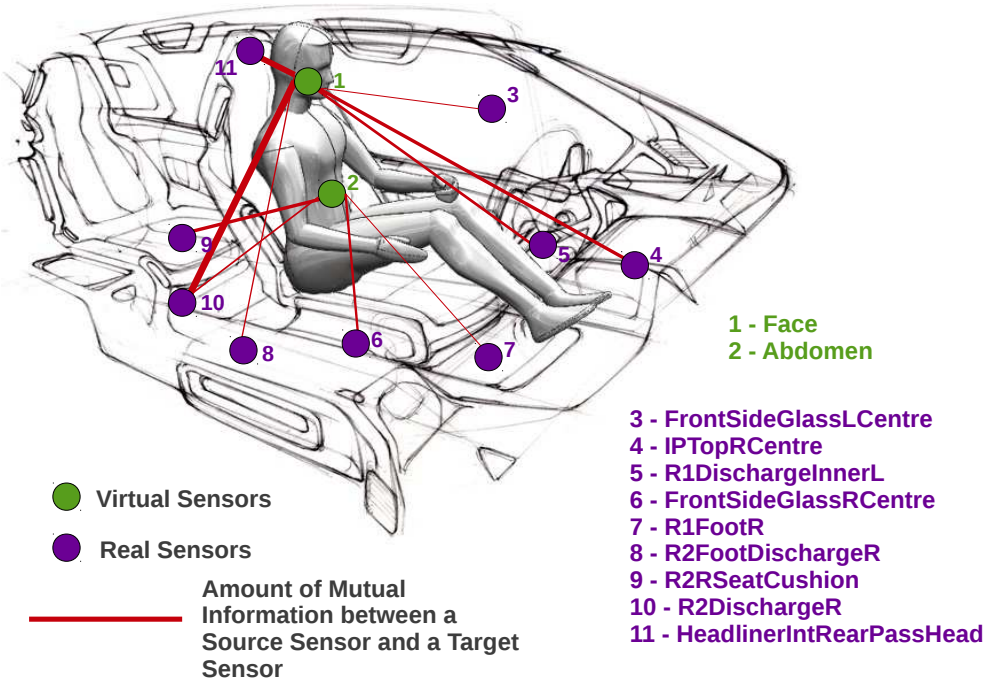

Fig. 4. MI relations between the two target sensors and some of the source sensors

Target Sensor: Face			Temperature Estimation
Source Sensor 1	Source Sensor 2	MI	RMSE(℃)(mean±std)
R2DischargeR	R2FootR	1.19	0.62±0.10
R2DischargeR	HeadlinerIntRearPassHead	1.17	0.64±0.08
R2DischargeR	R2FootL	1.16	0.66±0.09
PassengerSeatCushion	HeadlinerIntRearPassHead	1.15	0.66±0.09
R2DischargeR	R1FootL	1.14	0.66±0.09
Target Sensor: Abdomen			Temperature Estimation
Source Sensor 1	Source Sensor 2	MI	RMSE(℃)(mean±std)
DriverSeatCushion	PassengerSeatCushion	0.756	0.49±0.04
R2RSeatCushion	IPTopRCentre	0.683	0.524±0.06
R2RSeatCushion	PassengerSeatCushion	0.683	0.526±0.06
R1DischargeOuterR	R1FootL	0.682	0.527±0.04
R2FootR	R2RSeatCushion	0.679	0.526±0.06

Table 2. Best five MI scores for face and abdomen selected as target sensors

5 Conclusions and Further Work

The work described a method of identifying optimal sensor locations for estimating temperature at defined target locations, such as the face or abdomen of a cabin's occupant. A first step towards this aim was to establish a robust method for accurately quantifying how closely related various sensor data streams are. The Mutual Information between sensors was found to be an appropriate measure for the application at hand.

For the face selected as target location, the "R2DischargeR" source sensor delivered the highest MI value, leading to an estimation accuracy of 0.7 ℃. For the abdomen selected as target location, an estimation accuracy of 0.52 ℃ was obtained with "R2RSeatCushion" as a source sensor. The method was extended to multiple sources in order to find combinations of sensors which lead to a better estimation of the target sensor. The estimation accuracy was further improved to 0.62 ℃ for the face as target with "R2DischargeR" and "R2FootR" as source sensors. For the abdomen as target, the estimation accuracy was increased to 0.49 ℃ with "DriverSeatCushion" and "PassengerSeatCushion" as source sensors.

With regard to future work, it is planned to estimate the overall comfort of all occupants within a car cabin. Several source and target locations will be used with the purpose of maximizing the MI among them. It is also planned to implement a reinforcement learning HVAC algorithm used to train the system to adjust set-points. Embedding this algorithm into the car's HVAC system implies that the HVAC control will gradually learn user's preferences with the purpose of reducing the instances of user intervention whilst maintaining the occupants' comfort and reducing the energy consumption.

Acknowledgements

The Low Carbon Vehicle Technology Project (LCVTP) is a collaborative research project between leading automotive companies and research partners, revolutionising the way vehicles are powered and manufactured. The project partners include Jaguar Land Rover, Tata Motors European Technical Centre, Ricardo, MIRA LTD., Zytek, WMG and Coventry University. The project includes 15 automotive technology development work-streams that will deliver technological and socio-economic outputs that will benefit the West Midlands Region. The £19 million project is funded by Advantage West Midlands (AWM) and the European Regional Development Fund (ERDF).

References

1. Alec Cameron and Hugh Durrant-Whyte. A bayesian approach to optimal sensor placement. *The International Journal of Robotics Research*, 9, 1990.
2. Thomas M. Cover and Joy A. Thomas. *Elements of Information Theory*. John Wiley & Sons, Inc., 1991.

3. P.O. Fanger. *Thermal Comfort.* PhD thesis, Technical University of Denmark, 1970.
4. Carlos Guestrin, Andreas Krause, and Ajit Paul Singh. Near-optimal sensor placements in gaussian processes. In *ICML '05 Proceedings of the 22nd international conference on Machine learning*, 2005.
5. J. M. Gutierrez, V. Kreinovich, R. Osegueda, C. Ferregut, and M. J. George. Maximum entropy approach to optimal sensor placement for aerospace non-destructive testing. In *Maximum Entropy and Bayesian Methods*, 1998.
6. C. Huizenga, H. Zhang, T. Duan, and E. Arens. An improved multinode model of human physiology and thermal comfort. In *Building Simulation*, 1999.
7. Xiaonan Luo, Wenbang Hou, Yi Li, and Zhong Wang. A fuzzy neural network model for predicting clothing thermal comfort. *Computers & Mathematics with Applications*, 53:pp. 1840-1846, 2007.
8. Liam Paninski. Estimation of entropy and mutual information. *Neural Computation*, 15:pp. 1191-1253, 2003.
9. Costas Papadimitriou, James L.Beck, and Siu-Kui Au. Entropy-based optimal sensor location for structural model updating. *Journal of Vibration and Control*, 6:pp. 781-802, 2000.
10. RadTherm©. ThermoAnalytics Inc., Heat Transfer Analysis Software. http://www.thermoanalytics.com/products/radtherm/index.html; Accessed on the 6th of April 2011.
11. P. C. Shah and F. E. Udwadia. A methodology for optimal sensor locations for identification of dynamic systems. *Journal of Applied Mechanics*, 45:pp. 188-197, 1978.
12. Elizabeth Amudhini Stephen, Mercy Shnathi, P. Rajalakshmy, and M. Melbern Parthido. Application of fuzzy logic in control of thermal comfort. *International Journal of Computational and Applied Mathematics*, 5:pp.289-300, 2010.
13. Jose Luis Torres and Marcelo Luis Martin. Adaptive control of thermal comfort using neural networks. *Argentine Symposium on Computing Technology*, 2008.
14. H. Zhang. *Human Thermal Sensation and Comfort in Transient and Non-Uniform Thermal Environments.* PhD thesis, University of California, Berkeley, 2003.

Appendix D

Ethical Approval

The work in this thesis has been put through the universities ethical approval process. The ethical approval follows: